DYNAMIC MULTIVALENCY FOR THE RECOGNITION OF PROTEIN SURFACES.

Philipp Reeh

Dipòsit Legal: T 1579-2014

Dynamic Multivalency for the Recognition of Protein Surfaces

DOCTORAL THESIS

By

Philipp Reeh

Supervised by

Prof. Javier de Mendoza Sans

Institut Català d'Investigació Quimica

and

UNIVERSITAT ROVIRA I VIRGILI

Tarragona

2014

ICIQ
Institut Català d'Investigació Química

Av. Països Catalans, 16
43007 Tarragona
Tel.977 920 200
Fax. 977 920 222

UNIVERSITAT ROVIRA I VIRGILI

Departament De Química
Analítica I Química Orgànica
C/ Marcel.lí Domingo s/n
Campus Sescelades
43007 Tarragona
Tel. 977 55 97 69
Fax. 977 55 84 46

Prof. JAVIER DE MENDOZA, group leader at the Institute of Chemical Research of Catalonia (ICIQ),

Certifies, that the present Doctoral Thesis entitled "**Dynamic Multivalency for the Recognition of Protein Surfaces**" presented by PHILIPP REEH to obtain the degree of doctor, has been carried out under his supervision in the Institute of Chemical Research of Catalonia (ICIQ).

Tarragona, 13th of March 2014

PhD Thesis Supervisor

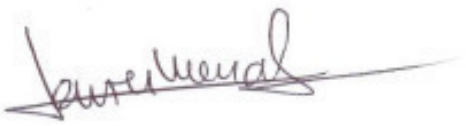

Prof. Javier de Mendoza

Acknowledgements

Most of all, I'd like to thank my parents for the decades of support they gave me. Without their help and understanding I would have never been able to start this project, let alone finishing it! I always expected to be a nervous wreck by the end of my thesis; however that is not the case. Why? The care that I got from Gizem gave me the tranquillity to relax and start with a rested mind every morning.

In spring 2009 I was looking for "a PhD somewhere abroad". Prof. Javier de Mendoza gave me the opportunity to come to the ICIQ in Tarragona. The position in this perfectly equipped institute, working on an interesting thesis topic and all of that in beautiful town beside the sea, felt like having won the lottery. Javier put me on a new topic and gave me the freedom to conduct all main parts of my research by myself. This sensation of freedom but also own responsibility for my results, was something that motivated me more than control or strict orders could have done. Therefore, I am very thankful for his insightful comments, suggestions and creative ideas but particularly, for his trust. The relaxed way we could discuss problems, especially in stressful times, made me continue even when thinking all was lost.

I felt immediately welcome in the lab thanks to people like Núria, Vera, Augustin, James, Caterina, Gerald, Elisa and Julian. Aritz helped me to do my first steps in this new place and Sara (Sattin) introduced me to the (sometimes not so) sweet world of sugars, thank you! Laura and I shared two rotovaps, many hours and our good and bad moods (though, as a well-mannered British she never showed me how nerve breaking a pedantic German can be). I owe very special thanks to Ondrej and Sara Pasquale for cheering up the work days and for good friendship.

Without the encouragement and help of one lab-mate I probably would have never started one of the best parts of my thesis project. Matt's expertise and support (even after he left our lab) helped me to successfully starting off into the right direction.

As the years passed the group continuously shrunk and finally only few were left in the lab. From this last guard; I'd like to thank Eva, firstly for being a good friend and secondly for her patient technical support in the lab. Jin lightened up my workdays and has probably shared more breakfasts with me than my girlfriend has. Qixun has to be thanked for his

patience when I kept occupying the MS system for days. With Berta I have not only shared the experience of doing a PhD but also a flat for almost four years. The biggest part of the Spanish (both Catalan and Castellan) I learned, originates from chatting along in kitchen, with her.

Nothing would have been possible without the people who kept all those precious devices running, that are so necessary for us every day. Therefore, many thanks go to the mass- and the NMR- spectrometry units that always kept the machines in perfect shape and ready to use. Special thanks to the chromatography unit, without them I would have never even started with some parts of my project. I also owe to Mariona who helped me to purify some of my most unpleasant reaction mixtures.

Right before the end my time in the ICIQ, I urgently needed to perform some ITC experiments. Therefore, I am particularly grateful for the assistance given by Prof. Pau Ballester; without his patient guidance I would not have been able to perform those measurements in any reasonable timeframe.

And finally, my deepest gratitude to anybody who is going to read this thesis.

List of Abbreviations

Ac: Acetyl

ACN: Acetonitrile

aq.: Aqueous

Ar: Aromatic

atm: Atmosphere

bn: Benzyl

Ts: Tosyl

Boc: Tert-butoxycarbonyl

tBu: tert-butyl

DCC: Dynamic Combinatorial Chemistry

DCL: Dynamic Combinatorial Library

DCM: Dichloromethane

DMF: *N,N'*-dimetylformamide

EI-MS: Electron Impact Mass Spectrometry

ESI-MS: Electrospray Ionization Mass Spectrometry

eq.: Equivalent

Et: Ethyl

Et_3N: Triethylamine

FAB-MS: Fast Atom Bombardment Mass Spectrometry

Hex/Hexa: Hexane

HPLC :High Performance Liquid Chromatography

HRMS: High Resolution Mass Spectrometry

HSQC: heteronuclear single quantum correlation

ITC: isothermal titration calorimetry

MALDI: matrix-assisted laser desorption/ionization sprectrometry

Me: methyl

Ms: Methanesulfonyl or mesyl

MS-TOF: time of flight spectrometry

LC-MS: Liquid chromatography-mass spectroscopy

PG: Protecting group

Ph: Phenyl

ppm: Parts per million

r.t.: Room temperature

RP: Reverse phase

TFA: trifluoroacetic acid

Tf_2O: trifluoromethanesulfonic acid anhydride or triflic anhydride

THF: tetrahydrofurane

TLC: thin layer chromatography

UV-vis: Ultraviolet-visible

Explanatory Notes:

Literature references have been treated independently in each chapter.

Compounds are numbered consecutively throughout the thesis.

In Chapter 2 and Chapter 3, in some cases, letters are used for labelling. For certain sugar based compounds this is supposed to make binding preferences more visual. For compound libraries, letters are used to distinguish them from single compounds.

Table of Contents

Chapter 1:
Introduction to Dynamic Combinatorial Chemistry and its Application in Carbohydrate Protein Recognition

Chapter 2:
Dynamic Covalent Combinatorial Libraries

Chapter 3:
Metal Based Dynamic Systems

Chapter 1

Introduction to Dynamic Combinatorial Chemistry and its Application in Carbohydrate Protein Recognition

1.1 Dynamic Combinatorial Chemistry

1.1.1 Background

The assumption that features of living things and probably even the universe have developed through natural selection,[1] rather than through intelligent-design[2] is commonplace not only among scientists. Nevertheless, the way substances for biological applications are made by chemists follows a different approach. Typically, structures are designed according to the state-of-the-art knowledge about structure, properties and interactions, and then created by synthesis. Thus the features a compound needs to inherit to be useful for a certain application are assumed, not tested (or evolved). Extended synthetic effort is common to afford kinetically stable products in reproducible yields. All this synthetic effort may have been useless if the compound does not exhibit the expected properties.

Combinatorial Chemistry (CC) is an alternative approach aimed at rendering this work more efficient. Prefabricated building blocks are reacted simultaneously inside a single reaction vessel to connect in varieties of combinations. In this way large libraries of related compounds (combinatorial libraries) can be generated. The most useful constituents of these mixtures are found by subsequent screening with an appropriate method of analysis.

Dynamic combinatorial chemistry (DCC) is CC under thermodynamic control. In contrast to combinatorial libraries, dynamic combinatorial libraries (DCL's) are formed by connecting the building blocks over reversible bonds. As all self-organising processes

---

1 Darwin, C., *On The Origin of Species*; John Murray, Ed. **1859**.
2 www.discovery.org/.

(including natural selection and binding interactions occurring in molecular recognition events) the formation of such DCL's is thermodynamically driven.[3] The thermodynamic equilibrium in between the DCL members defines their concentrations in solution (see the distribution of species on the different energy levels in Scheme 1). A template or guest molecule that is added into the equilibrating mixture can establish supramolecular interactions with the library members. It will selectively bind those entities that inherit matching features. DCC is based on the idea that the best match between target and ligand exhibits the lowest free energy. As a consequence of Le Chatelier's principle, the equilibrium between the library members will be driven towards the least constrained arrangement.

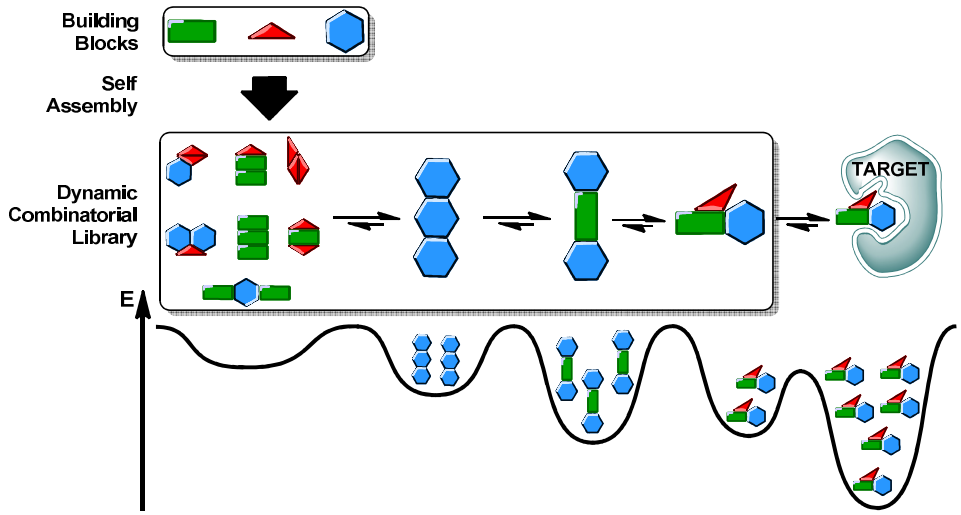

Scheme 1 *A DCL build up from three building blocks interacting with a target.*

Consequently, excess amounts of the most successfully binding molecules are created, like in biological evolution.[4] The concentration of the most stable complex rises, and this is often called "overexpression" or "amplification".[5]

For the set-up of DCLs several prerequisites have to be considered: The formed library

[3] Hoelzer, G. A.; Smith, E.; Pepper, J. W. *J. Evolution. Biol.* **2006**, *19*, 1785.
[4] Cougnon, F. B. L.; Sanders, J. K. M. *Acc. Chem. Res.* **2011**, *45*, 2211.
[5] Beeren, S. R.; Sanders, J. K. M. in *Dynamic Combinatorial Chemistry*; Reek, J. N. H., Otto, S., Eds.; Wiley-VCH, **2010**, p 1.

members have to present attractive supramolecular interactions with the target. These include ionic, charge-charge, or hydrophobic interactions, as well as hydrogen bonds and van der Waals forces. On the other hand the scrambling process between the different DCL species has to be assured. To establish reversible bonds between the building blocks all types of labile interactions can be used, although in most cases reversible covalent bonds or metal ligand exchange is employed. The most relevant reversible covalent interactions are imine formation,[6] esterification of boronic acids with alcohols,[7] hydrazone formation,[8] oxidation of thiols to disulphides,[9] Michael/retro-Michael addition (thiol enone exchange),[10] or hemithioacetal formation[11] (Scheme 2). Metal ligand coordination can often be a reversible process too, that is why a variety of metals has been used for dynamic combinatorial purposes, the most common ones being Co^{II},[12] Fe^{II},[13] Zn^{II},[14] and even Pb^{II}.[15] The final application of the DCL (molecular recognition, structural explorations, etc., see below) and the technique used for its analysis determine the choice of reversible bond. Therefore the reversible reaction should proceed chemoselectively and exclusively perform the exchange process, secondary interactions to a molecular target or other components of the experiment should not occur. Additionally, the reversible bonds have to be sufficiently stable to resist the method of analysis that is used to elucidate the composition of the DCL.

---

6 a) Zameo, S.; Vauzeilles, B.; Beau, J.-M. *Eur. J. Org. Chem.* **2006**, 5441. b) Herrmann, A. *Org. Biomol. Chem.* **2009**, *7*, 3195.

7 a) Demetriades, M.; Leung, I. K. H.; Chowdhury, R.; Chan, M. C.; McDonough, M. A.; Yeoh, K. K.; Tian, Y.-M.; Claridge, T. D. W.; Ratcliffe, P. J.; Woon, E. C. Y.; Schofield, C. J. *Angew. Chem., Int. Ed.* **2012**, *51*, 6672. b) Leung, I. K. H.; Brown Jr, T.; Schofield, C. J.; Claridge, T. D. W. *Med. Chem. Commun.* **2011**, *2*, 390.

8 Hochgürtel, M.; Biesinger, R.; Kroth, H.; Piecha, D.; Hofmann, M. W.; Krause, S.; Schaaf, O.; Nicolau, C.; Eliseev, A. V. *J. Med. Chem.* **2003**, *46*, 356.

9 a) Liénard, B. M. R.; Selevsek, N.; Oldham, N. J.; Schofield, C. J. *ChemMedChem* **2007**, *2*, 175. b) Liénard, B. M. R.; Hüting, R.; Lassaux, P.; Galleni, M.; Frère, J.-M.; Schofield, C. J. *J. Med. Chem.* **2008**, *51*, 684.

10 Shi, B.; Stevenson, R.; Campopiano, D. J.; Greaney, M. F. *J. Am. Chem. Soc.* **2006**, *128*, 8459.

11 Caraballo, R.; Dong, H.; Ribeiro, J. P.; Jiménez-Barbero, J.; Ramström, O. *Angew. Chem. Int. Ed.* **2010**, *49*, 589.

12 Goral, V.; Nelen, M. I.; Eliseev, A. V.; Lehn, J.-M. *Proc. Natl. Acad. Sci. U.S.A.* **2001**, *98*, 1347.

13 Sakai, S.; Shigemasa, Y.; Sasaki, T. *Tetrahedron Lett.* **1997**, *38*, 8145.

14 Klekota, B.; Hammond, M. H.; Miller, B. L. *Tetrahedron Lett.* **1997**, *38*, 8639.

15 Ulrich, S.; Lehn, J.-M. *Chem. Eur. J.* **2009**, *15*, 5640.

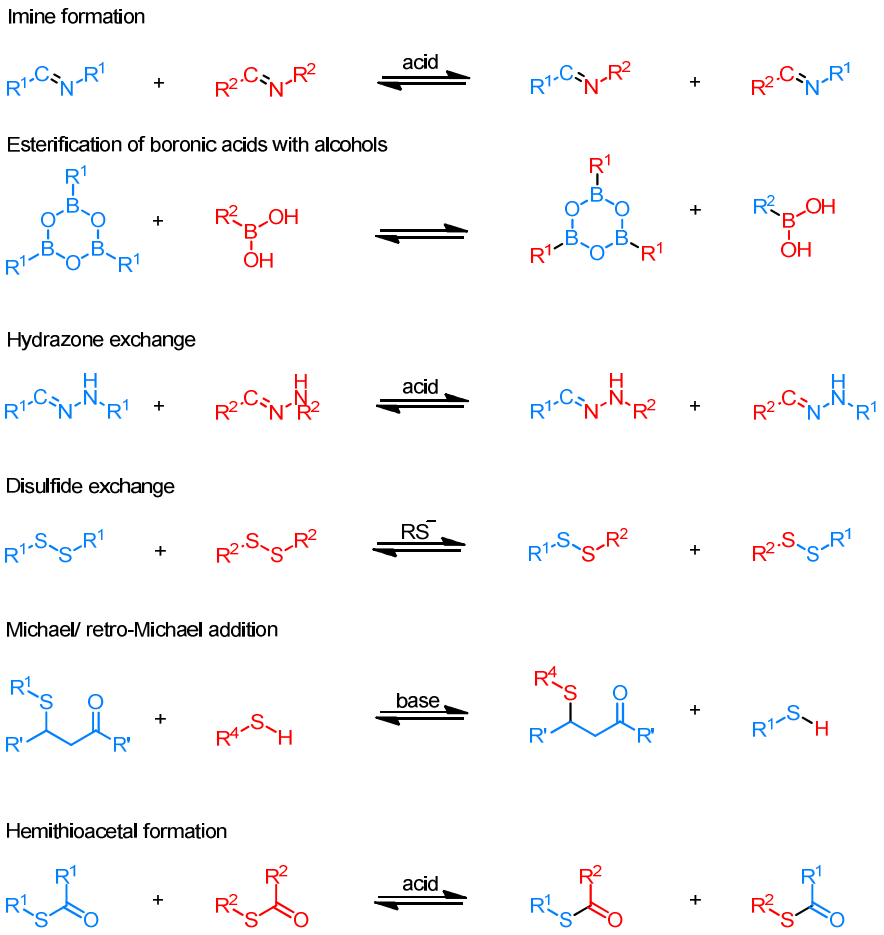

Scheme 2 *Examples for covalent but reversible reactions.*

Formation and application of dynamic libraries has been explored for more than 15 years now. In the following the available choice of applications, conditions and methods of analysis will be illustrated by discussing some of the main advances in the field of DCC.

1.1.2 Applications and Approaches

1.1.2.1 Template Effects and Early Dynamic Combinatorial Libraries

In order to yield a desired product the thermodynamic properties of an esterification can be deliberately altered by removing water during the reaction.[5] Similar protocols are common in many synthetic procedures. In a more specific method to increase thermodynamic control a suitable template is added to non-covalently bind the reaction partners in spatial proximity or a favourable orientation.[16] This concept was first identified as the crucial step in the formation of a product by Busch *et al.* in 1962.[17] Two reaction partners where brought into close proximity by coordination around a nickel centre. As a result the yield of the macrocyclic product rose (Scheme 3). Similar procedures have widely been applied thereafter to obtain macrocyclic compounds.[18]

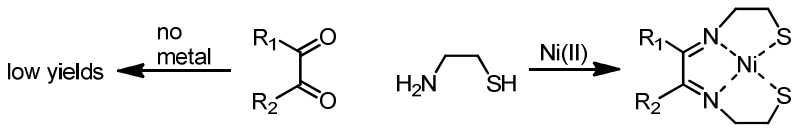

Scheme 3 *Formation of a macrocycle with Ni^{II} and without a metal template.*[18]

DCC for molecular recognition follows the same concept; due to the thermodynamic influence of the molecular target the best binding partner is produced in excess. Early examples for target directed DCC date back to 1995 when Hamilton *et al*. used dynamic interchange of chelating ligands around a central metal ion to bind simple di-carboxylate and di-ammonium terminated alkyl chains.[19]

Soon thereafter Lehn and Sanders developed this idea into a new concept. Lehn's

---

16 Make, D.; Sherman, J. C., *Templated Organic Synthesis*; Wiley-VCH, **2000**.
17 Thompson, M. C.; Busch, D. H. *J. Am. Chem. Soc.* **1962**, *84*, 1762.
18 Gerbeleu, N. V.; Arion, V. B.; Burgess, J., *Template Synthesis of Macrocyclic Compounds*; Wiley-VCH, **1999**.
19 Goodman, M. S.; Jubian, V.; Linton, B.; Hamilton, A. D. *J. Am. Chem. Soc.* **1995**, *117*, 11610.

findings in the field were related to his previous work on metal helicates. Those studies revealed that the size of circular helicates formed by tris-bipyridines around a Fe^{II} centre depends on the counter-anion present during self-assembly.[20] At the same time the group of Sanders developed first DCLs based on dynamic interchange over labile covalent bonds.

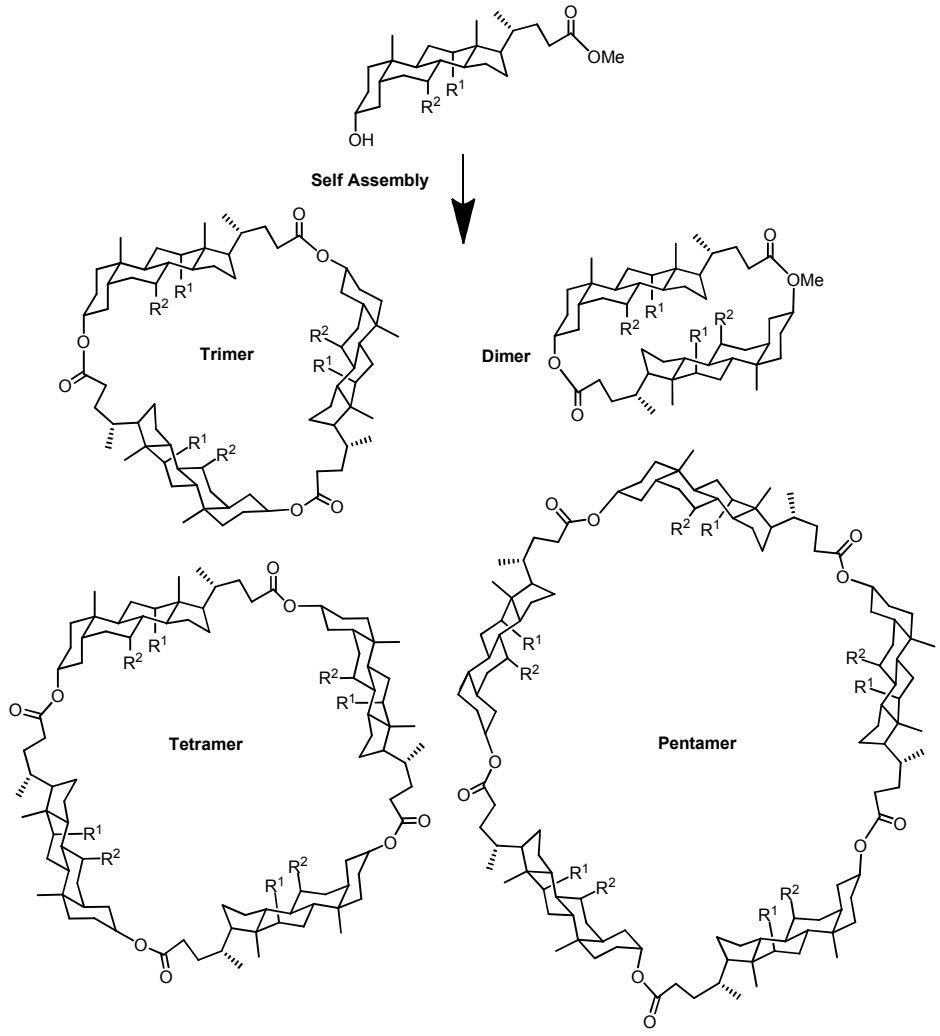

Scheme 4 *A DCL of four types of macrocycles formed by transesterification.*[21]

[20] Hasenknopf, B.; Lehn, J.-M.; Boumediene, N.; Dupont-Gervais, A.; Van Dorsselaer, A.; Kneisel, B.; Fenske, D. *J. Am. Chem. Soc.* **1997**, *119*, 10956.

For instance, they used methoxide-catalysed transesterification under reversible equilibrium conditions to set-up a dynamic library consisting of ester-linked macrocyclic oligomers (dimer-pentamer) (Scheme 4).[21]

Over the late 90s dynamic combinatorial chemistry rapidly developed into an own field and the application of DCLs under the influence of external stimuli was the main object of research.

1.1.2.2 DCLs for Small Molecule Recognition

The entities formed in DCLs can act as ligands for large molecules (such as proteins) or as receptors for small molecules. In context of the latter, finding receptor molecules for anions has been one focus. DCC is helpful to overcome the inherent obstacles in the design of anion receptors, in particular their unfavourably larger radius as compared to cations of similar atomic weight, the strong solvation or the smaller electrostatic interactions. The ability to adapt to the needs of the recognised molecule made dynamic combinatorial approaches successful in addressing those challenges.[22]

Interestingly, the strongest known binding constant to an anion in water was set-up using a dynamic system of macrocycles formed by cyclopeptides. This was achieved due to a delicate balance between rigidity and flexibility in the structure of the receptor, a fine tuning more easily accessible using a dynamic combinatorial strategy.[23]

Cation recognition is a common topic of supramolecular chemistry and, has naturally also been addressed using DCLs.[24] For example, Sanders *et al.* used a hydrazone based DCL to show how certain macrocyclic library members can selectively bind cationic

---

[21] Brady, P. A.; Bonar-Law, R. P.; Rowan, S. J.; Suckling, C. J.; Sanders, J. K. M. *Chem. Commun.* **1996**, 319.

[22] a) Bru, M.; Alfonso, I.; Burguete, M. I.; Luis, S. V. *Angew. Chem. Int. Ed.* **2006**, *45*, 6155. b) Beeren, S. R.; Sanders, J. K. M. *Chem. Sci.* **2011**, *2*, 1560. c) Bru, M.; Alfonso, I.; Bolte, M.; Burguete, M. I.; Luis, S. V. *Chem. Commun.* **2011**, 283.

[23] Rodriguez-Docampo, Z.; Eugenieva-Ilieva, E.; Reyheller, C.; Belenguer, A. M.; Kubik, S.; Otto, S. *Chem. Commun.* **2011**, 9798.

[24] a) Saggiomo, V.; Luning, U. *Chem. Commun.* **2009**, 3711. b) Xu, X.-N.; Wang, L.; Wang, G.-T.; Lin, J.-B.; Li, G.-Y.; Jiang, X.-K.; Li, Z.-T. *Chem. Eur. J.* **2009**, *15*, 5763.

alkaline earth metal ions over alkali metal ions.[25]

Unlike anions and cations, many biologically relevant small molecules are neutral. Therefore, a different selection of non-electrostatic interactions is necessary to bind those guests. This was demonstrated by Otto *et al.* who described a synthetic receptor for nicotine, which was selected from a dynamic combinatorial library of aromatic macrocycles. Binding experiments at different pHs showed that affinity of the library members to nicotine is independent from its protonation state and therefore unrelated to charge interactions. A combination of hydrophobic and π-π interactions was found to be responsible for binding (Scheme 5).[26]

Molecules like spermine,[27] cytidine[28] or CO_2[29] constitute further examples of neutral molecular targets studied by DCC.

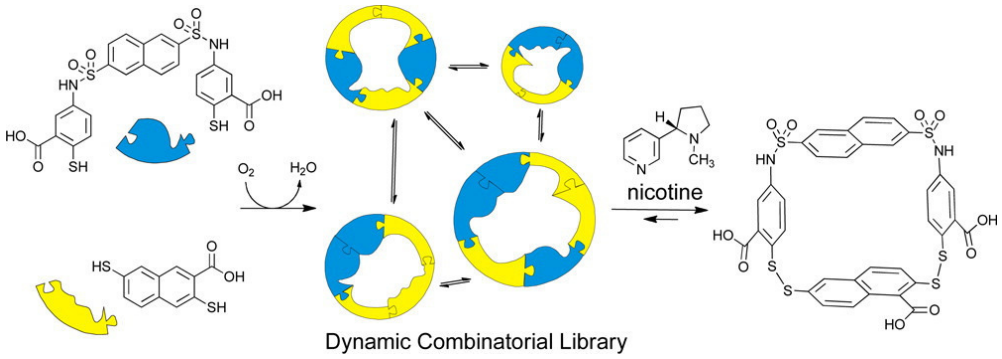

Scheme 5 *The DCL designed to recognise nicotine set-up from two building blocks and the structure of one of the best binding constituents.*[26]

[25] Klein, J. M.; Saggiomo, V.; Reck, L.; Luning, U.; Sanders, J. K. M. *Org. Biomol. Chem.* **2012**, *10*, 60.

[26] Hamieh, S.; Ludlow, R. F.; Perraud, O.; West, K. R.; Mattia, E.; Otto, S. *Org. Lett.* **2012**, *14*, 5404.

[27] Vial, L.; Ludlow, R. F.; Leclaire, J.; Pérez-Fernández, R.; Otto, S. *J. Am. Chem. Soc.* **2006**, *128*, 10253.

[28] Chung, M.-K.; Severin, K.; Lee, S. J.; Waters, M. L.; Gagne, M. R. *Chem. Sci.* **2011**, *2*, 744.

[29] Leclaire, J.; Husson, G.; Devaux, N.; Delorme, V.; Charles, L.; Ziarelli, F.; Desbois, P.; Chaumonnot, A.; Jacquin, M.; Fotiadu, F.; Buono, G. *J. Am. Chem. Soc.* **2010**, *132*, 3582.

1.1.2.3 Catalysis in Dynamic Combinatorial Chemistry

A three-dimensional receptor that fully wraps around the target is commonly referred to as a capsule. Structures like cages, capsules and other macromolecular entities can modify physical and chemical properties of an enclosed molecule. In some cases, this may lead to stabilisation of otherwise unstable entities, such as air-unstable white phosphorus in a self-assembled tetrahedral capsule.[30]

In supramolecular chemistry such structures have been investigated and synthesised in many different ways for many different purposes.[31] A lot of these examples rely on reversible bonding and self-assembly to make the structures accessible. The dynamic combinatorial approach is based on the same combination of interactions. Consequently, Otto and Sanders used their expertise in disulphide based exchange reactions to form an assortment of cage-like arrangements using a dynamic combinatorial protocol.[32] In another account by Reinhoudt *et al*. diethyl barbiturate and calix[4]arene dimelamine were mixed to set-up a DCL of molecular boxes assembled by hydrogen-bonding. Amplification effects were subsequently detected for an alizarin trimer and alizarin-like guests.[33]

Compounds can be trapped by dynamically acting capsules and in analogy to supramolecular catalysis this is opening the way to dynamic combinatorial catalysis. The confined space inside a capsule increases spatial proximity and thereby raises activities of reaction partners. Additionally the restricted possibilities for orientations only permit specific arrangements and reactions. Thus, Fujita *et al*. exploited those advantages and employed a water soluble organopalladium cage as an encapsulating catalyst. Inside the cage a Diels-Alder reaction between anthracene and phthalimide takes place at a terminal rather than central anthracene ring, a rather unusual regioselectivity for such

---

30 Mal, P.; Breiner, B.; Rissanen, K.; Nitschke, J. R. *Science* **2009**, *324*, 1697.

31 a) Horiuchi, S.; Murase, T.; Fujita, M. *J. Am. Chem. Soc.* **2011**, *133*, 12445. b) Pluth, M. D.; Bergman, R. G.; Raymond, K. N. *Science* **2007**, *316*, 85. c) Adriaenssens, L.; Escribano-Cuesta, A.; Homs, A.; Echavarren, A. M.; Ballester, P. *Eur. J. Org. Chem.* **2013**, *2013*, 1494.

32 a) West, K. R.; Bake, K. D.; Otto, S. *Org. Lett.* **2005**, *7*, 2615. b) Stefankiewicz, A. R.; Sambrook, M. R.; Sanders, J. K. M. *Chem. Sci.* **2012**, *3*, 2326.

33 Kerckhoffs, J. M. C. A.; Mateos-Timoneda, M. A.; Reinhoudt, D. N.; Crego-Calama, M. *Chem. Eur. J.* **2007**, *13*, 2377.

cycloaddition.[34]

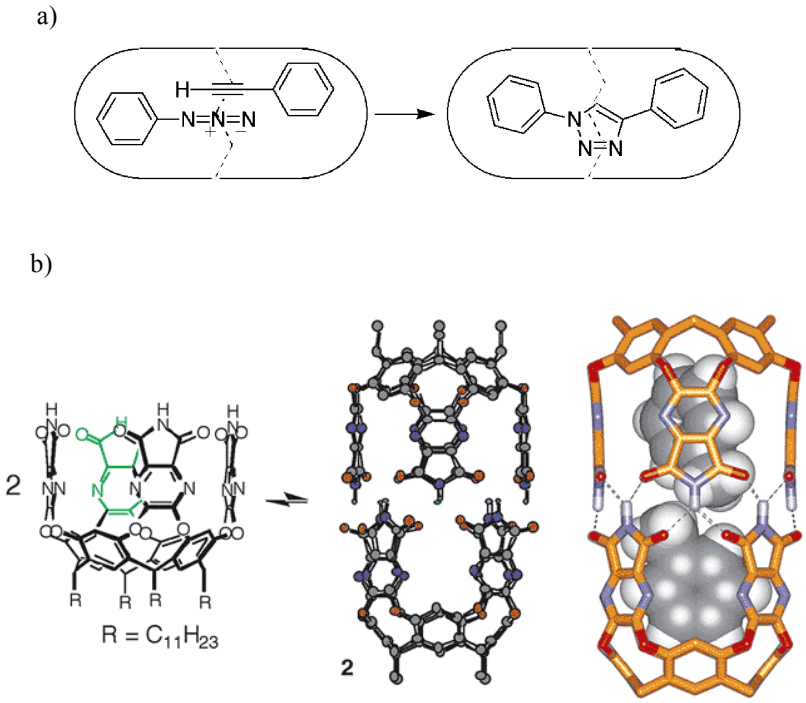

Scheme 6 *a) Schematic representation of a regioselective 1,3-dipolar cycloaddition inside a capsule. b) Formula and molecular modelled structures of the resorcinarene subunit and the dimeric capsule. Two toluene molecules are encapsulated in the energy-minimised complex (right).*[35]

The effect of an encapsulating catalyst also became evident in a study on the classical 1,3-dipolar cycloaddition of azide and acetylene. Under uncatalysed conditions the reaction proceeds slowly and gives equal amounts of 1,4- and 1,5-disubstituted triazoles. Rebek *et al.* demonstrated that inside a cylindrical hydrogen-bonded capsule, the reaction proceeds with full regioselectively for the 1,4-disubstituted isomer (Scheme 6).[35]

Although those findings paved the way for catalytic DCLs, real catalytic applications of

[34] Yoshizawa, M.; Tamura, M.; Fujita, M. *Science* **2006**, *312*, 251.
[35] Chen, J.; Rebek, J. *Org. Lett.* **2002**, *4*, 327.

DCC are still scarce. Gasparini *et al.* described a dynamic combinatorial system[36] using a template method that was later also used in a study by Nicholas *et al*. A pro-transition state analogue (similar in structure to the transition state of the catalysed reaction) was added to template the dynamic library of imine-zinc^{II} complexes.[37] This template served as mould to amplify the most active complex for promoting an ester hydrolysis. Despite this pioneering work it must be concluded that DCC approaches for catalysis, even in transition metal catalysis, is still at an initial stage.[38]

1.1.2.4 DCLs for Biomolecule Recognition

The most efficient procedure to find binding partners for biological molecular targets is a combinatorial method from molecular biology called SELEX (Systematic Evolution of Ligands by Exponential Enrichment).[39] It is based on a self-evolving system of complementary strands of oligonucleotides, the so-called aptamers (from the Latin *aptus* = fit, and Greek *meros* = part). Particularly structures build from nucleotides, the building blocks of DNA and RNA, can be bound in a very selective manner. Nevertheless successful recognition of proteins, cells, tissues and even organisms has also been reported.[40]

DCC relies on self-evolving systems too; instead of oligonucleotides it uses pre-synthesized building blocks. Synthetic approaches to the recognition of biological systems are challenging as the targets are often pH-sensitive and require the use of buffered aqueous systems.

These requirements limit the choice of reversible exchange reactions to those that can proceed in water. The typical DCLs for biomolecule recognition are based on imines (including hydrazones and oximes), disulphide exchange and metal coordination. Despite these limitations, almost all classes of biomolecules have been addressed. Enzymes,

---

36 Gasparini, G.; Prins, L. J.; Scrimin, P. *Angew. Chem. Int. Ed.* **2008**, *47*, 2475.
37 Matsumoto, M.; Estes, D.; Nicholas, K. M. *Eur. J. Inorg. Chem.* **2010**, 1847.
38 Dydio, P.; Breuil, P.-A. R.; Reek, J. N. H. *Isr. J. Chem.* **2013**, *53*, 61.
39 Svobodová, M.; Pinto, A.; Nadal, P.; O' Sullivan, C. K. *Anal. Bioanal. Chem.* **2012**, *404*, 835.
40 Famulok, M. *J. Am. Chem. Soc.* **1994**, *116*, 1698.

receptor proteins, oligonucleotides, whole cells and sugar binding proteins were targeted with DCLs. Those were set-up from building blocks such as amino acids, nucleotides, carbohydrates and a variety of non-natural substances.[41]

1.1.2.4.1 Oligonucleotides and Cells

Like the SELEX process described above, also DCC was used to study nucleotide binding. Metal complexes have been the preferred basis for the library set-up. In one early account the DCL was built around Zn^{II} centres that coordinate salicylaldimine ligands. The dynamic system was then screened against oligo(A-T) nucleotides and the binding entities were detected analysing the mixtures by HPLC.[14] Also RNA was targeted by DCLs. For example, Miller *et al.* determined binding constants of prime binders towards RNA from a library of 27 square planar complexes formed by Cu^{II} salicylamides.[42]

Cells are multimolecular arrangements and very different targets compared to the strands of oligonucleotides described above; nevertheless recognition of cell surfaces has also been addressed with DCLs. Inspired by the structure of marine natural product psammaplin A, a ditopic 3000 members dynamic library of interchanging disulphide analogues was setup. Three promising lead compounds for further development as antibacterial agents against *S. aureus* were identified (Scheme 7).[43]

[41] Corbett, P. T.; Leclaire, J.; Vial, L.; West, K. R.; Wietor, J.-L.; Sanders, J. K. M.; Otto, S. *Chem. Rev.* **2006**, *106*, 3652.
[42] Karan, C.; Miller, B. L. *J. Am. Chem. Soc.* **2001**, *123*, 7455.
[43] Nicolaou, K. C.; Hughes, R.; Pfefferkorn, J. A.; Barluenga, S.; Roecker, A. J. *Chem. Eur. J.* **2001**, *7*, 4280.

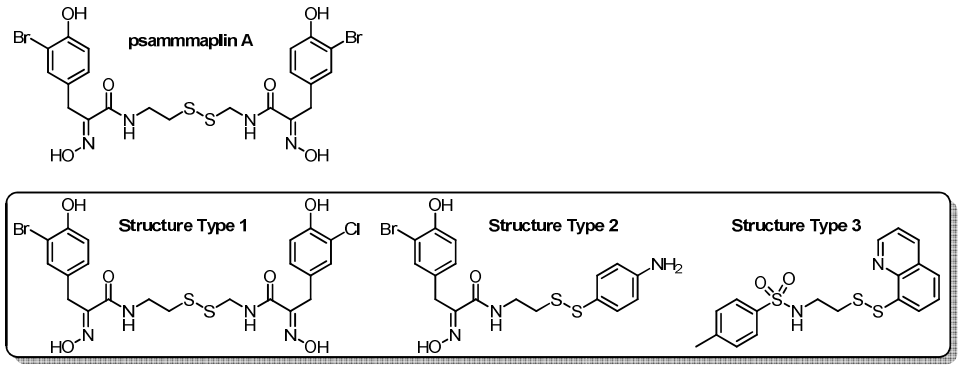

***Scheme** 7 Marine natural product psammaplin A and examples for the three best binding structural types identified from a DCL.*[41]

1.1.2.4.2 Enzymes

Enzymes are crucial in many biochemical pathways and therefore pharmacologically relevant targets for molecular recognition. Synthetic ligands or substrates can inhibit their natural catalytic task. Adequate methods of analysis can follow this inhibition processes. As the analysis of dynamic systems is often the most difficult part of a study this opens interesting opportunities in DCC chemistry.[44]

Carbonic anhydrase (CA) is an enzyme involved in the interconversion of CO_2 and bicarbonate. As it is inexpensive and easy to handle it was used in a number of dynamic combinatorial setups. Its advantages were used early in the history of DCC. A contribution from 1997 describes how the binding preferences of CA towards an imine-based dynamic library were tested. Three aldehydes and four amines were mixed to give a 12-membered DCL that was equilibrated in presence of CA. Subsequently the imine library members where reduced to amines to freeze the relative amount of the DCL members and thus facilitate the quantitative analysis of the library by HPLC. It was found that the entities which exhibit structures that fit better to the active centre of the enzyme were formed

[44] Ramström, O.; Amorim, L.; Caraballo, R.; Norberg, O. in *Dynamic Combinatorial Chemistry*; Reek, J. N. H., Otto, S., Eds.; Wiley-VCH Verlag GmbH & Co. KGaA, **2010**, p 109.

preferably.[45]

Bornaghi *et al.* used a different type of exchange reaction in a dynamic combinatorial study on the same enzyme. Cross-metathesis promoted by a Grubbs-type catalyst was employed to vary combinations of building blocks and to form a number of different alkenes containing DCLs. The DCLs were separately applied onto the enzyme and analysed by fluorescence to detect members with high binding affinities.[46]

A similar analytical method was applied for a binding study on acetylcholinesterase, an enzyme that catalyses the hydrolysis of the neurotransmitter acetylcholine into acetate and choline. The enzyme presents two binding sites selective for positively charged functionalities. A dynamic strategy was used to determine appropriate spacer lengths between positively charged end groups of potential binders. The reversible connection of 13 hydrazide and aldehyde building blocks afforded DCLs of interconverting acyl-hydrazone species. Each of these entities contained two positively charged end groups connected by spacers of different lengths. The optimal library members were identified by a protocol named *dynamic deconvolution* (by Lehn[47]). The technique is based on sequentially removing starting building blocks to afford DCLs of different sizes and compositions. This is followed by measuring the respective activity of each full library. From those values the binding properties of the single library members can be deducted.

This method is a feasible though tedious procedure. More elegantly, DCLs can be resolved by a kinetic process known as *dynamic combinatorial resolution* (DCR). An experiment by Ramström and co-workers using acetylcholinesterase and a DCL of thioesters illustrates the procedure. The enzyme first recognizes the fitting entity from the DCL. As it is able to catalyse hydrolysis, the binder is transformed to the corresponding thiol and *stable* acid. This step can be regarded as a kinetic "trap" that draws the equilibrium of the library irreversibly into the direction of the best binder. As a consequence the binding thioesters disappeared from the solution; this process could be

[45] Huc, I.; Lehn, J.-M. *Proc. Natl. Acad. Sci. U.S.A.* **1997**, *94*, 2106.
[46] Poulsen, S.-A.; Bornaghi, L. F. *Biorg. Med. Chem.* **2006**, *14*, 3275.
[47] Bunyapaiboonsri, T.; Ramström, O.; Lohmann, S.; Lehn, J.-M.; Peng, L.; Goeldner, M. *ChemBioChem* **2001**, *2*, 438.

followed by NMR (Scheme 8).[48]

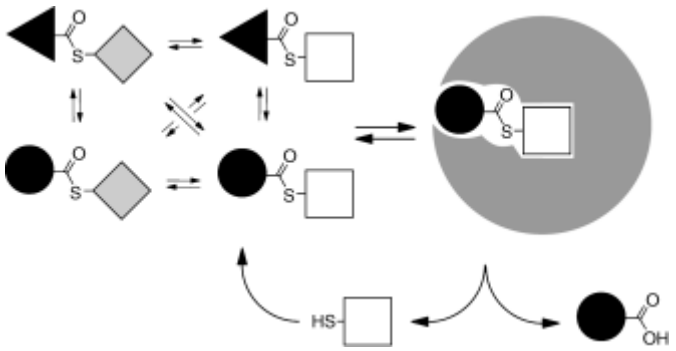

Scheme 8 *Dynamic combinatorial resolution (DCR) of a thiolester DCL (left side) by enzyme acetylcholinesterase (right side in grey).*[48]

The number of different enzymes tested using dynamic combinatorial approaches is large, and more complete lists can be found elsewhere, those include aurora kinase (and other kinases), glutathione *S*-transferase, neuramidase (key enzyme of influenzavirus), lipases and sugar transforming enzymes like galactotransferases.[49]

1.1.2.4.3 Sugar Binding Proteins (Lectins)

Enzymes are not the only proteins able to recognize specific molecular patterns. The ability of sugar binding lectins (see below) to selectively bind oligosaccharides has also attracted the attention of DCC. Actually one of the earliest examples of a prototype DCL was targeted on a lectin.[13] Sasaki *et al.* synthesised a homoleptic Fe^{II} complex from a galactosamine substituted 2,2'-bipyridine (bipy) ligand. The compound exhibits four different stereochemical configurations that are able to merge into each other intramolecularly. The system is reversible and its equilibrium was shifted towards one specific stereoisomer in the presence of *Vicia villosa B4* lectin.

Later Lehn *et al.* developed a similar DCL based on the intermolecular exchange

[48] Larsson, R.; Pei, Z.; Ramström, O. *Angew. Chem. Int. Ed.* **2004**, *43*, 3716.

between two tertpyridyl ligands around a Co^{II} centre. However, the strategy was not employed for protein recognition.[12] Another report from the same group uses concanavalin A (ConA) lectin as target. The fact that it is commercially available, economically priced and sold in a variety of solid supported conjugates make it a convenient object of study. The DCL that was used to test binding was prepared from an assembly of aldehydes bearing different sugars and simple scaffolds presenting hydrazides. The acyl hydrazone library members were then tested using an enzyme-linked lectin assay to detect the ligands with highest affinity for concanavalin A (ConA).[50]

ConA binding has also been addressed with the popular disulphide exchange motif. This reversible reaction offers a number of favourable properties for lectin directed DCLs- It proceeds in water, exhibits high chemoselectivity and can be locked and unlocked by pH changes. In an account from 2000 six symmetric *bis* glycol-disulphide dimers, connected through the anomeric position, were scrambled under slightly basic conditions to afford heterodimers. The 21-membered library was mixed with ConA and equilibrated. The exchange reaction was then conveniently stopped by simply lowering the pH. Detection of the amplified binders by HPLC was facilitated by the use of solid supported lectin, this revealed one of the pre-synthesised disulphides as the best binder (Scheme 9).[51]

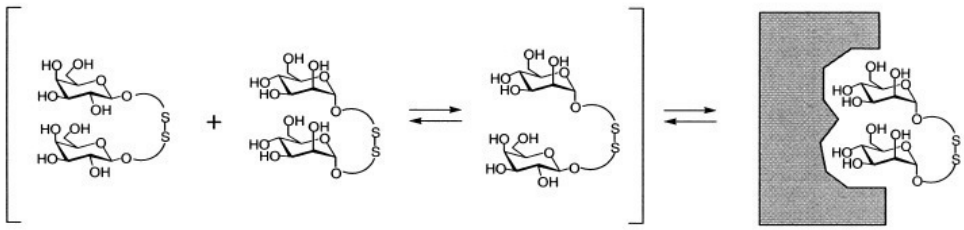

Scheme 9 *Representative scrambling of two library members and binding to ConA of the entity of highest affinity.*[51]

[50] Ramström, O.; Lohmann, S.; Bunyapaiboonsri, T.; Lehn, J.-M. *Chem. Eur. J.* **2004**, *10*, 1711.

[51] Ramström, O.; Lehn, J.-M. *ChemBioChem* **2000**, *1*, 41.

Amino acid based structures can be an easy way to obtain water soluble scaffold molecules. Aoyama *et al.* combined the disulphide approach with the use of peptides. The peptide scaffold and thio-sugar moieties could be mixed in aqueous solution to form various sugar–peptide conjugates that could be resolved by HPLC. In a separate experiment, surface plasmon resonance (SPR) measurements showed that the library contained species capable of cross-linking peanut lectin molecules.[52]

Peptide arrangements built from cysteine offer a further advantage, as they already contain thiol groups that can act as reversible connecting points. A DCL of this type was described by Davis and co-workers. The dipeptides were able to connect with monomeric thio-carbohydrates that serve as recognition moieties for the lectin. The DCL could conveniently be analysed by MS showing amplification of one of the library members.[53]

1.1.3 Conclusions

Within the last 15 years DCC has grown into an independent field of research and varieties of problems have been addressed. Basic structural studies, ion and small molecule interactions and dynamic encapsulations have been investigated. Further uses like DCC in catalysis still remain at a proof-of-concept stage. It can be summarized that DCC is an inherently flexible method that allows accessing complex structures and helps to improve knowledge on molecular interactions. Being inspired by nature, DCC is a useful tool for better understanding the origins of complex matter. Consequently, it can be and has been put into the quest for the "Origins of Chemical Evolution".[54]

---

52 Sando, S.; Narita, A.; Aoyama, Y. *Bioorg. Med. Chem. Lett.* **2004**, *14*, 2835.
53 Hotchkiss, T.; Kramer, H. B.; Doores, K. J.; Gamblin, D. P.; Oldham, N. J.; Davis, B. G. *Chem. Commun.* **2005**, 4264.
54 Lynn, D.; Burrows, C.; Goodwin, J.; Mehta, A. *Acc. Chem. Res.* **2012**, *45*, 2023.

1.2 Carbohydrate-Protein Recognition

1.2.1 Background

Carbohydrates (CHs) are the most abundant biomolecules in nature and they constitute the most frequent variation naturally introduced to proteins.[55] Traditionally, the role of storage and transfer of biological information was ascribed to nucleic acids and proteins, carbohydrates being merely considered as structural blocks and energy sources. However, oligosaccharides provide a huge structural diversity as the sugar units can be connected through a variety of positions. For instance, the possible linkages of two different monomeric pyranose units provide a total of 20 different potential structures.[56] Also ring sizes and anomeric configurations can differ which still increases the number of possible arrangements (Scheme 10).[57]

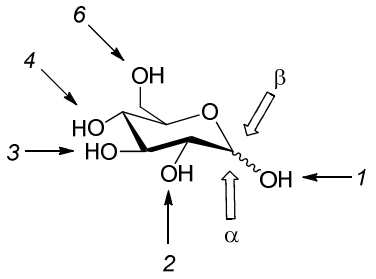

Scheme 10 *Positions and configurations for connections available for a single glucose monomer.*[57]

Two D-glucose molecules of identical anomeric configurations, differing only in the connection of a single position on one of the sugar rings give rise to substantially distinct compounds: Sophorose (known form the sweetener stevioside), laminaribiose (an algal polysaccharide), cellobiose (the basic structural unit of cellulose), and gentiobiose (a bitter tasting component of the *Gentiana lutea* root) (Scheme 11).[57] Increasing the number of sugar units in the arrangement exponentially raises the number of potential structures.

[55] Bernardi, A.; Cheshev, P. *Chem. Eur. J.* **2008**, *14*, 7434.
[56] Jayaraman, N. *Chem. Soc. Rev.* **2009**, *38*, 3463.
[57] Gabius, H.-J.; Siebert, H.-C.; André, S.; Jiménez-Barbero, J.; Rüdiger, H. *ChemBioChem* **2004**, *5*, 740.

Today, it is well established that this amount of information, storable in the potential permutations offered by glycosidic combinations, has not been neglected by nature. Important biological processes such as protein folding, host defence pathways and cell-cell adhesion are controlled by CHs.

Already in 1894, while investigating the effect of CH digesting enzymes, Emil Fischer understood that glycosides and their corresponding enzymes are asymmetric compounds. He concluded that to catalyse a reaction an enzyme needs to have a matching geometrical structure to the sugar.[58]

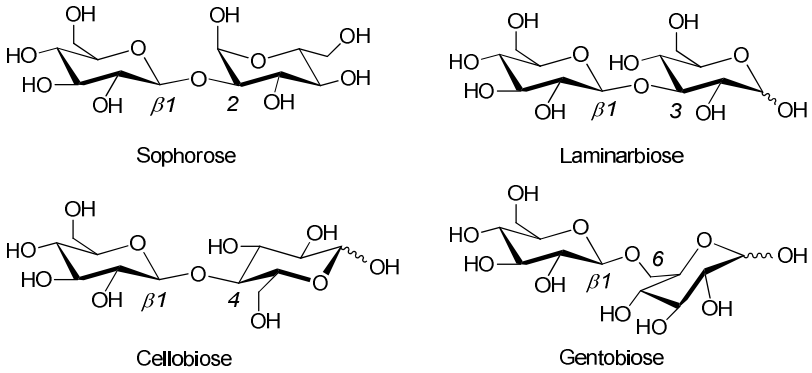

Scheme 11 *Structures of several regioisomers of β-diglucosides.*[57]

The "lock and key" analogy for enzymatic transformations was proposed by Fischer who realised that cellobiose, as the building block of cellulose, exhibits essentially different properties than its anomeric variant maltose, which is the building block of starch and glycogen (Scheme 12).

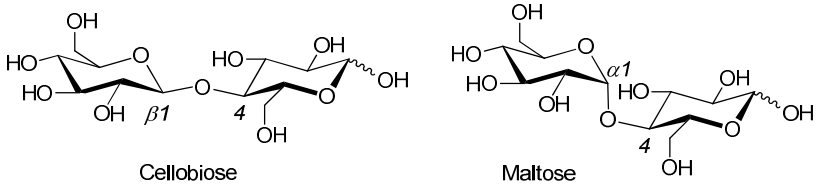

Scheme 12 *Cellobiose and maltose only differ in the configuration of the anomeric carbon.*

[58] Fischer, E. *Chem. Ber.* **1894**, *27*, 2985.

Apart from early discoveries about the selective transformations conducted by enzymes, it become slowly apparent how biological systems process sugar encoded information. The key to understand how the so-called "sugar code" can be read-out was the discovery of lectins.[57]

1.2.2 Lectins: Specific Carbohydrate-Binding Proteins

The first experiment observing the action of a lectin (later identified as a C-type lectin) was described in 1860: pigeon's blood agglutinated (clumped) upon addition of rattlesnake poison. The active protein of the venom was interacting with specific saccharides present on the outside of red blood cells (see below).[59] Almost 80 years later, starch, glycogen and mucin were precipitated using the lectin concanavalin A (ConA). This gave rise to the idea that CHs may act as ligands for lectins. The ability of sucrose to inhibit the hem-agglutination caused by ConA confirmed this assumption.[60] Blood groups can be discriminated by the presence of oligosaccharide antigens on their surface.[61] It was found that specific blood groups agglutinate in the presence of ConA. This behaviour was a first strong evidence of lectin selectivity for specific carbohydrate-based structures. Still today the main property exploited for detection of lectins in e.g. plant materials (mainly seeds) is their capacity to agglutinate cells (mostly mammalian red blood cells). Their most prominent feature is their specificity for certain sugar configurations and arrangements without being catalytically active. Lectins take part in biological recognition processes and are particularly involved in viral infection pathways.[62] However, the importance of lectins as biological recognition molecules was only recognized during the 1970s. About 500 lectins, mainly from plant origin, where discovered since then. The notion of lectins as non-catalysing (in contrast to enzymes) sugar binding proteins got accepted and gave rise to various applications, such as:[62]

Cell identification and separation (cancer detection).

Detection, isolation, and structural studies of glycoproteins.

---

59 Mitchel, S. W. *Smithsonian Contr. Knowl.* **1860**, 89.
60 Sumner J. B.; Howell, S. F. *J. Bacteriol.* **1936**, *32*, 137.
61 Lodish, H. B. A.; Zipursky S. L., *Molecular Cell Biology*; Freeman: New York, **2000**.
62 Sharon, N.; Lis, H. *Glycobiology* **2004**, *14*, 53R.

Investigation of carbohydrates on cells and subcellular organelles:
Histochemistry and cytochemistry.
Mapping of neuronal pathways.
Mitogenic stimulation of lymphocytes (in clinical use).
Purging of bone marrow for transplantation (in clinical use).
Selection of lectin-resistant mutants.
Studies of glycoprotein biosynthesis.

1.2.2.1 Structure of Lectins

The complete amino acid sequence of less than ten lectins was known since the late 1970s. Comparison of the X-ray crystallographic structural elucidation and the sequential data of ConA and wheat germ agglutinin (WGA) showed that "although lectins have many biological properties in common, they represent a diversified group of proteins with respect to size, composition and structure" (Scheme 13).[62] The general structural appearance can be classified into three types:

1. Simple, mostly found in plant seeds. They aggregate to render themselves active.
2. Mosaic or multidomain, mostly found in animal lectins, composed from different active domains.
3. Macromolecular, mostly found on bacteria. The lectin is expressed on their surface to enable attachment to cells.[56]

Their common feature is the ability for selective recognition of oligosaccharides. This capacity resides in a limited space on the lectin surface which has been called carbohydrate recognition domain (CRD). The CRD is structurally determinant and therefore has been used for the differentiation of lectin types.[62]

a)

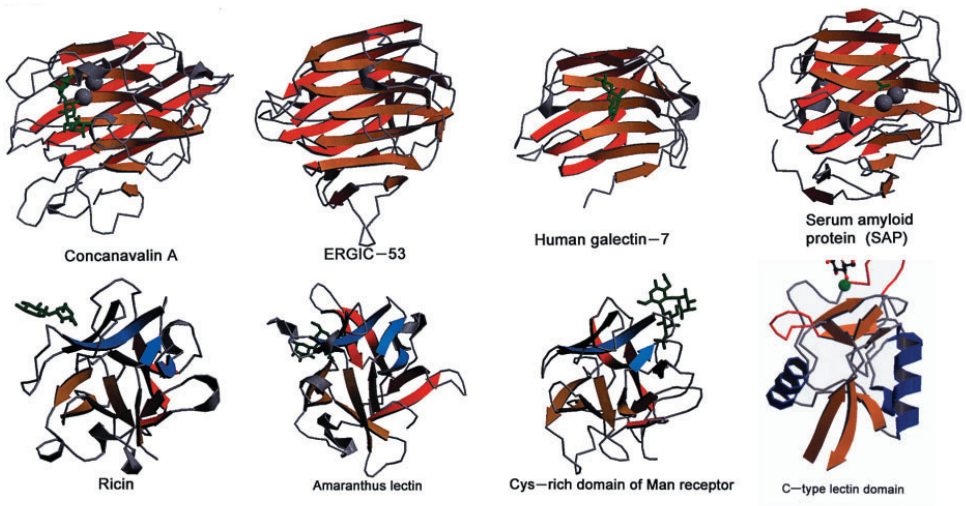

b)

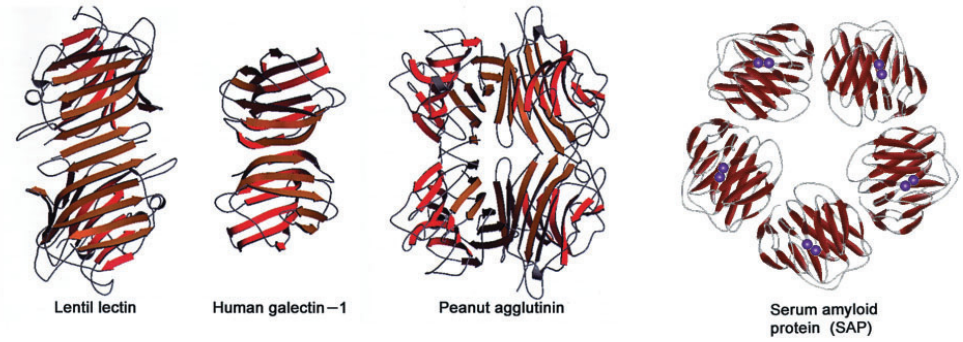

Scheme 13 *Structures of various lectins. a) Lectin monomers from different sources that share the "jelly roll" or lectin fold. First three examples (from left) in the lower row all exhibit the α-trefoil fold. b) Variations in quaternary lectin structures. The gray spheres represent metal ions; bound carbohydrate is shown in ball-and-stick representation.* **Error! Bookmark not defined.**

1.2.2.2 The Influence of Multivalency on Binding

1.2.2.2.1 Background

Lectins are carbohydrate binding proteins with strong selectivities for certain sugar moieties and larger oligosaccharide structures. The recognition event is based on supramolecular interactions between saccharide and lectin. Most of this binding relies on hydrogen bonding of the sugar hydroxyl groups with polar side chains of the protein structure. Association to metal-ions (such as calcium), ionic interactions and hydrophobic stacking add further to the overall binding enhancement.[63] Since these interactions are labile, they need to combine and act in a concerted fashion to achieve significant affinities. This compensates the entropic loss caused by motional freedom and solvation.[55] The carbohydrate recognition domain (CRD) recognizes specific sugar configurations. In most naturally occurring systems the monosaccharide is linked to a larger oligomeric structure which serves as a scaffold to align this anchoring moiety.[55] Simple mono- or disaccharides bind lectins only weakly with low mM or μM dissociation constants. Multivalent presentation of binding subunits is known to enhance affinity in biological interactions like between antibody and antigen.[62] Therefore efforts were centred to proof the concept of multivalency for lectin-carbohydrate interactions as well.[64]

1.2.2.2.2 Neoglycoproteins and Oligosaccharides

Early approaches to investigate multivalent carbohydrate-lectin interactions used the so-called neoglycoproteins. They can serve as multivalent platforms that can be functionalized with varying amounts of sugars. Delmontte *et al.* connected different

---

[63] Gabius, H.-J.; André, S.; Jiménez-Barbero, J.; Romero, A.; Solís, D. *Trends Biochem. Sci* **2011**, *36*, 298.

[64] a) Krishnamurthy, V. M.; Estroff, L. A.; Whitesides, G. M. *Methods Princ. Med. Chem.* **2006**, *34*, 11. b) Pavel, I. K.; Joanna, M. S.; George, M.; Glen, D. A.; Hong, L.; Navraj, S. P.; Randy, J. R.; David, R. B. *Nature* **2000**, *403*, 669. c) Fan, E.; Zhang, Z.; Minke, W. E.; Hou, Z.; Verlinde, C. L. M. J.; Hol, W. G. J. *J. Am. Chem. Soc.* **2000**, *122*, 2663. d) Arosio, D.; Fontanella, M.; Baldini, L.; Mauri, L.; Bernardi, A.; Casnati, A.; Sansone, F.; Ungaro, R. *J. Am. Chem. Soc.* **2005**, *127*, 3660.

numbers of sugar subunits to bovine serum albumin (protein). The capacity of this synthetic glycoprotein to inhibit lectin binding of a naturally occurring glycoprotein was measured. The analysis revealed that the inhibition potency increased along with the sugar content.[65]

The same effect was observed by Brewer *et al.* using purely sugar containing structures. Consecutive addition of sugar entities into a polysaccharide ligand raised the binding constant to ConA lectin. Again, the affinity depends on the number of binding determinants (Scheme 14).[66]

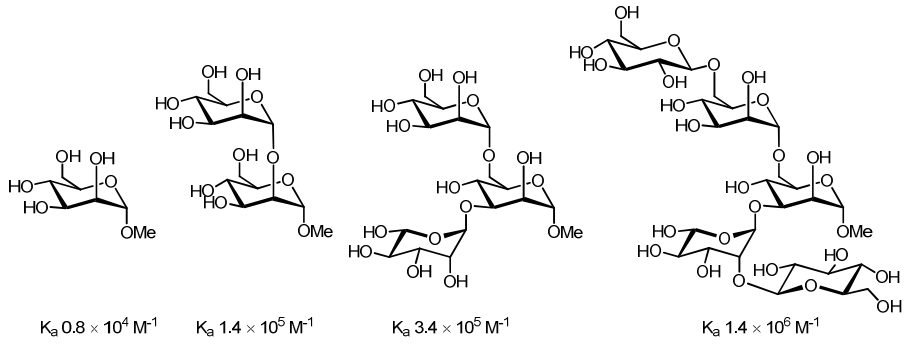

Scheme 14 *Mono-, di-, tri- and pentasaccharides based on a D-mannose structure and their association constants to ConA.*[66]

1.2.2.2.3 Peptide Scaffolds

Crystal structures of natural sugar oligomers bound to lectins showed that not all the saccharide is in contact with the protein surface.[67] Thus, it is not necessary that protein ligands consist completely of sugars. Easily accessible structures that serve solely as scaffolds, can be synthesized and later be decorated with binding sugar moieties. Apart from the already mentioned neo-glycoprotein approach, smaller amino acid based structures (peptides) were used to facilitate ligand design. Those so-called cluster

[65] Monsigny, M.; Roche, A.-C.; Sene, C.; Maget-Dana, R.; Delmotte, F. *Eur. J. Biochem.* **1980**, *104*, 147.
[66] Mandal, D. K.; Kishore, N.; Brewer, C. F. *Biochemistry* **1994**, *33*, 1149.
[67] Naismith, J. H.; Field, R. A. *J. Biol. Chem.* **1996**, *271*, 972.

glycosides help to access specifically desired structural properties like branched architectures. Lee *et al.* showed how peptide based structures presenting two or three β-lactoside moieties on their extremities were able to inhibit binding of a glycoprotein to mammalian liver lectin (Scheme 15).[68]

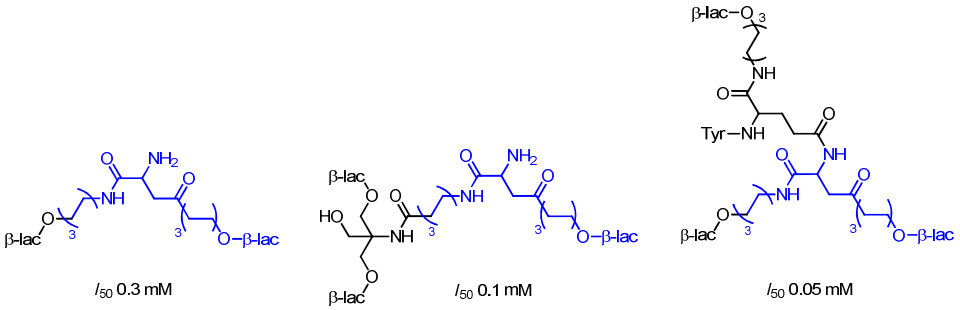

Scheme 15 *Three peptide based scaffolds and their IC_{50} values for inhibition of a naturally occurring lectin ligand.*[Error! Bookmark not defined.]

The technique allowed for the introduction and analysis of different spacers to connect the CH units to a central peptide backbone. Different inhibitory properties (I_{50} values) were observed for each of the varieties. These studies revealed that, apart from the number of sugar subunits, the length of the linker also has a crucial influence on the binding properties.

1.2.2.2.4 Polymers

The demand for extended structures as carriers for CHs raised as the importance of multivalency for efficient lectin binding became evident. Polymers functionalised with sugar moieties in a multivalent fashion are an obvious extension to the existing choice of backbones. Glycopolymers have the advantage that the number of mole fractions of sugars attached to a polymeric structure is controllable. The way different levels of multivalency improve binding was thereby analysable by variation of the sugar loading on the polymeric structure.[69] This was demonstrated by Nishimura *et al.*: glycopolymers of different

[68] Lee, R. T.; Lin, P.; Lee, Y. C. *Biochemistry* **1984**, *23*, 4255.
[69] Matrosovich, M. N.; Mochalova, L. V.; Marinina, V. P.; Byramova, N. E.; Bovin, N. V. *FEBS Lett.* **1990**, *272*, 209.

densities of *N*-acetyl-D-glucosamine residues were synthesised. Some of the multivalent structures showed up to four orders of magnitude higher affinity than the monomeric sugar (Scheme 16).[70]

a)

b)

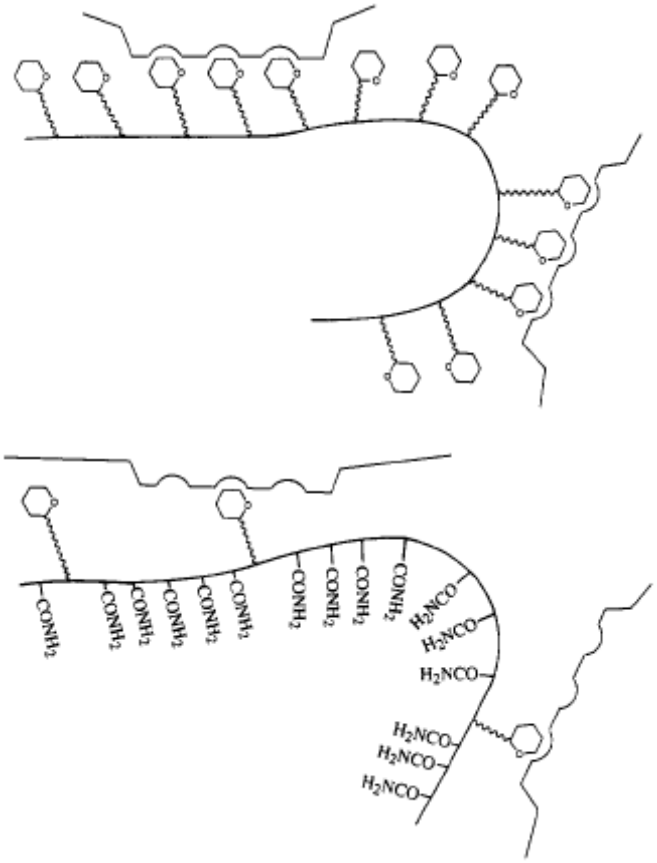

Scheme 16 *Polymeric GlcpNAc ligands as models of varying levels (a) high density and (b) low density multivalent binding to WGA subsites.*[70]

1.2.2.2.5 Micelles, Vesicles and Liposomes

Other multivalent arrangements to probe binding to lectin surfaces includes self-

[70] Nishimura, S.-I.; Furuike, T.; Matsuoka, K.; Maruyama, K.; Nagata, K.; Kurita, K.; Nishi, N.; Tokura, S. *Macromolecules* **1994**, *27*, 4876.

assembling systems like micelles, vesicles and liposomes. In 1980, Rando *et al.* managed to assemble small unilamellar liposomes from a group of glycolipids containing a cholesterol group. Those sugar-presenting vesicles were screened for their binding capacities against the *Ricinus communis* lectin. The experiment again showed the decisive influence of multivalency and spacer length on the affinity towards the protein surface.[71] In another account, a multivalent sialyl Lewis x tetrasaccharide ligand was designed to bind E-selectin. It proved to inhibit its natural binder more efficiently if incorporated into a liposome than when attached to a peptide.[72] A more detailed liposome-based study by Jayaraman *et al.* revealed that the improvement of binding by multivalency has limitations. Rising mole fractions of glycol moieties on the lipid bi-layer increase binding, but only up to a level where accessibility gets hampered by steric effects.[73]

1.2.2.2.6 Nanoparticles

More recently, the growing expertise in the preparation and analysis of nanoparticles offered opportunities to easily access high levels of multivalency. Gervay-Hague and co-workers employed a gold glyconanoparticle decorated with approximately 120 galactosides to bind to gp 120 HIV-associated glycoprotein. In a competitive binding analysis it was shown that binding is more than 300 times better than for the competing monomeric galactoside.[74] A mannoside gold nanoparticle described in a report from Wu's lab exhibits similar properties. Mannose-specific adhesin FimH, a sugar binding protein in *Escherichia coli,* exhibited high affinity for the multivalent arrangement. Free monomeric mannose had to be applied in at least 2000 times excess to compete with the glyconanoparticle. Most interestingly, the nanoparticles bind selectively to the surface of FimH expressed on the wild type bacterium. This level of selectivity opens up possibilities for labelling specific proteins on cell surfaces (Scheme 17).[75] In this context it is

---

71 Slama, J. S.; Rando, R. R. *Biochemistry* **1980**, *19*, 4595.
72 Stahn, R.; Schäfer, H.; Kernchen, F.; Schreiber , J. *Glycobiology* **1998**, *8*, 311.
73 Bandaru, N. M.; Sampath, S.; Jayaraman, N. *Langmuir* **2005**, *21*, 9591.
74 Nolting, B.; Yu, J.-J.; Liu, G.-y.; Cho, S.-J.; Kauzlarich, S.; Gervay-Hague, J. *Langmuir* **2003**, *19*, 6465.
75 Lin, C.-C.; Yeh, Y.-C.; Yang, C.-Y.; Chen, C.-L.; Chen, G.-F.; Chen, C.-C.; Wu, Y.-C. *J. Am. Chem. Soc.* **2002**, *124*, 3508.

noteworthy that some glycol-metal nanoparticles give UV responses upon binding to a lectin.

These inherent optical properties have been used to determine lectin concentrations.[76]

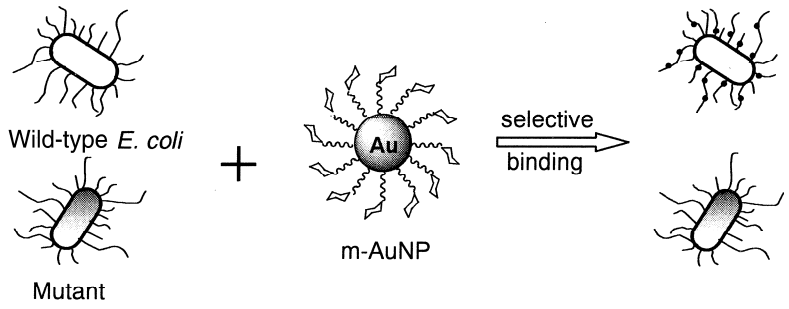

Scheme 17 *A high affinity mannoside Au nanoparticle selectively binds wild-type E. Coli.*[75]

1.2.2.2.7 Dendrimers and Hyperbranched Scaffolds

In contrast to techniques that use the concerted assembly of ready-made sugar building blocks into self-sorting arrangements (like liposomes or nanoparticles), dendrimers or hyperbranched scaffolds are generally obtained following classical synthetic procedures.[77] To prove the concept of multivalency for this kind of scaffolds, structures with different levels of branching were synthesised. Magnuson *et al.* have set-up simple mono-, di-, tri- and tetravalent arrangements containing CHs. Comparison of the different structures showed that higher valency can enhance the ability to inhibit hemagglutination by *Streptococcus suis* by several hundred times.[78] In a seminal work from Bundle *et al.*, a tailor-made pentavalent ligand for *Escherichia coli* shiga-like toxin was shown to exhibit an inhibitory activity 1-10 million-fold higher than univalent ligands, the best inhibitor ever found for Shiga-like toxins I and II (Scheme 18).[79]

---

[76] Hone, D. C.; Haines, A. H.; Russell, D. A. *Langmuir* **2003**, *19*, 7141.
[77] Astruc, D.; Boisselier, E.; Ornelas, C. *Chem. Rev.* **2010**, *110*, 1857.
[78] Hansen, H. C.; Haataja, S.; Finne, J.; Magnusson, G. *J. Am. Chem. Soc.* **1997**, *119*, 6974.
[79] Kitov, P. I.; Sadowska, J. M.; Mulvey, G.; Armstrong, G. D.; Ling, H.; Pannu, N. S.;

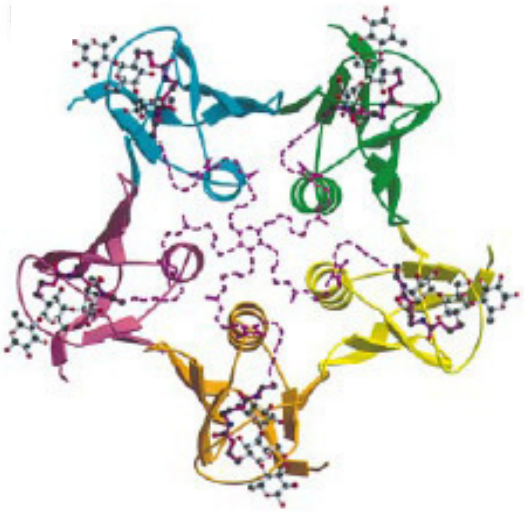

Scheme 18 *Mode of binding for tailor-made pentavalent ligand to the pentameric Escherichia coli shiga-like toxin I.*[79]

Following a similar approach another pentavalent ligand matching the pentameric binding domain of cholera toxin B (CTB) was recently presented by Casnati and Zuilhof.[80] The structure was constructed from a calix[5]arene, each phenolic portion carrying one mimic of a natural ligand for CTB, the oligosaccharide of ganglioside GM1 (GM1os). The structure achieved a picomolar inhibition potency (IC_{50} = 450 pM) for the toxin, as evaluated by competitive inhibition assay (Scheme 19). The binding strength benefits from a significant multivalency effect which is intensified by the matching valency.

Read, R. J.; Bundle, D. R. *Nature* **2000**, *403*, 669.

[80] Garcia-Hartjes, J.; Bernardi, S.; Weijers, C. A. G. M.; Wennekes, T.; Gilbert, M.; Sansone, F.; Casnati, A.; Zuilhof, H. *Org. Biomol. Chem.* **2013**, *11*, 4340.

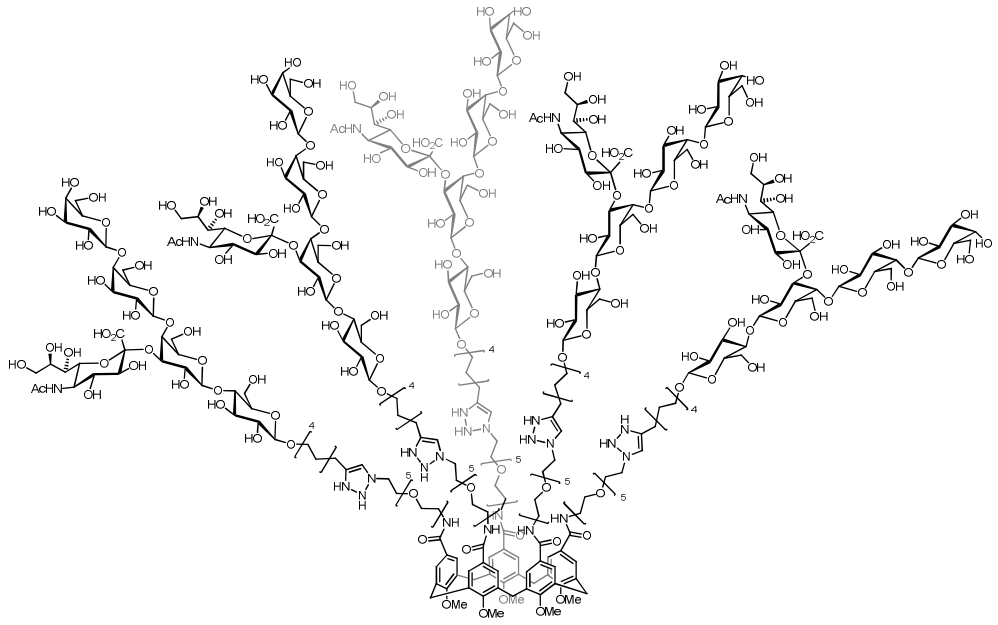

Scheme 19 *A cholera toxin B inhibitor based on a calix[5]arene based pentavalent GM1 presenting ligand.*[80]

1.2.2.3 Mechanism of Binding

The above examples highlight the crucial influence of multivalency on the binding affinities of ligands constructed for sugar binding lectins. The reason why the multivalency effect has such strong influence on the binding properties of lectin ligands could be due to two main effects: *chelation* and *statistical rebinding*. A binding mode that includes chelation of various binding sites at the same time is an obvious way to enhance binding or inhibition. The entropic penalty for the aggregation has already been paid upon binding to the first binding site. Any further chelating connection should increase affinity. The binding strength then only depends on the careful choice of the spacing between the binding anchors. The impressive impact of chelation on affinities has been shown in the above mentioned examples of tailor-made ligands matching in valency and size to their toxin targets.

However, apart from chelation, a further affinity enhancing effect must be operative.

The CRDs of ConA are *ca*. 70Å apart from each other. None of the structures shown in Scheme 14 would be large enough to span this distance with two or more of their sugar moieties. Despite this shortcoming the multivalent presentation of sugar monomers still seems to significantly increase affinities towards the lectin. Binding to protein surfaces is notoriously weak. The dissociation of the binding entities back into solution determines the binding strength. The off-rate, the thermodynamic value describing this process, is lowered in multivalent ligands.[81] The mechanism responsible could be understood as a localized concentration effect: Binding a first carbohydrate moiety to the recognition domain brings further binding units close and enables them to bind more readily than free ligands from solution.

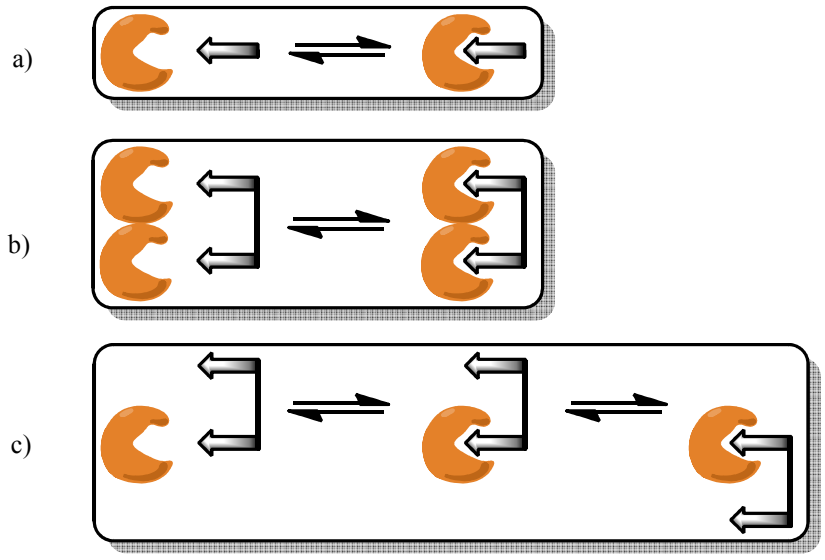

Scheme 20 *Different modes of binding. a) monovalent. b) multivalent, chelating. c) multivalent, statistical rebinding.*

In thermodynamic terms, the multivalent presentation increases the effective concentration of binders compared to ligands of lower valency. The effect, termed as *statistical rebinding* or *bind and slide* appears to be smaller than that of chelation. Though,

[81] Pieters, R. J. *Org. Biomol. Chem.* **2009**, *7*, 2013.

for small multivalent ligands that do not span the distance between binding sites, it is the decisive factor determining the overall binding strength (Scheme 20).[82]

The type of multivalent ligand architecture that facilitates statistical rebinding is not fully understood. Kiessling and co-workers have evaluated the effect of multivalent scaffold structures on the binding mechanism.[83] Large globular entities showed to be most efficient inhibitors for ConA lectin as indicated by this study and others.[84] The surface of round shaped ligands is generally more even and the distances from one binding moiety to the next are minimized. Compared to non-globular structures, all binding determinants have the same surrounding and therefore are all binding equally well. This features support statistical effects- A shifting movement from one anchoring point to the next is eased, in the same way as a round wheel rolls with lesser effort than one of irregular shape.

1.2.3 Conclusions

The above described studies have proven why multivalency is a key factor for affinity enhancements in ligands for carbohydrate-protein recognition. Glycoproteins, peptides, oligosaccharides, polymeric structures, micelles, liposomes nanoparticles and dendrimers have been used to achieve multivalent presentation of binding entities. The mechanism and the binding mode are determined by the type of multivalent structure. They can follow different principles that may be summarized into two main concepts- *chelation* and *statistical rebinding*. The way these different effects governing the binding process can cooperate and what are the structural requirements for maximizing them has not yet been fully elucidated. It is still unclear to what extend the classical *lock and key* analogy applies for the whole of an extended multivalent ligand structure. How does a perfect fit to a molecular target interplay with the effect of *statistical rebinding*? Could structural variety, harvested from a suitable DCL, help to answer the above questions? If so, it has first to be understood how the concept of multivalency applies in dynamic combinatorial systems.

---

[82] Dam, T. K.; Brewer, C. F. *Biochemistry* **2008**, *47*, 8470.

[83] Gestwicki, J. E.; Cairo, C. W.; Strong, L. E.; Oetjen, K. A.; Kiessling, L. L. *J. Am. Chem. Soc.* **2002**, *124*, 14922.

[84] Sánchez-Navarro, M.; Muñoz, A.; Illescas, B. M.; Rojo, J.; Martín, N. *Chem. Eur. J.* **2011**, *17*, 766.

Chapter 2

Dynamic Covalent Combinatorial Libraries

2.1 Conception of the Chapter

The main task to be addressed in this work was to implement the concept of multivalency (for lectin binding) into a dynamic combinatorial library. Most DCC approaches to lectin recognition have relied on the reversible exchange of two building blocks. The concept of multivalency has mostly been neglected for the set-up of protein recognising DCLs (see Introduction). The advantages of introducing multivalency to a protein-directed dynamic library are clear cut. To enhance binding affinities of a ligand to a protein surface, multivalent presentation of binding units is the most potent modification on the ligand molecule.[1] For sugar binding proteins this phenomenon is known as "glycoside-cluster effect". Along with the rising number of sugar units in oligosaccharides, affinity is increasing dramatically.[2] This is a concept that is catching growing attention in the quest for anti-pathogenic agents.[3] Apart from the sheer number of binding units on a single ligand, also the level of multivalency, configuration, distances, geometrical orientation and other more subtle structural needs of the recognized protein are of importance.[4] To access variations of multivalent structures, DCLs seemed a convenient choice to analyse the influence of those parameters.

A variety of reversible covalent interactions was evaluated to set-up different DCLs, all following the same general concept. A multivalent central structure with at least three connection points was used as a platform. Sugar binding lectins were chosen as protein targets. Consequently the building blocks of the libraries should contain sugar moieties as

[1] Jayaraman, N. *Chem. Soc. Rev.* **2009**, *38*, 3463.
[2] a) Lundquist, J. J.; Toone, E. J. *Chem. Rev.* **2002**, *102*, 555. b) Dimick, S. M.; Powell, S. C.; McMahon, S. A.; Moothoo, D. N.; Naismith, J. H.; Toone, E. J. *J. Am. Chem. Soc.* **1999**, *121*, 10286. c) Luczkowiak, J.; Sattin, S.; Sutkevičiūtė, I.; Reina, J. J.; Sánchez-Navarro, M.; Thépaut, M.; Martínez-Prats, L.; Daghetti, A.; Fieschi, F.; Delgado, R.; Bernardi, A.; Rojo, J. *Bioconjugate Chem.* **2011**, *22*, 1354.
[3] Cummings, R. D.; Kornfeld, S. *J. Biol. Chem.* **1982**, *257*, 11230.
[4] Weis, W. I.; Drickamer, K. *Annu. Rev. Biochem.* **1996**, *65*, 441.

binding subunits to form reversible covalent interactions with the proteins. When the sugar building blocks and the multivalent scaffold are mixed in solution, they should assemble a multivalent dynamic combinatorial library (DCL, Scheme 1). The library members bind to the protein surface upon mixing, *via* their sugar anchors. The affinities of the different library members should vary depending on their structural properties and their composition.

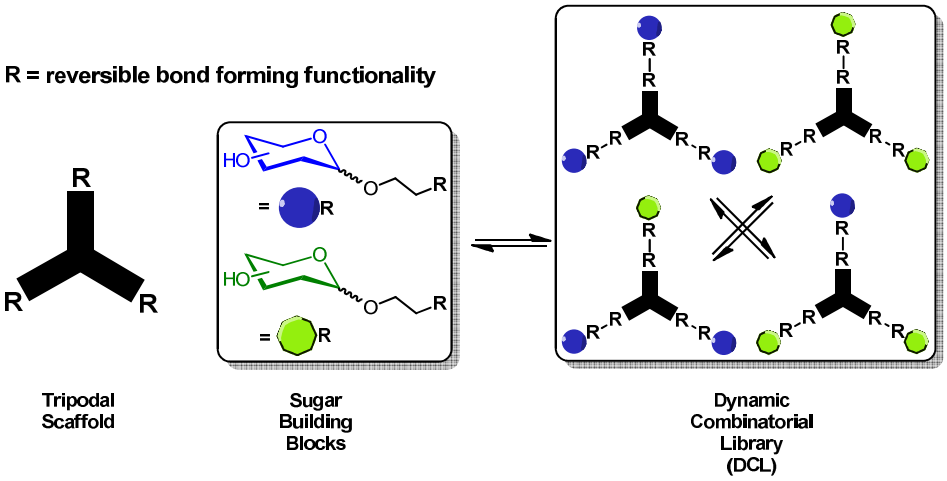

Scheme 1 *Schematic depiction of a basic scaffold for a DCL.*

The sugar binding lectin ConA was chosen as an easy to handle target protein. Its application has been described by Lehn *et al.*,[5] among others. ConA is available immobilized as a solid supported sepharose conjugate and quantities allowing analysis by a HPLC-MS system are commercially available at reasonable prices. Therefore a filtration elution procedure combined with HPLC-MS analysis was chosen to evaluate affinities for each member of a DCL from solution (see section 2.2).

2.2 Analytical Method

It is difficult to determine the relative affinities of the members of a DCL to a molecular

[5] Ramström, O.; Lehn, J.-M. *ChemBioChem* **2000**, *1*, 41.

binding partner in solution, since all entities may exhibit affinities for the target of interest. Owing to the dynamic properties of the system the structures usually cannot be analysed separately. Methods like Isothermal Titration Calorimetry (ITC), Surface Plasmon Resonance (SPR), Inhibition of Hemagglutination Assays (HIA) or Enzyme-Linked Lectin or Enzyme-Linked Immuno Sorbent (ELISA) assays all require the potential binding partners in a pure form or the mixture has to be evaluated as a whole. NMR techniques can be more flexible as has been shown by Ramström and Jiménez-Barbero, who used Saturation Transfer Difference NMR (STD) to analyse large protein binding libraries *in-situ*.[6] Nevertheless, the presence of particular NMR signals, that make the different binders distinguishable, is required. In a dynamic library that contains species with similar NMR responses it is difficult to discriminate the different binding affinities.

For carbohydrate containing systems, reverse phase HPLC can be applied, as it is able to resolve different sugar configurations. The combination of different sugars in one structure can result in different retention times on HPLC columns.[5] A mixture of sugar containing ligands can be analysed directly, as the previous separation of the binding constituents is not required. This and the advantages of an immobilized target protein were exploited in the present study. Solid phase supported ConA enables separation of protein bound and non-protein bound fractions by filtration (Scheme 2). As a standard protocol the DCLs were mixed with ConA immobilized on sepharose beads. After an equilibration time the suspension was filtered (over Amicon YM-100 filter discs). The non-protein bound fraction could then be analysed directly from the filtrate using a HPLC-MS system. The filter residue was re-suspended in 0.5 M HCl (Scheme 2b and 2c). The sugar binding ability of ConA lectin is dependent on a calcium cation located inside the carbohydrate recognition domain (CRD). The drop in pH removes the ion and triggers a release of the bound constituents. Renewed filtration yields a solution containing the bound fraction of the DCL. In that mixture, the abundance of the different sugar containing library members depends on their relative affinities to the CRD. An HPLC-MS system was then used to identify the library members and to determine the respective abundances. The measured

[6] Caraballo, R.; Dong, H.; Ribeiro, J. P.; Jiménez-Barbero, J.; Ramstrom, O. *Angew. Chem.* **2010**, *49*, 589.

values can be compared to those of a reference sample without protein interaction.

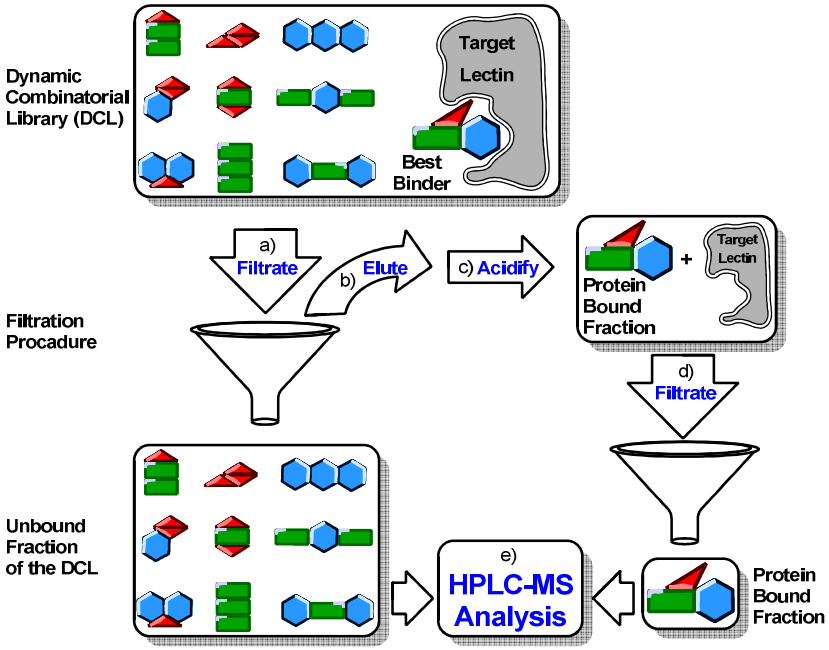

Scheme 2 *a) Filtration of DCL and target lectin. b) Elution of filter residue containing the lectin and bound DCL members. c) Acidification breaks bonds between lectin and DCL binding partners. d) Renewed filtration to separate lectin and protein bound fraction. e) Quantification of binding by HPLC.*

The differences in abundances are a relative measure for their affinity to the protein, a higher abundance of one species in the protein bound fraction indicates its preferred binding.

2.2.1 Testing the Analytical Method

To verify the analytical procedure, compound **RR84** (Scheme 3), synthesized by Rojo *et al.* was used as a reference to test the above described filtration/elution procedure. The test ligand exhibits a tetrapodal structure with four D-mannose units, since the multivalent nature of the molecule assures good affinity to the mannose binding ConA surface.

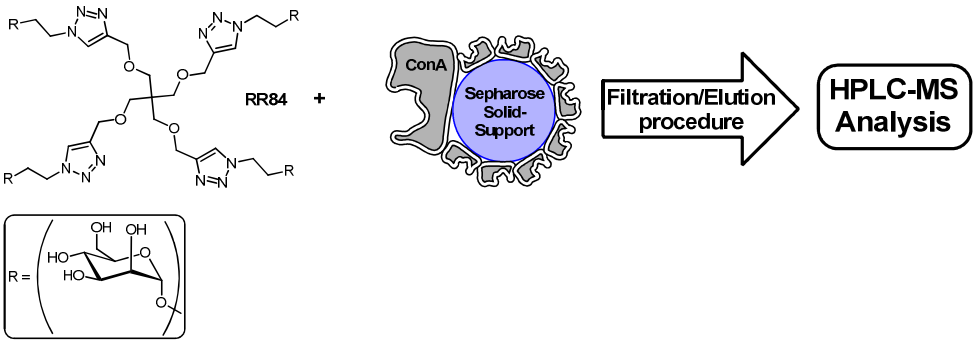

Scheme 3 *Binder model for the procedure described in Scheme 2.*

A 3 mM aqueous solution of **RR84** was mixed with ConA immobilized on a sepharose-based solid support (beads). The mixture was set-up in a 20/1 **RR84**/lectin ratio. After several days equilibration time the solution was filtered and the filtrate was re-suspended in 0.5 M HCl (same volume as the equilibrating mixture before). After 20 min the suspension was filtered and the filtrate analysed by HPLC-MS (Figure 1). The compound was detected as a clearly visible single peak in the chromatogram (Figure 1b), and its identity was confirmed by mass spectrometry.

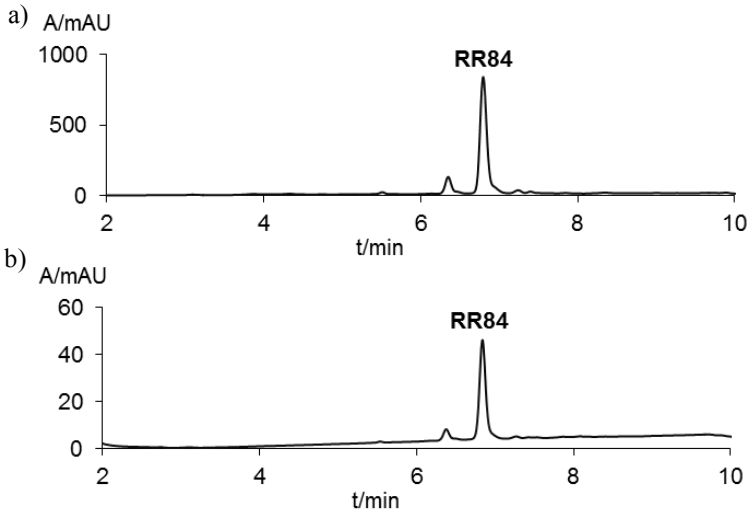

Figure 1 *a) Reference chromatogram of **RR84**. b) Protein bound fraction showing binding partner **RR84** at lower intensity.*

2.2.2 Conclusions

In this section a filtration/elution protocol was described that allows for the detection of lectin binding partners. The method had already been used successfully in Lehn's laboratory,[5] it was expected to also apply to the systems examined here. Thus, the experiment on a model compound confirmed that the chosen protocol for analysis of ConA binding partners is manageable and can afford detectable results.

2.3 Disulphide-based Dynamic Combinatorial Libraries

Formation and application of dynamic libraries formed by disulphide exchange is a well-studied field and a variety of practical experimental and analytical details are available.[7] Atmospheric oxygen is sufficient to drive an oxidation reaction between two thiols to form a disulphide bridge (Scheme 4). Under basic conditions free thiolate can attack this bridge to launch the scrambling process. The conditions required to maintain the dynamic properties do not interfere with the final application of the resulting DCL-protein binding. Moreover, the exchange process is highly chemoselective. It shows rapid interchange of thiol units at pH values above 7 and forms stable bonds at pH values below 5, thus the reaction can be "locked" and "unlocked".

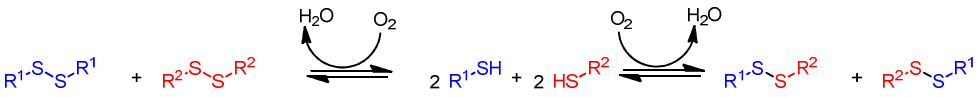

Scheme 4 *Disulphide exchange.*

[7] a) Corbett, P. T.; Leclaire, J.; Vial, L.; West, K. R.; Wietor, J.-L.; Sanders, J. K. M.; Otto, S. *Chem. Rev.* **2006**, *106*, 3652. b) Ponnuswamy, N.; Cougnon, F. B. L.; Clough, J. M.; Pantoş, G. D.; Sanders, J. K. M. *Science* **2012**, *338*, 783. c) Au-Yeung, H. Y.; Dan Pantoş, G.; Sanders, J. K. M. *J. Am. Chem. Soc.* **2009**, *131*, 16030. d) Pei, Z.; Larsson, R.; Aastrup, T.; Anderson, H.; Lehn, J.-M.; Ramström, O. *Biosens. Bioelectron.* **2006**, *22*, 42.

The groups of Lehn and Sanders, among others, have contributed a large number of systems relying on this particular reversible covalent bond forming reaction.[7] Simple proofs of concept as well as applications for protein recognition and even dynamic libraries of cages and large macromolecular structures have been reported. At the starting point of this work the likely closest enhancement of valence was chosen. The goal was to extend the divalent systems of earlier examples to an exchange-based on three attachment points, to proof usefulness and applicability of multivalent systems in DCLs. Thus, a scaffold was synthesised (see section 2.3.2.1) that provided three reversible connecting points in the form of thiol units (schematically in Scheme 5).

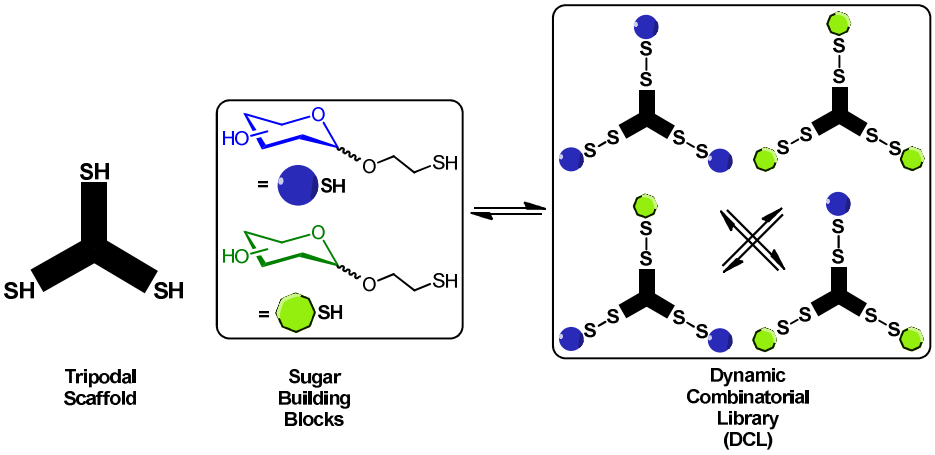

Scheme 5 *Disulphide scrambling based on a tripodal scaffold and two sugar units.*

The counterpart sugar building blocks were endowed with short ethylene linkers also bearing thiol functions. The DCL evolved by connecting the tripodal scaffold and those binding anchors *via* disulphide bridges. If two sugar building blocks are used, four permutations around the central core should be found (Scheme 5).

In that way a small DCL can be set-up that could later be extended by addition of further sugar-based building blocks.

2.3.1 Synthesis of Thio-Sugar Derivatives

Mannose containing structures have high affinities for ConA. Hence, as a first building block, a D-mannoside (**Man**) was synthesised. The derivative was obtained following a well-known protocol for a variety of similar compounds,[8] based on Lewis acid ($BF_3{\cdot}Et_2O$) activation of the anomeric position in peracetylated D-mannose **1**. In this way, bromoethanol was attached to the pyranose ring. Neighbouring group assistance by the acetyl group at position 2 forms an oxonium intermediate that facilitates formation of the α-isomer **2** in 62% yield.

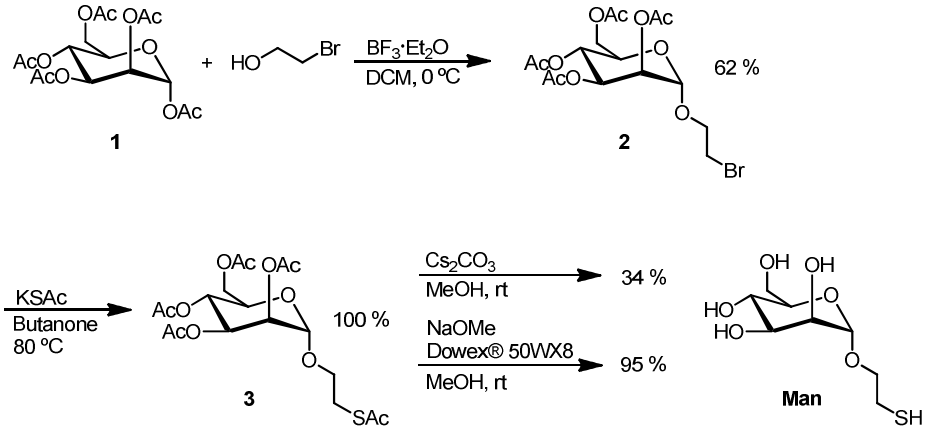

Scheme 6 *Synthesis of thioethyl α-D-mannopyranose (**Man**).*

Bromide was readily substituted upon addition of KSAc in butanone. An attempt to remove the acetyl protection of **3** with cesium carbonate resulted in low yields. Though, sodium methoxide in methanol cleanly deprotected both the hydroxyl and thiol groups, and acidification by acidic ion exchange resin afforded the pure product (**Man**) in 95% yield. Use of chloroethanol as nucleophile in the glycosidation step (Scheme 7) improved the yield and facilitated purification (no column chromatography was necessary). The subsequent substitution of chloride (in compound **4**) by thioacetate did not proceed as efficiently as with bromide **2**, resulting in a slight reduction of the overall yield.

---

[8] Revell, D. J.; Knight, J. R.; Blyth, D. J.; Haines, A. H.; Russell, D. A. *Langmuir* **1998**, *14*, 4517.

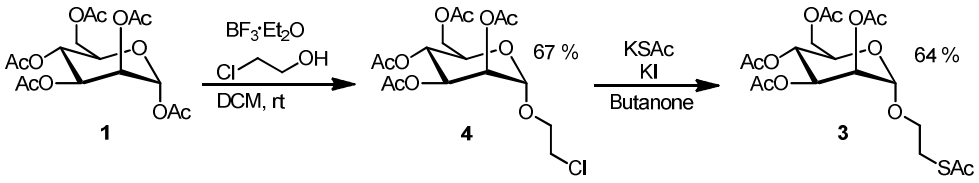

Scheme 7 *Chloroethanol variation for synthesis of thioethyl α-D-galactopyranose* (**Man**).

An analogous D-galactoside derivative (**Gal**) was obtained following the same procedure. Despite the low yields observed in the **Man** synthesis, the cleaner chloroethanol variation of the reaction pathway was chosen in order to avoid column chromatography. Deprotection with cesium carbonate did not afford satisfactory amounts of fully deprotected product **Gal** (Scheme 8). The combination of sodium methoxide and ion exchange resin for the work-up was again more efficient and much cleaner.

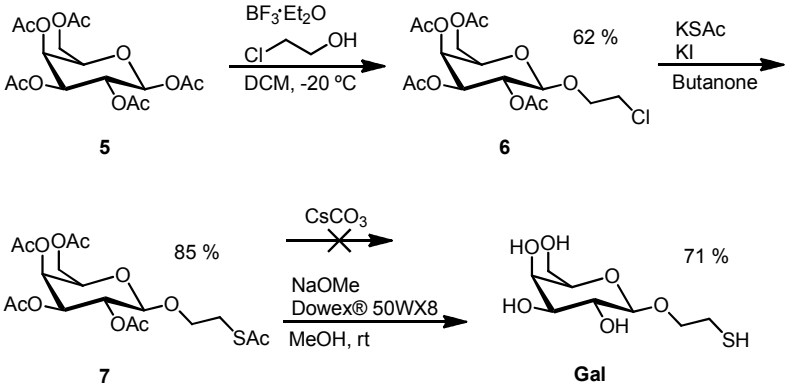

Scheme 8 *Synthesis of thioethyl β-D-galactopyranose (**Gal**)*

2.3.1.1 Set-up of a Prototype Dynamic Library

To test formation and analysis of a prototype DCL, thiolated sugars **Man** and **Gal** (see section 3.1) were used.

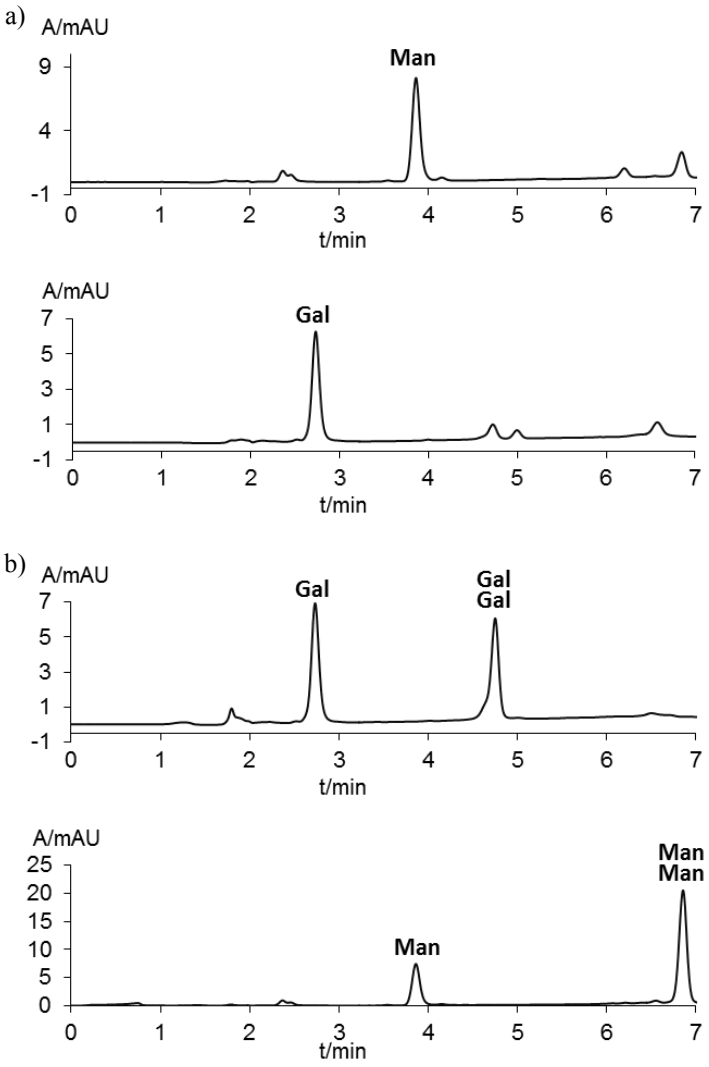

Figure 2 *Chromatograms of thioethyl α-D-mannopyranose (**Man**) and thioethyl β-D-galactopyranose (**Gal**). a) Freshly dissolved. b) After six days having formed homo-dimers.*

To determine the retention times of the homodimeric species of **Man** and **Gal**, the dimerization of the respective thiols was monitored by HPLC. For this purpose 3 mM aqueous solutions of **Man** and **Gal** where separately set-up. Over the course of several days (Figure 2) changes were followed by HPLC. After six days the initial thiols were partly transformed (Figure 2b). The new species were detected at larger retention times indicating lower polarity. As expected and later confirmed by HPLC-MS analysis, these where the respective disulphide-connected dimers **ManMan** and **GalGal**. Both dimer containing solutions were then mixed. After one week, a third dimer was formed besides the two homodimers. Due to its retention time midway between **ManMan** and **GalGal** the new entity was assumed to be the heterodimer **ManGal** (Scheme 9), which was later confirmed by HPLC-MS (Figure 3b). Addition of a small amount of hydrogen peroxide fully oxidised the remaining monomers (Figure 3c).

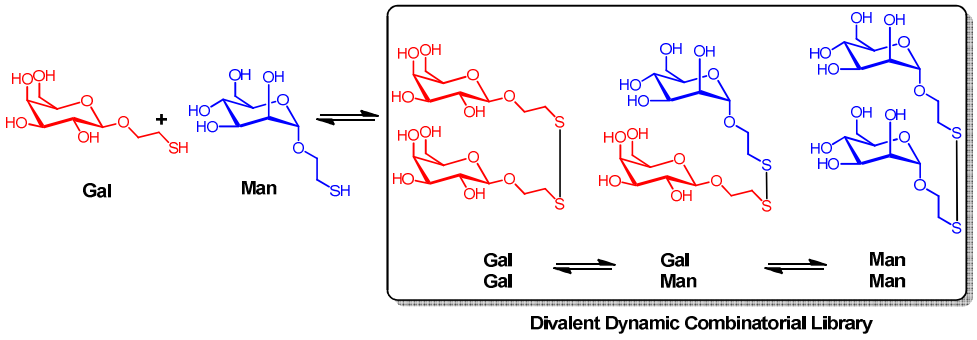

Scheme 9 *A small* ***DCL A*** *composed of three different sugar-based dimers* ***(GalGal)*** *(**ManGal**) and (**ManMan**)*

A small dynamic library containing the three possible combinations of the two starting sugar derivatives (**DCL A**) was thus created. Mixed entities have a higher probability to form. The statistical (Gaussian) distribution favouring the heterodimer was indeed well visible in the chromatogram (Figure 3c) indicating similar stabilities of the different compositions.

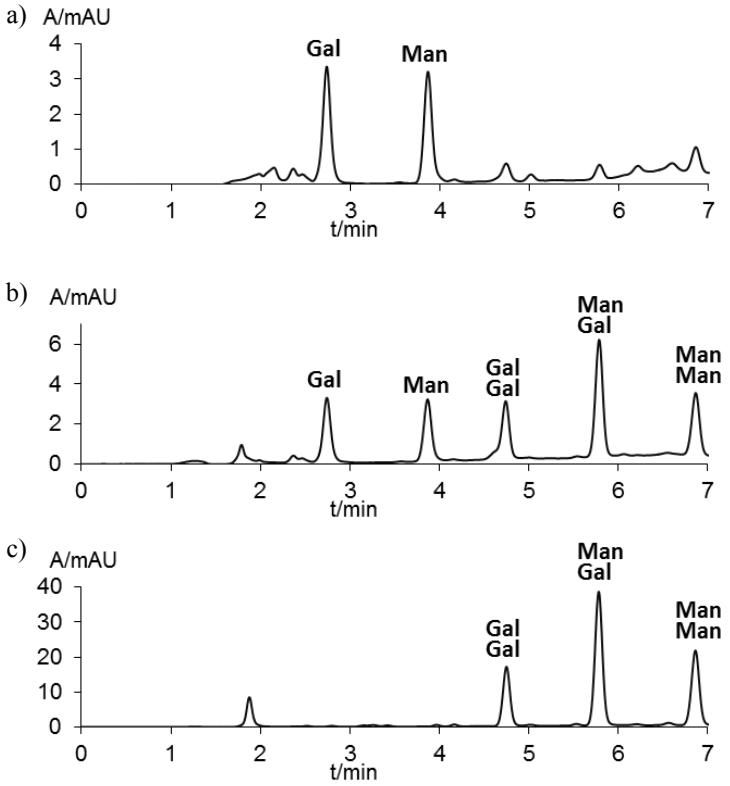

Figure 3 *a) HPLC analysis of a fresh mixed solution of thioethyl α-D-mannopyranose (**Man**) and thioethyl β-D-galactopyranose (**Gal**). b) Mixture after 6 days. c) Mixture after addition of H_2O_2.*

Thus, a small DCL had been generated using preformed dimers, highlighting their dynamic properties to form a new library member. In further experiments similar conditions will be employed to set-up a DCL on a molecular platform.

2.3.1.2 Detection of Protein Selectivity in a Dimeric DCL

In section 1.1 it was described how a model ligand binds to a protein and can be detected by filtration/elution. Next we tested if selectivity could be monitored using the same analytical method with **DCL A.** Lehn *et al.* had previously shown that the method was sensitive enough to detect binding preferences[5] (Scheme 10).

a) b)

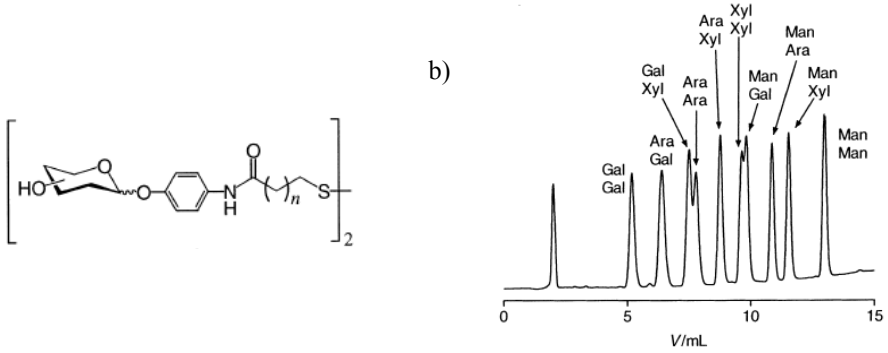

Scheme 10 *a) General structure of the dimers used by Lehn to form the DCL. b) Chromatogram of the DCL from solution. Every peak is assigned to one dimer.*[5]

Relative affinities of different sugars and sugar containing structures to a large number of proteins are available from comparative studies of an online project.[9] The data shows that D-galactosides bind significantly weaker to ConA than D-mannosides. Therefore **DCL A** (Scheme 9), consisting of thioethyl D-mannopyranose (**Man**) and thioethyl D-galactopyranose (**Gal**), was expected to exhibit distinct binding affinities for the different library members. The dynamic library was mixed with the solid supported protein and the binding partners were determined as described in section 1.1. Surprisingly, no selectivity could be observed, a result that seems to contradict later findings using more extended systems.

For a better discriminating system, we selected thioethyl L-fucose (**Fuc**) (synthesis see Experimental Section) instead of the D-galactose derivative, since L-fucose does not bind to the ConA CRD.[9]

The two homodimers were first tested separately (Scheme 11). The sugar derivatives (at 3 mM, in water) were mixed with an immobilised ConA suspension and equilibrated.

[9] www.functionalglycomics.org

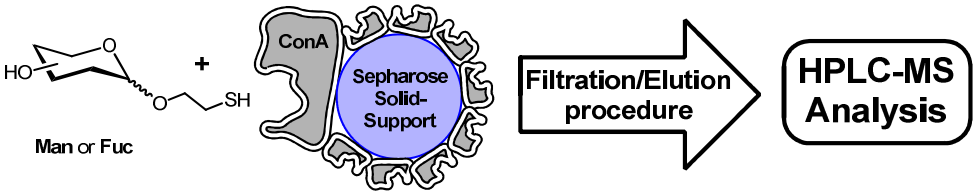

Scheme 11 *Detecting binding of thioethyl α-D-mannopyranose (**Man**) to ConA.*

Filtration/elution followed by HPLC-MS analysis revealed that L-fucoside (**Fuc**) was not bound to the protein surface, as expected. Then, the small **DCL B** library (Scheme 12) was generated by mixing the two **Man** and **Fuc** solutions as previously described for **Man** and **Gal** (see section 2.3.1.1). The three entities found in the dynamic mixture were di-D-mannoside (**ManMan**), di-L-fucoside (**FucFuc**), and the (**ManFuc**) heterodimer. According to the known binding preferences of ConA, di-mannoside (**ManMan**) should be prevalently bound. Thus, the equilibrated **DCL B** was mixed with the immobilised protein in a 20:1 relation of library members/ConA and stirred for several days.

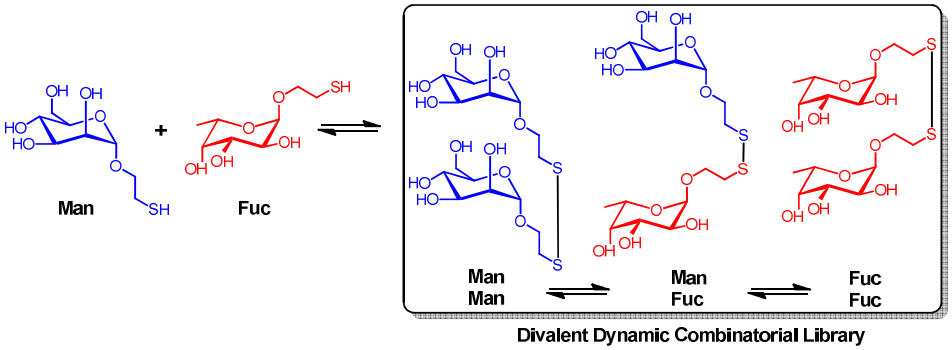

Scheme 12 *Small **DCL B** with dimers (**ManMan**), (**ManFuc**), and (**FucFuc**).*

After a work up as described in section 1.1 the protein bound fraction was analysed by HPLC-MS (Figure 4b). Absorptions of the species can be assumed equal due to their structural similarity. Solutions of the pure compounds at same concentrations exhibit identical absorptions. Therefore, integration and comparison of the peaks (Figure 5) showed that **ManMan** was almost twice as abundant in the protein bound fraction as in the reference sample (Figure 4a). The procedure therefore proved to be manageable for

detecting selectivity in DCLs.

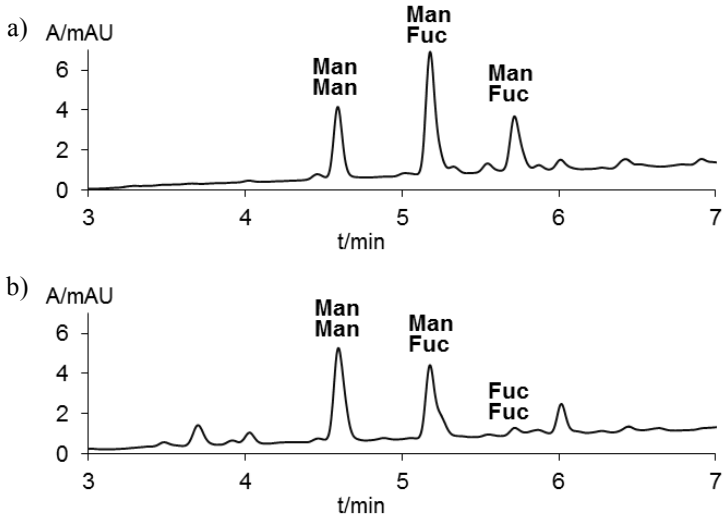

Figure 4 *Analysis of* ***DCL B*** *by HPLC. a) Reference sample (no protein interaction). b) Protein bound fraction.*

A closer look at the abundance change (Figure 5) reveals a hint of what is to be discussed on later examples (Chapter 3): The **ManFuc** heterodimer would be expected to exhibit a no change in abundance. The fact that a decrease of **ManFuc** is visible may be owed to strong binding of **ManMan** due to a multivalency effect. The equilibrium (Chapter 1) is shifted, taking the well binding **ManMan** into a thermodynamical minimum, thus favouring its formation. As a consequence thereof, the amount of **ManFuc** gets reduced by providing **Man** fragments. This interpretation is just tentative, since the effect is small and only visible on a single DCL member.

The experiments proved the ability of the analytical method to detect selectivity for different DCL members. This opened the way for the analysis of other, more complex (multivalent) DCLs.

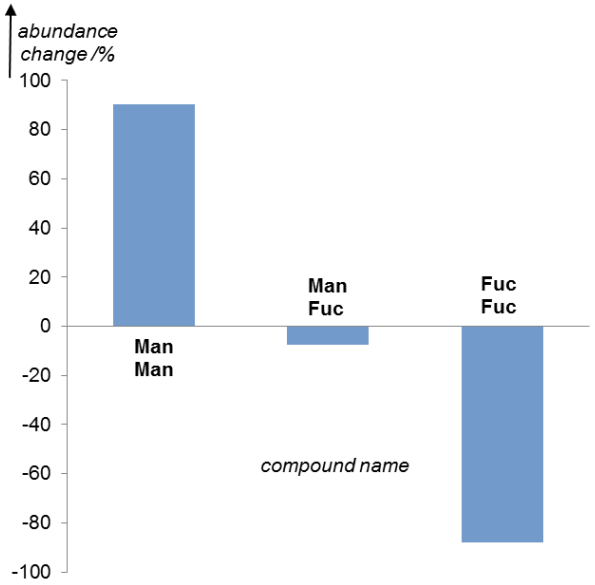

Figure 5 *Abundance change for the different library components. Equilibrated* ***DCL B*** *in absence of protein and protein bound fraction of* ***DCL B*** *are compared (determined from the respective HPLC chromatograms, see Figure* ***4****).*

2.3.2 Flexible Trivalent Scaffold

A small multivalent **DCL C** was created allowing thio-sugars **Man** and **Gal** (see section 2.3.1) to connect with a multivalent scaffold bearing thiol subunits under oxidative conditions (basic pH, air) (Scheme 13). Three thiol groups were connected to a galic-acid backbone through suitable glycol spacers. In addition, the acid function was esterified with a triglycolmethyl ether to render the scaffold soluble in water. The resulting structure (compound **8**) was soluble in aqueous solutions up to a concentration of 1 mM, which was used for all further experiments. Mixing the previously described thio-sugar derivatives (**Man**, **Gal**, **Fuc**) and scaffold **8** was expected to form a multivalent dynamic library with the building blocks anchored around the central subunit.

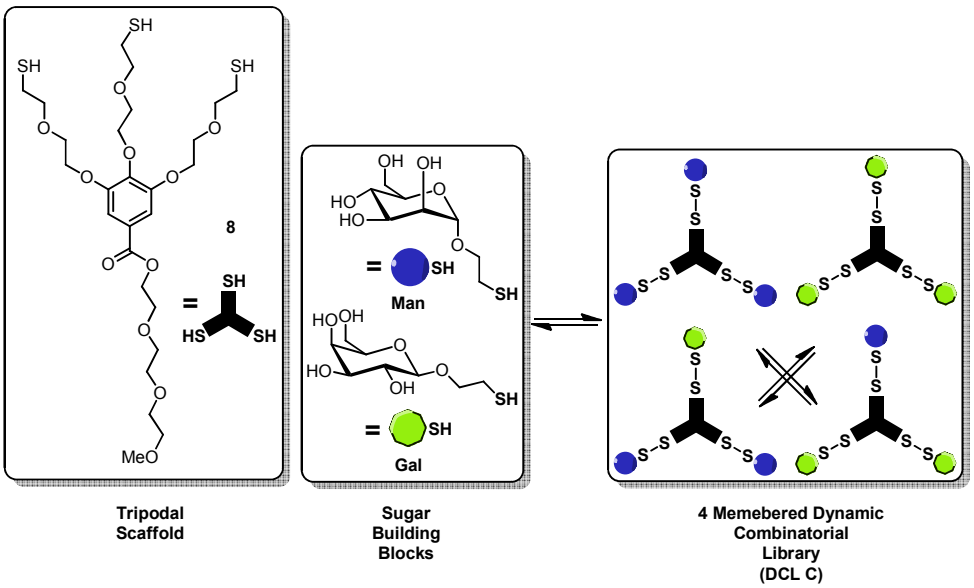

***Scheme 13 DCL C** should have formed by **Man** and **Gal** binding to the platform.*

2.3.2.1 Scaffold Synthesis

The precursor of the thiol linker **10** was prepared by monosubstitution of one tosyl group of ditosylate **9** by tritylthiol. The thiol nucleophile was deprotonated by NaH and then slowly added to a solution of **9**. Use of potassium *tert*-butoxide gave poorer yields. In addition, the procedure described by Tsuji[10] to attach the glycol branch to the galic acid core under basic conditions in acetone was unsuccessful.

[10] Fujihara, T.; Yoshida, S.; Terao, J.; Tsuji, Y. *Org. Lett.* **2009**, *11*, 2121.

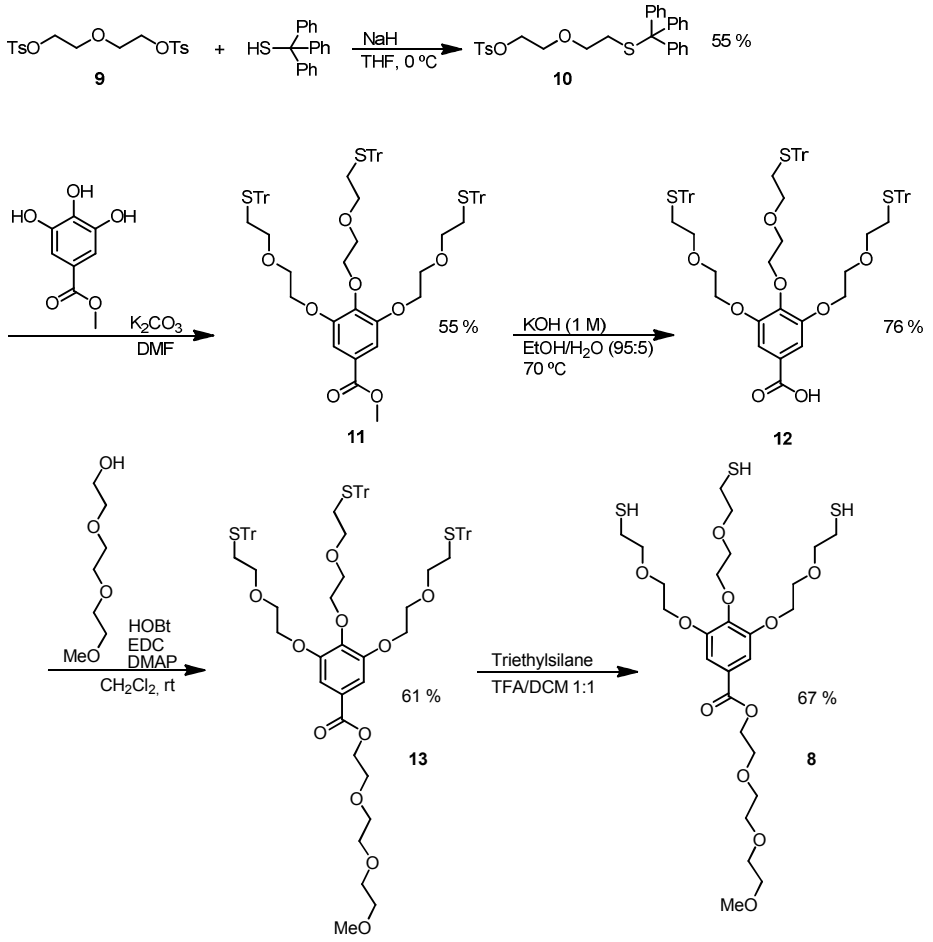

Scheme 14 *Synthesis of the first tripodal thiol-bearing scaffold.*

DMF was required to dissolve all reaction partners and to promote the nucleophilic substitution. This afforded methylester **11** in 55% yield. Deprotection of **11** in KOH solution gave the crude acid **12**, which was purified by flash chromatography (CombiFlash) to afford the final compound in 76% yield. The acid **12** was then activated by a combination of three different coupling agents [1-Hydroxybenzotriazole (HOBt), 1-(3-Dimethylaminopropyl)-3-ethylcarbodiimide (EDC) and 4-dimethylaminopyridine (DMAP)], prior to esterification with tetraethyleneglycol monomethyl ether to give ester **13** in 81% yield. To obtain thiol bearing structure **8** the trityl protecting groups where

Solvents Untreated	*Solvents Deoxiganted By Bubbling With Argon*	*Solvents Degassed By Pump-Thaw*	*Purification Under Air*	*Purification Under Inert Conditions*	***Pure Product***
		✓		✓	✓
✓			✓		✗
	✓		✓		✗
	✓			✓	✓

Table 1 *Conditions for deprotection of* ***13****.*

cleaved by TFA in DCM, in the presence of triethylsilane as hydride donor. The reaction was monitored by the disappearance of colour. As the free thiol groups are prone to intramolecular oxidation reactions, deprotection of scaffold **13** was tested under a variety of conditions (Table 1).

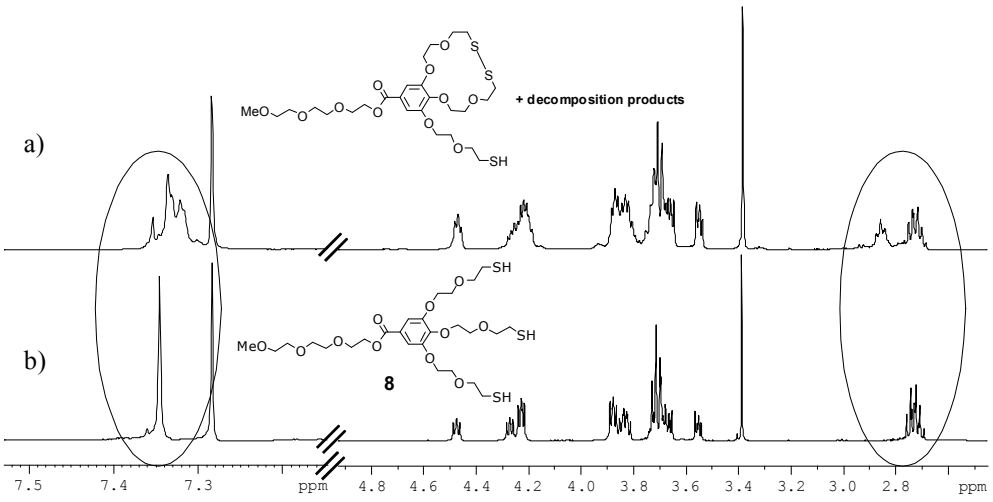

Figure 6 *Comparison of the* ^{1}*H NMR spectra of the oxidised a) and unoxidised b) Platform* ***8****.*

It proved to be sufficient to remove the oxygen by bubbling the solvents with argon prior to use. However it was even necessary to conduct the purification under inert conditions The reaction was monitored by ^{1}H NMR (Figure 6). The undesired intramolecular disulphide (Figure 6a) could be identified by its NMR spectrum exhibiting a broken symmetry. The unoxidised product shows a singlet for the aromatic protons at 7.3 ppm, whereas the unwanted product exhibits a multiplet. Also, the signal for one of the CH_2 groups at 2.75 ppm splits in the disulphide. HPLC and mass analysis confirmed those findings.

2.3.2.2 Homoadduct Models

The attachment of thio-sugars to platform **8** was first attempted separately for each sugar derivative. Two identical experiments were set-up using thioethyl-α-D-mannopyranose (**Man**) and thioethyl-β-D-galactopyranose (**Gal**). Both sugar derivatives (at 3 mM concentrations) were mixed in water with compound **8** (1 mM) in stoichiometric amounts relative to their free thiol groups. Under these conditions the oxidation rate was slow. To accelerate the formation of conjugation products, hydrogen peroxide was added later. Both experiments were followed by HPLC. After one week new species had formed (Figure 7b and 7c). The known peak for the free platform **8** (Figure 7a) had disappeared and new peaks were visible at shorter retention times in both experiments, indicating a higher polarity. The HPLC results indicated that platform **8** and sugar derivatives (**Man** and **Gal**) combine to form one single conjugation product each. Also, carbohydrate dimers (**ManMan** or **GalGal**) were visible. At this time, no HPLC-MS system was readily available in our laboratory, thus immediate determination of the new products by mass spectrometry from solution was not performed. Nevertheless, formation of the triple conjugated compounds was expected, as outlined in Scheme 13.

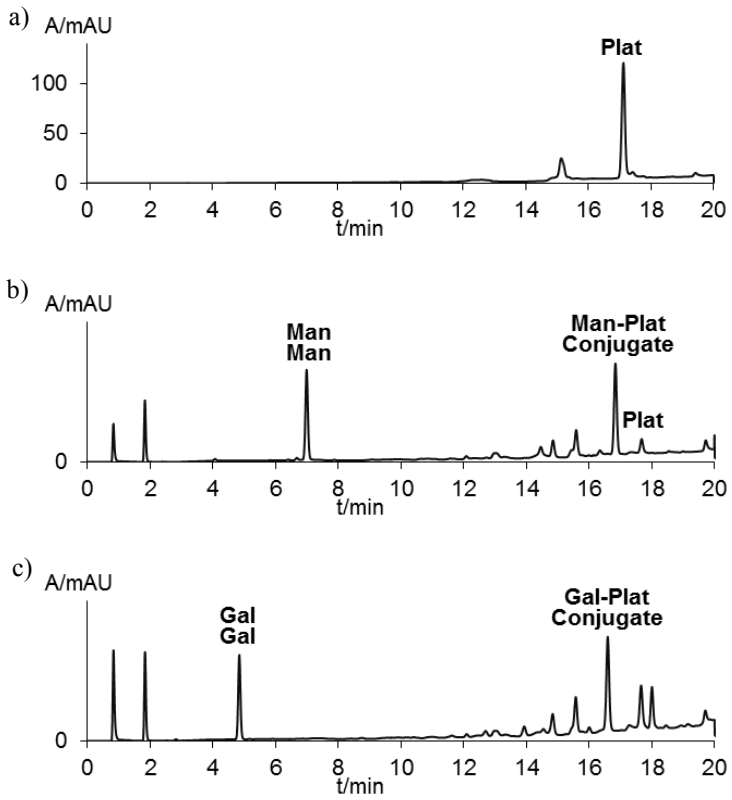

Figure 7 *Chromatograms of solutions of platform* ***8*** *(1 mM aq.) and sugar derivatives* ***Man*** *and* ***Gal*** *(3 mM aq.).*

2.3.2.3 DCL Set-up and Analysis

The indications given by the initial experiments (see section 2.3.1.2) with platform and building blocks interacting under oxidising conditions prompted us to generate a DCL. Thus, a water solution was prepared containing both receptor units **Man** and **Gal** (3 mM each) and the multivalent scaffold **8** (1 mM). After equilibration for one week in an open vial the mixture was analysed by HPLC-MS (Figure 8).

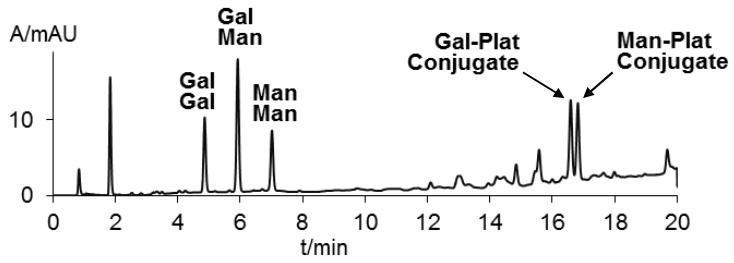

Figure 8 *Equilibrated mixture of* ***Man*** *and* ***Gal*** *with* ***8.***

At the left side of the chromatogram the three known peaks from the sugar derivative dimers (**ManMan, GalMan, GalGal**) were observed. In addition, two new peaks emerged at the right side, with identical retention times as the previously observed homo-conjugates (Figure 7). Analysis by HPLC-MS confirmed the identity of the three carbohydrate dimers (**ManMan, GalMan, GalGal**), but the two new peaks at longer retention times were identified as mono-conjugates of the scaffold **8** with the D-mannoside (**Man**) and the D-galactoside (**Gal**) (Scheme 15). Thus, an internal oxidation occurred, with two linker arms of the platform reacted to form a cycle. Therefore only one sugar unit can attach to the scaffold and a multivalent entity was not formed. No bis- or tris-conjugated species were detectable in the mixture.

.

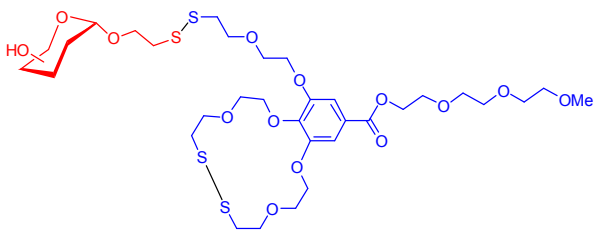

Scheme 15 *Internally oxidised conjugate with one pyranoside unit bound*

2.3.2.4 Intramolecular Oxidation Examined

To better understand the mechanism of the intramolecular oxidation, its progress was monitored periodically (Figure 9). A 1 mM solution of **8** in water was left under air. To

slow down the oxidation process for observation, the HPLC vial was closed to avoid additional circulation of air and abundant presence of oxygen.

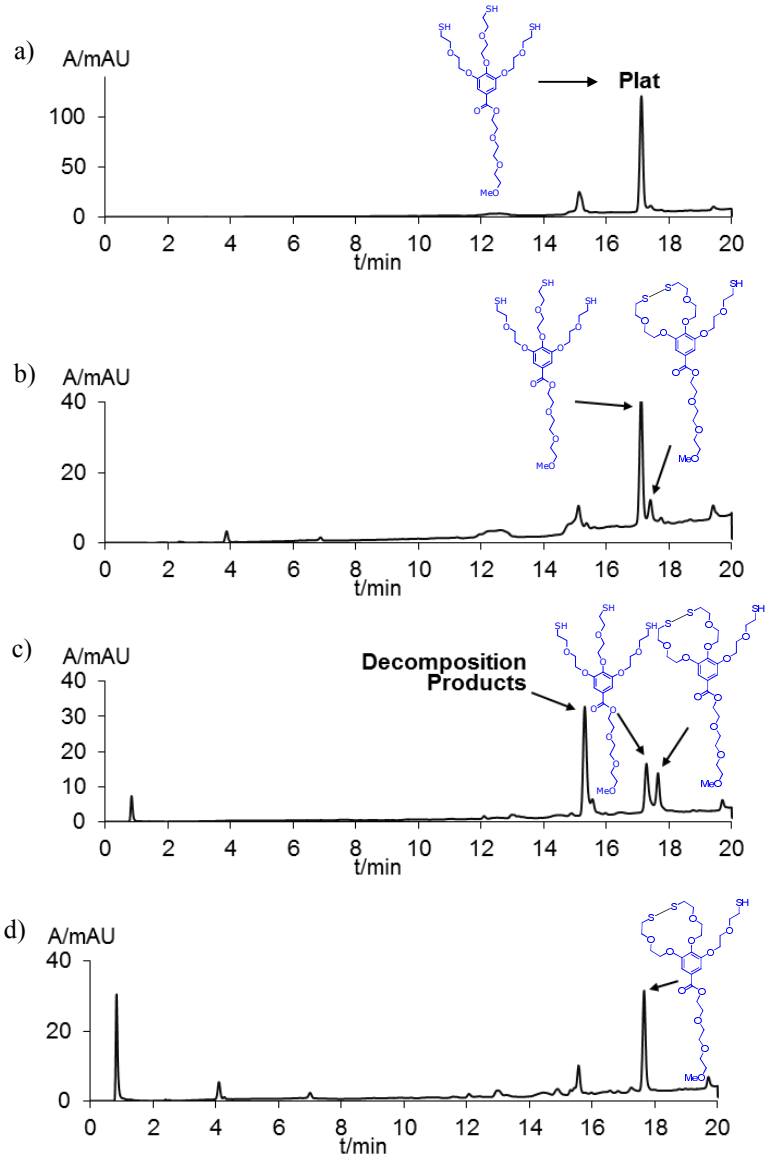

Figure 9 *Intramolecular oxidation of platform* ***8*** *followed by HPLC. a) Freshly deprotected platform. b) After 1 day. c) After 3 days. d) After one week.*

After one day both species were visible as two separate peaks in the chromatogram (Figure 9b). After three days a 1:1 ratio of open and closed species of the scaffold had developed (Figure 9c), and the ring closing proceeded to completion after one week (Figure 9d).

2.3.2.4.1 Ring Closing vs. Conjugation

Formation of the internally oxidised species of sugar building blocks (**Man**, **Gal**, and platform **8**) is favoured at stoichiometric ratios, (see section 2.3.2.3). In order to push the equilibrium towards higher conjugates, a higher concentration of sugar derivative (**Man**)

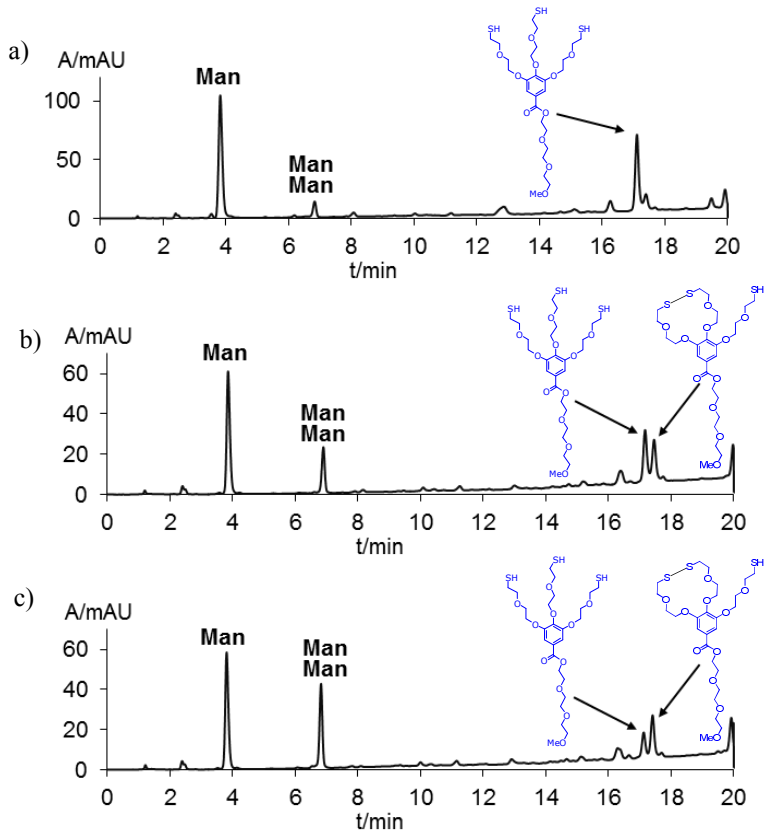

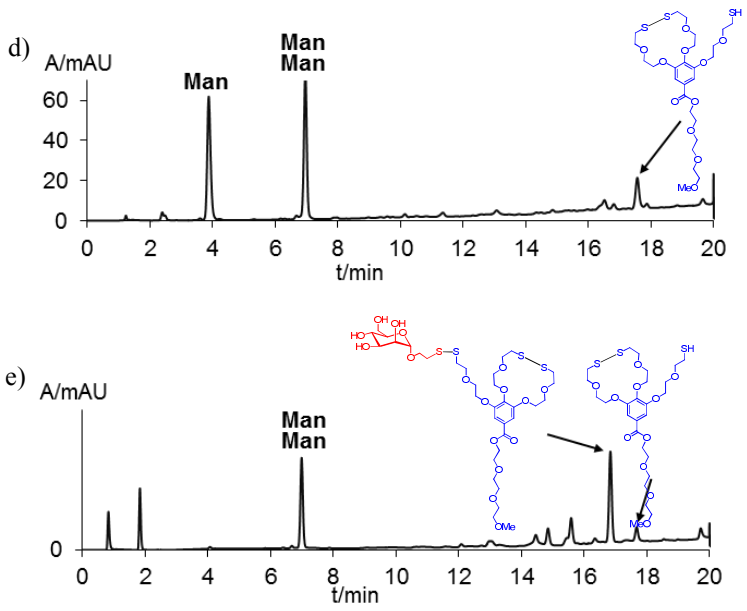

Figure 10 *Conjugation of Platform* ***8*** *and* ***Man*** *followed by HPLC. a)* ***Man*** *and* ***8*** *freshly deprotected. b) After 1 day. c) After 2 days. d) After one week. e) After 10 days.*

was used. Thus, **Man** (40 mM) was dissolved at in a solution of **8** (1 mM), and the solution was monitored by HPLC over ten days (Figure 10). After one week the platform was fully transformed into its internally oxidized counterpart, and no bis- or tris-sugar substituted species were detectable. Internal oxidation continued until all open type platforms were transformed. Subsequently, in a second separate step, the conjugation of the thio sugar derivative happened (Figure 10d). After 10 days, the closed scaffold had almost fully reacted with the sugar derivative, the mono-**Man**-conjugate becoming the prevalent species (Figure 10e).

Those results showed that the internal ring closing is a highly favoured process. However, in the presence of the protein target, a template effect was expected to support the formation of higher conjugates.

2.3.2.5 Alternative Tripodal Scaffold Synthesis

Previous experiments had revealed that platform **8** and sugar derivatives form conjugates that are analysable by HPLC. Although, the quality of the experiments suffered from low solubility and decomposition of **8**. In order to conduct experiments in the presence of the target protein ConA, it was necessary to improve the scaffold.

The ester connection at the gallic acid core is prone to hydrolysis, especially in the aqueous and basic conditions used. Therefore a more stable amide bond was introduced. Additionally the length of the glycol chain was increased to improve water solubility. Its precursor **15** was prepared following a procedure described by Bawendi *et al*. The protocol avoided the use of pyridine as reagent/solvent to tosylate the alcohol **14**. A mixture of THF and aqueous NaOH was used instead.[11] The tosyl group was then substituted by azide following standard procedures (Scheme 16).[12]

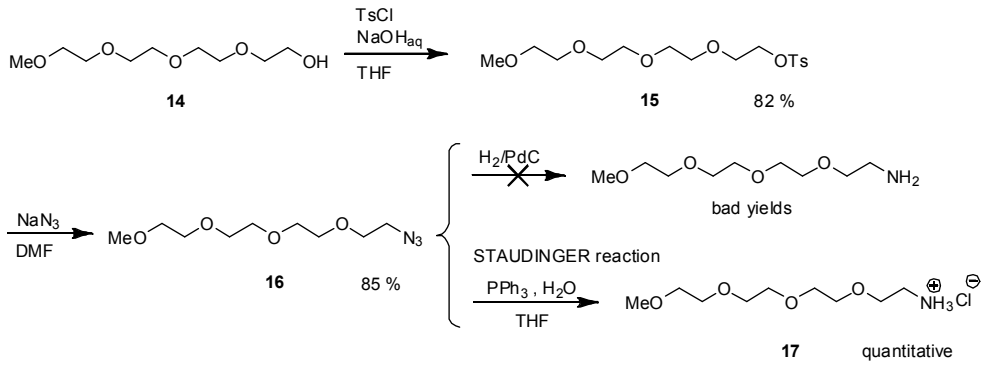

Scheme 16 *Glycol chain amination.*

Catalytic hydrogenation of azide **16** afforded the amine in low yields. On the other hand, direct amination of the tosylate with concentrated ammonia did not yield the desired product. Finally, a Staudinger protocol using triphenylphosphine afforded the desired amine **17** as its hydrochloride in quantitative yield (Scheme 16).

[11] Allen, P. M.; Liu, W.; Chauhan, V. P.; Lee, J.; Ting, A. Y.; Fukumura, D.; Jain, R. K.; Bawendi, M. G. *J. Am. Chem. Soc.* **2009**, *132*, 470.
[12] Silva Serra, M. E.; Murtinho, D.; Rocha Gonsalves, A. M. d. A. *Appl. Organomet. Chem.* **2008**, *22*, 488.

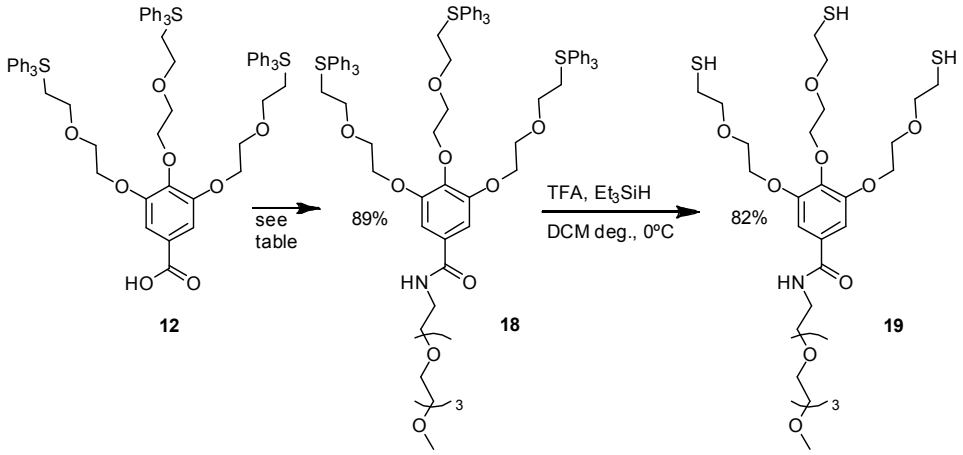

Scheme 17 *Activation of the carboxylic acid and subsequent amidation.*

A number of conditions were screened (Table 2) to couple the aminoglycol chain to the previously synthesized acid **12** (Scheme 17). The amide was most efficiently formed when a combination of EDC/HOBt as activating agents and DIPEA as base were employed. The thiol groups were deprotected in TFA/DCM (degassed) and hydride donor triethysilane was used to trap the free trityl carbocations.

Solvent	***Coupling Agents***	***Yield of 18***
DMF	HBTU, DIPEA	-
DCM	EDC, DMAP, HOBt	60 %
DCM	EDC, DMAP	50 %
DCM	EDC, HOBt, DIPEA	82 %

Table 2 *Conditions used for amidation of* ***18****.*

2.3.2.6 DCL Protein Interaction

So far, reversible covalent interchange of platform **8** and sugars (**Man**, **Gal**), did not yield detectable amounts of tris-sugar substituted conjugates (see section 2.3.2.3). However, a number of examples in the literature show that the templating effect can play a

decisive role in the evolution of a DCL.[13] As library members bind to a target (such as the protein surface) their formation becomes favoured by equilibration into an enthalpic minimum (see Introduction). In the present case, the templating target ConA was expected to shift the equilibrium. Multivalent entities like a tris-sugar conjugated scaffold (Scheme 13) could exhibit enhanced affinity. According to the general concepts of DCC, they should be produced in excess. To test this hypothesis, the different building blocks were mixed as previously described for **DCL C** with the only variation of using the alternative scaffold **19** instead of **8**. Under identical conditions as can be seen in section 2.3.2.5 sepharose immobilized ConA was added. After equilibrating this mixture for 11 days the distribution of species found in the ConA bound fraction of the library was analysed as explained earlier (see section 2.2).

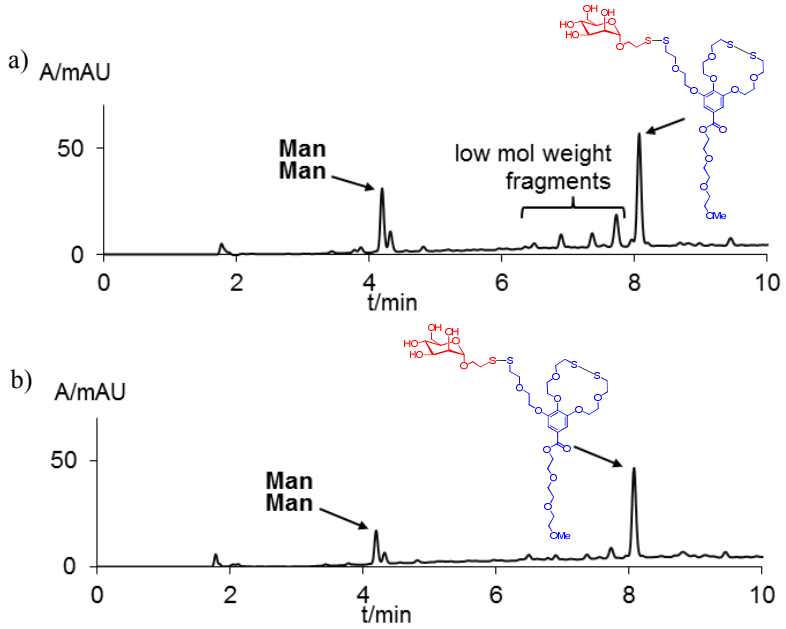

Figure 11 *Testing the influence of protein (ConA) interaction on the conjugation process between* ***Man*** *and* ***8****. a) Non-protein bound fraction. b) Protein bound fraction.*

[13] a) Nasr, G.; Petit, E.; Supuran, C. T.; Winum, J.-Y.; Barboiu, M. *Bioorg. Med. Chem. Lett.* **2009**, *19*, 6014. b) Rauschenberg, M.; Bomke, S.; Karst, U.; Ravoo, B. J. *Angew. Chem. Int. Ed.* **2010**, *49*, 7340.

Unfortunately the result was similar to the equilibration experiment conducted without the protein. No detectable amounts of tris-adducts were formed, neither in the non ConA bound, nor in the fraction cleaved from the immobilised protein (Figure 11).

Scaffold **8** and likewise **19** do not form stable enough bonds to the sugar derivatives to compete with the intramolecular ring closing. Neither does the template effect of the protein give sufficient additional thermodynamic contribution to drive the formation of higher conjugates. Thus, it became evident that the examined system does not allow formation of a multivalent DCL. On the other hand, platform **19** is still only scarcely soluble in water and therefore concentrations cannot be high enough to favour intermolecular disulphides. This renders UV-detected HPLC difficult and complicates the detection and quantification of the species present in the protein bound fraction. Better solubility would allow higher concentrations facilitating the analysis and detection of small amounts of the formed entities, but also favouring formation of higher conjugates.

2.3.3 Benzene-trithiol Scaffold

Benzene-trithiol (**20**), a commercially available compound, seemed an easy alternative to the previously used scaffolds **8** and **19**. As described before (see section 2.3.2) the three thiol groups could serve as reversible connecting points. Moreover, their direct attachment to the aromatic centre prevents intramolecular ring closing. The thio-sugar building blocks can be connected *via* disulphide bridges to form **DCL D** (Scheme 18).

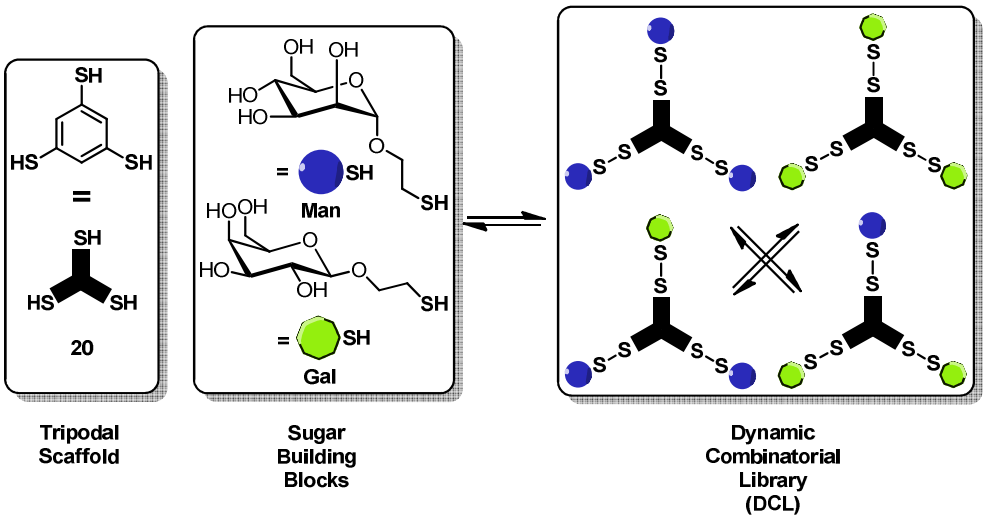

***Scheme 18 DCL D** should have formed by **Man** and **Gal** binding to platform **20**.*

As a first experiment solubility of **20** in water at different pH values was tested, showing that at pH 9 sufficient solubility for the planned experiments was achieved. However, a precipitate forms after stirring a 0.03 M solution of **20** at pH 9 for one night in the air, indicating polymerization. This could likely be prevented by using an excess of thio-sugar derivatives to compete with the polymerisation process.

2.3.3.1 Homoadduct Model

Homoconjugates of the monomeric sugars and benzene-trithiol **20** were tested first. At 0.03 M in water (pH 9), **20** was mixed with 5 eq. of thioethyl-α-D-mannopyranose (**Man**). The solution was monitored by HPLC for three weeks. However, no formation of

conjugates between the sugar building block and tripodal platform could be detected. After a few hours a precipitate formed, indicating that polymerization had taken place.

To increase solubility an analogous experiment in methanol was set-up. As for the experiment in water, a white powder precipitated after a few hours. After several weeks none of the expected library species was found by HPLC-MS analysis.

2.3.4 Tetrapropoxy-p-mercaptomethylcalix[4]arene Scaffold

Calixarene-based structures bearing covalently bound sugar moieties have been used successfully for binding sugar transforming enzymes or sugar binding lectins.[14]

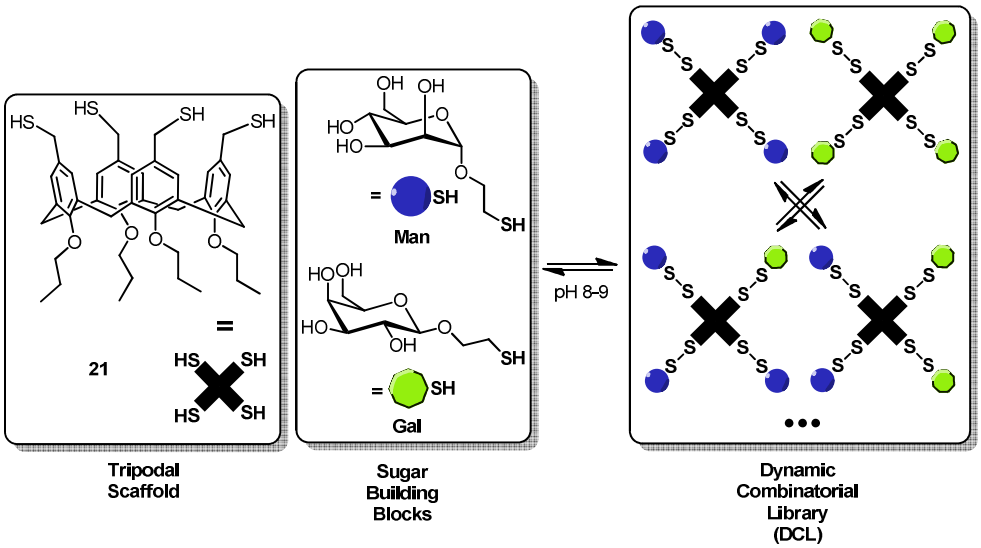

Scheme 19 DCL E *was intended to be formed by* ***Man*** *and* ***Gal*** *binding to the platform. Not all possible permutations of the DCL are shown.*

In one account Casnati *et al.* used a pentavalent calix[5]arene with covalently attached sugar pending arms to bind cholera toxin B with picomolar inhibition potency.[15] Thus, tetrapropoxy–*p*-mercaptomethylcalix[4]arene (**21**), a compound available from another

[14] Sansone, F.; Casnati, A. *Chem. Soc. Rev.* **2013**, *42*, 4623.
[15] Arosio, D.; Fontanella, M.; Baldini, L.; Mauri, L.; Bernardi, A.; Casnati, A.; Sansone, F.; Ungaro, R. *J. Am. Chem. Soc.* **2005**, *127*, 3660.

project in our laboratory, was evaluated for DCL set-up. The previously synthesised thio-pyranosides **Man** and **Gal** were used as sugar building blocks. As described earlier, a DCL (**DCL E**) would develop then by scrambling of different sugar units over the reversible disulphide bonds (Scheme 19).

2.3.4.1 Homoadduct Model

Formation of a homoconjugate of thiocalixarene **21** and one of the sugar units was first evaluated. Thus, the calixarene scaffold (0.1 M) and thioethyl-β-D-galactopyranose **Gal** were mixed in a 1/10 ratio. DMF was used initially in order to fully dissolve all the components. A second trial was conducted in water, in which the calixarene does not fully dissolve. **DCL E** members were expected to form by disulphide bonds linking platform **21** to four hydrophilic sugar moieties. Therefore formation of the library members was expected to yield water soluble entities. The two solutions (DMF and aqueous) where adjusted to pH = 8-9 by addition of NaOH. Both experiments were then monitored by HPLC and mass spectrometry over three weeks, but disappointingly no formation of sugar calixarene conjugates could be observed. Further DCL forming experiments using this calixarene (**21**) were therefore not conducted. A scaffold with higher solubility in water could more readily form the desired species (see section 2.3.5).

2.3.5 *N,N′,N′′*-(1,3,5-Benzenetriyltricarbonyl)tris-L-cysteine Scaffold

The previous attempts of forming multivalent disulphide linked species *via* a central platform (see section 2.3.2, 2.3.3 and 2.3.4) did not yield detectable amounts of higher conjugated products. Water solubility and sufficient distance between the thiol connecting points on the scaffold seemed to be crucial factors determining the formation of a multivalent DCL. Recently, the groups of Sanders and Otto described the use of an aromatic tris-cysteine derivative for the *in situ* set-up of a library of cage-like structures.[16] The building blocks were interconnected *via* disulphide bonds. The cysteine moieties

[16] a) West, K. R.; Bake, K. D.; Otto, S. *Org. Lett.* **2005**, *7*, 2615. b) Stefankiewicz, A. R.; Sanders, J. K. M. *Chem. Commun.* **2013**, *49*, 5820.

display two advantages: their thiol functionalities can reversibly connect with other thiols from thiol bearing building blocks, and the free acids strongly enhance water solubility. A further positive point is that internal oxidation has not been reported. Therefore, the scaffold employed in the study seemed ideal for the set-up of a carbohydrate decorated multivalent DCL for lectin binding.

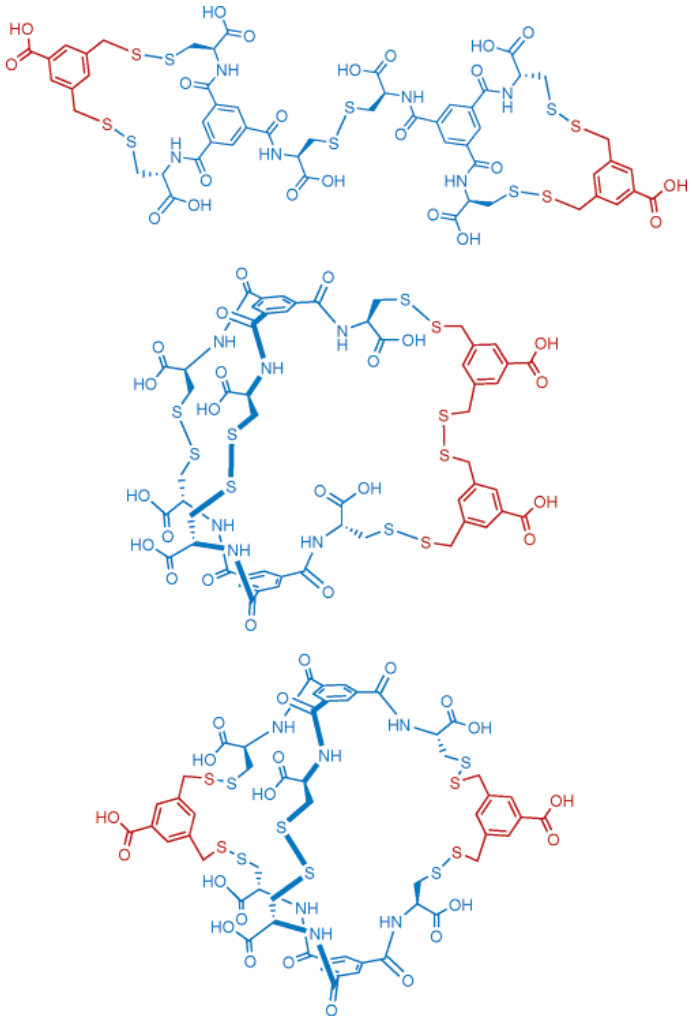

Scheme 20 *DCLs of cages formed using an aromatic tris-cysteine structure.*[15a)]

2.3.5.1 Scaffold Synthesis

The synthesis of the tris-cysteine scaffold was carried out as described in the literature with a slight variation in protecting groups. From *N*-(*tert*-butoxycarbonyl)-L-cysteine methyl ester **22** a protection/deprotection procedure afforded trityl-L-cystein methyl ester **24** in quantitative yield. Subsequently, **24** was reacted with benzene-1,3,5-tricarbonyl trichloride in DCM under basic conditions. The original protocol enables concerted removal of the protecting groups as the acid functionality is protected by a *tert*-butyl ester. However, this method requires that "ethanethiol had to be added to prevent migration of the *tert*-butyl group to the cysteine thiol".[16]

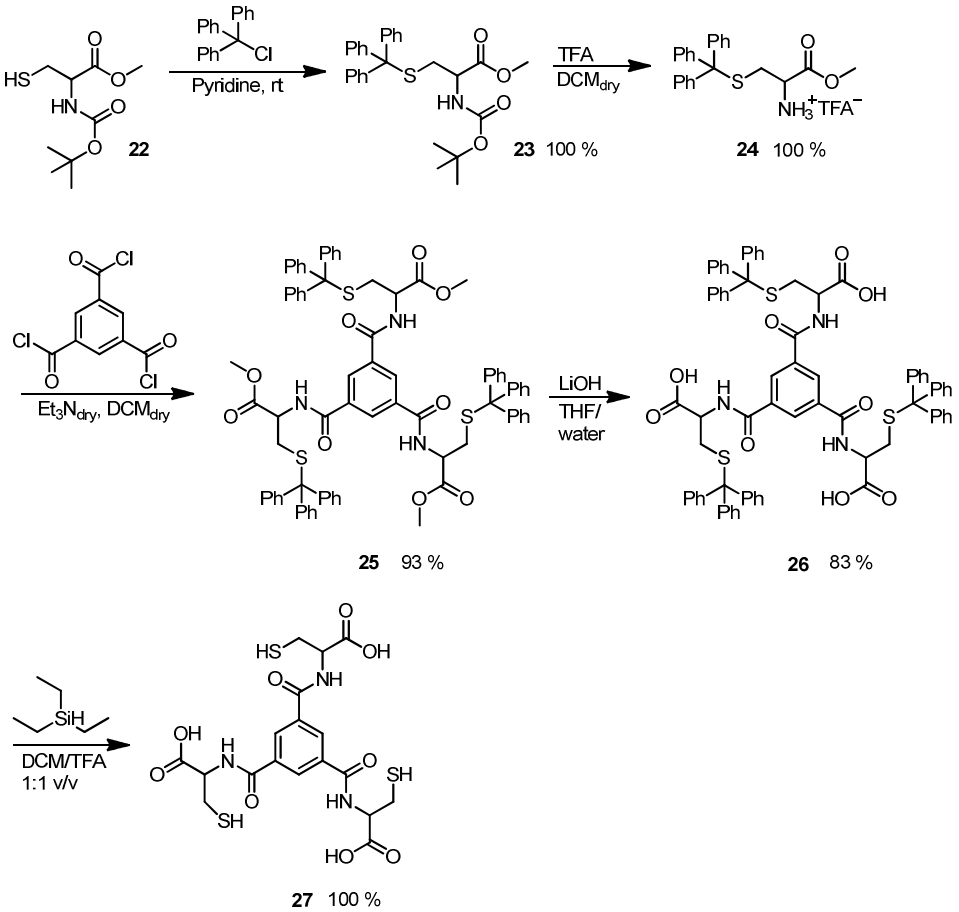

Scheme 21 *Synthesis of tris-cysteine scaffold **27**.*

In contrast, the methyl ester **24** could be orthogonally protected as a tritylthioether. This modification avoided to add (very) unpleasant ethanethiol. In a second deprotection step simple hydrolysis in a THF/water mixture containing LiOH yielded the free acid **26** in 84% yield after acidification. The trityl group was then removed under the deoxygenated conditions previously evaluated in section 2.3.2.1, yielding compound **27** quantitatively.

2.3.5.2 Homoadduct Model

The new scaffold **27** (10 mM) was mixed with **Man** (0.16 M) in water to test if a tris-homoadduct could be formed. After a few minutes, the mass of the desired tris-mannoside (structural variation **Y**, Scheme 22) could be detected from the solution.

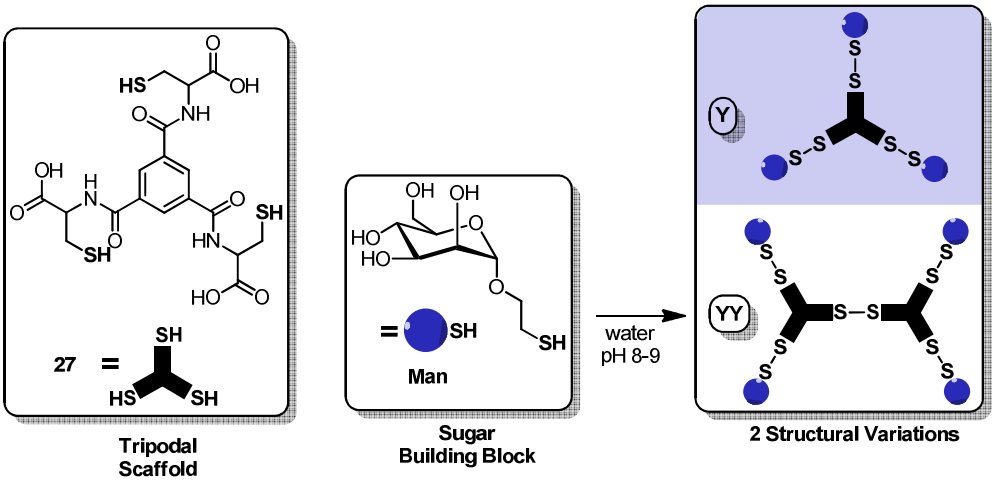

Scheme 22 *Two structural variations evolve upon mixing scaffold* ***27*** *and thioethyl-α-D-mannopyranose (****Man****).*

Besides, a second mass was visible, corresponding to a structure consisting of two scaffold molecules **27** connected *via* a disulphide bridge and four mannoside moieties decorating the remaining four cysteine thiols. This larger structural type **YY** is only visible as its dianionic mass. The HPLC chromatogram of the same mixture (Figure 12) shows two close peaks, one for the double centred tetrakis-mannoside species (**YY** type) and a

second one for the single centred tris-mannoside (**Y** type). A second experiment employing galactose **Gal** showed an analogous result at shorter retention times on the HPLC column.

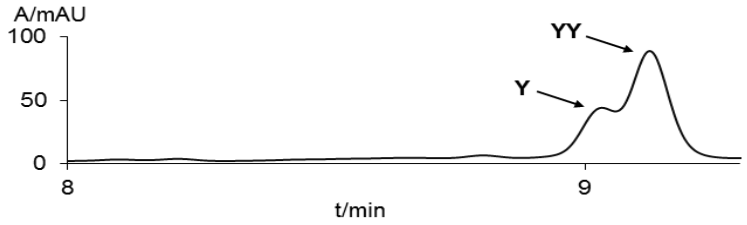

Figure 12 *Conjugates of platform* ***27*** *and thioethyl-α-D-mannopyranose (****Man****) form in two structural variations,* ***Y*** *and* ***YY****, visible as separate peaks in this HPLC chromatogram.*

A clear difference in retention times between the **Man** and the **Gal-based** structures was visible. This indicated that mixed species containing both types of sugars would be distinguishable too.

2.3.5.3 DCL Set-up and Analysis

A DCL formed by two thio-sugar derivatives arranging themselves around **Y** and dimeric **YY** should afford four arrangements for the **Y** variety and 20 for the **YY** variety (Scheme 23). The existence of stereo and regiosomers in the case of **YY** was ignored for the moment as they were not expected to be resolvable on the HPLC column. For the set-up of a **DCL F**, solutions of both chosen sugar derivatives (**Man**, **Gal**) were mixed with the central multivalent scaffold **27** in a 1:8 ratio of scaffold (10 mM) and sugar derivative (0.16 M). The solution was adjusted to a pH = 8-9 by addition of NaOH. After a few minutes a developing library was visible in the UV-detected HPLC chromatogram taken directly from the solution (Figure 13). Between the two peaks already known for each of the homo conjugates (see section 2.3.5.2) a number of new peaks were developing. After one week equilibration no more exchange was visible in the chromatogram (Figure 13a). Electrospray mass analysis (negative polarisation) showed that the UV-detected peaks (Figure 13a) correspond to masses of the expected library members. The overlay of the separate mass traces of structural type **Y** and **YY** coincide

almost exactly with the UV detected one (Figure 13b). This indicates formation of the expected **DCL F** (Scheme 23). The mass detected chromatogram for **Y** showed the expected four species resolved as peaks (Figure 13b).

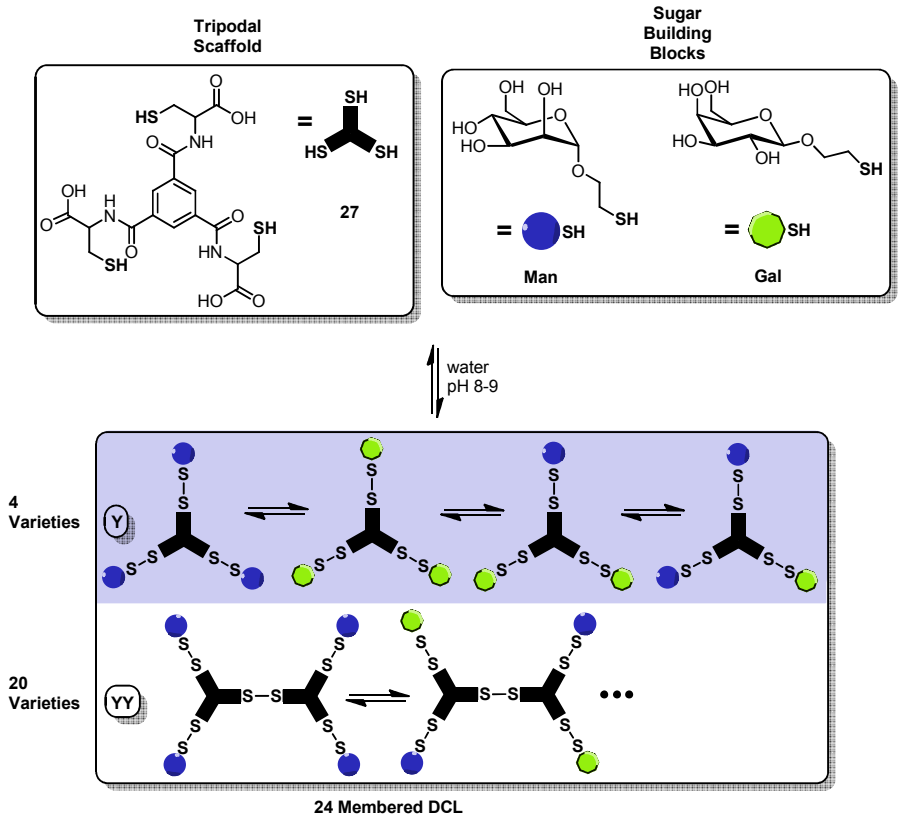

Scheme 23 *Formation of* ***DCL F*** *by conjugation of* ***Man*** *and* ***Gal*** *to scaffold* ***27****. The library members form two structural variations resulting in 4+20 members.*

For **YY** type arrangements distinct signals were visible too. However, overlapping and broadening of the peaks prevented the assignment of single species. Various gradients for the HPLC analysis were unsuccessfully evaluated to further resolve the chromatogram. To improve resolution, the **DCL F** species would have to exhibit larger differences in polarity. Likely, exchange of one of the pentahydroxy pyranoses for a mono deoxy-sugar, such as L-fucose, could increase differences in retention times and improve the separation of the peaks.

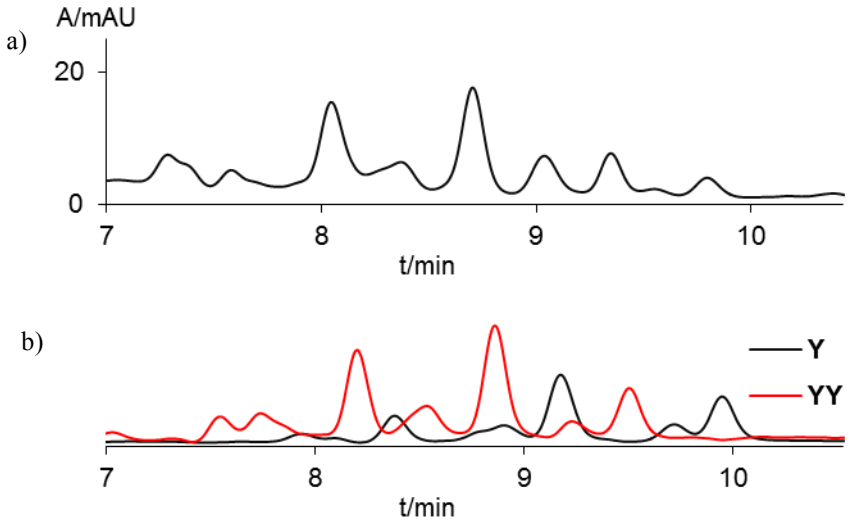

Figure 13 *HPLC analysis of* ***DCL F*** *using different detection methods- a) UV-trace of* ***DCL F****. b) Separate MS-traces for structural types* ***Y*** *and* ***YY****.*

2.3.5.4 DCL F with Protein Interaction

To test if particular species of the library could be selectively extracted by the target protein (ConA) the procedure described in section 2 was applied. **DCL F** (1.3 mM) (Scheme 23) and sepharose-bound ConA (0.26 mM) solutions were mixed in a 5:1 ratio. After one week equilibration the protein bound fraction was separated and analysed. Despite the high concentration of library members used and their good absorption in the UV detector the detectability was very poor. This and the above mentioned problems of overlapping peaks made an interpretation of the chromatogram impossible.

In view of the failure to analyse protein interactions we decided not to further pursue this part of the project. Nevertheless, we demonstrated that identification of the library members was possible and several of the previously encountered problems, such as internal oxidation, lack of solubility or polymerisation had not occurred. Therefore a similar system based on this approach could still successfully yield a DCL enabling also the determination of affinities to the protein.

2.3.6 Conclusions

The known concept of dynamic exchange of building blocks over disulphide bridges is easily applicable for lectin binding, using systems that form small dimeric constituents. This has also been demonstrated in this section.

As soon as scaffolds were employed to allow for a multivalent dynamic exchange, problems occurred. The oxidation reactions do not only take place with building blocks but also the connectors on the scaffolds are prone to react with each other. This caused internal bridging or in another case polymerisation of scaffold subunits seemed to take place. The introduction of cysteine moieties helped overcoming the problem of water solubility and gave more flexibility in the choice of concentrations.

Nevertheless, practical issues prevailed. Unwanted bridging complicated the developing DCLs and made analysis tedious. The large structures formed by the scrambling process do not appear to be stable enough, to be easily detectable after going through the analytical procedure. Though, more fine-tuned experimental conditions may render such analysis possible. Even so, the different types of arrangements shown in section 2.3.5.3 are not equally stable. Their abundance in a lectin bound fraction would therefore not only be related to their affinity towards the protein. For those reasons we considered other ways to access multivalent dynamic exchange of binding sugar moieties for lectin binding.

2.4 Imine-based Dynamic Exchange

The well-established disulphide approach for DCLs caused difficulties when it was applied on the systems described in section 2.3. Intramolecular oxidation or interconnection of the multivalent scaffolding entities hampered the evolution of multivalent entities or their analysis. To avoid this, a reversible binding mode which relies on different functionalities between scaffold and building blocks was evaluated.

Primary amines react with aldehydes to form imines in a reversible reaction. The groups of Barboiu,[13] Lehn and Ramström have used the process for a variety of applications in dynamic combinatorial chemistry.[17] The resulting Schiff bases are labile, although reduction to the respective amine can "lock" the DCL members in their original ratios.

2.4.1 Tetrahydroxy-p-formylcalix[4]arene Scaffold and Sugar Building Blocks

An upper rim tetraformylcalix[4]arene **28** was chosen to serve as a scaffold. On the other hand, the synthesis of two sugar derivatives is described in Chapter 3. The free pyranosides were prepared in quantitative yields by stirring the acetyl protected precursors for two hours in MeOH containing sodium methoxide followed by acidification with acidic ion exchange resin.

[17] a) Herrmann, A. *Org. Biomol. Chem.* **2009**, *7*, 3195. b) Ramström, O.; Lohmann, S.; Bunyapaiboonsri, T.; Lehn, J.-M. *Chem. Eur. J.* **2004**, *10*, 1711. c) Hafezi, N.; Lehn, J.-M. *J. Am. Chem. Soc.* **2012**, *134*, 12861.

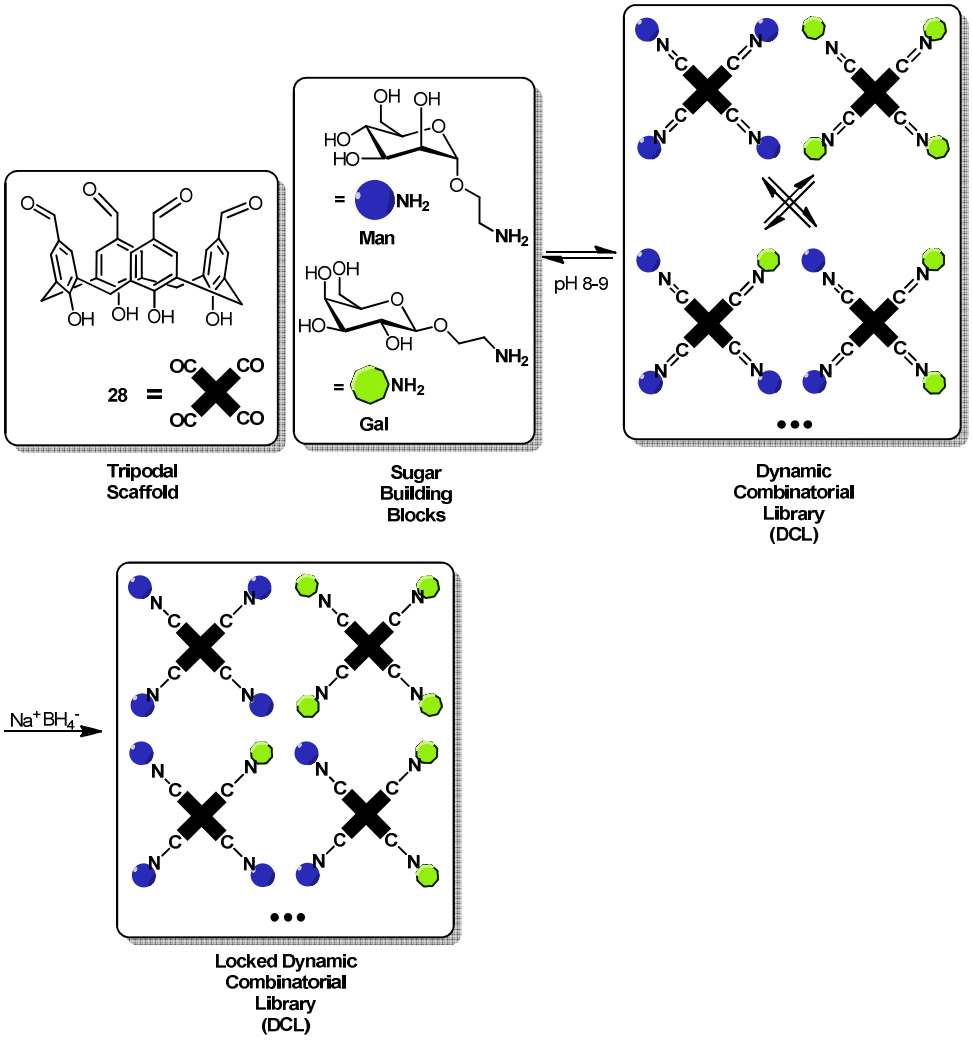

***Scheme 24** Formation of a **DCL G** by imine exchange on tetraformylcalixarene **28**.*

2.4.1.1 Reaction with a Phenol as a Calixarene Model

To test if imine formation and subsequent reduction would be feasible using formylcalixarene **28**, 4-hydroxy-3,5-dimethylbenzaldehyde **29** was employed as a model compound.

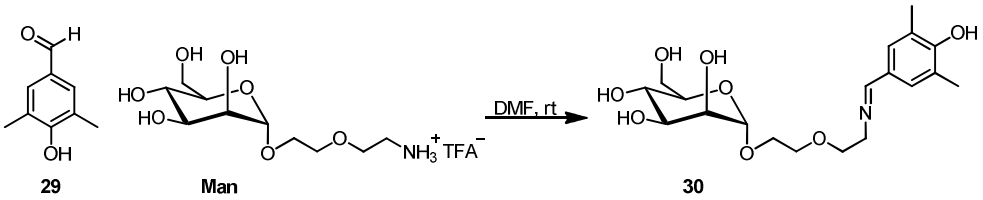

Scheme 25 *Imine formation using a phenol as a calixarene model compound.*

The reaction was tested at different temperatures (rt-60 ºC), different concentrations (0.05 M - 0,3 M of aldehyde) and different ratios between the two components **29** and the D-mannoside derivative. All trials successfully yielded the expected imine **30** without visible side products (*in situ* HPLC-MS analysis). Therefore, room temperature and stoichiometric ratios of the reaction partners seemed adequate.

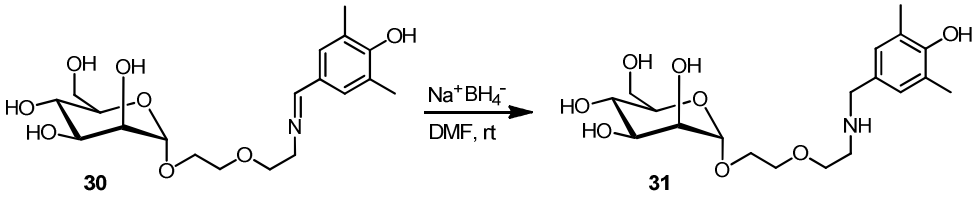

Scheme 26 *Imine reduction to "lock" the current structure.*

In situ reduction of the imine **30** to amine **31** in order to lock the arrangement in an irreversible manner was achieved by action of sodium borohydride in DMF at room temperature. HPLC-MS analysis of the reaction mixture indicated full transformation to the amine.

2.4.1.2 Homoadduct Model

A 0.1 M solution of calixarene **28** and a 0.8 M solution of the D-mannoside derivative were mixed to test the formation of a homoconjugate. Two experiments were run, the first in DMF and the second in water. After two hours MS analysis was performed, directly injecting from the DMF solution, showings trace amounts of mono **32** , bis **33** and tris **34** conjugated products (Scheme 27). A tetrakis-conjugate **35** was not observed. Detection of corresponding peaks by UV and mass traced HPLC chromatograms was unsuccessful, the amounts of compounds being too low. Further trials included addition of 1 eq. TFA per formyl group or heating the mixture at 50ºC. Formation of larger amounts of higher conjugates was still not observed.

Unfortunately, the experiment in water did not give any observable response by ESI mass spectrometry. It was assumed that the calixarene would transfer into the aqueous phase upon formation of the imine bonds to the hydrophilic sugar moieties, Apparently, solubility of the connecting platform is crucial.

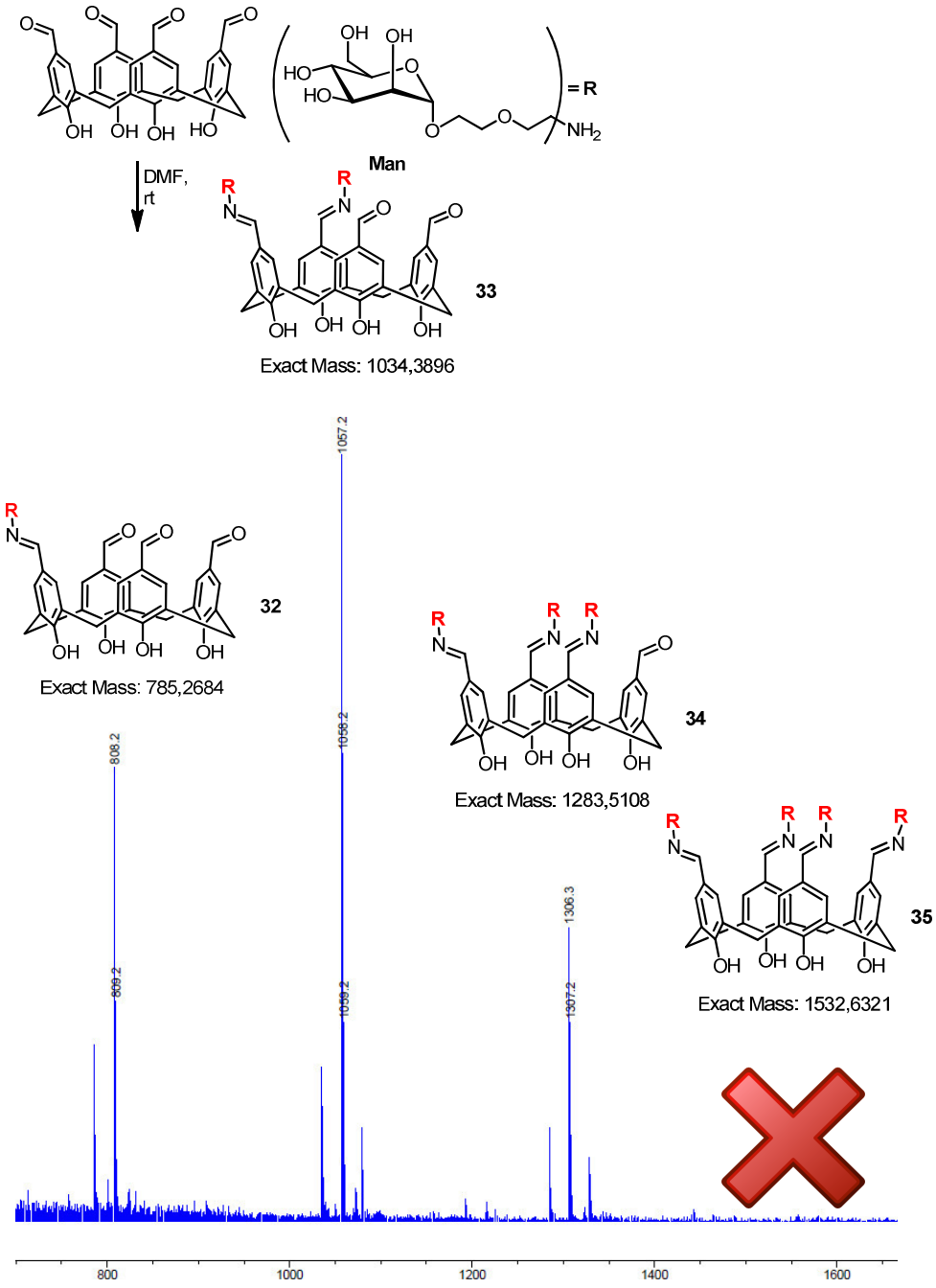

Scheme 27 *Partial formation of* ***DCL G*** *observed by mass spectrometry.*

2.4.2 Conclusions

The reversible exchange over imine bonds was chosen to avoid interactions of the connectors on the scaffold molecule. Model systems for a calixarene-type platform gave promising results. A calix[4]arene was chosen as a multivalent platform, offering four aldehyde units as connecting points for imine formation.

Water solubility of the scaffold was again insufficient. Using an alternative solvent, trace amounts of partial adducts were then found.

The result showed that multivalent conjugation of the imine platform with amine sugar building blocks is generally possible. However, the system is not ready to be used for lectin recognition. Water solubility is crucial and would require more synthetic effort, like addition of long glycol chains on the lower rim.

In view of the negative results, due to incomplete transformation of the reacting partners, the imine approach to multivalent DCL employing calixarene scaffold **28** was abandoned.

2.5 Experimental Section

Materials and methods

All reagents were commercial and used without further purification. Triethylamine was distilled over CaH_2. If not stated differently all reactions were performed under an argon atmosphere using dry solvents and flame dried reaction vessels. NMR spectra were recorded at 293 K, using 300, 400 or 500 MHz spectrometers. Deuterated solvents used are indicated in each case. Shifts are referenced relative to deuterated solvent residual peaks. Complete signal assignments from 1D and 2D NMR spectroscopy were based on COSY, HSQC correlations and phase sensitive DEPTQ45, DEPTQ135 spectra. High-resolution electrospray injection times of flight (HR-ESI-ToF) mass spectra were recorded using a Bruker spectrometer. Anhydrous solvents were obtained from a solvent purification system (SPS). Thin layer chromatography (TLC) was performed on pre-coated TLC-plates SIL G-25 UV254 (Macherey-Nagel) glass supported with detection by UV at 254 nm and/or Pancaldi, Vanilin or KMnO4 stain. Column chromatography was carried out using silica gel from SDS (Silica Gel 60 A) and SDS (Silica Gel C18 “reverse phase” 60A, 40–63 μm). For automated flash column chromatography a CombiFlash Companion apparatus running RediSep® columns was used. High-Pressure Liquid Chromatography (HPLC) chromatograms were recorded on an Agilent Technologies 1200 (UV-detector) and an Agilent Technologies 6130 Quadropole Liquid chromatography/mass (LC/MS) detector (recording in ESI mode) connected to and analytical HPLC running a reverse phase (RP) C18 Waters Symetry 300TM C18 5μm. The mobile phase consisted of a CH_3CN–H_2O mixture containing 0.1 % TFA. The solvents were provided by Scharlau and Carlo Erba (HPLC gradient grade).

Generation and analysis of the dynamic combinatorial libraries A, B, C, D, E, F (Sections 2.3.1.1, 2.3.1.2, 2.3.2.3, 2.3.3, 2.3.4 and 2.3.5)

Aqueous solutions of **Man**, **Gal** or **Fuc** were set-up in deoxygenated water (concentrations are stated in the respective paragraphs 2.3.1.1, 2.3.1.2, 2.3.2.3, 2.3.3, 2.3.4 and 2.3.5). For DCL generation the solutions were mixed in equal volumes and equilibrated (times are stated in the corresponding paragraph 2.3.1.1, 2.3.1.2, 2.3.2.3, 2.3.3, 2.3.4 and 2.3.5).

For platform based DCL set-ups the respective sugar derivatives were mixed with the platforms in different solvents and at different pH values (as stated in the corresponding paragraphs 2.3.2.3, 2.3.3, 2.3.4 and 2.3.5).

Reference samples

For reference samples the same amounts of pure solvent was added as in the respective binding experiment using ConA suspension.

ConA interaction analysis of **DCL A, B, C, D, E** (Sections 2.3.1.1, 2.3.1.2, 2.3.2.3, 2.3.3 and 2.3.4)

The previously prepared solutions of protein binders (DCLs or single binders) were mixed with Con A-sepharose suspension in a 20:1 relation, binders/ConA (respective to ConA monomers).

The mixtures were then agitated for the time stated in the respective paragraph. After equilibration the suspension was filtered (Millipore Ultrafiltration Membrane YM100). The sepharose particles on the filter membrane were then re-suspended in HCl (0.5 M, same volume as the original mixture) to release the bound complexes, after renewed filtration the filtrate was analysed by HPLC-MS (see below).

HPLC experiments

The library compositions were analysed by RP-HPLC-MS (column: Waters Symmetry 300TM C18 5μm). The elution was monitored with a UV detector (see above) set at 254 nm. Masses of the eluting peaks were determined using electrospray injection in positive or negative polarisation.

Injection volume:		10 µl		
Eluent:		H_2O(0.1% TFA)	/	MeOH(0.1% TFA)
Gradient:	0 min	95%	/	5%
	20 min	0%	/	100%

ConA interaction analysis of **DCL F** (Section 2.3.5)

DCL F was mixed with Con A-sepharose suspension in a 5:1 relation, **DCL F**/ConA (respective to ConA monomers).

HPLC experiments for **DCL F**

The library compositions were analysed by RP-HPLC-MS (column: Waters Symmetry 300TM C18 5µm). The elution was monitored with a UV detector (see above) set at 254 nm. Masses of the eluting peaks were determined using electrospray injection in negative polarisation.

Injection volume:		10 µl		
Eluent:		H_2O(0.1% TFA)	/	AcN(0.1% TFA)
Gradient:	0 min	88%	/	12%
	15 min	75%	/	25%
	17 min	0%	/	100%

Synthesis

α/β-D-Mannose pentaacetate (1), **α/β-D-Galactose pentaacetate (5)**, **1,2,3,4-tetraacethyl-β-L-fucopyranose** were prepared according to standard procedures.[18]

Acetylthioethyl 2,3,4,6-tetra-O-acetyl-α-D-mannopyranoside (3)

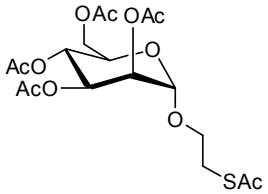

Chloroethyl 2,3,4,6-tetra-O-acetyl-α-D-mannopyranoside (**4**) (2.1 g, 5.1 mmol) was dissolved in butanone (50 ml). Potassium thioacetate (4.1 g, 36.0 mmol) and potassium iodide (0.68 g, 4.1 mmol) where added and the mixture was stirred overnight at 80 ºC. Then solvent was evaporated and the residue was dissolved in DCM and water. The organic phase was washed with 0.5 M HCl and then evaporated to afford dark red syrup. TLC analysis in PE/EA 1:1 was used to determine a gradient for automated flash chromatography. **Yield:** 1.5 g, 64 % - **^{1}H-NMR:** (400 MHz, $CDCl_3$) δ_H= 5.26-5.31 (m, 2 H, H-3 H-4); 5.24 (m, 1 H, H-2), 4.83 (s, 1 H, H-1), 4.24 (dd, 1 H, $J_{H6a,H5}$= 5.3 Hz, $J_{H6a,H6b}$= 12.2 Hz, H-6a), 4.09 (dd, 1 H, $J_{H6b,H5}$= 1.9, $J_{H6b,H6a}$= 12.2 Hz, H-6b), 4.01-4.06 (m, 1 H, H-5), 3.74 (m, 1 H, CH_2), 3.59 (m, 1 H, CH_2), 3.10 (t, 2 H, $J_{H,H}$= 6.3 Hz, CH_2), 2.36 (s, 3 H, MeCOS), 2.15, 2.09, 2.05, 1.99 (s, 3 H, CH_3CO) ppm. Spectroscopic data was found to be in agreement with literature.[8]

[18] Kramer, J. R.; Deming, T. J. *J. Am. Chem. Soc.* **2010**, *132*, 15068.

Chloroethyl 2,3,4,6-tetra-O-acetyl-α-D-mannopyranoside (4)

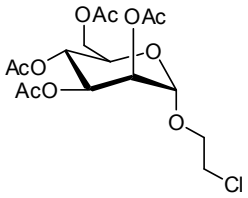

α/β-D-Mannose pentaacetate (2.8 g, 7,17 mmol) was dissolved in dry DCM (24 ml) and chloroethanol (0,63 ml, 9,33 mmol) was added. The solution was cooled to 0 ºC and BF_3Et_2O (4.07 g, 3.53 ml, 28.9 mmol) was added slowly. After half an hour the reaction was allowed to reach room temperature and stirring was continued overnight. The mixture was poured onto ice and the aqueous phase was extracted with DCM. The combined organic extracts where washed with brine and water and were then evaporated. Column chromatography yielded the pure product. **Yield:** 2.0 g, 67 % - **^{1}H-NMR:** (400 MHz, $CDCl_3$) δ_H= 5.26–5.38 (m, 3 H, H-2, H-3, and H-4), 4.91 (d, 1 H, $J_{H1,H2}$= 1.5 Hz, H-1), 4.29 (m, 1 H, H-6_b), 4.17 (m, 1 H, H-6_a), 4.13 (m, 1 H, H-5), 3.95 (dt, 1 H, $J_{H,H}$= 5.8 Hz and J_{HaHb}= 11.1 Hz, $OCH_aH_bCH_2Cl$), 3.83 (dt, 1 H, $J_{H,H}$= 5.3 Hz and J_{HaHb}= 10.8 Hz, $OCH_aH_bCH_2Cl$), 3.67 (apparent t, 2H, J= 5.8 Hz, OCH_2CH_2Cl), 2.03, 2.09, 2.14, 2.20 (s, 3 H, CH_3CO), ppm. Spectroscopic data was found to be in agreement with literature.[19]

Chloroethyl 2,3,4,6-tetra-O-acetyl-β-D-galactopyranoside (6)

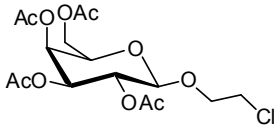

α/β-D-Galactose pentaacetate (2.8 g, 7.2 mmol) was dissolved in dry DCM (40 ml), chloroethanol (0.75 g, 0,626 ml, 9,33 mmol) was added and the solution was cooled to 0 ºC. Then BF_3Et_2O (4.07 g, 3.53 ml, 28.9 mmol) was slowly introduced and the mixture was allowed to reach room temperature. After stirring overnight TLC (ethyl

[19] Zhao, Y.; Tram, K.; Yan, H. *Carbohydr. Res.* **2009**, *344*, 2137.

acetate/hexane, 2:1) indicated full transformation of the starting material and a pure product. The solution was poured onto ice and the organic phase was washed with $NaHCO_3$ solution and water. After drying the organic phase over $MgSO_4$ it was evaporated. Recrystallization yielded colourless crystals. **Yield:** 2.0 g, 62 % - **^{1}H-NMR:** (400 MHz, $CDCl_3$) δ_H= 5.39 (dd, 1 H, $J_{H4,H5=}$ 1 Hz, $J_{H3,H4=}$ 3.4 Hz, H-4), 5.22 (dd, 1 H, $J_{H1,H2=}$ 7.9 Hz, $J_{H2,H3}$= 10.5 Hz, H-2), 5.02 (dd, 1 H, $J_{H3,H4}$= 3.4 Hz, $J_{H2,H3}$= 10.5 Hz, H-3), 4.54 (d, 1 H, $J_{H1,H2}$= 7.9 Hz, H-1), 4.20–4.09 (m, 3H, H-6a, H-6b, 1 H from OCH2), 3.92 (td, 1 H, $J_{H4,H5}$= 1.3 Hz, $J_{H5,H6a}$= $J_{H5,H6b}$= 6.7 Hz, H-5), 3.76 (ddd, 1 H, *J*= 6.6 Hz, *J*= 6.6 Hz, *J*= 11.1 Hz, 1H from OCH2), 3.64–3.51 (m, 2 H, CH_2Cl), 2.15, 2.07, 2.04, 1.98 (s, 3 H, CH_3CO) ppm. Spectroscopic data was found to be in agreement with literature.[20]

Acetylthioethyl 2,3,4,6-tetra-O-acetyl-β-D-galactopyranoside (7)

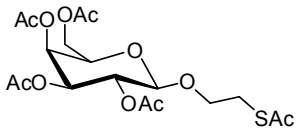

Chloroethyl 2,3,4,6-tetra-O-acetyl-β-D-galactopyranoside (**6**) (2.37 g, 5,7 mmol) was dissolved in butanone (60 ml). Potassium thioacetate (4.61 g, 40.4 mmol) and potassium iodide (0.76 g, 4.6 mmol) where added. The mixture was heated to reflux overnight. Then solvent was evaporated and the residue was dissolved in DCM. Solid residues where filtrated over celite and the organic filtrate was washed with water and slightly acidified water and was then evaporated. The crude residue was purified by column chromatography. **Yield:** 2.2 g, 85 % - **^{1}H-NMR:** (400 MHz, $CDCl_3$) δ_H= 5.38 (dd, 1 H, $J_{H4,H5}$= 0.9 Hz, $J_{3,4}$= 3.5 Hz, H-4), 5.19 (dd, 1 H, $J_{H1,H2}$= 7.9 Hz, $J_{H2,H3}$= 10.6 Hz, H-2), 5.01 (dd, 1 H, $J_{H3,H4}$= 3.4 Hz, $J_{H2,H3}$= 10.4 Hz, H-3), 4.49 (d, 1 H, $J_{H1,H2}$= 7.9 Hz, H-1), 4.19–4.09 (m, 2 H, H-6a, H-6b, and 1 H from OCH_2), 3.92 (td, 1 H, $J_{H4,H5}$= 1.3 Hz, $J_{H5,H6}$= $J_{H5,H6a}$= 6.7 Hz, H-5), 3.76 (ddd, 1 H, $J_{H,H}$= 6.6 Hz, $J_{H.H}$= 6.6 Hz, $J_{H,H}$= 11.1 Hz, 1 H from OCH2), 3.64–3.51 (m, 2 H, CH_2Cl), 2.15, 2.07, 2.04, 1.98 (s, 3 H, CH_3CO) ppm.

[20] Xue, J. L.; Cecioni, S.; He, L.; Vidal, S.; Praly, J.-P. *Carbohydr. Res.* **2009**, *344*, 1646.

Spectroscopic data was found to be in agreement with literature.[21]

Mercaptoethyl α-D-mannopyranoside (Man)

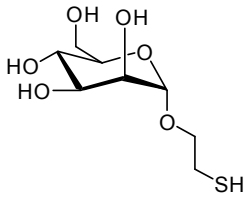

Acetylthioethyl 2,3,4,6-tetra-O-acetyl-α-D-mannopyranoside (**3**) (232 mg, 0,52 mmol) was dissolved in methanol (1 ml) previously deoxigenised with argon. Then sodium methoxide (28 mg, 0,52 mmol) was added and the mixture was stirred for 90 min, until TLC (MeOH/DCM 1:10) indicated full transformation of the starting material. The solution was then acidified with Dowex® 50WX8 hydrogen form ion exchange resin. After filtration the solvent was evaporated to yield the pure product. **Yield:** 148 mg, 35 % - **^{1}H-NMR:** (400 MHz, $CDCl_3$) δ_H= 2.70 (t, 2 H, $J_{H,H}$= 6.4 Hz, OCH_2CH_2SH), 3.56-3.86 (complex, 8 H, H-2, -3, -4, -5, -6a, -6b, $OCH_aH_bCH_2SH$, $OCH_aH_bCH_2SH$), 4.80 (d, 1 H, $J_{1,2}$= 1.46 Hz, H-1) ppm. Spectroscopic data was found to be in agreement with literature.[5]

Thioethyl 2,3,4,6-tetra-O-acetyl-β-D-galactopyranoside (Gal)

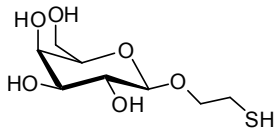

Acetylthioethyl 2,3,4,6-tetra-O-acetyl-β-D-galactopyranoside (**7**) (232 mg, 0,52 mmol) was dissolved in dry methanol (4 ml) previously deoxigenised with argon. Then sodium methoxide (56 mg, 1,03 mmol) was added and the mixture was stirred for 90 min, until TLC (MeOH/DCM 1:5) indicated complete transformation of the starting material. The

[21] Schofield, C. L.; Mukhopadhyay, B.; Hardy, S. M.; McDonnell, M. B.; Field, R. A.; Russell, D. A. *Analyst* **2008**, *133*, 626.

solution was then acidified with Dowex® 50WX8 hydrogen form ion exchange resin and the mixture was filtrated after 30 min. Evaporation of solvent yielded the product that could be used without further purification. **Yield:** 88 mg, 71 % - **^{1}H-NMR:** (400 MHz, D_2O) δ_H= 4.43 (d, 1 H, $J_{H1,H2}$= 7.6 Hz, H-1), 4.17 (m 1 H, C*Ha*Hb-SH) ,3.96 (m, 1 H, O-CHa*Hb*-SH), 3.91 (bd, 1 H, $J_{H3,H4}$= 3.6 Hz, H-4), 3.81-3.72 (m, 2 H, H-6a, H-6b), 3.68 (dd, 1 H, $J_{H3,H2}$= 9.6 Hz, $J_{H3,H4}$= 3.6 Hz H-3), 3.51 (dd, 1 H, $J_{H1,H2}$= 7.6 Hz, $J_{H2,H3}$= 9.6 Hz H-2), 3.01 (m, 2 H, CH_2) ppm. Spectroscopic data was found to be in agreement with literature.[3]

Mercaptoethyl β-L-fucopyranoside (Fuc)

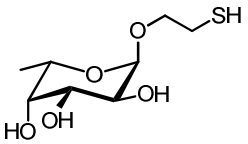

To a solution of 1,2,3,4-tetraacethyl-β-L-fucopyranose (1.0 g, 3.0 mmol) and 2-bromoethanol (0.26 ml, 0.46 g, 3.8 mmol) in dry CH_2Cl_2 (5 mL) at 0ºC, was added dropwise $BF_3.Et_2O$ (1.9 ml, 2.12 g, 15.1 mmol). Then the reaction was allowed to warm to room temeperature and was stirred for 15 hours. Once the reaction was finished, the solution was poured into ice water (~10 mL) and was then extracted with CH_2Cl_2. The combined organic fractions where washed with aqueous $NaHCO_3$ and water and dried over $MgSO_4$. Purification by column chromatography afforded **Bromoethyl 2,3,4-tri-*O*-acetyl-β-L-fucopyranose** as dark red syrup. **Yield:** 0.43 g, 36 % - **^{1}H-NMR:** (400 MHz, $CDCl_3$) δ_H= 5.34 (m, 2 H, H-4, H-3), 5.12 (m, 2 H, H-1, H-2), 4.27 (m, 1 H, H-5), 4.00 (td, 1 H, $J_{Ha,Hb}$= 11.5 Hz, $J_{vincinal}$= 5.74 Hz, C*H*$_a$H$_b$), 3.83 (td, 1 H, $J_{Ha,Hb}$= 11.48 Hz, $J_{vincinal}$= 5.74 Hz, CH$_a$*H*$_b$), 3.50 (t, 2 H, $J_{H,H}$= 5.74 Hz, C*H*$_2$), 2.15, 2.08, 1.98 (s, 3 H, CH_3CO), 1.14 (d, 3 H, *J*= 6.61 Hz, C*H*$_3$) ppm. Spectroscopic data was found to be in accordance to literature data.[21]

Bromoethyl 2,3,4-tri-O-acetyl-β-L-fucopyranose (0.433 g, 1.1 mmol) in butanone (10 ml) containing potassium thioacetate (0.87 g, 7.6 mmol) was heated to reflux (80ºC) for 3 h. The mixture was then filtered through celite. The filtrate was evaporated to dryness and the

residue was dissolved in EtOAc. The mixture was washed with water, subsequent evaporation of the solvent and purification by column chromatography yielded **Acetylthioethyl 2,3,4-tri-*O*-acetyl-β-L-fucopyranoside** as dark red syrup. **Yield:** 0.378 g, 88 % - **^{1}H-NMR:** (400 MHz, $CDCl_3$) δ_H= 5.32 (m, 2 H, H-4, H-3), 5.08 (m, 2 H, H-1, H-2), 4.45 (apparent q, 1 H, J= 6.5 Hz, H-5), 4.79 (td, 1 H, $J_{Ha,Hb}$= 10.46 Hz, $J_{vincinal}$= 6.43 Hz, CH_aH$_b$), 3.83 (td, 1 H, $J_{Ha,Hb}$= 10.46 Hz, $J_{vincinal}$= 6.12 Hz, CH$_a$$H_b$), 3.50 (t, 2 H, $J_{H,H}$= 6.12 Hz, CH_2), 2.32 (s, 3 H, SC(O)CH_3), 2.14, 2.07, 1.97 (s, 3 H, CH_3CO), 1.12 (d, 3 H, J= 6.61 Hz, CH_3) ppm. **^{13}C-NMR:** (400 MHz, $CDCl_3$) δ_C= 195.08 (*C*H$_3$COS), 169.20, 169.84, 169.73 (3 × *C*O), 96.22 (*C*-1), 71.10, 68.12, 67.96, 66.98 (3 × *C*H), 64.62 (*C*H$_2$CH$_2$SAc), 30.53 (*C*H3COS), 28.86 (*C*H$_2$SAc), 20.84, 20.69, 20.63 (3 × CO*C*H$_3$), 15.84 (*C*H$_3$) ppm. **IR:** $\tilde{\nu}$= 1649, 1591, 1550, 1441, 1311, 1058, 878, 801, 760, 676 cm^{-1}. **MS (TOF, ES$^+$)** *m/z*= 415.1 [M+Na$^+$].

Acetylthioethyl 2,3,4-tri-*O*-acetyl-β-L-fucopyranose (400 mg, 1,019 mmol) was dissolved in dry methanol (previously bubbled with argon). Sodium methoxide (110 mg, 2,04 mmol) was added and the mixture was stirred for 60 min. The solution was acidified with Dowex50WX8-200 hydrogen form ion exchange resin and filtrated. The filtrate was evaporated and washed with DCM. Then the aqueous phase was evaporated to yield **2-Mercaptoethyl β-L-fucopyranoside (Fuc)**. **Yield:** 100 mg, 43 % - δ_H= **NMR:** (400 MHz, $CDCl_3$) δ_H= 4.87 (d, 2 H, $J_{H1,H2}$= 3.0 Hz, H-1), 4.08-4.13 (m, 2 H, CH_2), 3.65-3.86 (m, H-2, H-3, H-4, H-5) 2.77 (dd, 2 H, $J_{H,H}$= 3.0 Hz, $J_{(H,H)}$= 6 Hz, CH_2), 1.28 (d, 3 H, $J_{H6,H5}$= 7 Hz, CH_3) ppm. All spectroscopic results were in accordance to literature data.[22]

2-(2-(tritylthio)ethoxy)ethyl 4-methylbenzenesulfonate (10)

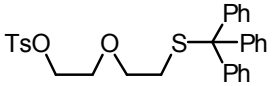

Under inert conditions triphenylmethanethiol (6.66 g, 24.1 mmol) was dissolved in THF

[22] Takahashi, T.; Tanaka, H.; Matsuda, A.; Doi, T.; Yamada, H. *Bioorg. Med. Chem. Lett.* **1998**, *8*, 3299.

and NaH (0.87 g, 60 % in mineral oil, 36.2 mmol) was added portion-wise at 0º C. After stirring for 60 min the mixture was slowly (within 60 min) introduced into a cooled (0º C) solution of diethylenglycol ditosylate (10 g, 24,1 mmol) in THF. Then the mixture was allowed to warm to room temperature and was stirred for 48 h. Remaining NaH was quenched with water (5 ml) and the solvent mixture was evaporated as an azoetrope under reduced pressure. The residue was triturated with chloroform and water was added. The organic phase was washed with water and brine and was evaporated under vacuum. Purification by column chromatography afforded the pure product as colourless oil. **Yield:** 6.97 g, 55.69 %. - **^{1}H-NMR:** (400 MHz, CDC_3) δ_H= 7.81–7.22 (m, 19 H, Ar*H*) 4.12 (t, 2 H, $J_{H,H}$= 4.97 Hz, CH_2), 3.51 (t, 2 H, $J_{H,H}$= 4.97 Hz, CH_2), 3.24 (t, 2 H, $J_{H,H}$= 6.75 Hz, CH_2), 2.45 (s, 3 H, CH_3), 2.40 (t, 2 H, J= 6.7 Hz, CH_2) ppm. **^{13}C-NMR:** (400 MHz, $CDCl_3$) δ_C= 144.75, 132.98, 129.81, 129.61, 127.98, 126.71 (Ar*C*), 69.73, 69.04, 68.15, 66.68 (*C*H_2), 31.59 (S*C*), 21.65 (*C*H_3) ppm. **MS (TOF, ES+)** *m/z*= 541.14 [M+Na]. Spectroscopic data was found to be in agreement with literature.[23]

Methyl 3,4,5-tris(2-(2-(tritylthio)ethoxy)ethoxy)benzoate (11)

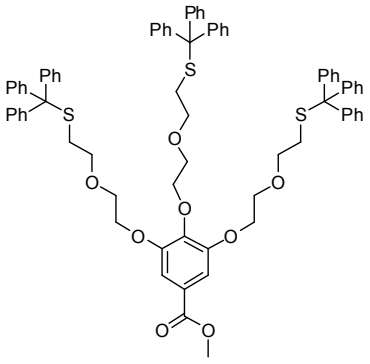

A mixture of methyl gallate (0.62 g, 3.37 mmol), 2-(2-(tritylthio)ethoxy)ethyl4-methylbenzenesulfonate (**10**) (7 g, 13.50 mmol) and potassium carbonate (8.39 g, 60.72 mmol) in dry DMF (70 ml) was stirred under reflux (80 ºC) for 48 h. After removal of DMF in *vacuo*, the residue was dissolved in CH_2Cl_2. The organic phase was sequentially

[23] Woehrle, G. H.; Warner, M. G.; Hutchison, J. E. *Langmuir* **2004**, *20*, 5982.

washed with saturated $NaHCO_3$ and water. The combined organic phases where dried over $MgSO_4$ and after evaporation of solvent, column chromatography yielded the product as a sticky white foam. **Yield:** 2.6 g, 62.98 % - **^{1}H-NMR:** (400 MHz, $CDCl_3$) δ_H= 7.28 (m, 47 H, Ar*H*), 4.10–4.07 (stack, 6 H, 3 CH_2), 3.87 (s, 3 H, CH_3), 3.65 (apparent t, 4 H, 2 CH_2), 3.56 (apparent t, 2 H, CH_2), 3.36 (stack, 6 H, 3 CH_2), 2.45 (t, 6 H, *J*= 6,69 Hz, 3 CH_2) ppm. **^{13}C-NMR:** (400 MHz, $CDCl_3$) δ_C= 166.60 (Ar*C*) 152.24 (*C*OOH), 144.90 (Ar*C*), 144.85 (Trityl-Ar*C*), 142.62 (Ar*C*), 129.65, 127.91, 127.90, 126.68, 126.64(Trityl-Ar*C*), 124.90, 109.21 (Ar*C*), 72.31, 70.23, 69.77, 69.49, 69.16, 68.73, 66.66, 66.54 (*C*H_2), 52.16 (*C*H_3) 31.88, 31.84 (*C*H_2S) ppm. **IR**: $\tilde{\nu}$= 3055, 2948, 2923, 2862, 1716, 1592, 1581, 1487, 1444, 1428, 1333, 1251, 1211, 1134, 1104, 1081, 1033, 1000, 907, 741, 726, 697, 674, 617 cm^{-1}. **MS (TOF, ES$^+$)** *m/z*= 1245.3 [M+Na$^+$]. **HRMS (TOF, ES$^+$)** calcd. for $C_{77}H_{74}NaO_8S_3$ *m/z*= 1245.4438 [M$^+$] found *m/z*= 1245.4450 [M$^+$].

3,4,5-tris(2-(2-(tritylthio)ethoxy)ethoxy)benzoic acid (12)

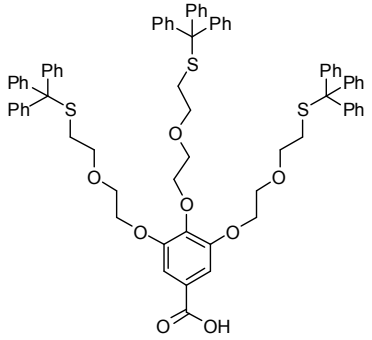

Methyl 3,4,5-tris(2-(2-(tritylthio)ethoxy)ethoxy)benzoate (**11**) (0.4 g, 0.35 mmol) was refluxed (70 ºC) in ethanol/THF (10 ml/10 ml) and KOH (0.14 g, 2.49 mmol) for 2 h. The solution was cooled to room temperature and was then acidified with 1 M HCl. Water (20 ml) was added to the mixture and the aqueous phase was extracted with CH_2Cl_2. The organic extracts were combined, dried over $MgSO_4$, filtered and evaporated, giving the product as sticky white foam. The crude product was analysed by TLC (EtOAc/CH_2Cl_2 1:2) and then purified by automated UV-detected flash chromatography. **Yield:** 0.33 g, 76 % - **^{1}H-NMR:** (400 MHz, $CDCl_3$) δ_H= 7.45–7.20 (m, 47 H, Ar*H*), 4.16 (t, 2 H,

$J_{H,H}$= 4.48 Hz, CH_2), 4.10 (t, 4 H, $J_{H,H}$= 4.48 Hz, CH_2), 3.65 (t, 4 H, $J_{H,H}$= 5.00 Hz, CH_2), 3.56 (t, 2 H, $J_{H,H}$= 5.00, CH_2), 3.52 (m, 6 H, CH_2), 2.45 (t, 4 H, $J_{H,H}$= 6,87 Hz, CH_2), 2.39 (t, 2 H, $J_{H,H}$= 6.87 Hz, CH_2) ppm. **^{13}C-NMR:** (400 MHz, $CDCl_3$) δ_C= 152.24 (*C*OOH), 144.87 (Ar*C*), 144.82 (Trityl-Ar*C*), 143.30 (Ar*C*), 129.64, 127.90, 127.88, 126.66, 126.63(Trityl-Ar*C*), 123.87, 109.74 (Ar*C*), 72.33, 70.23, 69.75, 69.47, 69.13, 68.71, 66.65, 66.52 (*C*H_2), 31.84, 31.78 (*C*H_2S) ppm. **IR**: $\tilde{\nu}$= 3053, 2923, 2863, 1715, 1682, 1592, 1580, 1487, 1444, 1429, 1354, 1325, 1134, 1108, 1033, 740, 697, 674 cm^{-1}. **MS (TOF, ES$^+$)** *m/z*= 1231.3 [M+Na$^+$]. **HRMS (TOF, ES$^+$)** calcd. for $C_{76}H_{72}O_8NaS_3$ *m/z*= 1231.4287 [M$^+$] found *m/z*= 1231.4347 [M$^+$].

Triethyleneglycol 3,4,5-tris(2-(2-(tritylthio)ethoxy)ethoxy) benzoate (13)

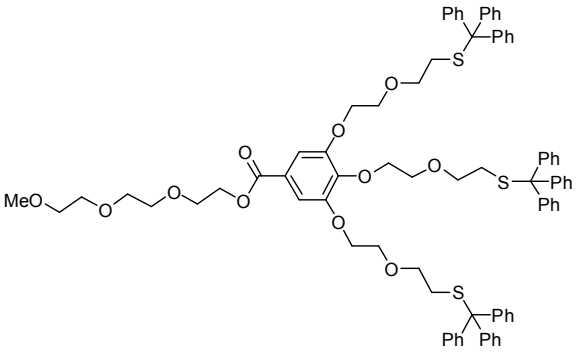

3,4,5-tris(2-(2-(tritylthio)ethoxy)ethoxy)benzoic acid (**12**) (1 g, 0.8 mmol) was dissolved in anhydrous CH_2Cl_2 (40 ml) and triethylene glycol monomethylether (271 mg, 0.8 mmol) was added. Then coupling agent 1-hydroxybenzotriazole (HOBt) (170 mg, 1.2 mmol), 1-(3-dimethylaminopropyl)-3-ethylcarbodiimide (EDC), (190 mg, 1.2 mmol, 0.2 ml), 4-dimethylaminopyridine (DMAP), (150 mg, 1.2 mmol) where introduced to activate the carboxylic acid. After a few days the mixture was diluted with CH_2Cl_2 (50 ml) and washed with water, the organic phases where combined and solvent was removed under reduced pressure. The mixture was analysed by TLC (EtOAc/Hexane 1:1) and purified by automated UV-detected flash chromatography. **Yield:** 0.693 g, 62 % - **^{1}H-NMR:** (400 MHz, $CDCl_3$) δ_H= 7.44–7.20 (m, 47 H, Ar*H*), 4.46 (t, 2 H, $J_{H,H}$= 4.90 Hz, CH_2), 4.11 (m, 6 H, CH_2), 3.83 (t, 2 H, $J_{H,H}$= 4.80 Hz, CH_2), 3.71 (stack, 10 H, CH_2), 3.5 (t, 4 H,

$J_{H,H}$= 5.04, CH_2), 3.41 (s, 3 H, CH_3), 3.37 (m, 6 H, CH_2) ppm. **^{13}C-NMR:** (500 MHz, $CDCl_3$) δ_C= 166.04 (ArC*q*), 152.19 (*C*=O), 144.82, 144.69 (Ar*Cq*), 129.63, 127.89, 127.65 (Trityl-Ar*C*H), 126.66 (Ar*Cq*), 109.30 (Ar*C*H), 72.30, 71.93, 70.65, 70.17, 69.75, 69.47, 69.14, 68.73 (*C*H_2), 66.64 (C*q*), 64.13 (CH_2), 59.04 (CH_3), 31.79 (CH_2) ppm. **IR**: $\tilde{\nu}$= 3055, 2957, 2923, 2862, 1780, 1592, 1580, 1488, 1444, 1429, 1356, 1331, 1238, 1172, 1122, 1083, 1032, 765, 738, 697, 673, 616 cm^{-1}. **MS (TOF, ES$^+$)** *m/z*= 1377.4 [M+Na$^+$]. **HRMS (TOF, ES$^+$)** calcd. for $C_{83}H_{86}NaO_{11}S_3$ *m/z*= 1377.5224 [M$^+$] found *m/z*= 1377.5235 [M$^+$].

Triethyleneglycol 3,4,5-tris(2-(2-thioethoxy)ethoxy) benzoate (8)

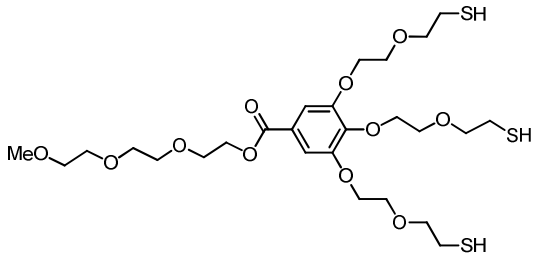

Under nitrogen atmosphere triethyleneglycol 3,4,5-tris(2-(2-(tritylthio)ethoxy)ethoxy)benzoate (**13**) (160 mg, 0.118 mmol) was dissolved in degassed DCM (3.5 ml), at 0 ºC. TFA (3.5 ml) was introduced and then triethylsilane (55 mg, 0.472 mmol) was added dropwise, as slowly as possible. After 60 min the whole reaction mixture was evaporated, the residue was dissolved in EtOAc and subjected to column chromatography (separation, collection of solvent and evaporation were all carried out under inert atmosphere) using degassed solvents (EtOAc/hexane 2:1). Evaporation of the solvents yielded the pure product quantitatively. **Yield:** 50 mg, 67 % - **^{1}H-NMR:** (400 MHz, $CDCl_3$) δ_H= 7.34 (s, 2 H, Ar*H*), 4.48 (t, 2 H, $J_{H,H}$= 4.74 Hz, CH_2), 4.27 (m, 6 H, CH_2), 3.88 (m, 8 H, CH_2), 3.72 (stack, 12 H, CH_2), 3.56 (m, 2 H, CH_2), 3.38 (s, 3 H, CH_3), 2.75 (m, 6 H, CH_2) 1.66 (m, 3 H, SH) ppm. **^{13}C-NMR:** (500 MHz, $CDCl_3$) δ_C= 166.05 (ArC), 152.26 (*C*=O), 134.79, 127.80 (Ar*C*), 109.27 (Ar*C*H), 72.97, 72.81, 72.36, 71.90, 70.63, 70.57, 70.31, 69.34, 69.25, 68.88, 64.20 (*C*H_2), 59.03 (CH_3), 27.52, 26.55, 24.41 (CH_2) ppm. **IR**: $\tilde{\nu}$= 2956, 2922, 2850, 1712, 1585, 1428, 1328, 1295, 1206, 1134, 1087, 762 cm^{-1}. **MS (TOF, ES$^+$)** *m/z*= 651.2 [M+Na$^+$].

Methoxy-3,6,9-trioxaundecyl *p*-toluenesulfonate (15)

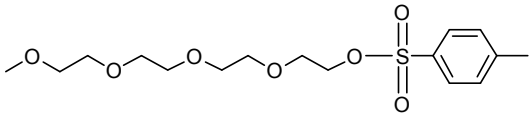

The reaction vessel was charged with a solution of 2,5,8,11-tetraoxatridecan-13-ol (3,0 ml, 14,4 mmol) in THF (5 ml). Upon vigorous stirring at 0 ºC, sodium hydroxide (1,15 g, 28,8 mmol) dissolved in water (5 ml) was added. To this mixture, a solution of tosylchloride (5,22 g, 27,4 mmol) in dry tetrahydrofuran (5 ml) was added drop wise over 15 min at 0ºC. The reaction mixture was allowed to warm to room temperature and stirring was continued for 1 h under argon. Then diethylether was added and the organic layer was separated and washed with 1 M aqueous NaOH and water. The organic phase was dried over $MgSO_4$ and evaporated to yield the product as a colourless liquid. Purification had to be performed by column chromatography (petrol ether/ethyl acetate 1:1 v/v and TFA 1% v). **Yield:** 4.3 g, 82 % - **^{1}H-NMR:** (400 MHz, $CDCl_3$) δ_H= 7.78 (d, 2 H, J_{HH}= 8.08 Hz, ArH ortho to OTs), 7.33 (d, 2 H, J_{HH}= 8.15 Hz, ArH ortho to OMe), 4.17 (t, 2 H, J_{HH}= 4.64 Hz, CH_2OTs), 3.53–3.70 (overlapping multiplets, 14 H, CH_2), 3.37 (s, 3 H, OCH_3), 2.44 (s, 3 H, CH_3). Spectroscopic data was found to be in agreement with literature.[24]

1-Azido-11-methoxy-3,6,9-trioxaundecane (16)

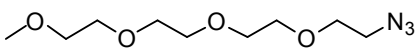

To 11-methoxy-3,6,9-trioxaundecyl *p*-toluenesulfonate (**15**) (200 mg, 0,55 mmol) in 7 ml of DMF, sodium azide (72 mg, 1,1 mmol) was added. The reaction was stirred at 100 ºC under an inert atmosphere overnight. Then solvent was removed and ethyl acetate and water were added to dissolve the residue. The aqueous phase was extracted with ethyl acetate and the organic phases were dried over MgSO4 and evaporated. **Yield:** 110 mg, 85 % - **^{1}H-NMR:** (400 MHz, $CDCl_3$) δ_H= 3.38 (s, 3 H, OCH_3), 3.40 (br s, 2 H, CH_2N_3)

[24] Kitto, H. J.; Schwartz, E.; Nijemeisland, M.; Koepf, M.; Cornelissen, J. J. L. M.; Rowan, A. E.; Nolte, R. J. M. *J. Mater. Chem.* **2008**, *18*, 5615.

3.54–3.57 (m, 2 H, CH_2), 3.64–3.69 (overlapping multiplets, 12 H, CH_2) ppm. **^{13}C-NMR:** (400 MHz, $CDCl_3$) $\delta_{C=}$ 50.7 (CN_3), 59.0 (OCH_3), 70.0, 70.5, 70.6, 70.6, 70.7, 70.7 71.9 (CH_2).ppm. Spectroscopic data was found to be in agreement with literature.[1]

2,5,8,11-Tetraoxatridecan-13-amine (17)

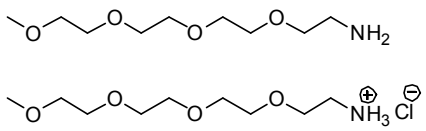

13-Azido 2,5,8,11 tetraoxatridecane (**16**) (572 mg, 2,452 mmol) was dissolved in THF (7 ml) and cooled to 0ºC, triphenylphosphine (707 mg, 2,70 mmol) was added and the mixture was allowed to reach room temperature. After strirring overnight water was added and stirring was continued for an hour, then solvent was evaporated. The product is water soluble and has to be retrieved from the aqueous phase. A concentrated solution of $NaHCO_3$ was added and the solution was mixed. The solvent was evaporated to a minimum and methanol was added to precipitate excess carbonate. After filtration the filtrate was evaporated. The residue was dissolved in DCM and 1 M HCl (necessary for separation of the phases) was added for washing. After evaporation of the organic phase a colourless oil was afforded. The spectrum of this hydrochloride differs significantly from the free amine (see below). The spectral data was found in accordance to literature. [25] **Yield:** 600 mg, 100 % -**^{1}H-NMR:** (400 MHz, $CDCl_3$) δ_H= 3.92- 3.88 (m, 2 H, CH_2), 3.77- 3.73 (m, 2 H, CH_2), 3.71- 3.64 (m, 8 H, CH_2), 3.43 (s, 3 H, CH_3), 3.26- 3.20 (m, 2 H, CH_2) ppm.

Free amine:

^{1}H-NMR: (400 MHz, $CDCl_3$) δ_H= 3.67- 3.57 (m, 10 H, CH2), 3.54- 3.50 (m, 2 H, CH_2), 3.50- 3.45 (m, 2H, CH_2), 3.35 (distorted s, 3 H, CH_3), 2.85- 2.80 (m, 2 H, CH2), 1.37 (s broad, 2 H, NH_2 exchangeable) ppm. **^{13}C-NMR:** (400 MHz, $CDCl_3$) $\delta_{C=}$ 73.48, 71.89, 70.58, 70.55, 70.55, 70.48, 70.25, 58.97, 41.79 ppm.

---

[25] Li, G.; Bhosale, S. V.; Wang, T.; Hackbarth, S.; Roeder, B.; Siggel, U.; Fuhrhop, J.-H. *J. Am. Chem. Soc.* **2003**, *125*, 10693.

_N_-(2,5,8,11-Tetraoxatridecan-13-yl)-3,4,5-tris(2-(2-(tritylthio)ethoxy)ethoxy) benzamide (18)

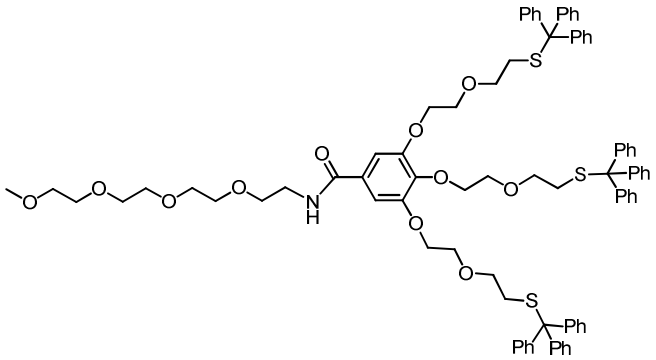

3,4,5-Tris(2-(2-(tritylthio)ethoxy)ethoxy)benzoic acid (**12**) (70 mg, 0,058 mmol) was dissolved in dry DMF (1 ml) and the solution was cooled to 0ºC. HOBT (8,86 mg, 0,058 mmol) EDC (11,09 mg, 0,058 mmol) and DIPEA (10,11 µl, 0,058 mmol) where added and after 10 min 3,4,5-tris(2-(2-(tritylthio)ethoxy)ethoxy)benzoic acid (13 mg, 0,053 mmol) was introduced. After stirring for 3h TLC indicated that starting material had completely disappeared. Solvent was evaporated and EtOAc was added to the residue. The solution was washed with HCl and the organic fraction was evaporated. **Yield:** 72 mg, 89 % - **^{1}H-NMR:** (400 MHz, MeOD) δ_H= 7.41-7.29 (m, 18 H, Trityl ArCH), 7.17-7.30 (m, 27 H, Trityl ArCH), 7.06 (s, 2 H, galat ArCH), 4.05 (m, 6 H, CH_2), 3.58 (stack, 16 H, CH_2), 3.49 (stack, 4 H, CH_2), 3.32 (stack, 8 H, CH_2, CH_3) 2.41 (t, 4 H, $J_{H,H}$= 6.6 Hz, CH_2), 2.37 (t, 2 H, $J_{H,H}$= 6.8 Hz, CH_2) ppm. **^{13}C-NMR:** (500 MHz, $CDCl_3$) δ_C= 152.38 (C*q*), 146.87 (*Cq*), 144.85, 144.80 (*Cq*), 129.61, 127.88 (Trityl-Ar*C*H) 127.25(Cq) 126.64 (Trityl-Ar*C*H), 109.72, 107.19 (Ar*C*H), 71.85, 70.54, 70.51, 70.39, 70.20, 69.73, 69.45, 69.22, 69.12, 68.91, 68.71 (*C*H_2), 66.63 (Cq), 58.90 (CH_3), 50.86 (CH), 39.80 (CH_2) ppm. **IR**: $\tilde{\nu}$= 3055, 2924, 2870, 1718, 1594, 1580, 1489, 1445, 1427, 1355, 1325, 1247, 1209, 1183, 1133, 1103, 1033, 766, 741, 697, 674, 617 cm^{-1}. **HRMS (TOF, ES$^+$)** calcd. for $C_{85}H_{91}NNaO_{11}S_3$ m/z= 1420.5646 [M$^+$] found m/z= 1420.5712 [M$^+$].

3,4,5-Tris(2-(2-thioethoxy)ethoxy)-*N*-(2,5,8,11-tetraoxatridecan-13-yl) benzamide (19)

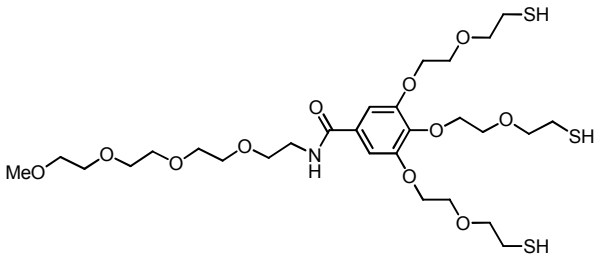

Under nitrogen atmosphere *N*-(2,5,8,11-tetraoxatridecan-13-yl)-3,4,5-tris(2-(2-(tritylthio)ethoxy)ethoxy)benzamide (**18**) (102 mg, 0,073 mmol) was dissolved in degassed DCM (1.8 ml). At 0 ºC, TFA (1.8 ml) was introduced and 10 min later triethylsilane (0,047 ml, 0,292 mmol) was added dropwise. After 30 min the mixture was evaporated and degassed DCM was added. The solution was washed with 1 M HCl and the organic layer was evaporated. The residue was instantly subjected to combiflash separation using a DCM/acetone eluent (previously bubbled with argon). **Yield:** 40 mg, 82 % - **^{1}H-NMR:** (400 MHz, MeOD) δ_H= 7.11 (s, 2 H, galat ArCH), 4.22 (m, 6 H, CH_2), 3.85 (t, 4 H, $J_{H,H}$= 4.7 Hz, CH_2), 3.80 (t, 2 H, $J_{H,H}$= 4.8 Hz, CH_2), 3.61 (stack, 20 H, CH_2), 3.51 (m, 2 H, CH_2), 3.35 (s, 3 H, CH_3), 2.70 (m, 6 H, CH_2) ppm. **^{13}C-NMR:** (500 MHz, MeOD) δ_C= 168.15 (C*q*), 152.43 (*Cq*), 140.87, 129.40 (*Cq*), 27.25(Cq), 106.53 (Ar*C*H), 72.87, 72.70, 72.23, 71.58, 70.22, 70.19, 70.14, 70.11, 69.99, 69.28, 69.14, 68.73 (*C*H_2), 57.78 (CH_3), 39.78, 38.55 (CH_2) ppm. **IR**: $\tilde{\nu}$= 2927, 2862, 1691, 1650, 1635, 1580, 1542, 1496, 1452, 1423, 1354, 1329, 1292, 1239, 1199, 1136, 1095, 1024, 945, 852 cm^{-1}. **HRMS (TOF, ES$^+$)** calcd. for $C_{28}H_{48}NO_{11}S_3$ *m/z*= 670.2395 [M$^-$] found *m/z*= 670.2393 [M$^-$].

BocCys(Trityl)OMe (23)

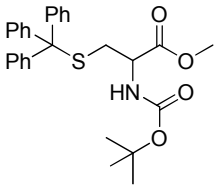

Trityl chloride (2 ml, 8,20 mmol) was added to a solution of BocCysOMe (1,75 g, 7,5 mmol) in pyridine (7 ml), at 0º. The mixture was stirred overnight. Then pyridine was evaporated into a receiving vessel containing 3 M HCl. The crude product was purified by column chromatography to afford the product in quantitative yield. **Yield:** 3.5 g, 100 % - **^{1}H-NMR:** (400 MHz, $CDCl_3$) δ_H= 7.42-7.20 (m, 15 H, Trityl-Ar*C*H), 5.02 (d, 1 H, $J_{H,H}$= 8.0 Hz, NH), 4.29 (m, 1 H, CH), 3.71 (s, 3 H, CH_3O), 2.59 (d, 2 H, $J_{H,H}$= 5.0 Hz, CH_2S), 1.44 (s, 9 H, CH_3) ppm. Spectroscopic data was found to be in agreement with literature.[26]

Cys(Trityl)OMe (24)

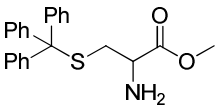

Under inert atmosphere BocCys(Trityl)OMe (**23**) (639 mg, 1,34 mmol) was dissolved in DCM (dry, 23 ml) and TFA (2,0 ml, 26,8 mmol) was added. After one night solvent and acid were evaporated, the residue was dissolved again in DCM and washed with $NaHCO_3$. Subsequently the organic phase was evaporated and the crude was subjected to column chromatography. **Yield:** 660 mg, 100 % - **^{1}H-NMR:** (400 MHz, $CDCl_3$) δ_H= 7.46-7.20 (m, 15 H, Trityl-Ar*C*H), 3.67 (s, 3H, OCH_3), 3.20 (m, 1 H, CH), 2.45-2.64 (m, 2 H, CH_2) ppm. Spectroscopic data was found to be in agreement with literature.[27]

[26] Ionita, P.; Volkov, A.; Jeschke, G.; Chechik, V. *Anal. Chem.* **2007**, *80*, 95.
[27] Liu, X.-h.; Suh, D.-Y.; Call, J.; Prestwich, G. D. *Bioconjugate Chem.* **2004**, *15*, 270.

2,2',2''-benzenetricarbonyl tris(cystein) (27)

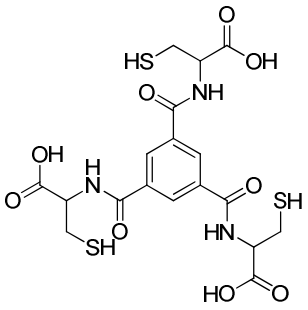

Cys(Trityl)OMe (**24**) (724 mg, 1,92 mmol) was dissolved in DCM (dry, 2 ml) at 0ºC. Triethylamine (dry, 535 µl, 3,84 mmol) was added and the solution was stirred for a while, then benzene-1,3,5-tricarbonyl trichloride (127 mg, 0,48 mmol) was introduced. After 12 h the solution was washed with 1 M HCl, $NaHCO_3$ and water. Solvent was evaporated and the crude was purified by column chromatography.

25 (554 mg, 0,43 mmol) was dissolved in THF/water 1:1 v/v (4 ml) and LiOH (61,8 mg, 2,6 mmol) was added. After 2 h 1 M HCl was introduced until pH 1 was reached. All liquid was evaporated and the crude was dissolved in EtOAc. The organic phase was washed with water and was then evaporated.

The residue (pure **26**) was now dissolved in a deoxygenated mixture of DCM/TFA 1:1 v/v. After 30 min triethylsilane (18 µl, 0,1 mmol) was added. Liquids were evaporated and the residue was dissolved in few ml of water (deoxygenated). The solution was then washed with DCM to remove remaining trityl residues. The aqueous phase was evaporated to yield the pure product. **Yield:** 249 mg, 78 % (over three steps)- **^{1}H-NMR:** (400 MHz, DMF) δ_H= 9.04 (apparent d, 3 H, $J_{H,H}$= 7.5 Hz) 8.73 (s, 3 H, ArCH) 4.78 (brm, 3 H) 3.19-3.11(brm, 6H) 2.58 (brt, 3H) ppm. Spectroscopic data was found to be in agreement with literature.[16a)]

Chapter 3

Metal Based Dynamic Systems

3.1 Conception of the Chapter

In the previous chapter we described multivalent dynamic combinatorial libraries (DCLs) based on covalent but reversible bonds. However, covalent bonds have not always been the first choice for the construction of such dynamic systems. In 1995 Hamilton *et al.* described a system relying on reversible exchange of two terpyridyl units around a ruthenium centre, one of the first reported examples applying a dynamic combinatorial concept.[1] Then in 1997, still before the term Dynamic Combinatorial Chemistry had been introduced, Sasaki *et al.* published a study directly pointing into this direction.[2] Unlike most dynamic combinatorial libraries developed later, those systems were based on metal coordination as the dynamic interchange mechanism. The trivalent arrangement of Sasaki was built-up around a Fe^{II} centre. It involved bipyridine as ligating moiety to which one galactopyranose unit was tethered over a CH_2 bridge (Scheme 1).

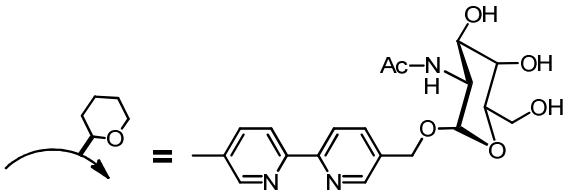

Scheme 1 *Ligating moiety for a dynamic system*[2]

Three bipyridine-sugar ligands coordinate to the Fe^{II} centre to form an octahedral complex. Due to the monosubstituted structure of the ligand, both meridional (*mer*) and facial (*fac*) stereoisomers can form. The inherent chirality of the arrangement gives rise to the existence of another pair of enantiomers, delta (Δ) and lambda (Λ). Therefore four different diastereomers develop that are able to reversibly interchange their configuration

[1] Goodman, M. S.; Jubian, V.; Linton, B.; Hamilton, A. D. *J. Am. Chem. Soc.* **1995**, *117*, 11610.
[2] Sakai, S.; Shigemasa, Y.; Sasaki, T. *Tetrahedron Lett.* **1997**, *38*, 8145.

(Scheme 2). When the complexes were mixed with the *Vicia Villosa* B_4 lectin, HPLC experiments showed that the equilibrium was shifted towards one specific isomer, clearly an adaptive behaviour. Use of the term dynamic combinatorial would be questionable here, as the system does not combine different constituents and is only intramolecularly exchanging a single ligand. Nevertheless, the system is dynamic and its full flexibility seems to indicate that also intermolecular exchange should be possible, should more ligands be employed. In addition, unlike in most examples of dynamic libraries for molecular recognition, the system relies on three independent recognition units. Thus, it can truly be called multivalent.

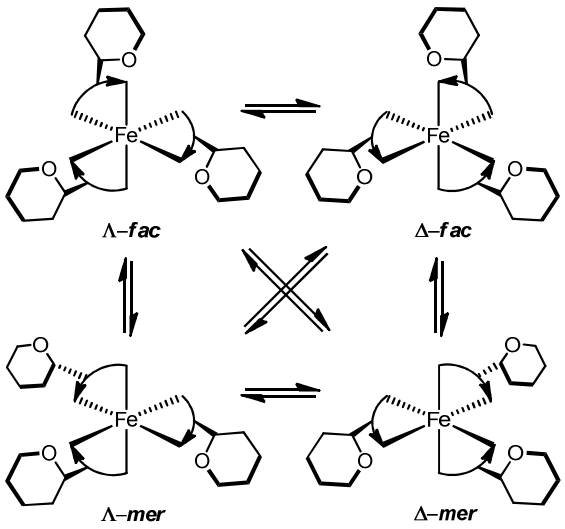

Scheme 2 *Dynamically interchanging diastereomers*[2]

Four years after Sasaki's publication, when the concept of dynamic combinatorial chemistry had already been established, Lehn's group examined the potential of transition metals to form intermolecularly exchanging complexes, using Co^{II} (Scheme 3). The trivalent terpyridyl ligands employed exchange in solution around the coordination sphere of the metal. Interestingly, the exchange between two homoleptic complexes coordinated with different ligands was faster than the exchange with free ligands from the solution.

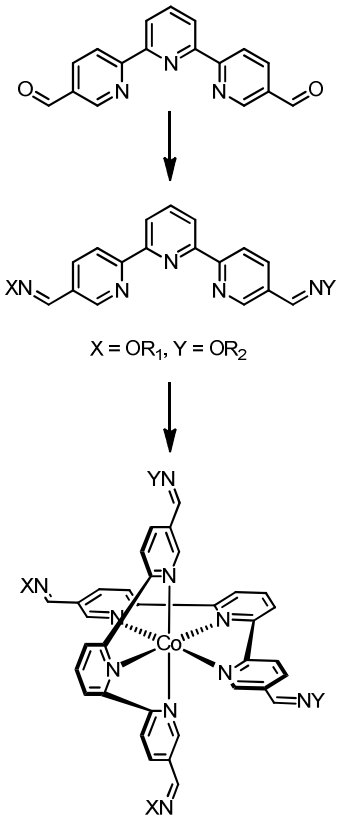

Scheme 3 *Complex formation with terpyridyl ligands*[3]

Despite the paramagnetic nature of these complexes it was possible to analyse the mixtures by proton NMR. ESI MS measurements confirmed the results obtained by NMR,[3] showing that free exchange of ligands took place.

Regardless of this initial success, the above ideas have not been combined so far to set up a multi-component exchanging DCL for protein recognition. Thus, we decided to exploit the driving force of metal-ligand coordination to form metal complexes coordinated to sugar-containing ligands that can be exchanged dynamically. These DCLs could then be used for lectin recognition.

The right combination of metal centre and coordinating ligands was key for an easy

[3] Huc, I.; Lehn, J.-M. *Proc. Natl. Acad. Sci. U.S.A.* **1997**, *94*, 2106.

ligand exchange. Many practical aspects such as solubility, sensitivity to oxidation, or suitability for easy analysis, among others, had to be evaluated.

3.2 Suitability of Different Metal Centres for DCC

To optimise the coordination process, three different metals where selected for evaluation of their ability to dynamically exchange ligands in solution.

3.2.1 Palladium (II)

Structures based on Pd-pyridine coordination are known to readily self-assemble to form impressive macromolecular frameworks. The level of structural diversity and the reliability of their formation have been shown in various examples in the inspiring work of Fujita *et al*, among others.[4] The dynamic behaviour of these constructs has not been explored in detail, however.

3.2.1.1 Palladium (II) Model Complexes

To understand if the coordinative behaviour of Pd^{II} complexes is suitable for DCL formation, two homoleptic Pd^{II} (**36** and **37**) complexes were synthesised with pyridine and 3-methylpyridine (Scheme 4). The two ligands are structurally distinguishable but should form similarly stable complexes as the methyl group in position 3 should have little influence on the electronic behaviour of the coordinative nitrogen atom. Therefore, the different members of the potential **DCL G** should be equally stable and the species observable in statistical distributions. The system enables a multivalent set-up as four

[4] a) Kusukawa, T.; Fujita, M. *J. Am. Chem. Soc.* **2002**, *124*, 13576. b) Yu, S.-Y.; Kusukawa, T.; Biradha, K.; Fujita, M. *J. Am. Chem. Soc.* **2000**, *122*, 2665. c) Harris, K.; Sun, Q.-F.; Sato, S.; Fujita, M. *J. Am. Chem. Soc.* **2013**, *135*, 12497. d) Inokuma, Y.; Yoshioka, S.; Ariyoshi, J.; Arai, T.; Hitora, Y.; Takada, K.; Matsunaga, S.; Rissanen, K.; Fujita, M. *Nature* **2013**, *495*, 461. e) Olenyuk, B.; Whiteford, J. A.; Fechtenkotter, A.; Stang, P. J. *Nature* **1999**, *398*, 796. f) Stang, P. J.; Olenyuk, B.; Muddiman, D. C.; Smith, R. D. *Organometallics* **1997**, *16*, 3094. g) Chakrabarty, R.; Mukherjee, P. S.; Stang, P. J. *Chem. Rev.* **2011**, *111*, 6810.

ligands get complexed in a square planar coordination sphere. Dynamic exchange of ligands should start upon mixing both homoleptic species **36** and **37**, to form a six membered DCL. HPLC, MS and NMR were chosen as suitable to analyse the evolving mixtures.

Complexes **1** and **2** were both obtained similarly. Palladium nitrate (0.06 M) was dissolved in acetone and 4.5 eq of pyridine or 3-methylpyridine were added, the product precipitating readily from the solution in quantitative yield. Both complexes were water soluble, a favourable aspect in view of their application in protein recognition. NMR spectra, measured in D_2O, were clean and coherent with the C_4 symmetry of a fully coordinated Pd^{II} centre in a square planar complexation pattern (Figure 1a and 1b).

Buffer solutions have to be used for experiments with proteins, as the salts contained in these mixtures may affect the stability of complexes. Thus, NMR spectra in a phosphate buffer solution were registered, but no differences from the spectra in pure water were detected. These findings were further confirmed by comparing the extinction coefficients of the pyridine-based complexes in water and in buffer solution.

3.2.1.2 DCL Set-up and Analysis

A small multicomponent DCL (Scheme 4) can arise by mixing both species **1** and **2** in solution. An interchange of ligands from one complex to the other would yield unsymmetrical species. Therefore, new signals should appear in the NMR spectrum of the mixture, after equilibration. Thus, **36** and **37** were dissolved in D_2O (0.06 M) in a 1:1 (v/v) ratio. After a few minutes the evolution of heteroleptic species was evidenced by a significant change in the ^{1}H-NMR spectrum (Figure 1, **36** and **37**).

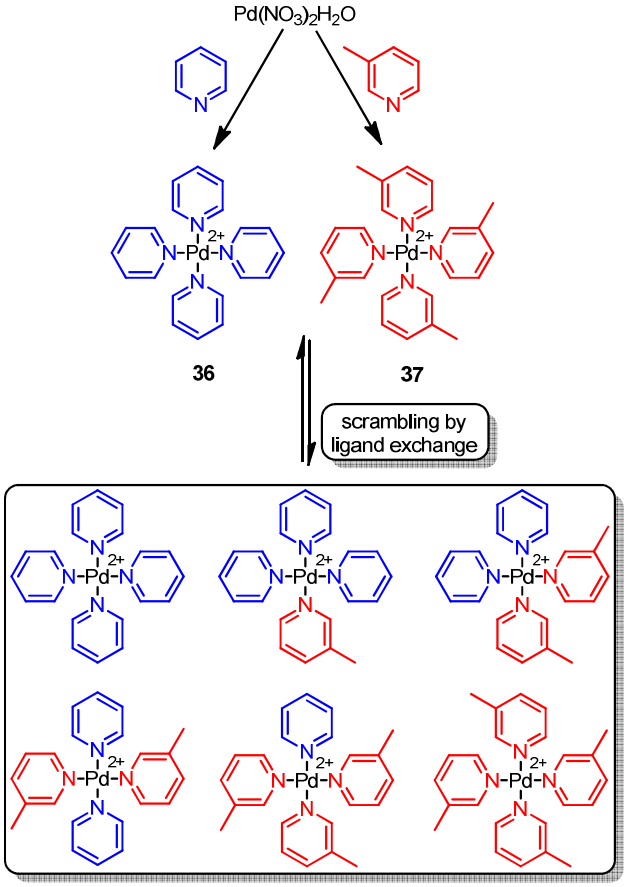

Scheme 4 *Synthesis of two homoleptic pyridine complexes, and formation of* **DCL G** *through scrambling by ligand exchange.*

Disappointingly further analysis of the developed DCL was hampered by several constraints. First, no mass analysis was feasible with the instrumentation available. Cryospray injection, as used by Fujita *et al.* to analyse palladium complexes would be necessary for detection.[4a-c)] Secondly, analysis by HPLC afforded only very broad signals or simply no peaks, and no adequate eluents were found to resolve the mixture. Those major disadvantages indicate that the analysis of more complex DCLs based on palladium coordination might be difficult or impossible, so alternative approaches were evaluated.

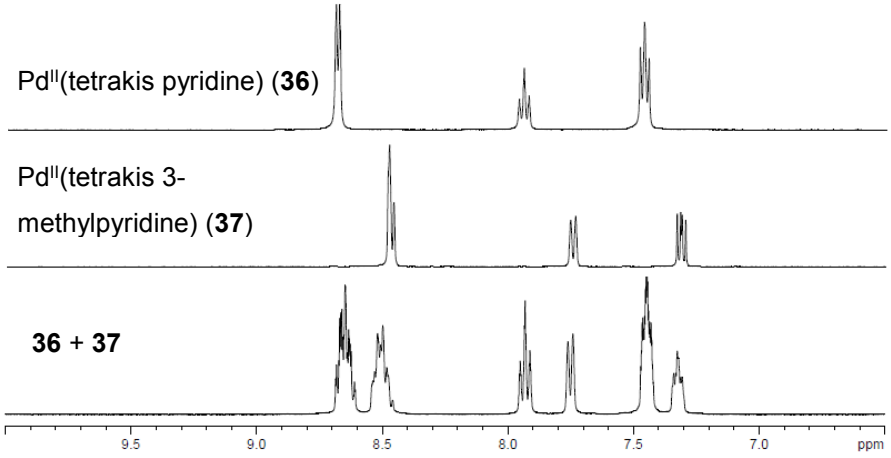

Figure 1 *^{1}H-NMR spectra of: a) Pd^{II}(tetrakispyridine) b) Pd^{II}(tetrakis-3-methylpyridine) and c) 1:1 mixture of a) and b)*

3.2.2 Cobalt (II) and Iron (II)

Co^{II} and Fe^{II} are neighbouring elements on the periodic table. Both can coordinate pyridine-type ligands in an octahedral coordination sphere. Therefore, coordination experiments can be conducted using similar ligands and conditions.

3.2.2.1 Cobalt (II)

Cobalt offers a number of favourable properties for the set-up of dynamic combinatorial libraries. Complexation of pyridine derivatives around the metal centre is in the right range of coordination strength to enable dynamic exchange of ligands around the coordination sphere, as it has been shown by Lehn *et al.* (see above).[3] Moreover, complexes are known to be relatively stable to air.

In addition, to use our analytical method, the complexes have to be stable under the HPLC conditions. This is also important as the paramagnetic character of Co^{II} complexes complicates studies by NMR. However, at the time, there was no reported example of HPLC analysis of cobalt-based DCLs.

3.2.2.2 Iron (II)

A major advantage of Fe^{II} bipyridine-type complexes over the previously considered metals is that the third binding constant is significantly larger than the first and second ones.[5] Formation of fully coordinated complexes is therefore favoured. Furthermore, the complexes exhibit proven dynamic properties and have been successfully analysed as was shown by the group of Sasaki. However, Fe^{II} is prone to oxidation and the corresponding Fe^{III} species are, unlike their Co^{III} counterparts, instable. Long equilibration times in aqueous buffer solutions might intensify that problem.

3.2.2.3 Iron (II) and Cobalt (II) Model Systems

To test the experimental properties, simple model systems were set up for both Fe^{II} and Co^{II} metals. Two commercially available bipyridines (2,2'-bipyridine and 4,4'-dimethyl-2,2'-bipyridine) were used to synthesise two homoleptic complexes for each metal (Scheme 5). Three ligands should complex each of the metal centres, in octahedral coordination.

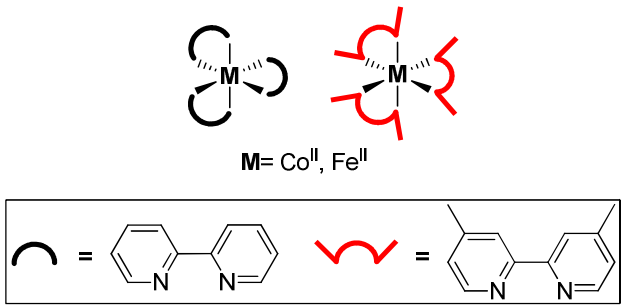

Scheme 5 *Homoleptic Fe^{II} and Co^{II} complexes (enantiomers of the complexes are omitted for clarity)*

Solutions of ammonium Fe^{II} sulphate (hexahydrate) and Co^{II} acetate (tetrahydrate) in methanol were prepared and stoichiometric amounts of each ligand (2,2'-bipyridine or 4,4'-dimethyl-2,2'-bipyridine) were added. Due to the paramagnetic nature of Co^{II}, NMR

[5] Sasaki, T.; Lieberman, M. *Tetrahedron* **1993**, *49*, 3677.

analyses were not performed.

The iron complexes (**38**, **39**) exhibited clean NMR spectra (Schemes 6a and 8b). No additional signals for free ligands were visible when excess ligand was added (Scheme 6b). This proved full coordination of the Fe^{II} centre in case that enough bipyridine ligand was present, as confirmed later by mass and HPLC analysis. Moreover, this result confirmed that the exchange of the ligand in and out of the Fe^{II} coordination sphere was slow enough on the NMR time scale to make both species visible, which allows use of this spectroscopy for Fe^{II} complexes.

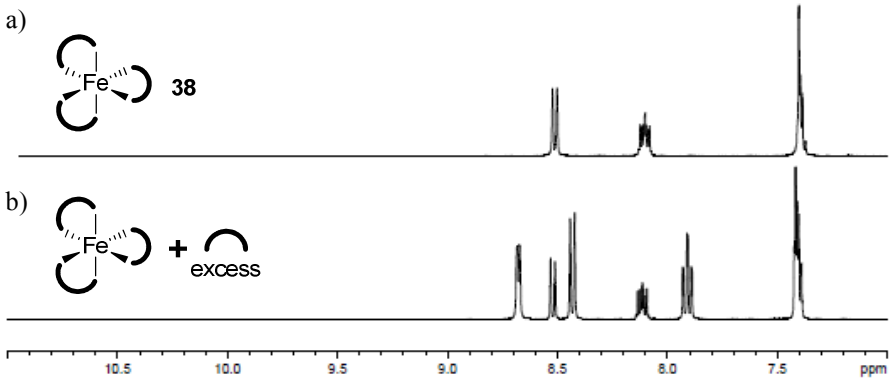

Scheme 6 *^{1}H NMR spectrum of: a) the iron-bipyridine complex and b) iron-bipyridine complex and excess ligand*

3.2.3 Model DCL Set-up and Analysis

To test the reversibility of the complex formation, a simple DCL (**DCL H**) was constructed by mixing solutions of the two homoleptic 2,2'-bipyridine and 4,4'-dimethyl-2,2'-bipyridine Fe^{II} complexes (Scheme 7). Another DCL (**DCL I**) was set up for the corresponding Co^{II} complexes (Scheme 7).

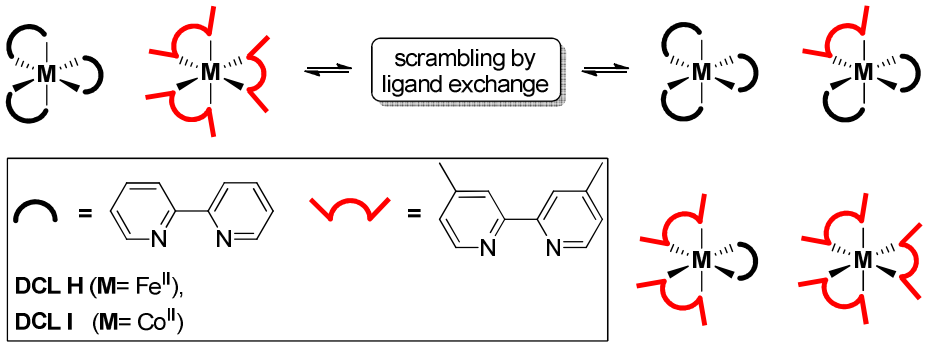

Scheme 7 *Formation of* ***DCL H*** *and* ***DCL I*** *by scrambling around a Fe^{II} or Co^{II} centre (enantiomers of the complexes are omitted for clarity).*

To analyse the Fe^{II} **DCL H** by NMR, two samples of identical concentrations of Fe^{II}(2,2'-bipyridine) and Fe^{II}(4,4'-dimethyl-2,2'-bipyridine) were prepared in D_2O. Both clean spectra were in agreement with the symmetry of the complexes (Scheme 8a and 8b). When similar volumes of the two samples were mixed, NMR analysis showed significant changes in the aromatic region, indicating the expected scrambling of ligands.

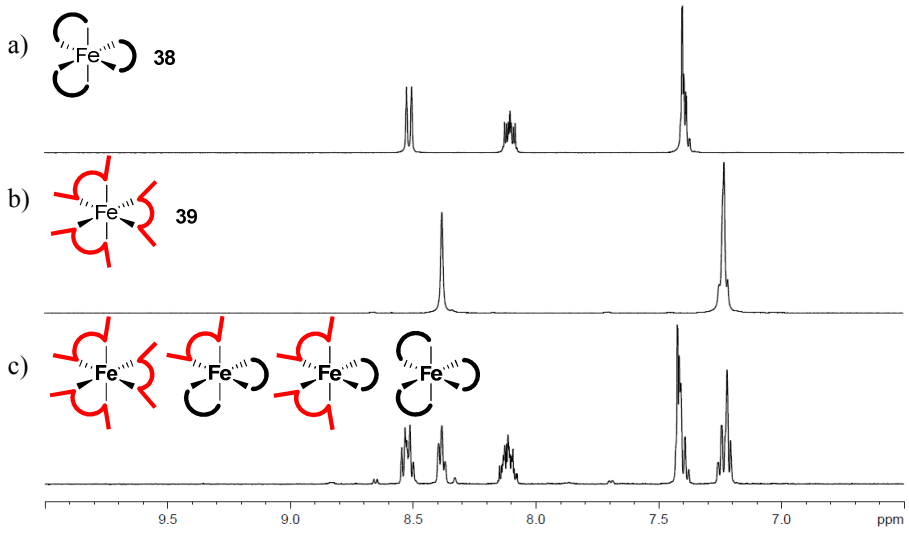

Scheme 8 *^1H NMR spectrums of: a) pure Fe^{II}(2,2'-bipyridine), b) pure complexes Fe^{II}(4,4'-dimethyl-2,2'-bipyridine) and c) a 1:1 mixture of a) and b)*

To further confirm the reversibility of the complex formation, both libraries (**DCL-H** and **DCL-I**) were also analysed by HPLC-MS. After five days in acetonitrile the Fe^{II} **DCL-H** was detected as expected (Figure 2), showing the four possible ligand combinations in statistical distribution (HPLC-MS analysis, Figure 2).

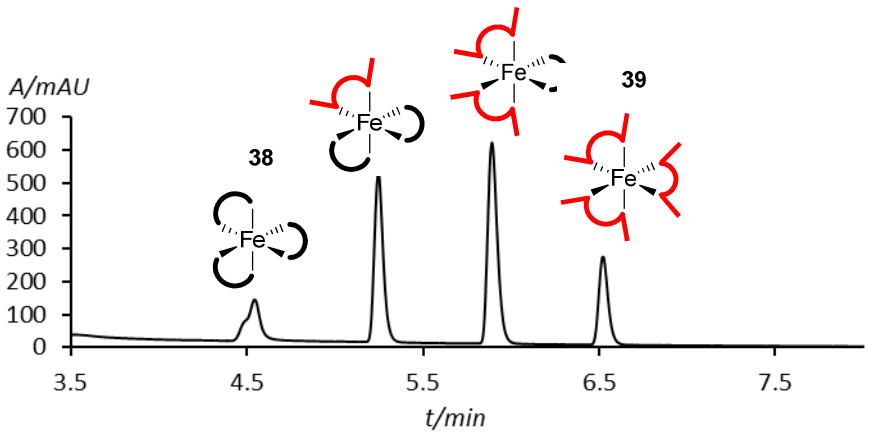

Figure 2 *UV detected HPLC chromatogram of the* Fe^{II} *based* ***DCL H*** *(reverse phase, acetonitrile-water)*

The same method was employed to analyse the Co^{II} based **DCL I**, for which NMR studies were not feasible. As before, all expected constituents were detected (Figure 3), though partially coordinated complexes were also detected in the equilibrated mixture. One complex visible as a peak in the chromatogram (confirmed by MS detection) was coordinated by two 4,4'-dimethyl-2,2'-bipyridine and one TFA anion (the eluent contains TFA for better separation). Moreover, distribution of the fully coordinated complexes was not statistical. This suggested that the arrangements differ in stability, a problem if mixtures of similar complexes have to be analysed quantitatively in binding experiments.

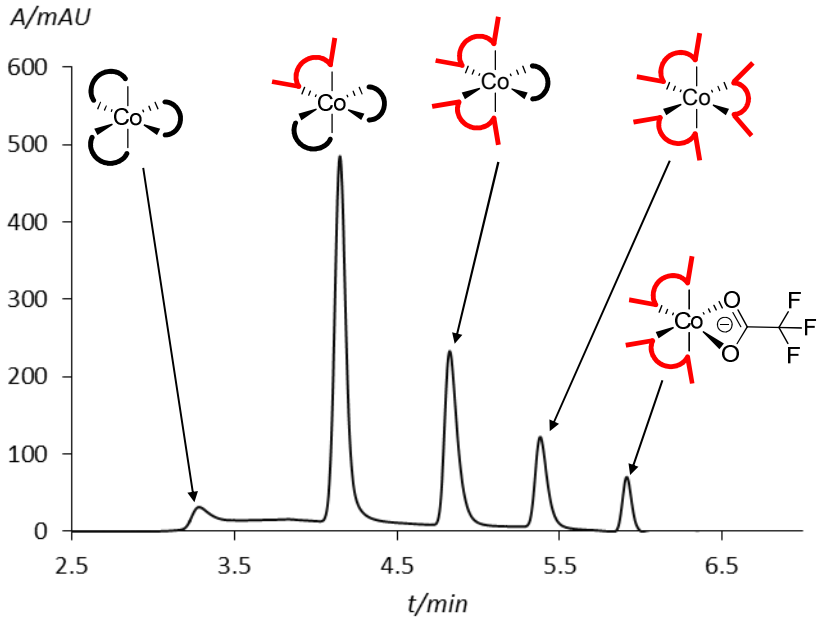

Figure 3 *UV detected HPLC chromatogram of the Co^{II}* ***DCL I*** *(reverse phase, acetonitrile-water)*

Thus, Co^{II} seemed less appropriate for the formation of DCLs, and further studies were all based on Fe^{II} complexes.

3.2.4 Conclusions

In summary, dynamic model systems, exploiting the concept of scrambling by ligand exchange around three different metal centres, were used to determine the most promising approach for the set-up of multivalent dynamic combinatorial libraries. Experiments with palladium were promising, according to NMR data. However, separation of the library constituents by HPLC-MS was not feasible.

On the contrary, both cobalt and iron model systems fulfilled those requirements, allowing detection of the expected library species, although cobalt complexes were not formed exclusively, so the expected statistical distribution was not observed. In particular, signals were found for complexes containing only two of the desired ligands; the third position is likely occupied by a TFA ligand (see Figure 3)

Therefore, Fe^{II} appeared to be the best candidate. The HPLC chromatogram showed all expected species in statistical distribution. No side products could be detected. For that reason the combination of an Fe^{II} centre and bipyridine-type ligands was chosen for the set-up of more complex dynamic systems.

3.3 Multivalent Sugar Containing DCLs for ConA Lectin Binding

Based on the preliminary experiments with a four membered DCL, the approach was extended to three-component DCLs of bipyridine-Fe^{II} complexes, based on a variety of carbohydrate-containing ligands, to study how the dynamic library interacts with concanavalin A (ConA).

Bipyridines with D-mannoside (**MMM**), D-galactoside (**GGG**) and L-fucoside (**FFF**) complexes (Scheme 10) were prepared to set up a 4- and then a 10-membered sugar containing adaptive library. The sugar moieties were connected to the coordinative bipyridine backbone by a spacer long enough to provide the necessary flexibility and distance to leave each of the saccharide clusters to a more individually induced-fit into the carbohydrate recognition domain (CRD) of the target lectin.[6] The choice of sugars was guided by their known binding affinities towards ConA (Man > Fuc or Gal),[7] and by their predictably easy HPLC separation and identification by mass spectrometry. It was likely that mannoside-containing complexes should prevail after contact with the protein.

3.3.1 Set-up of Multivalent DCLs

3.3.1.1 Synthesis of Building Blocks

The synthesis of the sugar containing ligands was straightforward (Scheme 9). Glycosylation of D-mannose or D-galactose with *N*-carboxybenzyl-protected diethyleneglycolamine in the presence of $BF_3 \cdot Et_2O$ exclusively provided the corresponding α-isomers in the cases of **40** and **42** and the β-isomer in the case of **41**.[8] For L-fucose, requiring a more active glycosyl donor, a trichloroacetimidate strategy was selected;[9] the

[6] a) Hasegawa, T.; Yonemura, T.; Matsuura, K.; Kobayashi, K. *Bioconjugate Chem.* **2003**, *14*, 728. b) Cecioni, S.; Praly, J.-P.; Matthews, S. E.; Wimmerová, M.; Imberty, A.; Vidal, S. *Chem. Eur. J.* **2012**, *18*, 6250. c) Fan, E.; Zhang, Z.; Minke, W. E.; Hou, Z.; Verlinde, C. L. M. J.; Hol, W. G. J. *J. Am. Chem. Soc.* **2000**, *122*, 2663. d) Deniaud, D.; Julienne, K.; Gouin, S. G. *Org. Biomol. Chem.* **2011**, *9*, 966.

[7] www.functionalglycomics.org

[8] Yang, Z.; Lin, W.; Yu, B. *Carbohydr. Res.* **2000**, *329*, 879.

[9] a) Schmidt, R. R.; Michel, J. *Angew. Chem., Int. Ed.* **1980**, *19*, 731. b) Schmidt, R. R.;

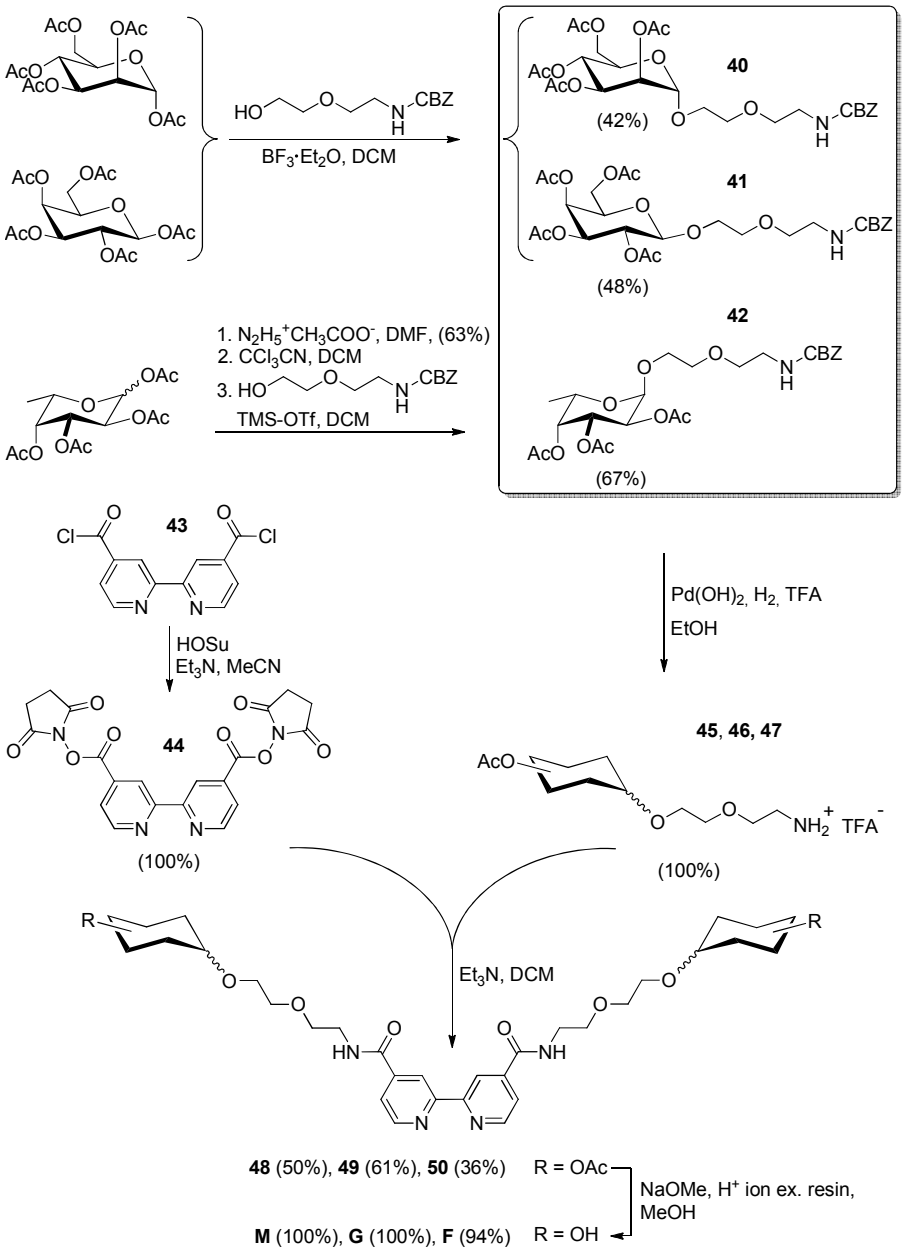

Scheme 9 *Preparation of sugar containing bipyridine based ligands **M**, **G** and **F** as building blocks*

Wegmann, B.; Jung, K.-H. *Liebigs Ann. Chem.* **1991**, *1991*, 121.

subsequent steps were similar for all three pyranosides: amine deprotection (palladium hydroxide, H_2, TFA, quantitative yield), followed by coupling to the succinimidoyl derivative (**44**) of 2,2'-bipyridine-4,4'-dicarboxylic acid (36-61% yields). It is noteworthy that when the analogous acid chloride **43** was treated with the free amines the reaction did not proceed selectively, and inseparable mixtures of nucleophilic substitution products were obtained. Therefore the crude acid chloride was treated with *N*-hydroxysuccinimide and triethylamine to afford the pure activated diester **44** in quantitative yield. After amide formation, deacetylation (94–100% yields) with NaOMe in methanol yielded the pure ligands **M**, **G**, **F**. Pure homoleptic tris-coordinated Fe^{II} complexes (**MMM**, **GGG** and **FFF**) were finally obtained by mixing stoichiometric amounts of the corresponding ligand and $FeCl_2 \cdot 4H_2O$ in water (Scheme 10).

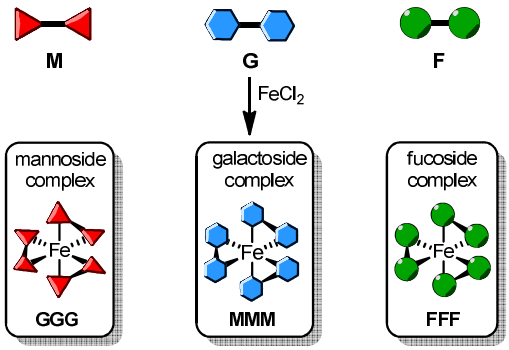

Scheme 10 *Formation of homoleptic complexes from ligands* **G**,**M** *and* **F**

3.3.1.2 Generation and Analysis of a Four Membered DCL

To gradually approach larger DCLs the three initial homoleptic library constituents were tried separately. By mixing two components the smallest possible library for the chosen system evolved. All combinations of the three available ligands were tested (Scheme 11). Aqueous complexes **MMM**, **GGG** or **FFF** were mixed in three separate experiments (Scheme 11, 0.3 mM aqueous solutions). In each mixture all expected species were detected by HPLC-MS analysis (Figure 4). The desired statistical distribution was roughly visible in all experiments after equilibration, indicating that the species are of similar stability. Further lectin binding studies should therefore be more reliable. Both the good

analysability and the found retention times indicated that a DCL generated from three initial homoleptic complexes could be directly screened against ConA lectin. Therefore, at this time, no further binding studies were performed for DCLs **J**, **K** and **L**.

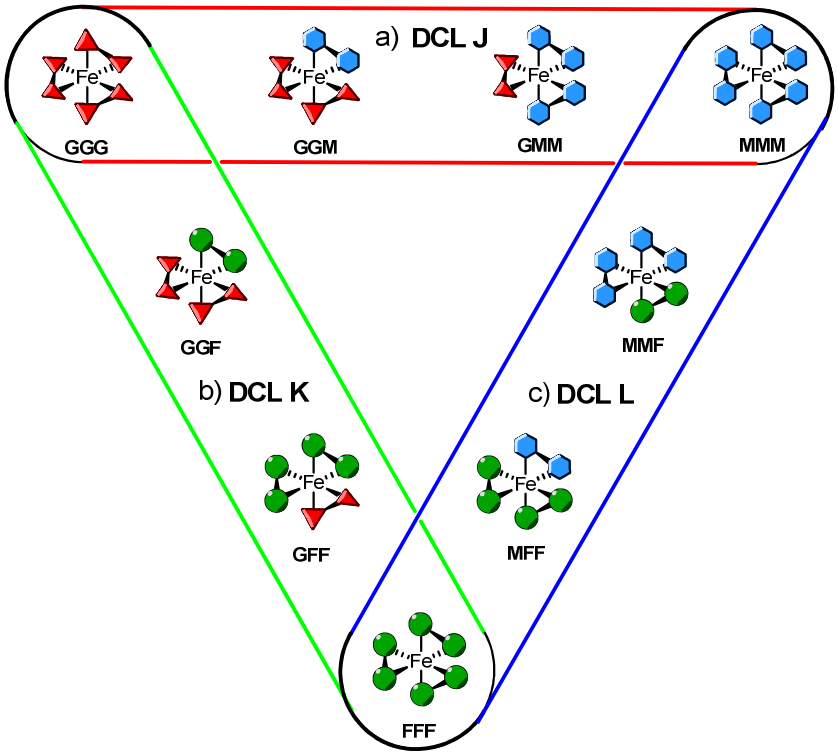

Scheme 11 *Generation of three four membered DCLs by mixing homoleptic complexes a)* ***GGG*** *with* ***MMM****, b)* ***GGG*** *with* ***FFF*** *or c)* ***MMM*** *with* ***FFF****.*

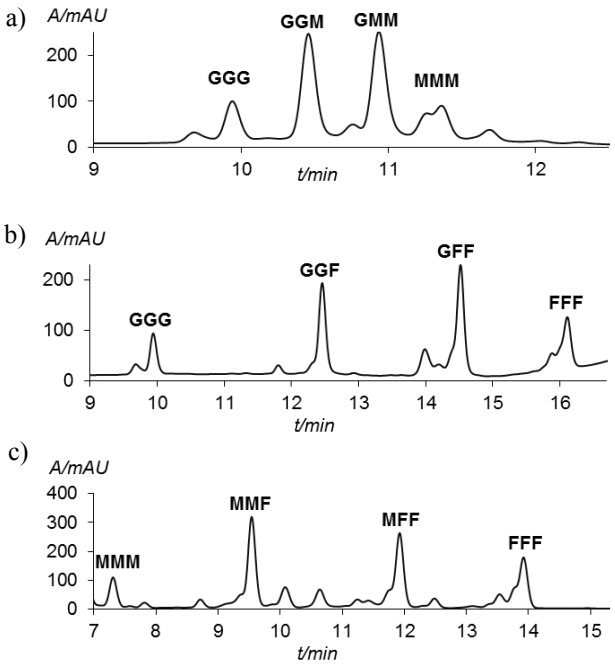

Figure 4 *UV-trace for a)* ***DCL J****, b)* ***DCL K*** *and c)* ***DCL L****. The identity of all species was confirmed by mass detection*

3.3.1.3 Generation and Analysis of a Ten Membered DCL

The results obtained for the four membered DCLs (**J**, **K** and **L**, section 3.2) prompted us to set-up a larger system for lectin binding studies. **DCL-M** containing all ten expected arrangements evolved after mixing aqueous solutions of complexes **MMM**, **GGG**, and **FFF**, within a few days (Scheme 12). Complexes of **DCL-M** tend to dissociate at room temperature at the given concentration, therefore a lower temperature (5 ºC) was employed. Equilibrium was established after 14 days, when the expected statistical distribution (Gaussian normal distribution) was reached. Stability of the library components was sufficient to be analysed by HPLC (reverse phase column, eluent: acetonitrile/water + 0.1 % TFA); their identity was again confirmed by HPLC-MS analysis (Figure 5a).

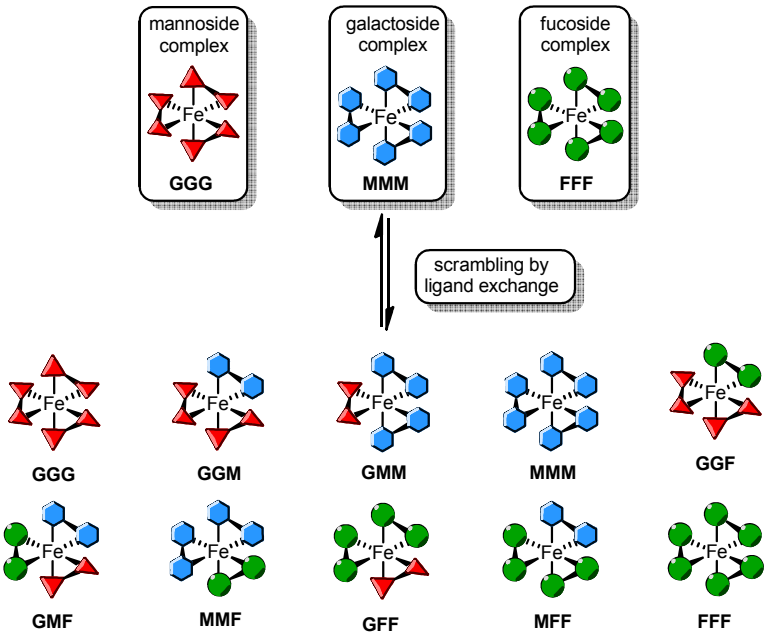

Scheme 12 *Set-up of a 10-member* ***DCL-M*** *from a three-complexes scrambling around a* Fe^{II} *center.*

Since the masses of D-galactose and D-mannose are identical, a combination of MS and retention-times interpolation was employed for peak assignments. The three initial homoleptic complexes were easily identified by comparison of their retention times with reference samples. The sequence of retention times **GGG** < **MMM** < **FFF** was subsequently employed to correctly locate peaks of identical masses by interpolation, such as **GGM** and **GMM** in the first set of signals, **GGF**, **GMF**, and **MMF** in the second set, and finally **GFF** and **MFF** at higher retention times. Minor peaks corresponding to uncomplexed glycoside-bipy ligands (**G, M, F**) were also detected in the chromatogram.

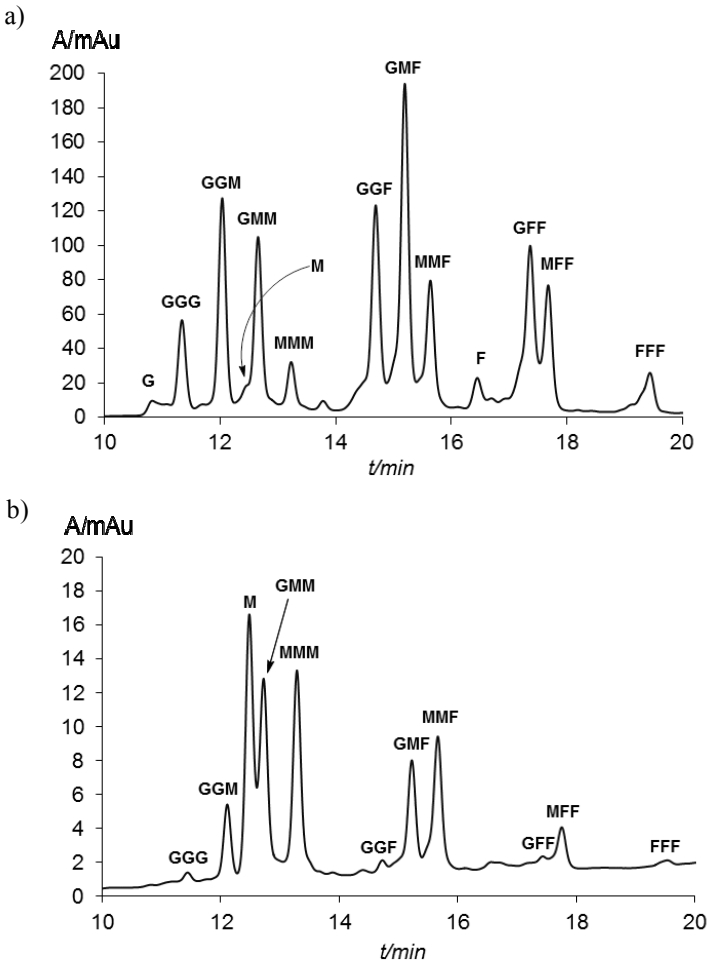

Figure 5 *a) Chromatogram of the equilibrated* ***DCL M*** *from left to right b) Fraction of* ***DCL M*** *bound to the protein surface complexes*

The same library as described in the previous paragraph was constructed, scrambling a mixture of the three initial homoleptic ligands in the presence of the target (sepharose-bound ConA) and the evolving library was allowed to equilibrate for 14 days. Equilibrium was assumed when no further changes in the proportions of library members in the reference sample were observed. The use of a solid phase supported ConA allowed the separation of binding and non-binding entities using a filtration/elution process (Chapter 2). The solid residue containing the protein and its bound counterparts was then

re-suspended in HCl (0.5 M) to release the bound complexes from the lectin surface. This method of cleavage was validated in a comparative study (see section 3.4). HPLC-MS analysis of this fraction showed the full mannoside complex **MMM** as the most prevalent species (Figure 5). Its overall abundance compared to the reference sample (with no protein interaction) was increased by more than 700% (Figure 6). Other compositions, containing mannoside ligand as high affinity recognition unit for the protein surface, were found to be enhanced according to the number of D-mannosides present in the arrangement. At least two D-mannoside-bipyridyl ligands are necessary to obtain a positive change in abundance in the protein bound fraction of the dynamic library as observed for **GMM** and **MMF** (Figure 6). Conversely, complexes containing only D-galactoside and/or L-fucoside ligands showed a lower affinity in the protein bound fraction. It became also apparent that both D-galactoside and L-fucoside appeared to have similar affinities for the protein, since **GGG**, **GGF, GFF** and **FFF** were comparably reduced in the ConA bound fraction.

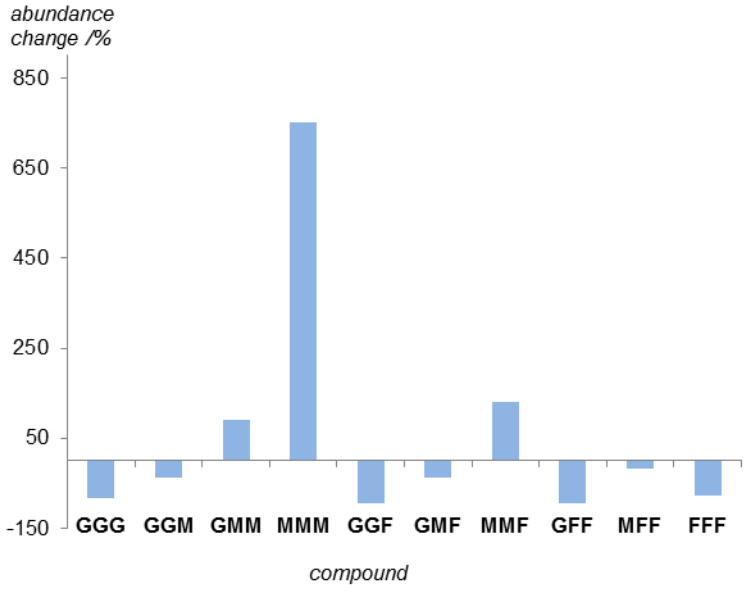

Figure 6 *Abundance change for the different library components. Equilibrated* ***DCL M*** *in absence of protein and the fraction of the* ***DCL M*** *bound to the protein are compared (determined from the respective HPLC chromatograms)*

Compared to the original amount of library members, approx. 80% remained in solution (due to the excess of library used) and 10% was bound to the protein and another 10% was destroyed during equilibration (deduced from integration in the chromatogram), but the only ligand that exhibited significant binding to the carbohydrate recognition domain (CRD) was mannoside **M**, dominant at a retention time of 12.5 min in the chromatogram (Figure 5).

Our results clearly confirm the expected higher affinity of the arrangements containing a large number of sugars with strong interactions to the protein surface. If we assume that complexes would bind to the protein only *via* a single building block, the resulting chromatogram would resemble the reference sample regarding distribution of species. However the strong bias towards DCL members bearing higher amounts of mannosides indicates that the well-known multivalency effect for protein recognition is also present for the dynamic multivalent system described here.

In a preliminary study, an analogous experiment was run employing an (approximately) equal amount of pure ConA lectin. The previously used filtration-elution procedure was not fully applicable for the small amount of sensitive, pure protein. Therefore only the first filtrate (showing the non- protein bound species) could be analysed. The proportions of the species found in that fraction were then compared to the non- protein bound fraction of the previous experiments. The values indicated that similar results can be obtained when using pure ConA lectin (instead of the sephrose bound one).

3.3.4 Method to Cleave Lectin Binding Partners - A Validation

A smaller dynamic library, namely **DCL L** (see section 3.2) was used to validate the method used for cleaving the lectin binding partners. The DCL contains D-mannose and L-fucose-based library constituents with very clear differences in selectivity for the ConA.

The binding studies presented in the previous paragraphs all employed the same method of cleavage, as it has been described by Ramström and Lehn.[10] The procedure relies on the fact that calcium and manganese ions located in the carbohydrate recognition domain are crucial for binding, and addition of acid demetallates the protein and releases bound

[10] Ramström, O.; Lehn, J.-M. *ChemBioChem* **2000**, *1*, 41.

entities.[11] Whether this method fully cleaves all protein binders has not been verified yet.

Thus, a variety of other methods to cleave binding partners from the lectin surface were tested. The experimental set-up was identical (concentrations, volumes, equilibration times) to those described above (see section 3.3.1). For the work-up of the filtrated residue four different procedures were employed:

The resin was:

1. Eluted in 0.4 ml of water and heated to 90 ºC for 2 h.
2. Eluted in 0.35 ml of water and 50 µl of 1 M HCl (Figure 7a).
3. Eluted in 0.4 ml of water and intensively stirred for one hour (Figure 7b).
4. Eluted in 0.4 ml of 8 M aqueous urea solution (Figure 7c).

The mixtures were then filtrated and the filtrate was analysed. The first experiment (heating) failed as the complexes were not stable enough under the conditions employed. For the remaining experiments, comparison to a reference sample without protein interaction gave again the abundance change for each constituent (Figure 7).

[11] Reeke, G. N.; Becker, J. W.; Cunningham, B. A.; Gunther, G. R.; Wang, J. L.; Edelman, G. M. *Ann. N.Y. Acad. Sci.* **1974**, *234*, 369.

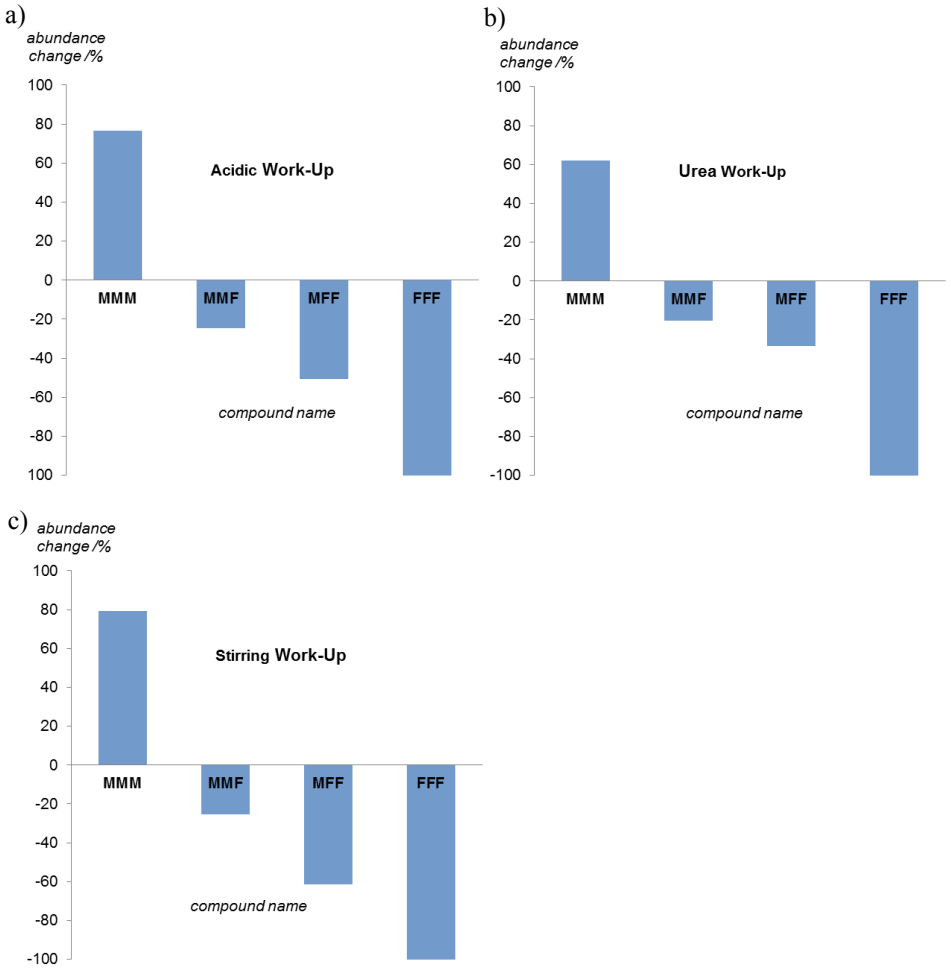

Figure 7 *The selectivities of three different workup conditions for ConA binding studies were compared. The change of abundance between reference sample and lectin bound fraction for each constituent were compared.*

As weakly bound entities would get cleaved first, partial cleavage would alter the observed selectivity. The methods discussed here have different potential to break bonds between the lectin and its binding partners. This should lead to variable or less pronounced results in selectivity for the different experiments. However, in all cases the same selectivity for ConA was clearly visible. This strongly indicates that all the acidic and the other methods induce full cleavage of the bound constituents from the lectin.

3.3.5 Conclusions

In summary, we have shown that dynamic combinatorial chemistry using metal ligand coordination as a reversible interaction and the well-known concept of enhanced binding to lectin surfaces by multivalent presentation of sugar subunits can be combined to analyse the binding properties of a multivalent dynamic combinatorial library. HPLC-MS was found as a method of choice to detect all possible structures resulting from the intermolecular exchange process. Analysis of the species bound to the protein surface showed an obvious bias towards the entities that are able to present larger numbers of carbohydrate units of high affinity to the protein surface. This example of a multivalent self-assembling system able to freely exchange its binding entities on multiple (more than two) connecting points to bind to a target proves that multivalency improves binding interactions in dynamic self-assembling systems too.

This approach can easily be extended to wider or more complex libraries, based on natural or unnatural components, presented under different orientations by a suitable choice of the position, length and rigidity of the linkers or the bipyridine anchoring.

3.4 Geometrical Preferences of Lectin Binding Evaluated by Dynamic Combinatorial Multivalency

In this section we wished to explore how the system was sensitive to geometrical binding preferences on ConA. Instead of varying the general compound type, as in other studies on multivalent ligand architectures,[12] or the nature of the sugar unit (as in the previous paragraphs), the more subtle discrimination induced by spacer length was investigated. The distance between two carbohydrate anchors is a well-known factor influencing the binding properties of small molecule ligands to protein surfaces. Affinity is diminished if the spacer does not match the necessary flexibility and length to leave each of the saccharide clusters close to an individually induced-fit into the carbohydrate recognition domain (CRD) of the lectin.[6] Rather than focusing on determining the optimal distance between two sugar subunits, we intended to explore the influence of the overall shape using combinations of spacer lengths.

3.4.1 Set-up of DCLs of Varying Shapes

To set-up DCLs of varying shapes, four α-D-mannoside bipyridine derivatives with different spacers (**S**, **M**, **L**, **X**, Scheme 14) were synthesized and coordinated around Fe^{II} cores. DCLs were then generated by mixing the homoleptic complexes in aqueous solution (see section 3.2 and 3.3). The resulting species are likely to adopt a variety of different shapes, from roughly spherical (the homoleptic **SSS**, **MMM**, **LLL**, and **XXX** members) to more distorted 3D architectures in the remaining heteroleptic complexes (Scheme 14).

Two set-ups were investigated: The first one was based on mixing three homoleptic complexes to obtain a 10-membered **DCL N** (Scheme 13, species highlighted in blue). The second 20-membered **DCL O** included one further initial library member, namely complex **XXX** bearing an α-D-mannoside moiety connected *via* a even longer linker.

[12] Gestwicki, J. E.; Cairo, C. W.; Strong, L. E.; Oetjen, K. A.; Kiessling, L. L. *J. Am. Chem. Soc.* **2002**, *124*, 14922.

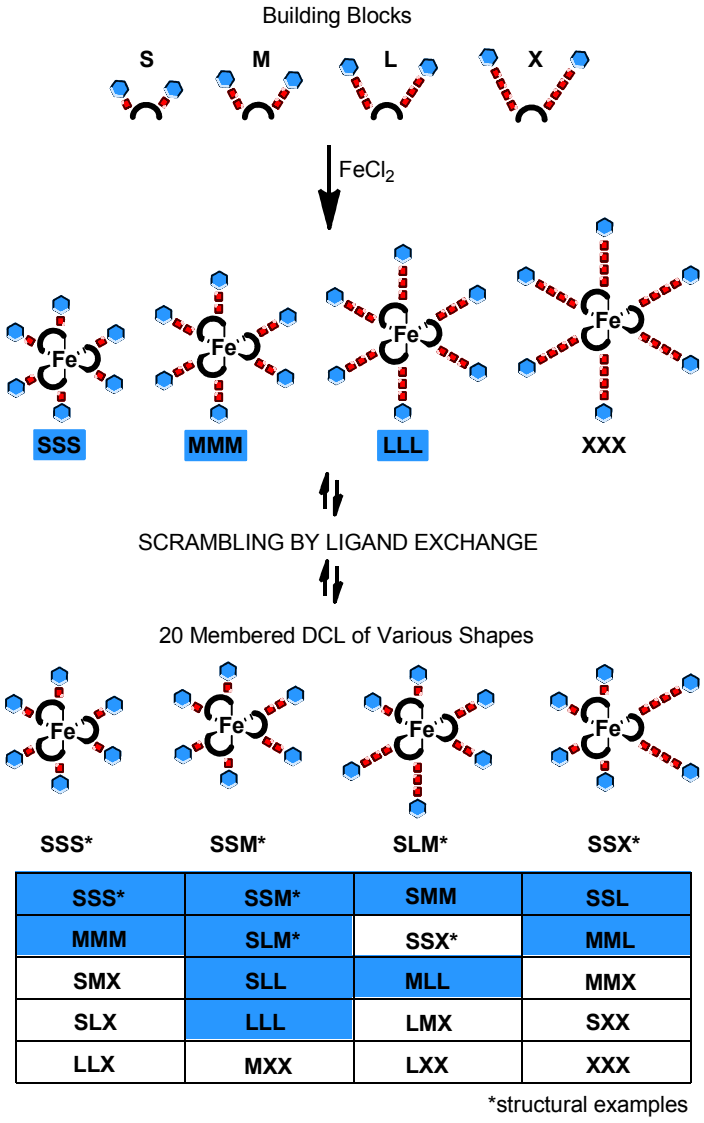

SSS*	SSM*	SMM	SSL
MMM	SLM*	SSX*	MML
SMX	SLL	MLL	MMX
SLX	LLL	LMX	SXX
LLX	MXX	LXX	XXX

*structural examples

Scheme 13 *a) Formation of four homoleptic complexes. b) Set-up of the 10-membered* ***DCL N*** *(blue) and the 20-membered* ***DCL O*** *(all species) from a three- or four-complexes scrambling around a* Fe^{II} *centre. Complexes are shown (from left to right) according to their order of appearance in the chromatogram (Figure 8). (Diastereomers omitted for clarity)*

3.4.1.1 Synthesis of Building Blocks

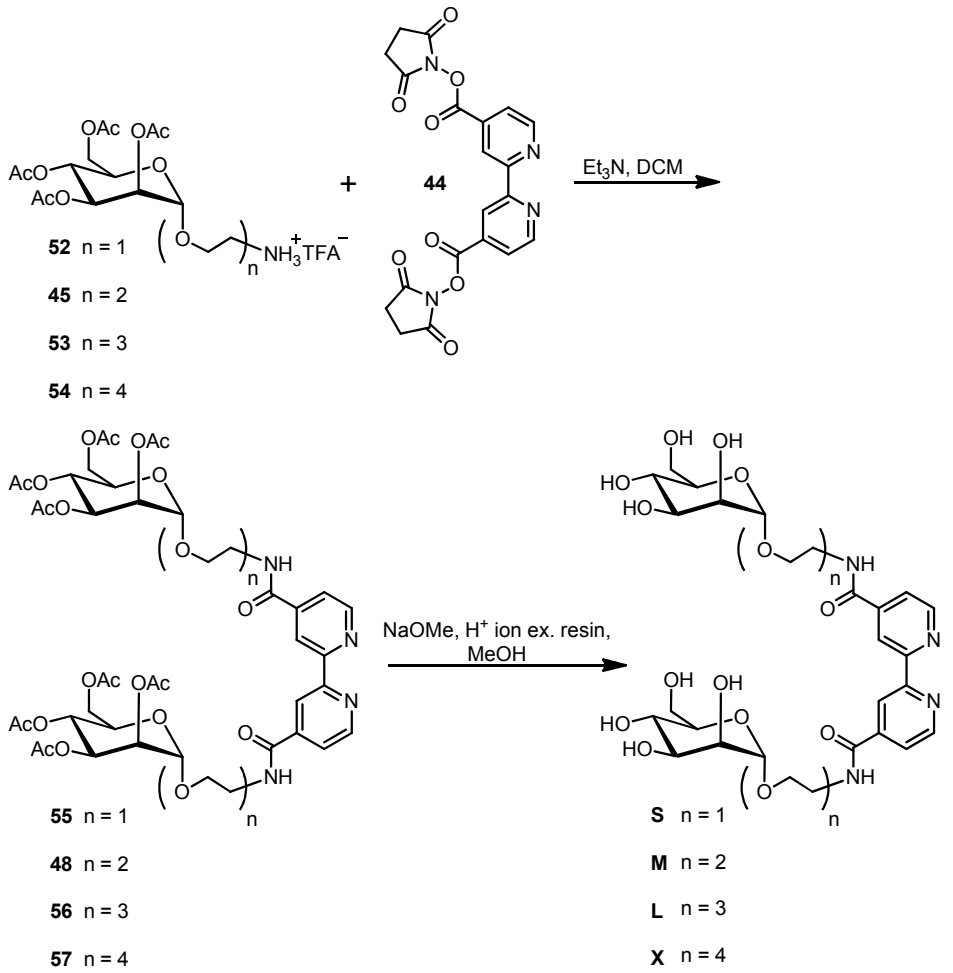

Scheme 14 *Preparation of bis D-mannoside bipyridine ligands with different spacer lengths.*

The synthesis of **M** was described in section 3.1. Precursors **52**, **53** and **54** (Scheme 14) were prepared according to literature procedures,[13] followed by coupling to the *N*-succinimidoyl derivative (**44**) of 2,2'bipyridine-4,4′dicarboxylic acid (44-56% yields of

[13] Engeldinger, E.; Puterová, Z.; Hiemenz, B.; Vos, J. G. *Inorg. Chim. Acta* **2008**, *361*, 341.

55, **56**, **57**), and deacetylation (100% yields of **S**, **M**, **L**, **X**). The pure homoleptic tris-coordinated Fe^{II} complexes (**SSS**, **MMM**, **LLL** and **XXX**) were finally formed by mixing 17 mM solutions of free (**S**, **M**, **L**, **X**) ligands with a stoichiometric amount of [$FeCl_2$ $4H_2O$] in the same volume of water, followed by dilution to 0.3 mM.

3.4.1.2 Generation and HPLC-MS Analysis of the DCLs

As before (see section 3.3.1), generation of the DCLs (**N** and **M**) was performed in water at 5 °C, as the complexes tend to dissociate at room temperature. The libraries were analysed by HPLC-MS (reverse phase column, acetonitrile/water + 0.1% TFA). The equilibrium was established after two weeks, when the expected statistical distribution (Gaussian normal distribution) was reached. All complexes gave rise to well resolved peaks in the chromatogram, together with minor peaks corresponding to uncomplexed bipyridine bis-D-mannoside ligands (**S**, **M**, **L**, **X**) (Figure 8a, for **DCL M**). Ten groups of complexes with identical masses can be identified: (**SSS)**, (**SSM)**, (**SMM**, **SSL)**, (**MMM**, **SSX**, **SLM**), (**MML**, **SLL**, **SMX**), (**MLL**, **MMX**, **SLX**), (**LLL**, **SXX**, **LMX**), (**LLX**, **MXX)**, (**LXX),** and (**XXX**). Fragments corresponding to the constituting ligands were observed in each individual spectrum, enabling unambiguous identification of every specific arrangement. The equilibrated libraries were mixed with the target (sepharose-bound ConA) and the mixture was allowed to equilibrate for another week. The use of the solid phase supported ConA again facilitates the separation of binding and non-binding entities by means of a filtration/elution process (see Chapter 2). The bound complexes were again easily released from the lectin surface by treatment with a 0.5 M HCl solution. The overall abundance of each library member in this protein bound fraction (Figure 8b, for **DCL M**) was compared to a reference sample (without protein interaction) to obtain a picture of the relative affinities for each complex (Figure 9).

The first experiments involving the 10 membered **DCL N** indicated that binding of complexes containing **S** or **M** ligands was significantly hampered. The effect is so strong that the only biasing factor detectable is the number of **L** ligands present in the respective constituent. This result confirmed the linker length of **L** as more advantageous for binding. However, a deeper insight into geometrical binding preferences of ConA was not obtained.

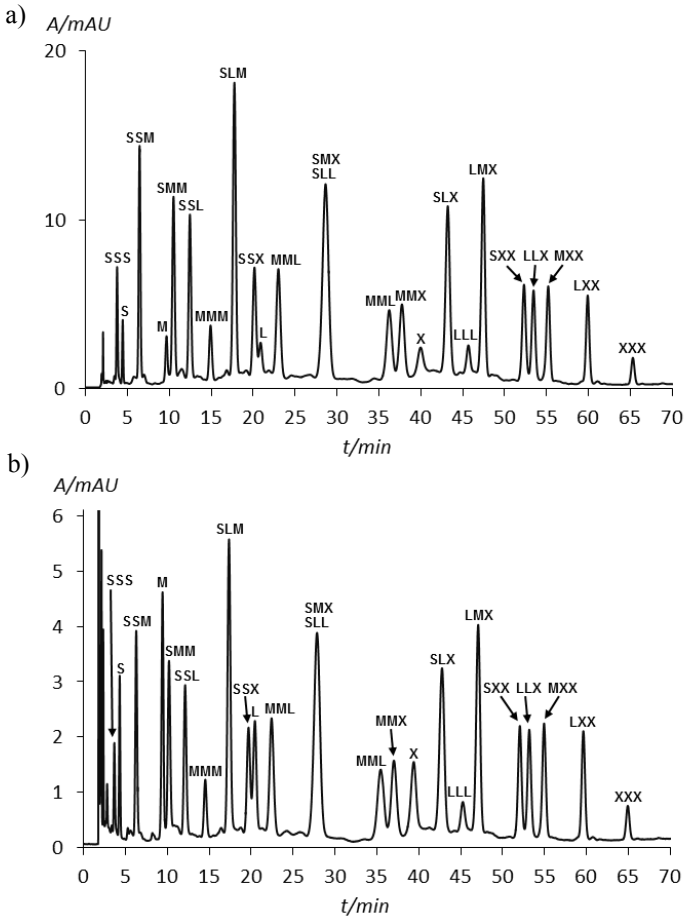

Figure 8 *a) Chromatogram of the equilibrated* ***DCL O*** *containing responses for 20 Fe^{II} complexes and 4 ligand species. b) Chromatogram of the protein bound fraction of the DCL. Overlapping peaks are indicated with marks on top of each other.*

In contrast, **DCL M** (which was set-up for this reason) also contains ligand **X,** varying from **L** by only one additional ethylene glycol subunit. This endowed the system with another spacer of appropriate length for binding, a more subtle variation. The change in abundance for the species of **DCL M** is shown in Figure 9.

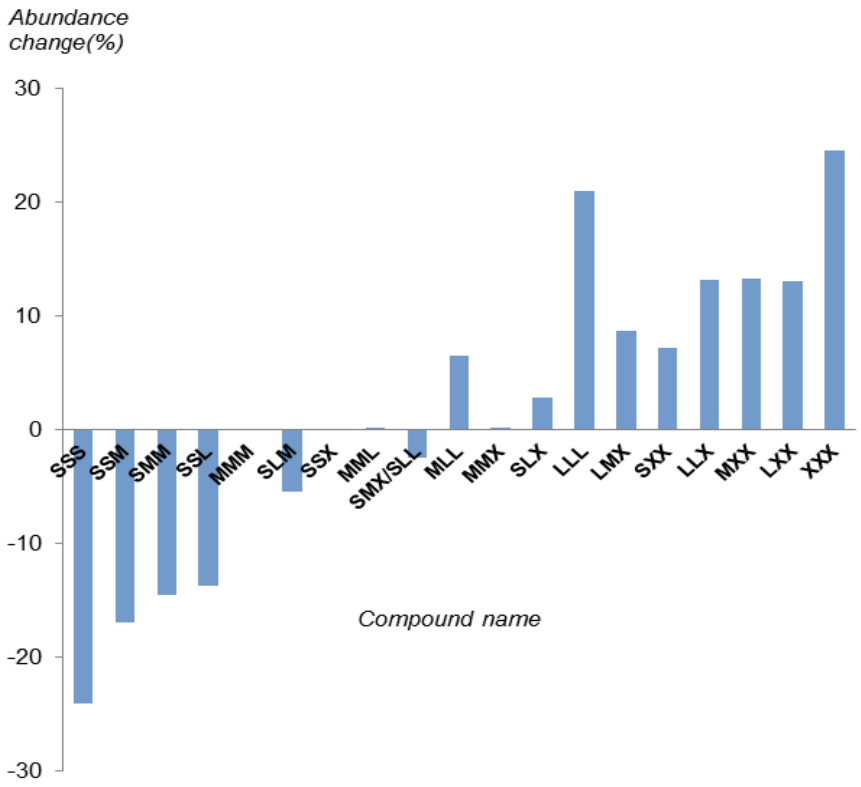

Figure 9 *Abundance changes for the different library components. The equilibrated DCL and the fraction of the DCL that gets bound to the protein are compared (determined from the HPLC chromatograms, Figure 8).*

Data from three independent equilibration/ConA binding experiments (see Experimental Part) were evaluated and revealed identical trends. However, standard deviations are relatively large, especially for the values of the homoleptic complexes. Their overall abundance is lower than for mixed entities due to statistic effects. For that reason, small variations can create large errors. Those errors are mainly produced during the work-up. The procedure includes washing of the filter residue (consisting of ConA with bound entities) to remove unspecifically bound species. As only small amounts of water can be used for that purpose, it was difficult to control the intensity of the washing. This can result in more or less pronounced selectivity. For that reason similar trends are always

visible but also disappointingly large errors (in the changes of abundance) were detected. Therefore, all final conclusions should be regarded as preliminary.

Nevertheless, some interesting indications could be deduced from the results. **LLL** and **XXX** were found to be the strongest bound species, whereas heteroleptic entities such as **LXX** and **LLX** were less prevalent. Expectedly, short ligands, such as **M** and **S**, were not found among the best binders. As mentioned in 3.3, under the experimental conditions, 80% of the library members did not bind to the protein and remained in solution (due to the excess of library employed), whereas 10% were bound to the protein and another 10% were destroyed during equilibration and acidic workup, releasing free ligands (**S**, **M**, **L**, **X**), abundantly visible in the chromatograms (Figure 8b). Most remarkably, heteroleptic complexes containing *both* **L** and **X** ligands (such as **LLX** and **LXX**) seemed to display a *lower* affinity to the protein than **LLL** or **XXX**. The more distorted shapes of the non-uniformly decorated complexes appear to be a disadvantage for binding to the lectin. The same trend was visible in all three experiments, though the abundance changes were not as pronounced as in our previous study.

3.4.1.3 Binding Analysis by Isothermal Titration Calorimetry

In order to explore another way to confirm the results of the previous section, isothermal titration calorimetry (ITC) was employed to determine binding constants. Due to the lack of solubility of the protein, the choice of concentrations was limited and thus the full sigmoidal curve of the thermogram could not be properly recorded. Low binding stoichiometries suggest that single hexavalent complexes are able to bind to multiple proteins at the same time. Therefore the interpretation of the data was limited to a qualitative comparison of binding constants. Separately, the homoleptic complexes **LLL** (at 0.4 mM) and **XXX** (at 0.4 mM) were titrated into a solution containing ConA. The heat released or absorbed during binding was measured as a function of the molar ratio of the sugar derivative to ConA. The obtained data shows that **LLL** binds better than **XXX** ($Ka_{(LLL)} = 8 \cdot 10^5\ M^{-1} > Ka_{(XXX)} = 2 \cdot 10^5\ M^{-1}$). A comparative study on the influence of spacer lengths for sugar binding to ConA reported by Page and Roy in 1997 provided values for

optimal distances.[14] For our system, model inspection of the ligands docked into the surface of the protein showed that ligand **L** containing a triethyleneglycol chain at each side of the bipyridyl core should indeed exhibit the optimal length for binding ConA. Addition of a further ethyleneglycol subunit at each arm (such as in ligand **X**) makes the spacer a bit too long and should lower the binding affinity. Although this difference was not visible from the HPLC data (it actually suggested a slightly reverse trend), the ITC titration may have given a more exact picture of the binding (two independent measurements gave the same results) as it directly compares only those two species.

Owing to the dynamic properties of the system, ITC experiments of the mixed species **LLX** and **LXX** cannot be measured individually, as for the homoleptic complexes. Nevertheless, binding properties of those heteroleptic species could be inferred from the affinity constant of a dynamic mixture of **LLL** and **XXX**. Therefore a 1:1 mixture of **LLL** and **XXX** of identical concentration as for the previous titrations (0.4 mM) was prepared. Scrambling by ligand exchange afforded a four member DCL containing **LLX** and **LXX** as emerging heteroleptic species. In the new mixture, **LLX** and **LXX** are worse binders than **LLL** and **XXX**, according to the HPLC data. Thus, this mixture should exhibit an affinity constant to ConA [$K_{a(MIXTURE)}$] significantly smaller than the mean of $K_{a(LLL)}$ and $K_{a(XXX)}$ binding constants, previously determined. The value of $K_{a(MIXTURE)}$ should be close to that of the homoleptic complex **XXX** of lower affinity. In agreement with these predictions ITC measurements indicated that the affinity constant of the mixture is comparable to that of **XXX** ($K_{a(MIXTURE)} = K_{a(XXX)} \approx 2 \cdot 10^5\ M^{-1}$). Those values seem to confirm the results obtained from the HPLC study. However, also these values do not exhibit large differences (orders of magnitude) and therefore, the results can only be regarded as indicative.

3.4.2 Conclusions

The observed phenomenon of worse binding for heteroleptic species could be explained by the concept of *statistical rebinding*. The theory describes a process that is assumed to account for a large portion of the enhanced binding through multivalency: a multivalent

[14] Page, D.; Roy, R. *Glycoconjugate J.* **1997**, *14*, 345.

binder changes its own position on the protein binding site by shifting from one of its (many) binding units to the next. Therefore the off-rate of the ligand to dissociate back into solution is slower than that of a monovalent one.[15] If this effect is dominant a concentrically (spherically) shaped binding partner containing only one type of spacer would facilitate the shifting movement and be advantageous for optimising binding interactions, as has recently been suggested from experimental data.[12]

Our results show how a multivalent DCL can be employed to analyse the geometrical preferences of a lectin, such as ConA. Particularly, this was evidenced by the fact that spherical shapes, presented by complexes uniformly decorated with either **L** or **X** ligands, seem to benefit from an additional advantage in affinity. This leads to conclude that the likely dominating mechanism is statistical rebinding, favouring concentric species, which facilitate a shifting movement. Thus, the classical *lock and key* analogy apparently applies only at the level of the monomeric unit distinguishing between different sugar subunits, as previously demonstrated (see Section 3.3).

The well-studied trimannoside core that is recognized by ConA with high affinity and selectivity contains pyranose rings connected through their 1,3 and 1,6 positions.[16] A further extension of the approach presented herein would require changing the linking positions, in the hope that some heteroleptic complexes would be selected as the best binders. To obtain more solid values, a different metal (e.g. ruthenium) could be used to obtain kinetically more stable complexes. This would allow for separation of the library members and subsequent determination of specific binding constants by alternative methods.

[15] Pieters, R. J. *Org. Biomol. Chem.* **2009**, *7*, 2013.
[16] Naismith, J. H.; Field, R. A. *J. Biol. Chem.* **1996**, *271*, 972.

3.5 Experimental Section

Materials and methods

All reagents were commercial and used without further purification. Triethylamine was distilled over CaH_2. If not stated differently all reactions were performed under an argon atmosphere using dry solvents and flame dried reaction vessels. NMR spectra were recorded at 293 K, using a 300, 400 or 500 MHz spectrometer. Deuterated solvents used are indicated in each case. Shifts are referenced relative to deuterated solvent residual peaks. Complete signal assignments from 1D and 2D NMR spectroscopy were based on COSY, HSQC correlations and phase sensitive DEPTQ45, DEPTQ135 spectra. High-resolution electrospray injection times of flight (HR-ESI-ToF) mass spectra were recorded using a Bruker spectrometer. Anhydrous solvents were obtained from a solvent purification system (SPS). Thin layer chromatography (TLC) was performed on pre-coated TLC-plates SIL G-25 UV254 (Macherey-Nagel) glass supported visualised by UV at 254 nm and/or Pancaldi, Vanilin or $KMnO_4$ stain. Column chromatography was carried out using silica gel from SDS (Silica Gel 60 A) and SDS (Silica Gel C18 "reverse phase" 60A, 40–63 μm). For automated flash column chromatography a CombiFlash Companion apparatus running RediSep® columns was used. High-Pressure Liquid Chromatography (HPLC) chromatograms were recorded on an Agilent Technologies 1200 (UV-detector) and an Agilent Technologies 6130 Quadropole Liquid chromatography/mass (LC/MS) detector (recording in ESI mode) connected to and analytical HPLC running a reverse phase (RP) C18 Waters Symetry 300™ C18 5μm. The mobile phase consisted of a CH_3CN–H_2O mixture containing 0.1 % TFA. The solvents were provided by Scharlau and Carlo Erba (HPLC gradient grade).

Synthesis

(2,3,4-Tri-O-acetyl-L-fucopyranosyl) trichloroacetimidate was prepared according to literature procedures.[9]

[Fe(2,2'-bipy)$_3$](PF$_6$)$_2$ (**38**) and **[Fe(4,4'-dimethyl-2,2'-bipy)$_3$](PF$_6$)$_2$** (**39**) were prepared according to literature procedures.[17]

[2,2'-Bipyridine]-4,4'-dicarbonyl dichloride (**43**) was purchased from Sigma-Aldrich (Spain).

Bis(succinimidoyl) 2,2' bipyridine-4,4'-dicarboxylate (**44**) were prepared according to literature procedures.[13]

Precursors **52**, **53** and **54** were prepared according to literature procedures.[13]

Preparation of (40) and (41)

α-D-mannose pentaacetate or β-D-galactose pentaacetate (1 eq.) was dissolved in DCM (0.14 M of pyranose pentaacetate), benzyl(2-(2-hydroxyethoxy)ethyl)carbamate (1 eq.) was added and the solution was cooled to 0 ºC. After boron trifluoride diethyl etherate (4 eq.) was slowly introduced, the solution was allowed to reach room temperature and then was heated to 45ºC and stirred overnight. The mixture was diluted and washed with aq. $NaHCO_3$ conc. and water. The organic phase was then dried and evaporated to yield the crude product mixed with starting material. Purification by column chromatography (ethylacetate/hexane,1:1) afforded a clear and colourless syrup.

[17] Bouzaid, J.; Schultz, M.; Lao, Z.; Bartley, J.; Bostrom, T.; McMurtrie, J. *Cryst. Growth Des.* **2012**, *12*, 3906Hong, Y.-R.; Gorman, C. B. *J. Org. Chem.* **2003**, *68*, 9019.

((2,3,4,6-Tetra-O-acetyl-α-D-mannopyranosyl)ethoxy)ethyl benzylcarbamate (40)

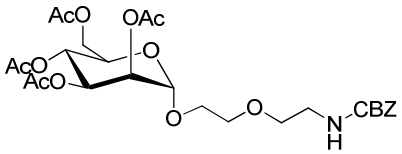

Yield: 3 g, 62 % - **^{1}H-NMR:** (400 MHz, $CDCl_3$) δ_H = 7.30 (m, 5 H, Ar-H), 5.35 (dd, 1 H, $J_{H\text{-}3,H\text{-}2}$ = 4 Hz, $J_{H\text{-}3,H\text{-}4}$ = 10 Hz, H-3), 5.24 (apparent t, 1 H, $J_{H\text{-}4,H\text{-}3}$ = 10 Hz, $J_{H\text{-}4,H\text{-}5}$ = 10 Hz, H-4), 5.24 (dd, 1 H, $J_{H\text{-}2,H\text{-}3}$ = 3 Hz, $J_{H\text{-}2,H\text{-}1}$ = 2 Hz, H-2), 5.11 (s, 2 H, CH_2-Ar), 4.89 (d, 1 H, $J_{H\text{-}1,H\text{-}2}$ = 2 Hz, H-1), 4.24 (dd, $J_{Ha\text{-}6,Hb\text{-}6}$= 12 Hz, $J_{Ha\text{-}6,H\text{-}5}$= 5 Hz, H_a-6), 4.04 (stack, 2 H, H_b-6, H-5), 3.77 (m, 1 H, C$H_a$$H_b$NH), 3.61 (stack, 3 H, C$H_a$$H_b$NH and CH_2), 3.54 (t, 2 H, $J_{H,H}$ = 5 Hz), 3.38 (dd, 2 H, $J_{H,Ha}$ = 10 Hz, $J_{H,Hb}$ = 5 Hz, CH_2), 2.13, 2.09, 2.01, 1.99 (s, 3 H, $COCH_3$) ppm. -**^{13}C-NMR:** (400 MHz, $CDCl_3$) δ_C = 170.6, 170.1, 169.7 (C=O), 128.4 (Ar-C), 128.0 (Ar-C), 97.5 (C-1), 70.2 (CH_2), 69.9 (CH_2), 69.6 (C-2), 68.9 (C-3), 68.4 (C-5), 67.1 (CH_aH_b), 66.6 (Ar-*C*H_2), 66.2 (C-4), 62.6 (C-6), 40.9 (*C*H_2NH), 20.8, 20.7, 20.6, 20.6 (OC*C*H_3) ppm. - **IR**: $\tilde{\nu}$ = 3388, 2937, 1742, 1519, 1454, 1367, 1216, 1133, 1080, 1043, 977, 776, 737, 698, 600, 464, 398 cm^{-1}. - **HRMS (TOF, ES$^+$)** calcd. for $C_{26}H_{35}NO_{13}Na^+$ 592.2006 [M+Na$^+$] found *m/z* = 592.2018 [M+Na$^+$].

((2,3,4,6-Tetra-O-acetyl-β-D-galactopyranosyl)ethoxy)ethyl benzylcarbamate (41)

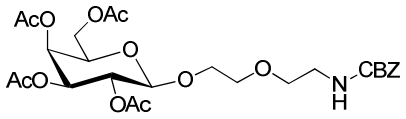

Yield: 510 mg, 49 % - **^{1}H-NMR:** (400 MHz, $CDCl_3$) δ_H = 7.32 (m, 5 H, Ar-H), 5.38 (apparent d, 1 H, *J* = 3 Hz, H-4), 5.20 (dd, 1 H, $J_{H\text{-}2,H\text{-}3}$ = 11 Hz, $J_{H\text{-}2,H\text{-}1}$ = 8 Hz, H-2), 5.13 (s, 2 H, CH_2), 5.01 (dd, 1 H, $J_{H\text{-}3,H\text{-}2}$ = 11 Hz, $J_{H\text{-}3,H\text{-}4}$ = 3 Hz, H-3), 4.54 (d, 1 H, $J_{H\text{-}1,H\text{-}2}$ = 8 Hz, H-1), 4.09 (m, 2 H, H_a-6, H_b-6), 3.93 (m, 1 H, pyranose-O-C$H_a$$H_b$), 3.87 (m, 1 H, H-5), 3.69 (m, 1 H, pyranose-O-C$H_a$$H_b$), 3.60 (m, 2 H, CH_2), 3.54 (m, 2 H, CH_2), 3.37 (m, 1 H, CH_2NH), 2.14, 2.05, 2.04, 1.99 (s, 3 H, $COCH_3$) ppm. - **^{13}C-NMR:** (400 MHz, $CDCl_3$) δ_C = 170.3, 170.2, 170.1, 169.5 (C=O), 128.5 (Ar-C), 128.1

(Ar-C), 128.1 (Ar-C), 101.2 (C-1), 70.8 (C-3), 70.7 (C-5), 70.1 (CH_2), 69.9 (CH_2), 68.8 (C-2), 68.8 (CH_aH_b) 67.0 (C-4), 66.6 (Ar-CH_2), 61.2 (C-6), 40.9 (CH_2NH), 20.7, 20.6, 20.6, 20.5 ($OCCH_3$) ppm. - **IR**: $\tilde{\nu}$ = 3393, 2938, 2878, 1746, 1521, 1366, 1208.65, 1040, 756, 698, 589 cm^{-1}. – **HRMS (TOF, ES$^+$)** calcd. for $C_{26}H_{35}NO_{13}Na^+$ 592.1998 [M+Na^+] found *m/z* = 592.2013 [M+Na^+].

((2,3,4-Tri-O-acetyl-α-L-fucopyranosyl)ethoxy)ethyl benzylcarbamate (42)

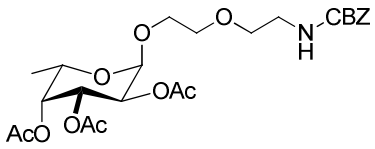

(2,3,4-Tri-O-acetyl-fucopyranosyl)trichloro acetimidate (mixture of isomers α and β, see above) (1,03 g, 2,38 mmol) was dissolved in DCM (19 ml), then molecular sieve (AW 300, powdered and activated overnight at 110ºC under vacuum) was added followed by benzyl (2-(2-hydroxyethoxy)ethyl)carbamate (1,14 g, 4,76 mmol). The solution was cooled to -20ºC and TMS-OTf (0,22 ml, 1,19 mmol) in 1 ml DCM is added slowly. After less than 40 min TLC indicated completion of the reaction and triethylamine (0,33 ml, 2,38 mmol) was introduced at 0 ºC. Stirring was continued for another 10 min then the solvent was evaporated and the residue was purified by column chromatography to yield a colourless syrup. **Yield:** 810 mg, 67 % - **^{1}H-NMR:** (400 MHz, $CDCl_3$) δ_H = 7.31 (m, 5 H, Ar-H), 5.32 (brs, 1 H, NH), 5.18 (stack, 2 H, H-4, H-2), 5.12 (s, 2 H, Ar-CH_2), 5.00 (dd, 1 H, $J_{H\text{-}3,H\text{-}4}$ = 11 Hz, $J_{H\text{-}3,H\text{-}2}$ = 4 Hz, H-3), 4.50 (d, 1 H, $J_{H\text{-}1,H\text{-}2}$ = 8 Hz, H-1), 3.32 (m, 1 H, glycol-H_a), 3.73 (m, 1 H, H-5), 3.64 (m, 1 H, glycol-H_b), 3.60 (m, 2 H, CH_2), 3.53 (m, 2 H, CH_2), 2.16 (s, 3 H, $COCH_3$), 2.03 (s, 3 H, $COCH_3$), 2.03 (s, 6 H, $COCH_3$), 1.99 (s, 3 H, $COCH_3$), 1.20 (d, 3 H, $J_{H\text{-}6,H\text{-}5}$ = 6 Hz, H-6) ppm. - **^{13}C-NMR:** (400 MHz, $CDCl_3$) δ_C = 170.6, 170.1, 169.6 (C=O), 156.4 (carbonyl C), 136.6 (Ar-C, C_q), 128.5 (Ar-CH), 128.1 (Ar-CH), 101.1 (C-1), 71.2 (C-3), 70.2 (C-4), 70.1 (glycol CH_2), 70.0 (glycol CH_2), 69.2 (C-5), 68.9 (C-2), 68.6 (CH_aH_b), 66.6 (Ar- CH_2), 40.9 (CH_2NH), 20.7, 20.6, 20.6 ($OCCH_3$), 16.0 (C-6) ppm. - **IR**: $\tilde{\nu}$ = 2939, 1744, 1521, 1454, 1366, 1217, 1174, 1127,

1056, 906, 734, 698, 594 cm^{-1}. - **MS (TOF, ES$^+$)** *m/z* = 534.2 [M+Na^+]. - **HRMS (TOF, ES$^+$)** calcd. for $C_{24}H_{33}NO_{11}Na^+$ *m/z* = 534.1952 [M+Na^+] found *m/z* = 534.1971 [M+Na^+].

Preparation of (45), (46) and (47)

((Per-O-acetyl-pyranosyl)ethoxy)ethyl benzylcarbamate (**5a**), (**6a**) or (**7a**) (1 eq.) was dissolved in EtOH (0.03 M of (**5a**), (**6a**) or (**7a**) not dry) and TFA (2 eq.) was introduced under argon. Palladium hydroxide on carbon (20 mass-%Pd, 1 eq.) was added and the flask was evacuated by membrane pump until solvent started to boil, then hydrogen was flushed in and the same cycle was repeated once more. After stirring overnight no more starting material could be detected by TLC and the reaction mixture was filtrated over celite®. Solvent was evaporated and the residue was subjected to filtration over silica gel, washing of impurities with an eluent of ethyl-acetate/hexane (3:2) and eluting the product then with DCM/MeOH (2:10) affording a pale syrup.

((2,3,4,6-Tetra-O-acetyl-α-D-mannopyranosyl)ethoxy)ethanaminium trifluoroacetate (45)

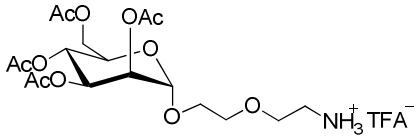

Yield: 1.98 g, 93 % - **^{1}H-NMR:** (400 MHz, $CDCl_3$) δ_H = 8.14 (s, 3 H, NH_3 exchanging), 5.29 (m, 1 H, H-1), 5.27 (m, 1 H, H-4), 5.24 (m, 1 H, H-2), 4.90 (s, 1 H, H-1) 4.23 (dd, 1 H, $J_{Ha\text{-}6,Hb\text{-}6}$= 12 Hz, $J_{Ha\text{-}6,H\text{-}5}$= 5 Hz, H_a-6), 4.13 (apparent d, 1 H, $J_{Hb\text{-}6,Ha\text{-}6}$= 12 Hz, H_b-6), 4.06 (m, 1 H, H-5), 3.68-3.83 (stack, 8 H, CH_2), 3.21 (s, 1 H, CH_2NH_3), 2.15, 2.11, 2.06, 2.00 (s, 3 H, $COCH_3$) ppm. - **^{13}C-NMR:** (400 MHz, $CDCl_3$) δ_C = 171.0, 170.4, 169.8 (C=O), 97.4 (C-1), 70.0 (CH_2), 69.5 (C-2), 69.1 (C-4), 68.4 (C-5), 66.9 (CH_2), 66.6 ($CH_2CH_2NH_3^+$), 66.1 (C-3), 62.6 (C-6), 39.8 ($CH_2NH_3^+$), 20.8, 20.7, 20.6, 20.6 ($OCCH_3$) ppm. - **IR**: $\tilde{\nu}$ = 2939, 1741, 1676, 1429, 1369, 1220, 1129, 1044, 978, 833, 798, 721, 600,

467 cm^{-1}. - **HRMS (TOF, ES$^+$)** calcd. for $C_{18}H_{30}NO_{11}^+$ *m/z* = 436,1813 [M^+] found *m/z* = 436.1812 [M^+].

((2,3,4,6-Tetra-O-acetyl-β-D-galactopyranosyl)ethoxy)ethanaminium trifluoroacetate (46)

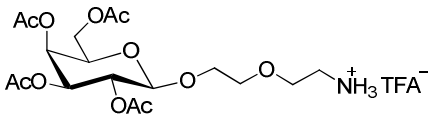

Yield: 420 mg, 99 % - **^{1}H-NMR:** (500 MHz, $CDCl_3$) δ_H = 8.13 (s, 3 H, NH_3 exchanging), 5.42 (apparent d, 1 H, *J* = 3 Hz H-4), 5.15 (dd, 1 H, $J_{H-2,H-3}$= 11 Hz, $J_{H-2,H-1}$= 8 Hz H-2), 5.05 (dd, 1 H, $J_{H-3,H-2}$= 11 Hz, $J_{H-3,H-4}$= 3 Hz H-3), 4.55 (d, 1 H, $J_{H-1,H-2}$ = 8 Hz, H-1) 4.23 (dd, 1 H, $J_{Ha-6,Hb-6}$= 11 Hz, $J_{Ha-6,H-5}$= 7 Hz, H_a-6), 4.13 (dd, 1 H, $J_{Hb-6,Ha-6}$ = 11 Hz, $J_{Ha-6,H-5}$= 7 Hz, H_b-6), 3.99 (m, 1 H, CH_2, C*H*$_a$H$_b$), 3.94 (t, 1 H, $J_{H-5,H-6}$ = 7 Hz, H-5) 3.69-3.77 (stack, 8 H, CH_aH_b + 2×CH_2), 3.20 (m, 2 H, CH_2NH_3), 2.18, 2.08, 2.07, 2.01 (s, 3 H, $COCH_3$) ppm. - **^{13}C-NMR:** (400 MHz, $CDCl_3$) δ_C = 170.5, 170.3, 170.2 170.1 (C=O), 101.2 (C-1), 70.8 (C-5), 70.6 (C-3), 69.9 (CH_2), 69.0 (C-2),68.7 (CH_2), 66.9 (C-4), 66.6 (CH_2), 61.2 (C-6), 39.6 ($CH_2NH_3^+$), 20.7, 20.6, 20.5, 20.5 ($OCCH_3$) ppm. **IR**: $\tilde{\nu}$ = 3502, 2941, 2885, 1747, 1369, 1221, 1200, 1130, 1038 cm^{-1}. **HRMS (TOF, ES$^+$)** calcd. for $C_{18}H_{30}NO_{11}^+$ *m/z* = 436,1813 [M^+] found *m/z* = 436.1793 , [M^+].

((2,3,4-Tri-O-acetyl-α-L-fucopyranosyl)ethoxy)ethanaminium trifluoroacetate (47)

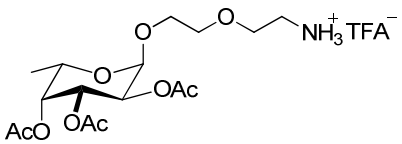

Yield: 550 mg, 100 % - **^{1}H-NMR:** (400 MHz, $CDCl_3$) δ_H = 7.95 (bs, 3 H, NH_3), 5.25 (dd, 1 H, $J_{H-3,H-4}$ = 1 Hz, $J_{H-3,H-4}$ = 3 Hz, H-3), 5.08 (dd, 1 H, $J_{H-2,H-1}$ = 8 Hz, $J_{H-2,H-3}$ = 11 Hz, H-2), 5.03 (dd, 1 H, $J_{H-4,H-3}$ = 3 Hz, $J_{H-4,H-5}$ = 11 Hz, H-4), 4.48 (d, 1 H, $J_{H-1,H-2}$ = 8 Hz, H-1), 3.99 (m, 1 H, pyranose-O-C*H*$_a$H$_b$), 3.82 (m, 1 H, H-5), 3.64 (stack, 5 H, CH_2), 2.00, 2.06, 2.18 (3 s, 9 H, $OCCH_3$), 1.22 (d, 3 H, $J_{H-6,H-5}$ = 6 Hz, H-6) ppm.

^{13}C-NMR: (400 MHz, $CDCl_3$) δ_C = 170.6, 170.6, 170.2 (OAc, quaternary C), 101.2 (C-1), 70.9 (C-4), 70.0 (C-3), 69.9 (CH_2), 69.4 (C-5), 69.1 (C-2), 68.7 (CH_2), 39.5 (CH_2NH), 20.7, 20.5, 20.5 ($OCCH_3$), 15.8 (C-6) ppm. **IR**: $\tilde{\nu}$ = 2943, 1744, 1676, 1517, 1429, 1369, 1220, 1201, 1171, 1132, 1057, 1021, 971, 933, 907, 834, 797, 721, 705, 594, 537, 518, 476.24, 406 cm^{-1}. **MS (TOF, ES$^+$)** calcd. for found *m/z* = 378.2 [M-TFA$^-$]. **HRMS (TOF, ES$^+$)** calcd. for $C_{16}H_{28}NO_9^+$ *m/z* = 378,1759 [M$^+$] *m/z* = 378.1771 [M^{+-}].

Preparation of (48), (49) and (50)

The trifluoroacetate (**40**, **41** or **42**) (2.2 eq.) was evaporated into a Schlenk flask from a solution of DCM. After drying the residue for 1h under oil pump vacuum DCM was added and the solution (0.1 M of **40**, **41** or **42**) was cooled to 0ºC. Then bis(2,5-dioxopyrrolidin-1-yl)[2,2'-bipyridine]-4,4'-dicarboxylate (**44**) (1 eq.) was introduced and triethylamine (2 eq.) was added. The temperature was kept at 0 ºC and the solution was stirred for two hours. After diluting with DCM and washing with HCl (1 M) and water the organic phase was dried over $MgSO_4$ and evaporated. The crude was subjected to column chromatography using a DCM/MeOH (10:1) mixture as eluent affording the pure product as colorless syrup.

N^4,*N*$^{4'}$-Bis((2,3,4,6-tetra-*O*-acetyl-α-D-mannopyranosyl))ethoxy)ethyl)-[2,2'-bipyridine]-4,4'-dicarboxamide (48)

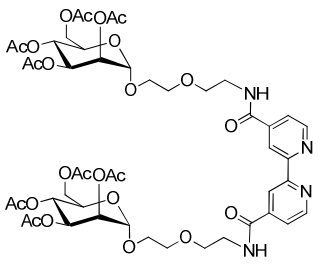

Yield: 270 mg, 50 % - **^{1}H-NMR:** (400 MHz, $CDCl_3$) δ_H = 8.80 (d, 2 H, J_{HH} = 5 Hz, *N*^{5}Ar-H, *N*$^{5'}$Ar-H), 8.76 (s, 2 H, *N*^{3}Ar-H, *N*$^{3'}$Ar-H), 7.81 (dd, J_{HH} = 5 Hz, *N*^{6}Ar-H, *N*$^{6'}$Ar-H), 7.35 (s, 2 H, NH), 5.36 (dd, 2 H, $J_{H\text{-}3,H\text{-}4}$ = 10 Hz, $J_{H\text{-}3,H\text{-}2}$ = 3 Hz, H-3), 5.29

(apparent t, 2 H, $J_{H\text{-}4,H\text{-}3}$ = 10 Hz, $J_{H\text{-}4,H\text{-}5}$ = 10 Hz H-4), 5.24 (dd, 2 H, $J_{H\text{-}2,H\text{-}3}$ = 3 Hz, $J_{H\text{-}2,H\text{-}1}$ = 2 Hz, H-2), 4.98 (d, 2 H, $J_{H\text{-}2,H\text{-}3}$ = 2 Hz, H-1), 4.25 (dd, 2 H, $J_{Ha\text{-}6,Hb\text{-}6}$ = 12 Hz, $J_{Hb\text{-}6,H\text{-}5}$ = 6 Hz, H_a-6), 4.14 (dd, $J_{Hb\text{-}6,Ha\text{-}6}$ = 12 Hz, $J_{Hb\text{-}6,H\text{-}5}$ = 3 Hz, H_b-6), 4.07 (ddd, $J_{H\text{-}5,Ha\text{-}6}$ = 5 Hz, $J_{H\text{-}5,Hb\text{-}6}$ = 3 Hz, $J_{H\text{-}5,H\text{-}4}$ = 10 Hz, H-5), 3.62 (stack, 16 H, CH_2), 2.13 (s, 6 H, $COCH_3$), 2.09 (s, 6 H, $COCH_3$), 2.03 (s, 6 H, $COCH_3$), 1.96 (s, 6 H, $COCH_3$) ppm. **^{13}C-NMR:** (400 MHz, $CDCl_3$) δ_C = 170.7, 170.3, 170.0, 165.6, 156.1 (C=O), 150.0 (N^6Ar-C, $N^{6'}$Ar-C), 142.8 (C_q), 122.1 (N^5Ar-C, $N^{5'}$Ar-C), 118.1 (N^3Ar-C, $N^{3'}$Ar-C), 97.5 (C-1), 70.1 (CH_2), 70.1 (CH_2), 69.8 (C-2), 68.9 (C-3), 68.4 (C-5), 67.2 (CH_2CH_2NH), 66.3 (C-4), 62.6 (C-6), 40.2 (CH_2NH), 20.9, 20.7, 20.6, 20.6 ($OCCH_3$) ppm. **MS (TOF, ES$^+$)** *m/z* = 1101.2, [M+Na$^+$], **IR**: $\tilde{\nu}$ = 1740, 1662, 2532, 1433, 1366, 1215, 1134, 1042, 976, 761, 687, 599, 466 cm^{-1}. **HRMS (TOF, ES$^+$)** calcd. for $C_{48}H_{62}N_4O_{24}Na^+$ *m/z* = 1101.3651 [M+Na$^+$] found *m/z* = 1101.3682 [M+Na$^+$], **Mp.:** 83.1ºC.

N^4,$N^{4'}$-Bis((2,3,4,6-tetra-*O*-acetyl-β-D-galactopyranosyl))ethoxy)ethyl)-[2,2'-bipyridine]-4,4'-dicarboxamide (49)

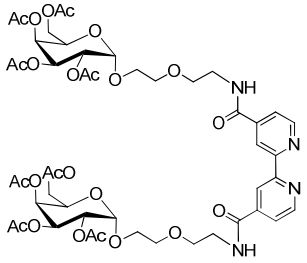

Yield: 120 mg, 61 % - **^{1}H-NMR:** (400 MHz, $CDCl_3$) δ_H = 8.83 (d, 2 H, $J_{H,H}$ = 5 Hz, N^5Ar-H, $N^{5'}$Ar-H), 8.76 (s, 2 H, N^3Ar-C, $N^{3'}$Ar-C), 7.81 (d, $J_{H,H}$ = 5 Hz, N^6Ar-H, $N^{6'}$Ar-H), 7.35 (s, 2 H, NH), 5.38 (d, 2 H, $J_{H\text{-}4,H\text{-}3}$ = 3 Hz, H-4), 5.18 (dd, 2 H, $J_{H\text{-}2,H\text{-}3}$ = 10 Hz, $J_{H\text{-}2,H\text{-}1}$ = 8 Hz, H-2), 4.99 (dd, 2 H, $J_{H\text{-}3,H\text{-}2}$ = 10 Hz, $J_{H\text{-}2,H\text{-}1}$ = 3 Hz, H-3), 4.54 (d, 2 H, $J_{H\text{-}1,H\text{-}2}$ = 8 Hz, H-1), 4.08 (m, 5 H, H_a-6), 3.99 (m, 2 H, H_b-6), 3.89 (apparent t, $J_{H\text{-}H}$ = 7 Hz, H-5), 3.68 (stack, 13 H, CH_2), 2.12 (s, 6 H, $COCH_3$), 2.04 (s, 12 H, $COCH_3$), 1.98 (s, 6 H, $COCH_3$) ppm. **^{13}C-NMR:** (400 MHz, $CDCl_3$) δ_C = 170.2, 170.1 (4 C_q), 150.0 (N^6Ar-C, $N^{6'}$Ar-C), 122.2 (N^5Ar-C, $N^{5'}$Ar-C), 118.4 (N^3Ar-C, $N^{3'}$Ar-C), 101.3 (C-1), 70.7 (C-3, C-5), 69.9 (CH_2), 69.7 (CH_2), 68.9 (C-6), 68.8 (C-2), 66.9 (C-4), 62.6 (C-6), 61.2

(CH_2), 40.0 (CH_2NH), 20.8, 20.6, 20.6, 20.5 ($OCCH_3$) ppm. **IR**: $\tilde{\nu}$ = 2920, 2850, 1748, 1213, 1068, 1055 cm^{-1}. **HRMS (TOF, ES$^+$)** calcd. for $C_{48}H_{62}N_4O_{24}Na^+$ *m/z* = 1101.3651 [M+Na^+] found *m/z* = 1101.3697 [M+Na^+], **Mp.:** 72ºC.

N^4,$N^{4'}$-Bis((2,3,4-tri-*O*-acetyl-α-L-fucoopyranosyl)) ethoxy)ethyl)-[2,2'-bipyridine]-4,4'-dicarboxamide (50)

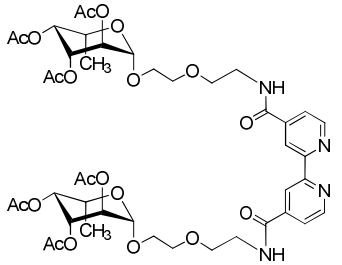

Yield: 33 mg, 36 % - **^{1}H-NMR:** (400 MHz, $CDCl_3$) δ_H = 8.83 (d, 2 H, $J_{H,H}$ = 5 Hz, N^5Ar-H, $N^{5'}$Ar-H), 8.76 (s, 2 H, N^3Ar-H, $N^{3'}$Ar-H), 7.81 (dd, 2 H, $J_{H,H}$ = 5 Hz, $J_{H,H}$ = 1 Hz, N^6Ar-H, $N^{6'}$Ar-H), 7.16 (bs, 2 H, amide NH), 5.21 (m, 2 H, H-4), 5.16 (dd, 2 H, $J_{H\text{-}2,H\text{-}1}$ = 10 Hz, $J_{H\text{-}2,H\text{-}1}$ = 8 Hz, H-2), 4.98 (dd, 2 H, $J_{H\text{-}3,H\text{-}2}$ = 10 Hz, $J_{H\text{-}3,H\text{-}4}$ = 3 Hz, H-3), 4.50 (d, 2 H, $J_{H\text{-}1,H\text{-}2}$ = 8 Hz, H-1), 3.98 (m, 2 H, CH_aH_b), 3.76 (m, 2 H, H-5), 3.65 (m, 15 H, CH_aH_b), 2.17, 2.04, 1.98 (3 s, 18 H, $OCCH_3$), 1.19 (d, 6 H, $J_{H\text{-}6,H\text{-}5}$ = 6 Hz, H-6) ppm. **^{13}C-NMR:** (400 MHz, $CDCl_3$) δ_C = 150.0 (N^6Ar-C, $N^{6'}$Ar-C), 122.0 (N^5Ar-C, $N^{5'}$Ar-C), 118.3 (N^3Ar-C, $N^{3'}$Ar-C), 101.2 (C-1), 71.1 (C-3), 70.1 (C-4), 70.0 (CH_2), 69.7 (CH_2), 69.2 (C-5), 68.9 (C-2), 68.8 (pyranose-O-CH_aH_b), 40.0 (CH_2-NH), 20.8, 20.6, 20.6 ($OCCH_3$), 16.0 (C-6) ppm. [M+Na^+]. **IR**: $\tilde{\nu}$ = 3350, 2939, 2874, 1743, 1656, 1595, 1535, 1457, 1433, 1366, 1301, 1217, 1173, 1130, 1056, 1020, 990, 970, 909, 859, 761, 727, 686, 666, 646, 594, 535, 476, 405 cm^{-1}; **MS (TOF, ES$^+$)** *m/z* = 985.3. **HRMS (TOF, ES$^+$)** calcd. for $C_{44}H_{58}N_4O_{20}Na^+$ *m/z* = 985.3541 [M+Na^+] found *m/z* = 985.3513 [M+Na^+]. **Mp.:** 75ºC.

Preparation of (M), (G) and (F)

N^4,$N^{4'}$-Bis((per-O-acetyl-pyranosyl))ethoxy)ethyl)-[2,2'-bipyridine]-4,4'-dicarboxamides ((**48**), (**49**) or (**50**)) (1 eq.) was dissolved in MeOH (0.03 M of (**48**), (**49**) or (**50**)) under argon and cooled to 0ºC. Then sodium methoxide (5 eq.) was added and the reaction was stirred for 1h until TLC indicated full disappearance of starting material. Dowex50 protic ion exchange resin was introduced until the solution was neutralized. Then the mixture was filtrated and the filtrate evaporated to yield a colourless syrup.

N^4,$N^{4'}$-Bis((α-D-mannopyranosyl))ethoxy)ethyl)-[2,2'-bipyridine]-4,4'-dicarboxamide (M)

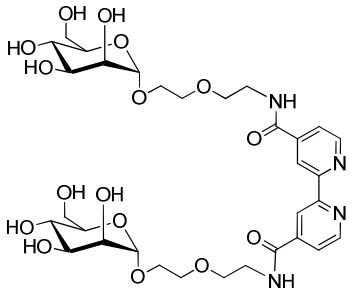

Yield: 110 mg, 100 % - **^{1}H-NMR:** (400 MHz, D_2O) δ_H = 9.11 (s, 2 H, N^3Ar-H, $N^{3'}$Ar-H), 9.03 (d, 2 H, $J_{H,H}$ = 5.46 Hz, N^5Ar-H, $N^{5'}$Ar-H), 8.26 (d, 2 H, $J_{H,H}$ = 5 Hz, N^6Ar-H, $N^{6'}$Ar-H), 4.81 (2 H, d, $J_{H,H}$ = 2 Hz, H-1, H-1'), 3.87-3.63 (stack, 16 H diethyleneglycol CH_2, 8 H pyranoside C*H*) ppm. **^{13}C-NMR:** (400 MHz, D_2O) δ_C = 164.8 (C=O), 149.9 (N^4 Ar-C_q, $N^{4'}$ Ar-C_q), 147.7 (N^6Ar-C, $N^{6'}$Ar-C), 146.7 (N^2 Ar-C_q, $N^{2'}$ Ar-C_q), 124.3 (N^5Ar-C, $N^{5'}$Ar-C), 121.1 (N^3Ar-C, $N^{3'}$Ar-C), 100.2 (C-1), 73.1 (C-2), 71.1 (C-3), 70.7 (C-5), 69.9 (CH_2), 68.9 (CH_2), 67.2 (C-4), 66.4 (CH_2), 61.5 (C-6), 40.0 (CH_2NH) ppm. **IR**: $\tilde{\nu}$ = 3289, 2925, 1654, 1599, 1548, 1441, 1308, 1052, 876, 806, 759, 679 cm-1. **MS (TOF, ES$^+$)** *m/z* = 765.2 [M+Na$^+$]., **HRMS (TOF, ES$^+$)** calcd. for $C_{32}H_{46}N_4O_{16}Na^+$ *m/z* = 765,2807 [M+Na$^+$] found *m/z* = 765.2815, [M+Na$^+$]. **Mp.:** 91.0ºC.

N^4,$N^{4'}$-Bis((β-D-galactopyranosyl))ethoxy)ethyl)-[2,2'-bipyridine]-4,4'-dicarboxamide (G)

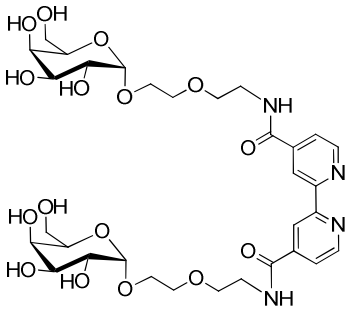

Yield: 40 mg, 100 % - **^{1}H-NMR:** (500 MHz, D_2O) δ_H = 8.64 (d, 2 H, $J_{H,H}$ = 5.0 Hz, N^6Ar-H, $N^{6'}$Ar-H), 8.20 (s, 2 H, N^3Ar-H, $N^{3'}$Ar-H), 7.66 (dd, 2 H, $J_{H,H}$ = 5 Hz, $J_{H,H}$ = 1 Hz N^5Ar-H, $N^{5'}$Ar-H), 4.32 (2 H, d, $J_{H,H}$ = 8 Hz, H-1, H-1'), 3.98-4.02 (m, 2 H, H_a-6), 3.79 (dd, 2 H, $J_{H\text{-}4,H\text{-}3}$ = 3 Hz, $J_{H\text{-}4,H\text{-}5}$ = 1 Hz, H-4), 3.54-3.78 (stack, 21 H diethyleneglycol CH_2, H_b-6), 3.49 (dd, 2 H, $J_{H\text{-}3,H\text{-}2}$ = 10 Hz, $J_{H\text{-}3,H\text{-}4}$ = 3 Hz, H-3), 3.41 (dd, 2 H, $J_{H\text{-}2,H\text{-}1}$ = 8 Hz, $J_{H\text{-}2,H\text{-}3}$ = 10 Hz, H-2) ppm. **^{13}C-NMR:** (500 MHz, D_2O) δ_C = 167.9 (C=O), 157.1 (N^4 Ar-C_q, $N^{4'}$ Ar-C_q), 150.1 (N^6Ar-C, $N^{6'}$Ar-C), 142.9 (N^2 Ar-C_q, $N^{2'}$ Ar-C_q), 122.0 (N^5Ar-C, $N^{5'}$Ar-C), 119.5 (N^3Ar-C, $N^{3'}$Ar-C), 102.8 (C-1), 75.1 (C-5), 72.7 (C-3), 70.72 (C-2), 69.6 (CH_2), 68.7 (2 C, C-6 and CH_2), 68.5 (C-4), 60.9 (CH_2), 39.6 (CH_2NH) ppm., **IR**: $\tilde{\nu}$ = 3334, 2927, 2878, 2495, 1649, 1544, 1455, 1072, 1040 cm^{-1}. **HRMS (TOF, ES$^+$)** calcd. for $C_{32}H_{46}N_4O_{16}Na^+$ *m/z* = 765.2807 [M+Na$^+$] found *m/z* = 765.2816 [M+Na$^+$].

N^4,$N^{4'}$-Bis((α-L-fucoopyranosyl))ethoxy)ethyl)-[2,2'-bipyridine]-4,4'-dicarboxamide (F)

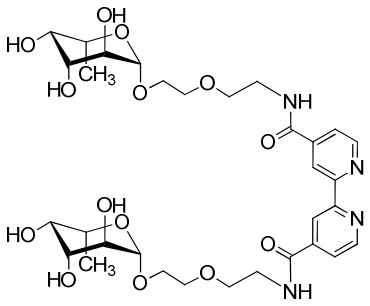

Yield: 66 mg, 94 % - **^{1}H-NMR:** (500 MHz, D_2O) δ_H = 8.66 (m, 2 H, Ar-H), 8.21 (m, 2 H, Ar-H), 7.70 (m, 2 H, Ar-H), 4.27 (2 H, d, $J_{H,H}$ = 7.8 Hz, H-1, H-1'), 3.92-3.96 (m, 2 H, CH_aH$_b$), 3.57-3.77 (stack, 19 H diethyleneglycol CH_2, C-6H_2), 3.45 (dd, 2 H, $J_{H-3,H-2}$ = 9.9 Hz, $J_{H-3,H-4}$ = 4 Hz, H-3), 3.35 (dd, 2 H, $J_{H-2,H-1}$ = 8 Hz, $J_{H-2,H-3}$ = 10 Hz, H-2) 3.26 (apparent s, 2 H, CH$_a$$H_b$) 1.10 (d, 3 H, $J_{H-6,H-5}$ = 7 Hz, CH$_3$) ppm. **^{13}C-NMR:** (500 MHz, D_2O) δ_C = 166.3 (C=O), 159.3 (N^4 Ar-C_q, $N^{4'}$ Ar-C_q), 154.9 (N^6Ar-C, $N^{6'}$Ar-C), 143.6 (N^2 Ar-C_q, $N^{2'}$ Ar-C_q), 124.7 (N^5Ar-C, $N^{5'}$Ar-C), 122.0 (N^3Ar-C, $N^{3'}$Ar-C), 102.7 (C-1), 72.8, 71.2, 70.8, 70.4 (4 H, pyranose C), 69.5 (CH_2), 68.6 (CH_2), 68.6 (CH_2), 39.8 (CH_2NH), 15.3 (CH_3) ppm., **IR**: $\tilde{\nu}$ = 325, 2935, 2872, 2488, 1666, 1542, 1310, 1053 cm^{-1}. **HRMS (TOF, ES$^+$)** calcd. for $C_{32}H_{46}N_4O_{14}$ Na^+ m/z = 733.2908 [M+Na^+] found m/z = 733.2881 [M+Na^+].

Preparation of (MMM), (GGG), (FFF)

N^4,$N^{4'}$-Bis((pyranosyl))ethoxy)ethyl)-[2,2'-bipyridine]-4,4'-dicarboxamide) (**M, G** or **F**) (3 eq.) was dissolved in D_2O (0.07 M of ((**M, G** or **F**), bubbled with argon for 15 min previously) and added to [$FeCl_2$•4H_2O] (1 eq.). After one night ^{1}H NMR and HPLC-MS analysis indicated full transformation and disappearance of free ligand. The solution was frozen and lyophilized to yield a deep red sticky solid.

[Tris(N^4,$N^{4'}$-bis((α-D-mannopyranosyl))ethoxy)ethyl)-[2,2'-bipyridine]-4,4'-dicarboxamide)] iron^{II} dichloride (MMM)

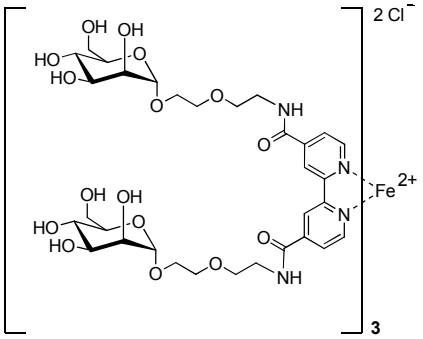

Yield: 60 mg, 100 % - **^{1}H-NMR:** (500 MHz, D_2O) δ_H = 8.97 (s, 2 H, N^3Ar-H, $N^{3'}$Ar-H), 7.72 (d, 6 H, $J_{H,H}$ = 5.7 Hz, N^5Ar-H, $N^{5'}$Ar-H), 7.62 (d, 6 H, $J_{H,H}$ = 6 Hz, N^6Ar-H, $N^{6'}$Ar-H), 4.82 (apparent s, 6 H, H-1), 3.32-3.86 (84 H, stack, diethyleneglycol CH_2 [48 H], pyranoside CH [36 H]) ppm. **^{13}C-NMR:** (500 MHz, D_2O) δ_C = 166.3 (C=O), 159.4 (N^4 Ar-C_q, $N^{4'}$ Ar-C_q), 155.0 (N^6Ar-C, $N^{6'}$Ar-C), 143.6 (N^2 Ar-C_q, $N^{2'}$ Ar-C_q), 124.7 (N^5Ar-C, $N^{5'}$Ar-C), 122.0 (N^3Ar-C, $N^{3'}$Ar-C), 99.8 (C-1), 72.7, 70.4, 69.9 (4 H, pyranose C), 69.3, 68.6 (CH_2), 66.7 (pyranose C), 66.3, 60.9 (CH_2), 39.8 (CH_2NH) ppm. **IR**: $\tilde{\nu}$ = 3300, 2928, 2871, 1666, 1544, 1456, 1403, 1310, 1232, 1055, 1022 cm^{-1}. **HRMS (TOF, ES$^+$)** calcd. for $C_{96}H_{138}FeN_{12}O_{48}^{2+}$ m/z = 1141,4032 [M^{2+}] found m/z = 1141.4012 [M^{2+}].

[Tris(N^4,$N^{4'}$-bis((β-D-galactopyranosyl))ethoxy)ethyl)-[2,2'-bipyridine]-4,4'-dicarboxamide)] iron^{II} dichloride (GGG)

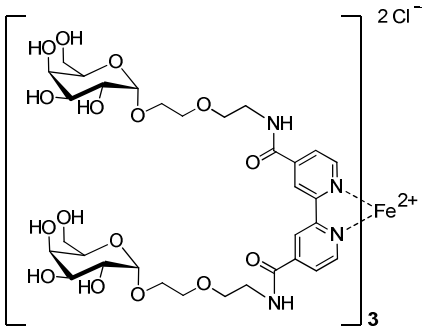

Yield: 30 mg, 100 % - **^{1}H-NMR:** (500 MHz, D_2O) δ_H = 8.64 (s, 6 H, N^3ArCH, $N^{3'}$ArCH), 7.40 (d, 6 H, $J_{H,H}$ = 5 Hz, N^5ArCH, $N^{5'}$ArCH), 7.29 (d, 6 H, $J_{H,H}$ = 6 Hz, N^6ArCH, $N^{6'}$ArCH), 4.05 (6 H, d, $J_{H,H}$ = 8 Hz, H-1, H-1'), 3.07-3.74 (stack, 21 H diethyleneglycol CH_2, H-6) ppm. **^{13}C-NMR:** (500 MHz, D_2O) δ_C = 168.8 (C=O), 166.4 (N^4 Ar-C_q, $N^{4'}$ Ar-C_q), 154.5 (N^6Ar-C, $N^{6'}$Ar-C), 143.5 (N^2 Ar-C_q, $N^{2'}$ Ar-C_q), 124.4 (N^5Ar-C, $N^{5'}$Ar-C), 121.8 (N^3Ar-C, $N^{3'}$Ar-C), 102.6 (C-1), 74.9, 72.4, 70.5 (4 H, pyranose *C*H), 69.3, 68.4, 68.4, 60.7, (CH_2), 48.8 (CH) 39.5 (CH_2NH) ppm. **IR**: $\tilde{\nu}$ = 3295, 2933, 2873, 2476, 1649, 1543, 1460, 1404, 1072, 1038, 761 cm^{-1}. **HRMS (TOF, ES$^+$)** calcd. for $C_{96}H_{138}FeN_{12}O_{48}$ *m/z* = 1141.4032 [M^{2+}] found *m/z* = 1141.4016, [M^{2+}].

[Tris(N^4,$N^{4'}$-bis((α-L-fucopyranosyl))ethoxy)ethyl)-[2,2'-bipyridine]-4,4'-dicarboxamide)] iron^{II} dichloride (FFF)

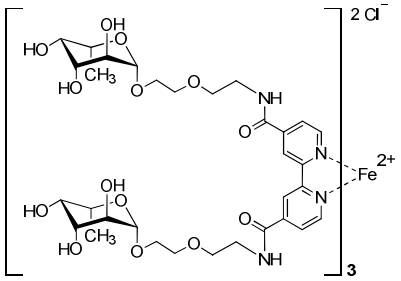

Yield: 27 mg, 100 % - **^{1}H-NMR:** (500 MHz, MeOD) δ_H = 8.92 (s, 6 H, N^3ArCH, $N^{3'}$ArCH), 7,69 (dd, 6 H, $J_{H,H}$ = 1 Hz, $J_{H,H}$ = 6 Hz, N^5ArCH, $N^{5'}$ArCH), 7.58 (d, 6 H, $J_{H,H}$ = 6 Hz, N^6ArCH, $N^{6'}$ArCH), 4.30 (6 H, d, $J_{H\text{-}1,H\text{-}2}$ = 8 Hz, H-1, H-1'), 3.93-3.96 (m, 6 H, CH_aH_b), 3.60-3.76 (stack, 54 H diethyleneglycol CH_2, pyranoside CH), 3.51 (m, 6 H, H-3), 3.36 (dd, 2 H, $J_{H\text{-}2,H\text{-}1}$ = 8 Hz, $J_{H\text{-}2,H\text{-}3}$ = 10 Hz, H-2), 1.11 (d, 18 H, $J_{H\text{-}2,H\text{-}1}$ = 7 Hz, CH_3) ppm. **^{13}C-NMR:** (500 MHz, MeOD) δ_C = 166.3 (C=O), 159.3 (N^4 Ar-C_q, $N^{4'}$ Ar-C_q), 155.0 (N^6Ar-C, $N^{6'}$Ar-C), 143.6 (N^2 Ar-C_q, $N^{2'}$ Ar-C_q), 124.8 (N^5Ar-C, $N^{5'}$Ar-C), 122.0 (N^3Ar-C, $N^{3'}$Ar-C), 102.7 (C-1), 72.8 (C-3), 71.2, 71.8 (pyranose C), 70.4 (C-2) 69.5 (CH_2), 68.7 (CH_2), 68.6 (CH_2), 39.8 (CH_2NH), 15.3 (CH_3) ppm., **IR**: $\tilde{\nu}$ = 3490, 2936, 2871, 1659, 1549, 1453, 1058, 763 cm^{-1}. **HRMS (TOF, ES$^+$)** calcd. for $C_{96}H_{138}FeN_{12}O_{42}$ *m/z* = 1093.4185 [M^{2+}] found *m/z* = 1093.4181 [M^{2+}].

Preparation of (55), (56) and (57)

General procedures: Trifluoroacetate (**52**, **53** or **54**) (2.2 eq.) was evaporated into a Schlenk flask from a solution of DCM. After drying the residue for 1h under oil pump vacuum, DCM (to reach a concentration of 0.1 M for **52**, **53** or **54**) was added and the solution was cooled to 0ºC. Then bis(2,5-dioxopyrrolidin-1-yl)[2,2'-bipyridine]-4,4'-dicarboxylate (**44**) (1 eq.) was introduced and triethylamine (2 eq.) was added. The temperature was kept at 0 ºC and the solution was stirred for 12 hours. After diluting with DCM and washing with HCl (1 M) and water, the organic phase was dried over $MgSO_4$

and evaporated. The crude was subjected to column chromatography using a DCM/MeOH (10:1) mixture as eluent affording the pure product as colorless syrup.

N^4,$N^{4'}$-Bis((2,3,4,6-tetra-*O*-acetyl-α-D-mannopyranosyl))ethyl)-[2,2'-bipyridine]-4,4'-dicarboxamide (55)

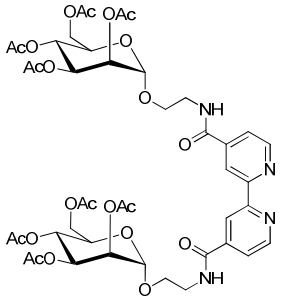

Yield: 107 mg, 56 % - **^{1}H-NMR:** (500 MHz, $CDCl_3$) δ_H = 8.84 (d, 2 H, J_{HH} = 5 Hz, N^5Ar-H, $N^{5'}$Ar-H), 8.75 (s, 2 H, N^3Ar-H, $N^{3'}$Ar-H), 7.80 (dd, J_{HH} = 5 Hz, J_{HH} = 2 Hz, N^6Ar-H, $N^{6'}$Ar-H), 7.08 (t, J_{HH} = 5 Hz, 2 H, NH), 5.36 (dd, 2 H, $J_{H\text{-}3,H\text{-}4}$ = 10 Hz, $J_{H\text{-}3,H\text{-}2}$ = 3 Hz, H-3), 5.30 (dd, 2 H, $J_{H\text{-}2,H\text{-}3}$ = 3 Hz, $J_{H\text{-}2,H\text{-}1}$ = 2 Hz, H-2), 5.26 (apparent q, 2 H, $J_{H\text{-}4,H\text{-}3}$ = 10 Hz, $J_{H\text{-}4,H\text{-}5}$ = 10 Hz H-4), 4.89 (d, 2 H, $J_{H\text{-}2,H\text{-}3}$ = 2 Hz, H-1), 4.28 (dd, 2 H, $J_{Ha\text{-}6,Hb\text{-}6}$ = 12 Hz, $J_{Ha\text{-}6,H\text{-}5}$ = 6 Hz, H_a-6), 4.15 (dd, $J_{Hb\text{-}6,Ha\text{-}6}$ = 12 Hz, $J_{Hb\text{-}6,H\text{-}5}$ = 2 Hz, H_b-6), 4.04 (ddd, $J_{H\text{-}5,Ha\text{-}6}$ = 6 Hz, $J_{H\text{-}5,Hb\text{-}6}$ = 2 Hz, $J_{H\text{-}5,H\text{-}4}$ = 10 Hz, H-5), 3.93 (m, 2 H, CH_2), 3.76 (stack, 6 H, CH_2), 2.16 (s, 6 H, $COCH_3$), 2.09 (s, 6 H, $COCH_3$), 2.01 (s, 6 H, $COCH_3$), 2.00 (s, 6 H, $COCH_3$) ppm. **^{13}C-NMR:** (400 MHz, $CDCl_3$) δ_C = 170.71, 170.18, 170.13, 169.81, 165.82 (C=O), 150.38 (N^6Ar-C, $N^{6'}$Ar-C), 142.63 (C_q), 122.23 (N^5Ar-C, $N^{5'}$Ar-C), 118.01 (N^3Ar-C, $N^{3'}$Ar-C), 98.01 (C-1), 69.51 (C-2), 69.08 (C-3), 69.06 (C-5), 67.63 (CH_2CH_2NH), 66.30 (C-4), 62.79 (C-6), 40.06 (CH_2NH), 20.98, 20.84, 20.81, 20.76 ($OCCH_3$) ppm. - **MS (TOF, ES$^+$)** *m/z* = 991.3 [M^+], **IR**: $\tilde{\nu}$ = 2940, 1741, 1651, 1534, 1432, 1367, 1304, 1216, 1135, 1081, 1041, 977, 908, 859, 794, 687, 599, 491 cm^{-1}. **HRMS (TOF, ES$^+$)** calcd. for C44H54N4O22+Na^+ *m/z* = 1013,3116 [M+Na^+] found *m/z* = 1013.3122 [M+Na^+].

N^4,$N^{4'}$-Bis((2,3,4,6-tetra-*O*-acetyl-α-D-mannopyranosyl))ethyl)ethoxy)ethoxy)-[2,2'-bipyridine]-4,4'-dicarboxamide (56)

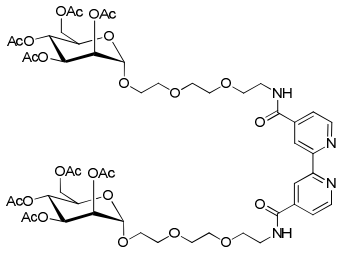

Yield: 140 mg, 47 % - **^{1}H-NMR:** (500 MHz, $CDCl_3$) δ_H = 8.78 (d, 2 H, J_{HH} = 5.0 Hz, N^5Ar-H, $N^{5'}$Ar-H), 8.74 (s, 2 H, N^3Ar-H, $N^{3'}$Ar-H), 7.79 (dd, J_{HH} = 5.0 Hz, J_{HH} = 1.6 Hz, N^6Ar-H, $N^{6'}$Ar-H), 7.08 (s, 2 H, NH), 5.31 (dd, 2 H, $J_{H\text{-}3,H\text{-}4}$ = 10.0 Hz, $J_{H\text{-}3,H\text{-}2}$ = 3.3 Hz, H-3), 5.27 (apparent t, 2 H, $J_{H\text{-}4,H\text{-}3}$ = 10.0 Hz, H-4) 5.23 (dd, 2 H, $J_{H\text{-}2,H\text{-}3}$ = 3.3 Hz, $J_{H\text{-}2,H\text{-}1}$ = 1.8 Hz, H-2), 4.84 (d, 2 H, $J_{H\text{-}2,H\text{-}3}$ = 1.6 Hz, H-1), 4.22 (dd, 2 H, $J_{Ha\text{-}6,Hb\text{-}6}$ = 12.2 Hz, $J_{Ha\text{-}6,H\text{-}5}$ = 5.0 Hz, H_a-6), 4.06 (dd, $J_{Hb\text{-}6,Ha\text{-}6}$ = 12.2 Hz, $J_{Hb\text{-}6,H\text{-}5}$ = 2.5 Hz, H_b-6), 4.01 (ddd, $J_{H\text{-}5,Ha\text{-}6}$ = 5.0 Hz, $J_{H\text{-}5,Hb\text{-}6}$ = 2.5 Hz, $J_{H\text{-}5,H\text{-}4}$ = 10.0 Hz, H-5), 3.77 (m, 2 H, CH_2), 3.63-3.70 (stack, 22 H, CH_2), 2.13 (s, 6 H, $COCH_3$), 2.07 (s, 6 H, $COCH_3$), 2.02 (s, 6 H, $COCH_3$), 1.96 (s, 6 H, $COCH_3$) ppm. **^{13}C-NMR:** (400 MHz, $CDCl_3$) δ_C = 170.72, 170.10, 170.04, 169.69, 165.50 (C=O), 155.91 (N^2Ar-C, $N^{2'}$Ar-C), 149.95 (N^5Ar-C, $N^{5'}$Ar-C), 143.09 (N^4Ar-C, $N^{4'}$Ar-C), 122.27 (N^6Ar-C, $N^{6'}$Ar-C), 118.09 (N^3Ar-C, $N^{3'}$Ar-C), 97.68 (C-1), 70.66, 70.34, 69.99, 69.63 (CH_2), 69.57 (C-2), 69.09 (C-3), 68.45 (C-5), 67.38 (CH_2CH_2NH), 66.12 (C-4), 62.42 (C-6), 40.06 (CH_2NH), 20.88, 20.75 ($OCCH_3$), 20.69 (2 C, $OCCH_3$) ppm. - **MS (TOF, ES$^+$)** *m/z* = 1167.4, [M^+], **IR**: $\tilde{\nu}$ = 2927, 2875, 2105, 1741, 1661, 1538, 1455, 1368, 1216, 1132, 1077, 1041, 977, 687, 599 cm^{-1}. **HRMS (TOF, ES$^+$)** calcd. for C52H70N4O26+Na^+ *m/z* = 1189,4165 [M+Na^+] found *m/z* = 1189.4227 [M+Na^+].

N^4,$N^{4'}$-Bis((2,3,4,6-tetra-*O*-acetyl-α-D-mannopyranosyl))ethyl)ethoxy)ethoxy)ethoxy)-[2,2'-bipyridine]-4,4'-dicarboxamide (57)

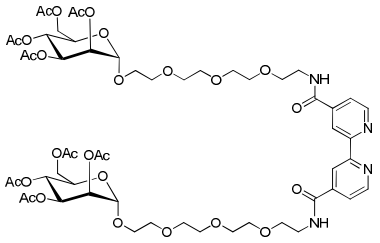

Yield: 50 mg, 44 % - **^{1}H-NMR:** (400 MHz, $CDCl_3$) δ_H = 8.78 (d, 2 H, J_{HH} = 5.1 Hz, N^5Ar-H, $N^{5'}$Ar-H), 8.73 (s, 2 H, N^3Ar-H, $N^{3'}$Ar-H), 7.78 (dd, J_{HH} = 4.9 Hz, J_{HH} = 1.6 Hz, N^6Ar-H, $N^{6'}$Ar-H), 7.29 (s, 2 H, NH), 5.30 (dd, 2 H, $J_{H\text{-}3,H\text{-}4}$ = 10.1 Hz, $J_{H\text{-}3,H\text{-}2}$ = 3.4 Hz, H-3), 5.26 (apparent t, 2 H, $J_{H\text{-}4,H\text{-}3}$ = 10.0 Hz, H-4) 5.22 (dd, 2 H, $J_{H\text{-}2,H\text{-}3}$ = 3.3 Hz, $J_{H\text{-}2,H\text{-}1}$ = 1.8 Hz, H-2), 4.82 (d, 2 H, $J_{H\text{-}2,H\text{-}3}$ = 1.6 Hz, H-1), 4.25 (dd, 2 H, $J_{Ha\text{-}6,Hb\text{-}6}$ = 12.2 Hz, $J_{Ha\text{-}6,H\text{-}5}$ = 4.9 Hz, H_a-6), 4.05 (dd, $J_{Hb\text{-}6,Ha\text{-}6}$ = 12.2 Hz, $J_{Hb\text{-}6,H\text{-}5}$ = 2.4 Hz, H_b-6), 4.01 (ddd, $J_{H\text{-}5,Ha\text{-}6}$ = 4.9 Hz, $J_{H\text{-}5,Hb\text{-}6}$ = 2.5 Hz, $J_{H\text{-}5,H\text{-}4}$ = 9.7 Hz, H-5), 3.74 (m, 2 H, CH_2), 3.58 (stack, 30 H, CH_2), 2.13 (s, 6 H, $COCH_3$), 2.07 (s, 6 H, $COCH_3$), 2.01 (s, 6 H, $COCH_3$), 1.96 (s, 6 H, $COCH_3$) ppm. **^{13}C-NMR:** (400 MHz, $CDCl_3$) δ_C = 170.73, 170.05, 169.93, 169.68, 165.50 (C=O), 156.00 (N^2Ar-C, $N^{2'}$Ar-C), 149.97 (N^5Ar-C, $N^{5'}$Ar-C), 143.03 (N^4Ar-C, $N^{4'}$Ar-C), 122.19 (N^6Ar-C, $N^{6'}$Ar-C), 118.10 (N^3Ar-C, $N^{3'}$Ar-C), 97.69 (C-1), 70.73, 70.56, 70.52, 70.28 69.92 (CH_2), 69.54 (C-2), 69.08 (C-3), 68.40 (C-5), 67.34 (CH_2CH_2NH), 66.11 (C-4), 62.41 (C-6), 40.04 (CH_2NH), 20.88, 20.75 ($OCCH_3$), 20.68 (2 C, $OCCH_3$) ppm. - **IR**: $\tilde{\nu}$ = 2928, 2872, 1742, 1657, 1535, 1456, 1368, 1301, 1215, 1174, 1132, 1041, 954, 915, 730, 589 cm^{-1}. **HRMS (TOF, ES$^+$)** calcd. for C56H78N4O28+Na^+ *m/z* = 1277,4695 [M+Na^+] found *m/z* = 1277.4692 [M+Na^+].

Preparation of (S), (L) and (X)

N^4,$N^{4'}$-Bis((per-O-acetyl-pyranosyl))ethoxy)ethyl)-[2,2'-bipyridine]-4,4'-dicarboxamides ((**55**), (**56**) or (**57**)) (1 eq.) was dissolved in MeOH (0.03 M of (**55**), (**56**), (**57**)) under argon and cooled to 0ºC. Then sodium methoxide (5 eq.) was added and the reaction was stirred for 1h until TLC indicated full disappearance of starting material. Dowex50 prFotic ion exchange resin was introduced until the solution was neutralized. Then the mixture was filtrated and the filtrate evaporated to yield a colourless syrup.

N^4,$N^{4'}$-Bis((α-D-mannopyranosyl))ethyl)-[2,2'-bipyridine]-4,4'-dicarboxamide (S)

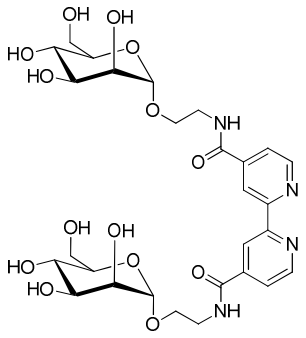

Yield: 30 mg, 100 % - **^{1}H-NMR:** (400 MHz, D_2O) δ_H = 8.69 (s, 2 H, N^3Ar-H, $N^{3'}$Ar-H), 8.20 (s, 2 H, N^5Ar-H, $N^{5'}$Ar-H), 7.69 (s, 2 H, N^6Ar-H, $N^{6'}$Ar-H), 4.91 (2 H, d, J_{HH} = 1.6 Hz, H-1, H-1'), 3.95 (dd, 2 H, $J_{H\text{-}2,H\text{-}3}$ = 3.3 Hz, $J_{H\text{-}2,H\text{-}1}$ = 1.7 Hz, H-2) 3.73-3.93 (stack, 12 H CH_2, 6 H pyranoside C*H*) ppm. **^{13}C-NMR:** (400 MHz, D_2O) δ_C = 167.90 (C=O), 155.11 (N^4 Ar-C_q, $N^{4'}$ Ar-C_q), 150.08 (N^5Ar-C, $N^{5'}$Ar-C), 142.80 (N^2 Ar-C_q, $N^{2'}$ Ar-C_q), 121.92 (N^6Ar-C, $N^{6'}$Ar-C), 119.41 (N^3Ar-C, $N^{3'}$Ar-C), 99.68 (C-1), 72.88 (pyranose CH), 70.50 (pyranose CH), 70.02 (C-2), 66.63 (pyranose CH), 65.69, 60.82 (CH_2), 39.64 (CH_2NH) ppm., **- IR**: $\tilde{\nu}$ = 3294, 2929, 2888, 2481, 1642, 1547, 1454, 1362, 1310, 1245, 1202, 1130, 1051, 974, 911, 857, 804, 756, 681, 578 cm^{-1}. **HRMS (TOF, ES$^+$)** calcd. for C28H38N4O14+Na^+ *m/z* = 677,2277 [M+Na^+] found *m/z* = 677.2272 [M+Na^+].

N^4,$N^{4'}$-Bis((α-D-mannopyranosyl))ethyl)ethoxy)ethoxy)-[2,2'-bipyridine]-4,4'-dicarboxamide (L)

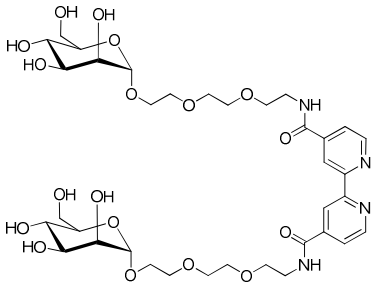

Yield: 30 mg, 100 % - **^{1}H-NMR:** (500 MHz, D_2O) δ_H = 8.58 (s, 2 H, N^3Ar-H, $N^{3'}$Ar-H), 8.12 (s, 2 H, N^5Ar-H, $N^{5'}$Ar-H), 7.61 (s, 2 H, N^6Ar-H, $N^{6'}$Ar-H), 4.74 (2 H, d, J_{HH} = 1.4 Hz, H-1, H-1'), 3.80 (dd, 2 H, $J_{H\text{-}2,H\text{-}3}$ = 3.3 Hz, $J_{H\text{-}2,H\text{-}1}$ = 1.6 Hz, H-2) 3.53-3.75 (stack, 12 H CH_2, 8 H pyranoside C*H*) ppm. **^{13}C-NMR:** (400 MHz, D_2O) δ_C = 167.55 (C=O), 154.96 (N^4 Ar-C_q, $N^{4'}$ Ar-C_q), 150.06 (N^5Ar-C, $N^{5'}$Ar-C), 142.66 (N^2 Ar-C_q, $N^{2'}$ Ar-C_q), 121.95 (N^6Ar-C, $N^{6'}$Ar-C), 119.27 (N^3Ar-C, $N^{3'}$Ar-C), 99.86 (C-1), 72.68 (pyranose CH), 70.49 (pyranose CH), 69.93 (C-2), 69.64, 69.53, 69.49, 68.68 (CH_2), 66.66 (pyranose CH), 66.26 (CH_2), 60.85 (CH_2), 39.67 (CH_2NH) ppm.. **IR**: $\tilde{\nu}$ = 3333, 2920, 2093, 1646, 1546, 1457, 1356, 1309, 1245, 1130, 1054, 975, 914, 879, 806, 759, 684, 575, 509 cm^{-1}. **HRMS (TOF, ES$^+$)** calcd. for C36H54N4O18+Na^+ *m/z* = 853,3325 [M+Na^+] found *m/z* = 853.3340 [M+Na^+].

N^4,$N^{4'}$-Bis((α-D-mannopyranosyl))ethyl)ethoxy)ethoxy)ethoxy)-[2,2'-bipyridine]-4,4'-dicarboxamide (X)

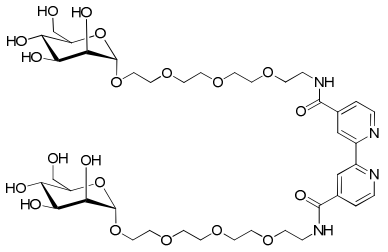

Yield: 37 mg, 100 % - **^{1}H-NMR:** (400 MHz, D_2O) δ_H = 8.75 (d, 2 H, $J_{H,H}$ = 4.0 Hz, N^5Ar-H, $N^{5'}$Ar-H), 8.31 (s, 2 H, N^3Ar-H, $N^{3'}$Ar-H), 7.69 (d, 2 H, J_{HH} = 4.6 Hz, N^6Ar-H, $N^{6'}$Ar-H), 4.79 (2 H, H-1, H-1'), 3.88 (dd, 2 H, $J_{H\text{-}2,H\text{-}3}$ = 3.4 Hz, $J_{H\text{-}2,H\text{-}1}$ = 1.7 Hz, H-2) 3.58-3.85 (stack, 23 H CH_2, 6 H pyranoside C*H*) ppm. **^{13}C-NMR:** (400 MHz, D_2O) δ_C = 167.81 (C=O), 155.20 (N^4 Ar-C_q, $N^{4'}$ Ar-C_q), 150.17 (N^5Ar-C, $N^{5'}$Ar-C), 142.95 (N^2 Ar-C_q, $N^{2'}$ Ar-C_q), 122.07 (N^6Ar-C, $N^{6'}$Ar-C), 119.52 (N^3Ar-C, $N^{3'}$Ar-C), 99.86 (C-1), 72.68 (pyranose CH), 70.47 (pyranose CH), 69.92 (C-2), 66.63 69.61, 69.58, 69.51, 69.41, 68.63 (CH_2), 66.67 (pyranose CH), 66.24, 60.86 (CH_2), 39.68 (CH_2NH) ppm. - [M+Na^+], **IR**: $\tilde{\nu}$ = 3285, 2930, 2874, 2481, 1641, 1547, 1455, 1362, 1310, 1245, 1202, 1130, 1050, 974, 910, 804 cm^{-1}. **HRMS (TOF, ES$^+$)** calcd. for C40H62N4O20+Na^+ *m/z* = 941,3850 [M+Na^+] found *m/z* = 941.3856 [M+Na^+].

Preparation of (SSS), (LLL), (XXX)

General procedures: (**S**), (**L**) or (**X**) (3 eq.) was dissolved in H_2O at 0.07 M and bubbled with argon for 15 min. After the solution was added to [$FeCl_2$ $4H_2O$] (1 eq.) it was stirred for one night. ^{1}H NMR and HPLC-MS analysis indicated full transformation by disappearance of the free ligand ((**S**), (**L**) or (**X**)). The solution was frozen and lyophilized to yield a deep red sticky solid.

[Tris(N^4,$N^{4'}$-bis((α-D-mannopyranosyl))ethyl)-[2,2'-bipyridine]-4,4'-dicarboxamide)] iron^{II} dichloride (SSS)

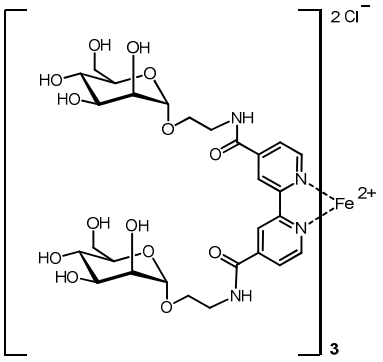

Yield: 49 mg, 100 % - **^{1}H-NMR:** (500 MHz, D_2O) δ_H = 8.66 (s, 6 H, N^3Ar-H, $N^{3'}$Ar-H), 7.42 (d, 6 H, J_{HH} = 4.8 Hz N^5Ar-H, $N^{5'}$Ar-H), 7.69 (d, 6 H, J_{HH} = 5.5 Hz N^6Ar-H, $N^{6'}$Ar-H), 4.91 (s, 6 H, H-1, H-1'), 3.09-3.60 (stack, 36 H CH_2, 18 H pyranoside C*H*) ppm. **^{13}C-NMR:** (500 MHz, D_2O) δ_C = 167.18 (C=O), 160.18 (N^4 Ar-C_q, $N^{4'}$ Ar-C_q), 155.82 (N^5Ar-C, $N^{5'}$Ar-C), 144.46 (N^2 Ar-C_q, $N^{2'}$ Ar-C_q), 125.60 (N^6Ar-C, $N^{6'}$Ar-C), 122.87 (N^3Ar-C, $N^{3'}$Ar-C), 100.39 (C-1), 73.75 (pyranose CH), 71.35 (pyranose CH), 70.80 (pyranose CH), 67.47 (pyranose CH), 66.47, 61.74 (CH_2), 40.68 (CH_2NH) ppm., **-IR**: $\tilde{\nu}$ = 3329, 2932, 1641, 15.48, 1452, 1414, 1131, 1053, 978, 854, 801, 761, 720, 674 cm^{-1}. **HRMS (TOF, ES$^+$)** calcd. for $^+$ *m/z* = 1009.3248 [M^{2+}] found *m/z* = 1009.3290 [M^{2+}].

[Tris(N^4,$N^{4'}$-bis((α-d-mannopyranosyl))ethyl)ethoxy)ethoxy)-[2,2'-bipyridine]-4,4'-dicarboxamide)] iron^{II} dichloride (LLL)

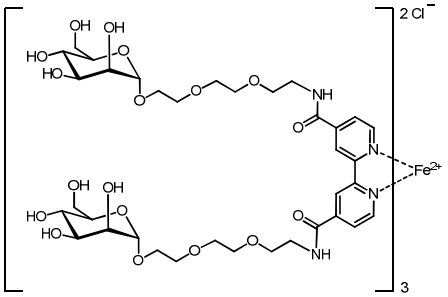

Yield: 16 mg, 100 % - **^{1}H-NMR:** (500 MHz, D_2O) δ_H = 8.91 (s, 2 H, N^3Ar-H, $N^{3'}$Ar-H), 7.67 (d, 2 H, J_{HH}) = 5.5 Hz, N^5Ar-H, $N^{5'}$Ar-H), 7.56 (d, 2 H, J_{HH} = 5.5 Hz, N^6Ar-H, $N^{6'}$Ar-H), 3.51-3.81 (stack, 84 H CH_2, 24 H pyranoside CH) ppm. **^{13}C-NMR:** (500 MHz, D_2O) δ_C = 166.21 (C=O), 159.28 (N^4 Ar-C_q, $N^{4'}$ Ar-C_q), 154.88 (N^5Ar-C, $N^{5'}$Ar-C), 143.62 (N^2 Ar-C_q, $N^{2'}$ Ar-C_q), 124.69 (N^6Ar-C, $N^{6'}$Ar-C), 121.95 (N^3Ar-C, $N^{3'}$Ar-C), 99.78 (C-1), 72.64 (pyranose CH), 70.40 (pyranose CH), 69.85 (pyranose CH), 69.49, 69.37, 69.31, 68.51 (CH_2), 66.61 (pyranose CH), 66.18, 60.81 (CH_2), 39.74 (CH_2NH) ppm. - **IR**: $\tilde{\nu}$ = 3334.19, 2927.99, 2473.04, 1642.83, 1548.67, 1451.72, 1414.35, 1353.26, 1305.12, 1233.58, 1056.33, 804.07, 761.25 cm^{-1}. **HRMS (TOF, ES$^+$)** calcd. for $^+$ *m/z* = 1273.4820 [M^{2+}] found *m/z* = 1273.4871 [M^{2+}].

[Tris(N^4,$N^{4'}$-bis((α-D-mannopyranosyl))ethyl)ethoxy)ethoxy)ethoxy)-[2,2'-bipyridine]-4,4'-dicarboxamide)] iron^{II} dichloride (XXX)

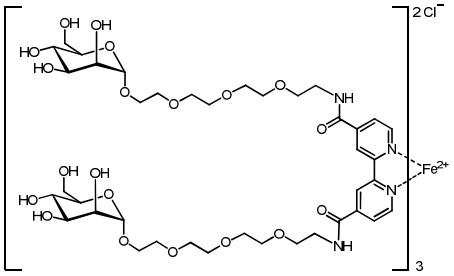

Yield: 31 mg, 100 % - **^{1}H-NMR:** (500 MHz, D_2O) δ_H = 8.77 (s, 2 H, N^3Ar-H, $N^{3'}$Ar-H), 7.52 (d, 2 H, J_{HH} = 4.9 Hz, N^5Ar-H, $N^{5'}$Ar-H), 7.69 (d, 2 H, J_{HH} = 5.4 Hz, N^6Ar-H, $N^{6'}$Ar-H), 4.6 (2 H, H-1, H-1'), 3.35-3.65 (stack, 23 H CH_2, 6 H pyranoside C*H*) ppm. **^{13}C-NMR:** (500 MHz, D_2O) δ_C = 166.05 (C=O), 159.19 (N^4 Ar-C_q, $N^{4'}$ Ar-C_q), 154.83 (N^5Ar-C, $N^{5'}$Ar-C), 143.58 (N^2 Ar-C_q, $N^{2'}$ Ar-C_q), 124.70 (N^6Ar-C, $N^{6'}$Ar-C), 121.89 (N^3Ar-C, $N^{3'}$Ar-C), 99.73 (C-1), 72.59 (pyranose CH), 70.35 (pyranose CH), 69.78 (C-2), 69.41 69.37, 69.27, 69.25, 69.40 (CH_2), 66.55 (pyranose CH), 66.13, 60.76 (CH_2), 39.66 (CH_2NH) ppm. - [M+Na^+], **IR**: $\tilde{\nu}$ = 3354.02, 2919.86, 2481.11, 1648.98, 1548.57, 1452.44, 1412.67, 1234.39, 1057.02, 806.64, 762.37 cm^{-1}. **HRMS (TOF, ES$^+$)** calcd. for $^+$ *m/z* = 1405.5606 [M^{2+}] found *m/z* = 1405.5639 [M^{2+}].

Generation and analysis of the dynamic combinatorial libraries H, I, J, K, L and M

Reference Samples:

The homoleptic complexes (**38** and **39** for **DCL H** and **DCL I)**, (**MMM**, **GGG**, and **FFF** for **DCL J**, **DCL K**, **DCL L** and **DCL M**) were mixed in deoxygenated water.

For **DCL H** and **DCL I** solutions of complexes (**38** and **39**) at a concentration of 0.6 mM were mixed 1:1 v/v. Equilibration took 5 days at rt.

For **DCL J**, **DCL K**, **DCL L** and **DCL M** the solutions of complexes (**MMM**, **GGG**, and **FFF**) at a concentration of 0.5 mM were mixed 1:1:1 v/v/v. Complexes of **DCL J**,

DCL K, **DCL L** and **DCL M** tend to dissociate at rt at the given concentration, therefore the set-up required a lower temperature (5 ºC) and 14 days of equilibration period.

All solutions were then analysed by HPLC-MS.

Samples with protein interaction (only for **DCL L** and **DCL M**):

To an aqueous solution of the homoleptic complexes **MMM**, **GGG** (only for **DCL M**), and **FFF** in deoxigenated water (0.85 mM concentration for each of the initial complexes, 0.7 ml) was added a suspension of Con A-sepharose (0.1 ml, approx. 0.1 mM ConA tetramers). After mixing for 14 days at 5ºC the suspensions were filtered (Millipore Ultrafiltration Membrane YM100 Dia: 25 mm). The filtrate was immediately analysed by HPLC-MS (see below). The sepharose particles on the filter membrane were re-suspended in HCl (0.5 M, 1.2 ml) to release the bound complexes, after renewed filtration the filtrate was analysed by HPLC-MS (see below) likewise.

HPLC experiments

The library compositions were analysed by RP-HPLC-MS (column: Waters Symetry 300^{TM} C18 5µm). The elution was monitored with a UV-detector (see above) set at 254 nm. Masses of the eluting peaks were determined using ES injection in positive polarity with a fragmentor voltage of 90 V.

For DCL-1: injection volume 5µl H_2O/MeCN (0.1% TFA) gradient: 0-15 min, 90:10 - 0:100.

For DCL-2: injection volume 15µl H_2O/MeCN (0.1% TFA) gradient: 0-15 min, 95:5 - 80:20.

HPLC results for DCL M (additional to main part)

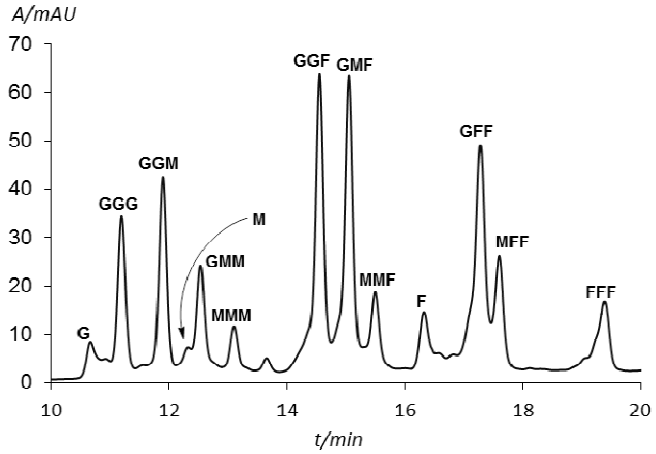

Figure 1 *Chromatogram of non-protein bound fraction of* ***DCL M***

Calculation of abundance changes for DCL M

Library member DCL1	*Reference sample[a],[b]*	*Protein bound fraction[a],[c]*	*Abundance Change (%)*
GGG	5.9	1.0	-82.8
GGM	13.9	8.8	-36.7
GMM	13.0	24.6	89.8
MMM	3.1	26.5	752.4
GGF	14.2	0.9	-93.5
GMF	21.2	13.3	-37.3
MMF	7.9	18.3	131.1
GFF	9.7	0.4	-95.9
MFF	6.1	5.0	-17.7
FFF	4.9	1.1	-78.0

Table 1 *Abundances of library members of* ***DCL M*** *and their change in abundance. [a] Integration area of overall abundance in % taken from the respective chromatogram (UV-254 nm detection).*

Generation and analysis of the dynamic combinatorial libraries N and O

Aqueous solutions of the homoleptic complexes **SSS**, **MMM**, **LLL**, **XXX** (only for **DCL O**) at 0.3 mM each in deoxygenated water were mixed and equilibrated for 7 days at 5ºC.

Reference sample:

54 µl of equilibrated solution (see above) were mixed with 10 µl deoxygenated water.

DCL mixed with Concanavalin A:

To 270 µl of equilibrated DCL solution (see above) 50 µl Con A-sepharose suspension was added. After mixing for 7 days at 5ºC the suspension was filtered (Millipore Ultrafiltration Membrane YM100). The filtrate was immediately analysed by HPLC-MS (see below). The sepharose particles on the filter membrane were suspended in HCl (0.5 M, 1.2 ml) to release the bound complexes, after renewed filtration the filtrate was likewise analysed by HPLC-MS (see below).

HPLC experiments:

The library compositions were analysed by RP-HPLC-MS (column: Waters Symmetry 300^{TM} C18 5µm). The elution was monitored with a UV-detector (see above) set at 254 nm. Masses of the eluting peaks were determined using electrospray injection in positive polarity with a fragmentor voltage of 100 V.

Injection volume: 10 µl

Eluent: **H_2O** (0.1% TFA) / **MeCN** (0.1% TFA)

Gradient:	0 min	92 /	8%
	15 min	90.5% /	9.5%
	30 min	90.5% /	9.5%
	70 min	86% /	14%

HPLC results (additional to main part)

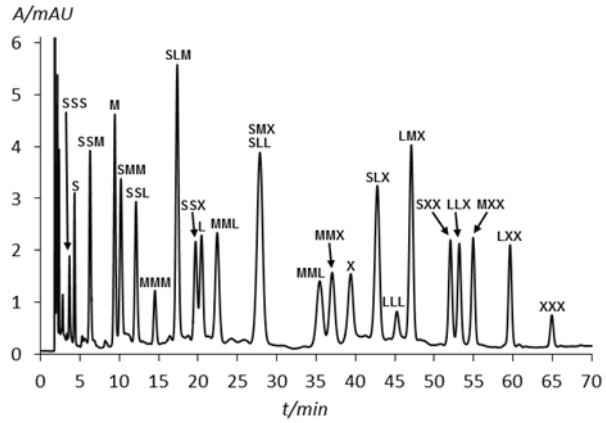

Figure 2 *Chromatogram of the protein bound fraction of* ***DCL O*** *(1st set-up). Overlapping peaks are labelled on top of each other (this figure is also shown in the main part).*

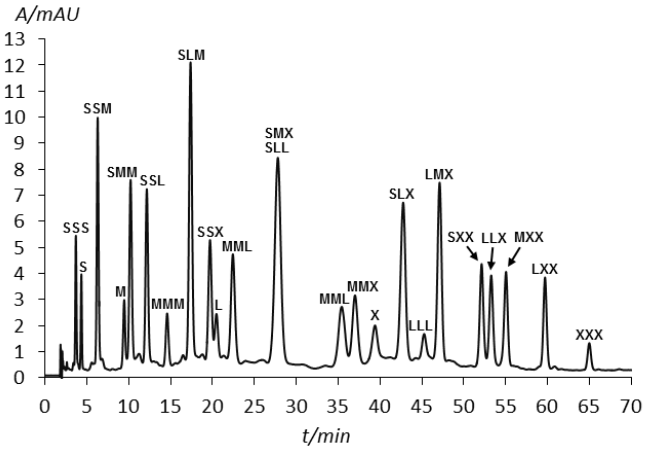

Figure 3 *Chromatogram of the non-protein bound fraction of* ***DCL O*** *(1st set-up). Overlapping peaks are labelled on top of each other.*

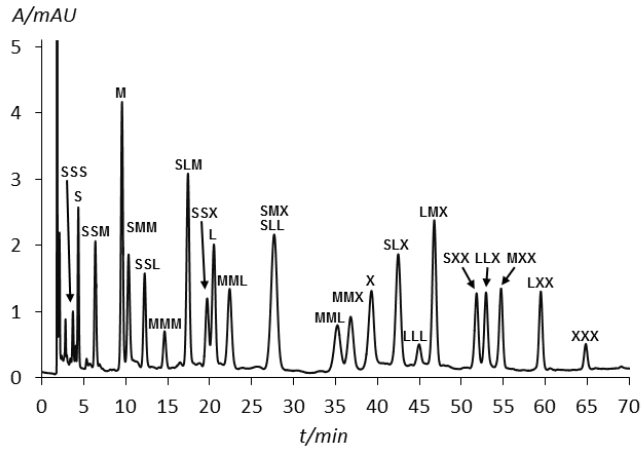

Figure 4 *Chromatogram of the protein bound fraction of* ***DCL O*** *(2nd set-up). Overlapping peaks are labelled on top of each other.*

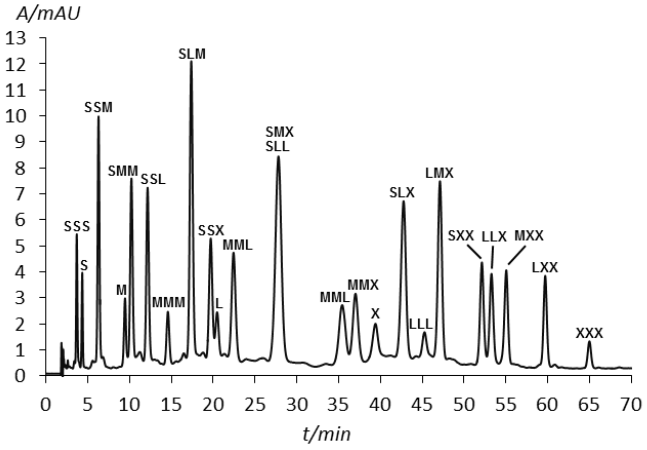

Figure 5 *Chromatogram of the non-protein bound fraction of* ***DCL O*** *(2nd set-up). Overlapping peaks are labelled on top of each other.*

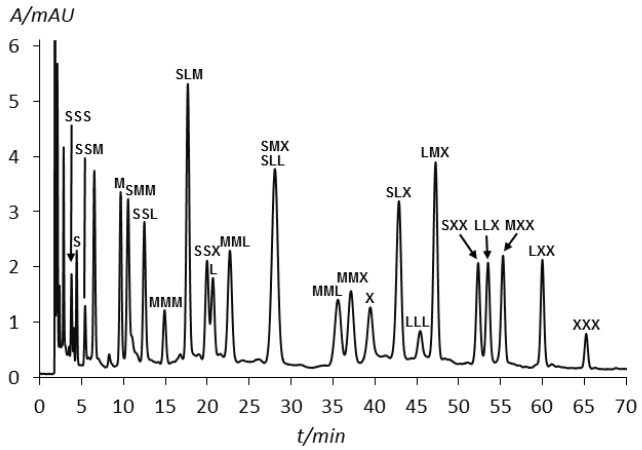

Figure 6 *Chromatogram of the protein bound fraction of* ***DCL O*** *(3rd set-up). Overlapping peaks are labelled on top of each other.*

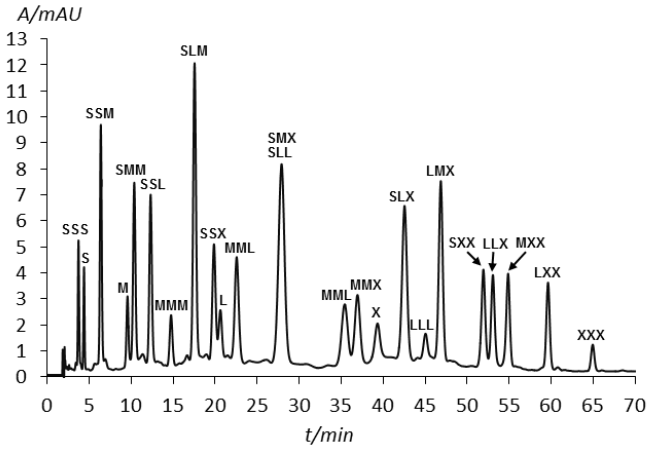

Figure 7 *Chromatogram of the non-protein bound fraction of* ***DCL O*** *(3rd set-up). Overlapping peaks are labelled on top of each other.*

Calculation of Abundance (and abundance change) of DCL members in reference sample and protein bound fractions:

Library member DCL1	*Reference sample*[a]	*Protein bound fraction*[a]	*Abundance Change (%)*
SSS	1.66	1.26	-24.09
SSM	5.43	4.51	-16.94
SMM	5.7	4.87	-14.56
SSL	5.41	4.67	-13.67
MMM	2.01	2.01	0
SLM	11.25	10.64	-5.42
SSX[b]	-	-	-
MML	5.8	5.81	0.17
SMX/SLL	15.84	15.45	-2.46
MLL	4.41	4.7	6.57
MMX	4.49	4.5	0.22
SLX	9.6	9.87	2.81
LLL	1.24	1.5	20.96
LMX	9.38	10.2	8.74
SXX	4.29	4.6	7.22
LLX	3.88	4.39	13.14
MXX	4.42	5.01	13.34
LXX	3.98	4.5	13.06
XXX	1.14	1.42	24.56

Table 2 *Abundances of library members of* ***DCL O*** *(1st set-up) and their changes in abundance. [a] Integration area of overall abundance in % taken from the respective chromatogram (UV-254 nm detection) [b] Omitted due to overlapping of peaks.*

Library member DCL O	***Reference sample[a]***	***Protein bound fraction[a]***	***Abundance Change (%)***
SSS	1.66	1.02	-38.55
SSM	5.43	4.1	-24.49
SMM	5.7	4.7	-17.54
SSL	5.41	4.36	-19.40
MMM	2.01	1.87	-6.96
SLM	11.25	10.27	-8.71
SSX[b]	-	-	-
MML	5.8	5.79	-0.17
SMX/SLL	15.84	15.32	-3.28
MLL	4.41	4.45	0.90
MMX	4.49	4.59	2.22
SLX	9.6	10.03	4.47
LLL	1.24	1.7	37.09
LMX	9.38	10.84	15.56
SXX	4.29	4.73	10.25
LLX	3.88	4.6	18.55
MXX	4.42	5.37	21.49
LXX	3.98	4.61	15.82
XXX	1.14	1.58	38.59

Table 3 *Abundances of library members of* ***DCL O*** *(2nd set-up) and their changes in abundance. [a] Integration area of overall abundance in % taken from the respective chromatogram (UV-254 nm detection) [b] Omitted due to overlapping of peaks.*

Library member DCL O	*Reference sample*[a]	*Protein bound fraction*[a]	*Abundance Change (%)*
SSS	1.66	1.15	-30.72
SSM	5.43	4.33	-20.25
SMM	5.7	4.61	-19.12
SSL	5.41	4.88	-9.79
MMM	2.01	1.97	-1.99
SLM	11.25	10.6	-5.77
SSX[b]	-	-	-
MML	5.8	5.84	0.68
SMX/SLL	15.84	15.59	-1.57
MLL	4.41	4.49	1.81
MMX	4.49	4.5	0.22
SLX	9.6	9.93	3.43
LLL	1.24	1.56	25.80
LMX	9.38	10.36	10.44
SXX	4.29	4.6	7.22
LLX	3.88	4.46	14.94
MXX	4.42	5.06	14.47
LXX	3.98	4.5	13.06
XXXL	1.14	1.47	28.94

Table 4 *Abundances of library members of* ***DCL O*** *(3rd set-up) and their changes in abundance. [a] Integration area of overall abundance in % taken from the respective chromatogram (UV-254 nm detection) [b] Omitted due to overlapping of peaks.*

Abundance Change Diagrams for DCL O (1st and 2nd set-up):

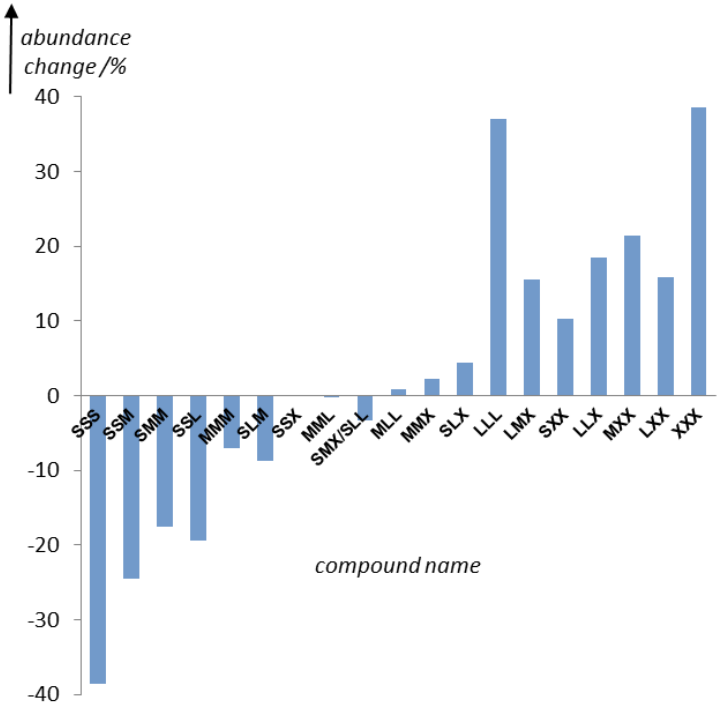

Figure 8 *Abundance change for the different library components of* ***DCL O*** *(2nd set-up). The equilibrated* ***DCL O*** *and the fraction of the DCL that gets bound to the protein are compared (determined from the HPLC chromatograms).*

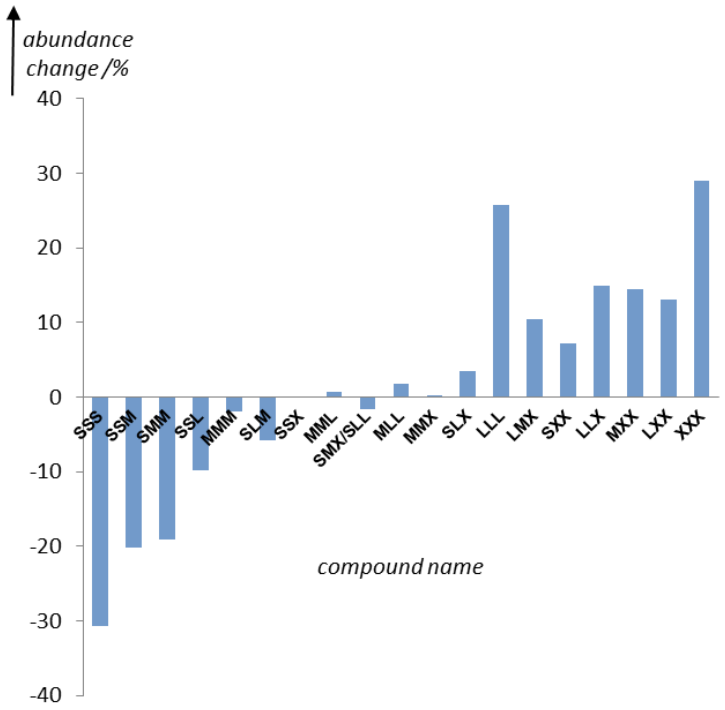

Figure 9 *Abundance change for the different library components of* ***DCL O*** *(3rd set-up). The equilibrated* ***DCL O*** *and the fraction of the DCL that gets bound to the protein are compared (determined from the HPLC chromatograms).*

Isothermal Titration Calorimetry (ITC) Experiments

Set-up of Titrant Solutions

Two solutions of **LLL** (0.4 mM) and **XXX** (0.4 mM) were set-up in 0.1 M acetate buffer containing 1 M NaCl, 1 mM $CaCl_2$, 1 mM $MnCl_2$, and 1 mM $MgCl_2$ in 50% ethanol. **MIX** (0.4 mM) was obtained by mixing **LLL** (0.4 mM) and **XXX** (0.4 mM) 1:1 v/v and equilibrating the mixture for 7 days.

ITC Measurements

ITC measurements were performed using a VP-ITC microcalorimeter from Microcal. Injections of 6 µL of glycol-Fe^{II} complexes (**LLL**, **XXX**) solution and the dynamic mixture **MIX** were added from a computer controlled 250 µL microsyringe at an interval of 200 seconds into de sample solution of Con A at 27ºC (cell volume= 1.453 mL). The solution in the titration cell was stirred at a speed of 300 revolutions min^{-1}. The concentrations of the lectin were 0.066 mM and the glycol-Fe^{II} complexes were 0.4 mM. Titration measurements were performed at pH= 6 in 0.1 M acetate buffer containing 1 M NaCl, 1 mM $CaCl_2$, 1 mM $MnCl_2$, and 1 mM $MgCl_2$ in 50% ethanol. Raw data were obtained as a plot of heating rate (µcal s^{-1}) against time (min). The raw data were then integrated to obtain a plot of observed enthalpy change per mole of injected glycoderivative (ΔH in kcal mol-1) against molar ratio (glycol-Fe^{II} complexes/ConA). Binding stoichiometries, enthalpies, and equilibrium association constants were determined by fitting the data to a one-site binding model with MicroCal Origin 7 using a nonlinear least-squares approach (Levenberg-Marquardt algorithm).

ITC Results for LLL

a)

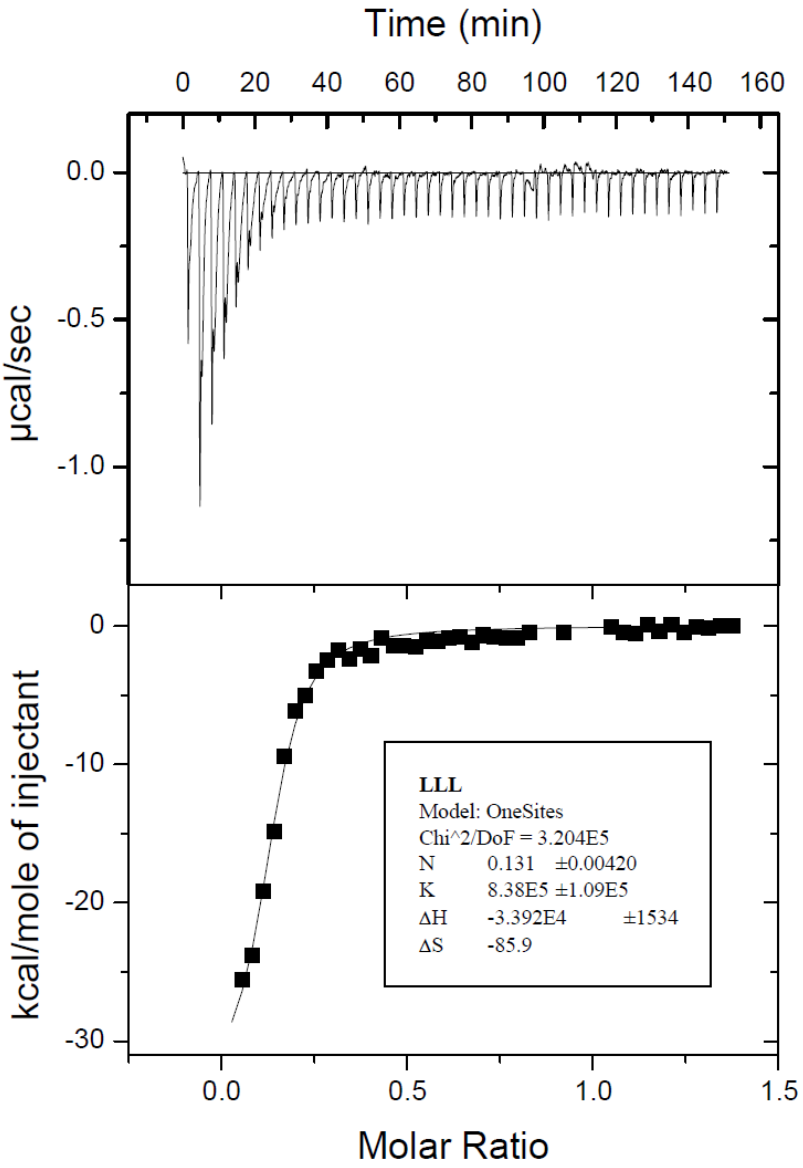

b)

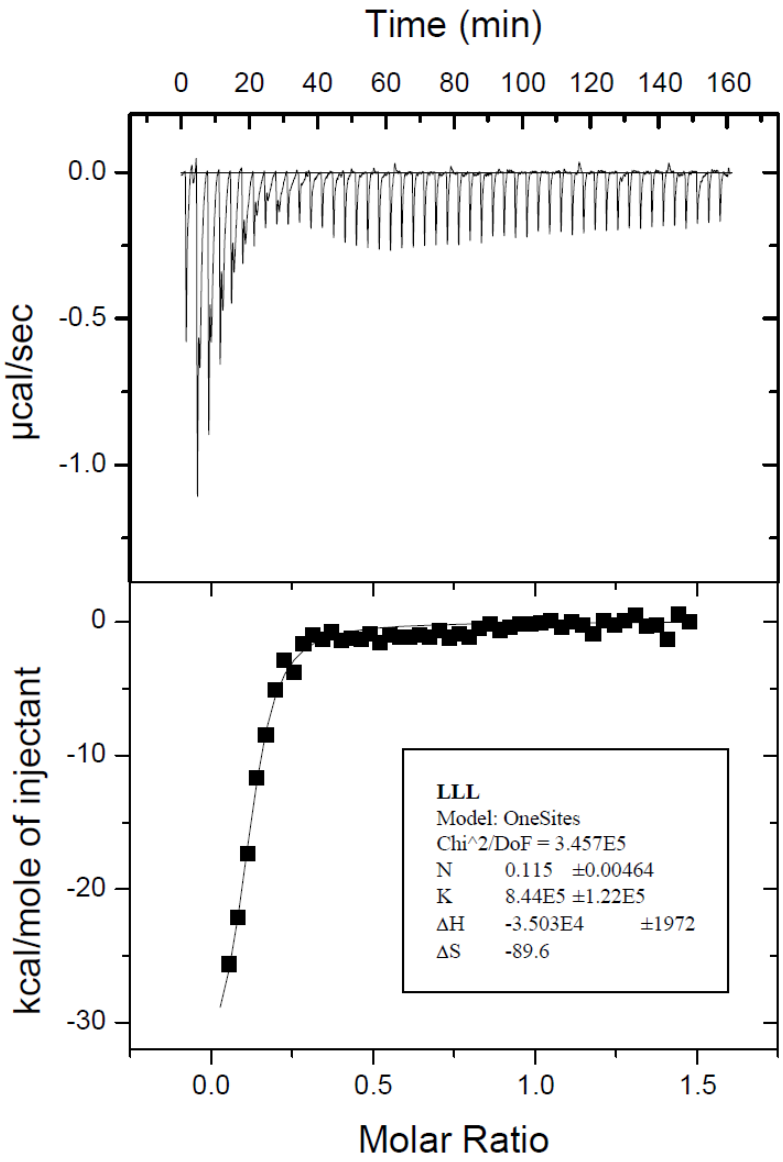

Figure 10 LLL *(0.4 mM) was titrated into a solution containing ConA (0.066 mM) in two independent ITC experiments a) and b). The heat released or absorbed during binding was measured as a function of the molar ratio of the sugar derivative to ConA.*

ITC Results for XXX

a)

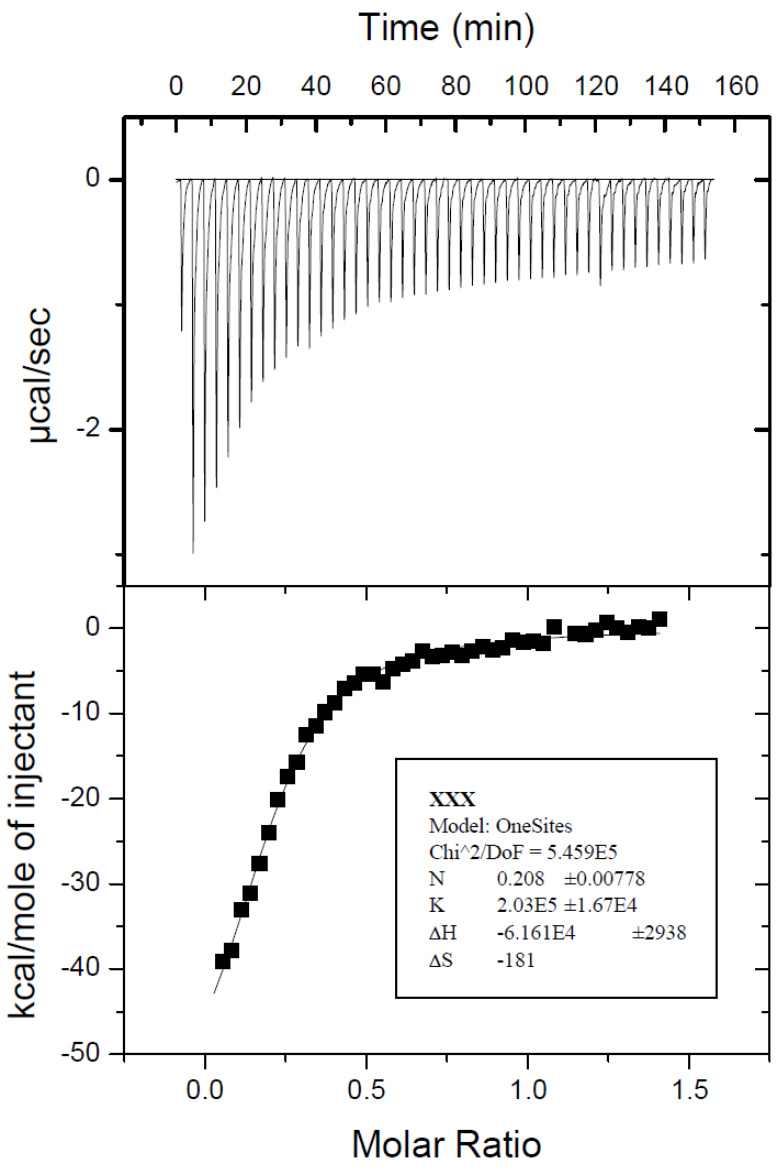

b)

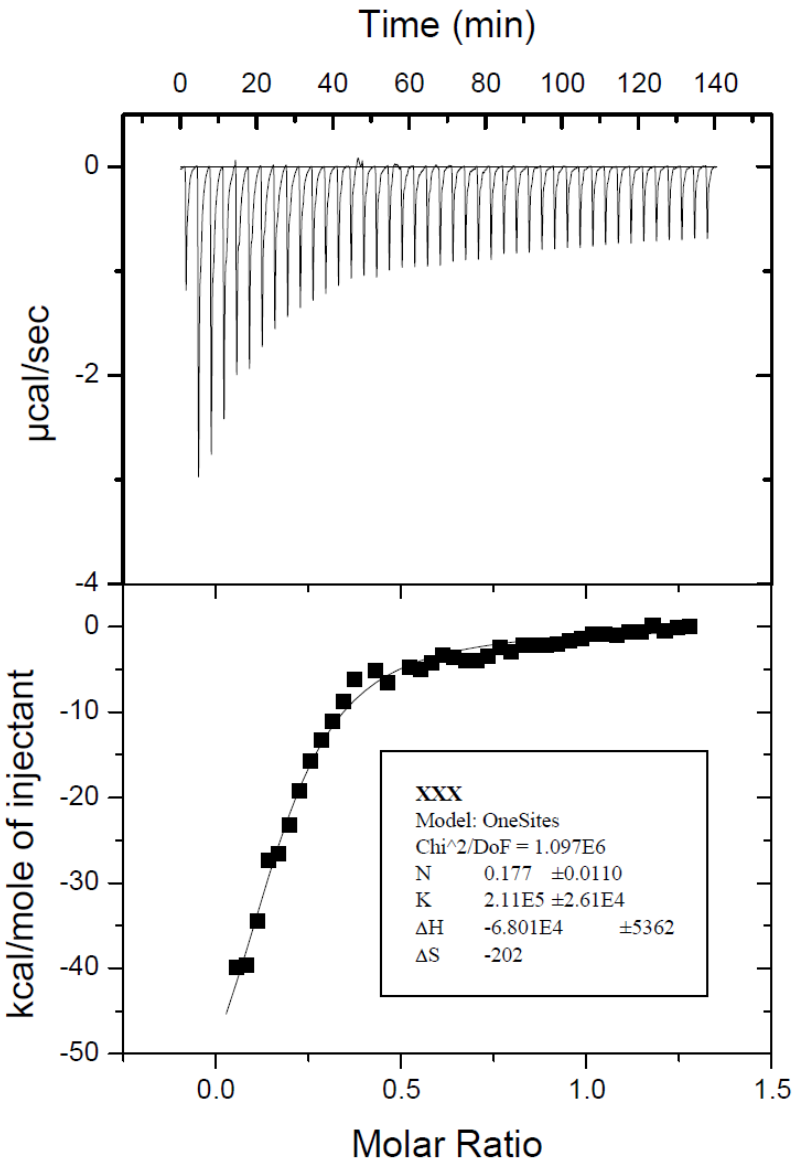

Figure 11 XXX *(0.4 mM) was titrated into a solution containing ConA (0.066 mM) in two independent ITC experiments a) and b). The heat released or absorbed during binding was measured as a function of the molar ratio of the sugar derivative to ConA.*

ITC Results for MIX

a)

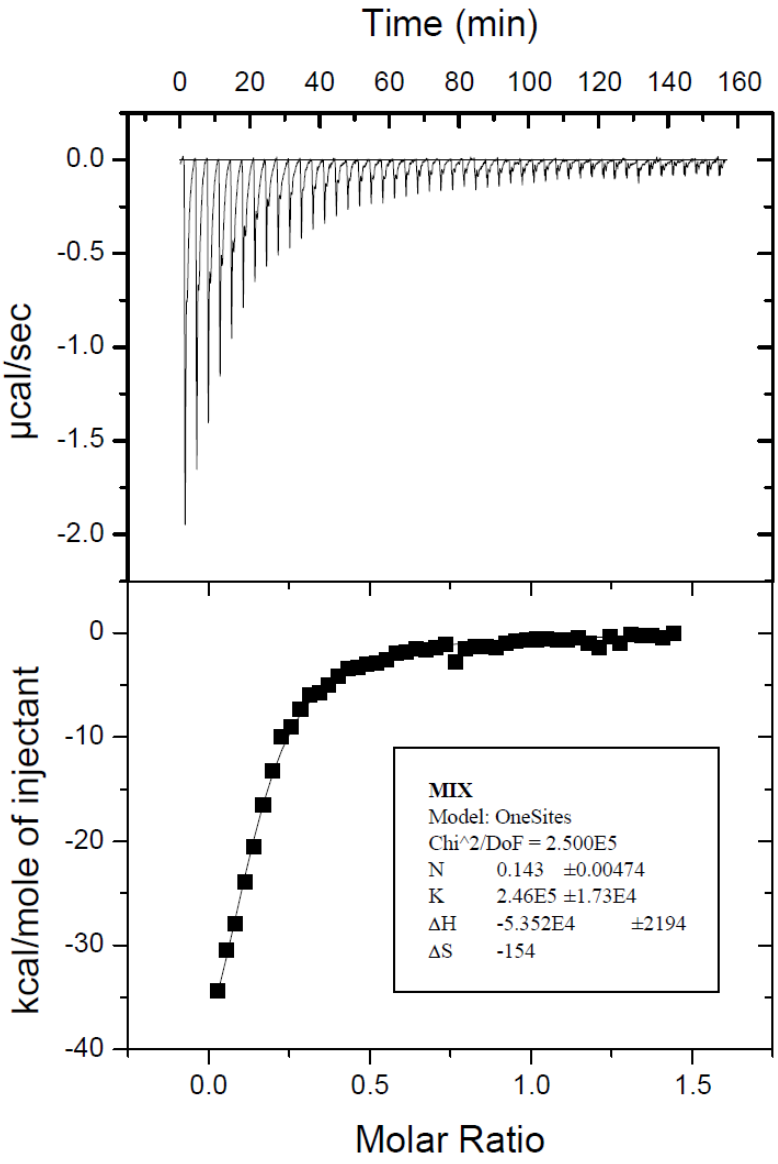

b)

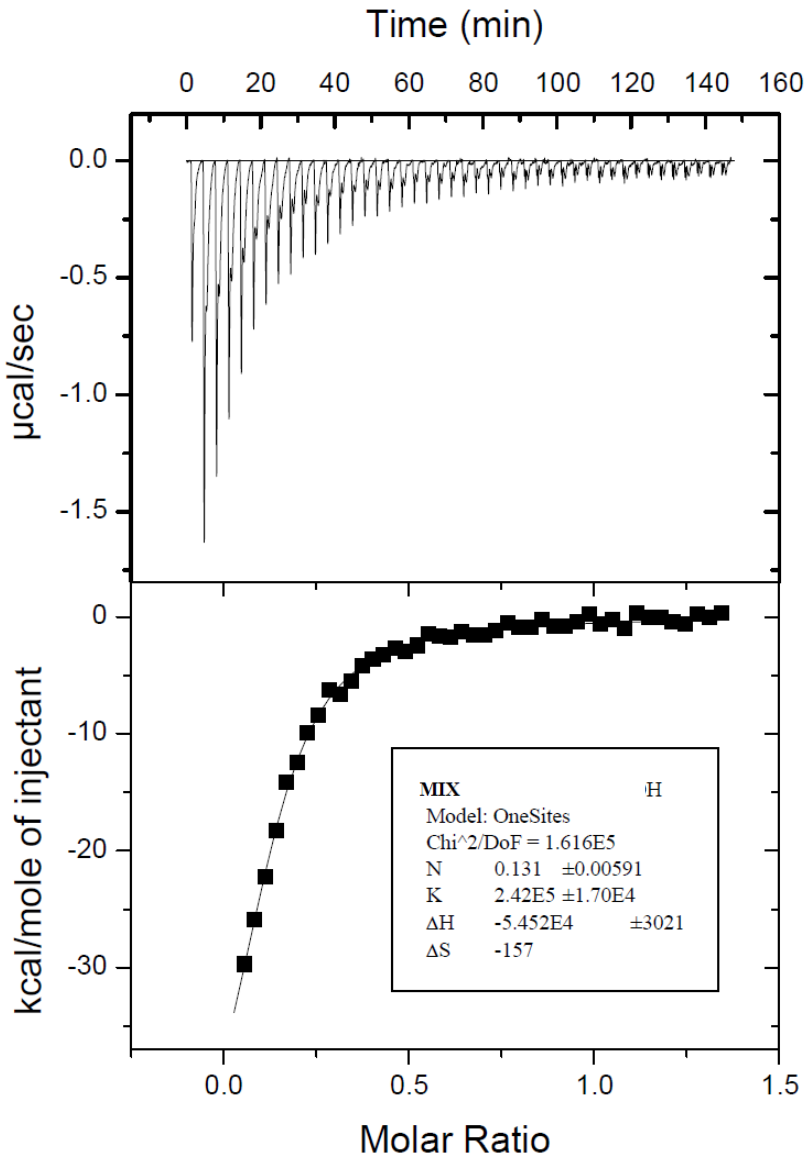

Figure 12 MIX *(0.4 mM) was titrated into a solution containing ConA (0.066 mM) in two independent ITC experiments a) and b). The heat released or absorbed during binding was measured as a function of the molar ratio of the sugar derivative to ConA.*

General Conclusions

In this doctoral thesis the concept of multivalency in sugar-protein (lectin) recognition was combined with the idea of dynamic combinatorial chemistry. This was attempted, not only to take advantage of the affinity enhancing effect of such multivalent systems but also to endow the system with a greater variety of constitutions and geometries. Determination of the relative binding affinities of dynamic combinatorial library members gave insights into the prerequisites for sugar- lectin binding.

Specific conclusions related to each of the topics covered in the manuscript have been highlighted in a separate section at the end of the corresponding Chapter. We will summarise here some general conclusions about the work performed.

The first approach (presented in Chapter 2), to accessing multivalent systems for lectin recognition, based on Dynamic Combinatorial Libraries (DCLs), employed well known strategies based on covalent but reversible bonds. In this part of the work the feasibility of the chosen analytical procedure was confirmed. Dimeric species, similar to those that had been known from experiments of other groups, show good analysability of the formed DCLs. The chosen analytical method (HPLC-MS) allowed detection of relative binding affinities and selectivities of these library constituents. A number of attempts to set-up multivalent dynamic combinatorial libraries based on the same concept were conducted. All relied on a central subunit providing multiple connecting points for reversible bonding. Specifically, disulphide bridges and imine formation were evaluated. Some of these studies turned out to be complicated by significant side problems, such as water solubility and unwanted side interactions of scaffolding units, mainly due to intramolecular reactions. Nevertheless, a multivalent dynamic combinatorial library presenting and exchanging sugar units, based on sulphide exchange to form disulphide bridges, was finally obtained and successfully analysed by HPLC-MS techniques. This was possible due to the water solubility of the scaffold, endowed with carboxylate subunits and by the use of short linkages between the thiol connecting points and the central structure, to prevent intramolecular linkages. However, even as the mentioned problems were controlled, the reliable and stable formation of the DCLs species remained challenging, due to substantial disintegration of the library members during the analysis step. Thus, subsequent

comparison of affinities of DCL members was not possible. Nonetheless, the presented approaches offer opportunities for further experiments and very careful choice of conditions should lead to success. Unfortunately, the time-frame of this thesis did not allow further pursuing such fine tuning as more promising leads had to be followed.

On the contrary, metal-ligand coordination, especially with bipyridine-type ligands around Fe^{II} centres, avoided most of the problems encountered earlier. This part has been developed in Chapter 3. Formation of complexes is very reliable under the conditions necessary for working with the chosen protein (ConA lectin) target. Sugar-decorated ligands as building blocks were obtained by straightforward synthetic procedures in good yields. Well-chosen HPLC methods enabled analysis of the formed DCLs and also determination of the relative binding affinities to ConA lectin. As a first proof of concept for a dynamic combinatorial behaviour, simple non-sugar containing DCLs based on bypyridine coordination were evaluated. Then sugar-containing DCLs were set-up and probed against the protein target. Quantification of the best binders supported the concept of multivalency for systems that dynamically exchange multiple recognition units.

Based on this study, other DCLs that incorporated constituents of varying shapes were developed. The relative affinities of those arrangements were compared to reveal what library members containing three-dimensional arrangements were most advantageous for binding to the lectin. Moreover, spherically shaped binding partners seemed to show highest affinity to the protein, in good agreement with the theory of statistical rebinding.

In summary, metal coordination-based (in contrast to dynamic covalent) DCLs have shown to constitute an easy way to to access multivalent exchange processes, providing new insights to unravel the rules of multivalent sugar-lectin interactions.